



Activity report

2014

Index

1. RFX-mod and RFP Physics	pag. 5
2. Eurofusion Tokamak & Stellarator WP	pag. 28
3. Broader Approach	pag. 40
4. ITER	pag. 46
5. DEMO	pag. 115
6. Applications	pag. 122
7. Education, Training and Information to the public	pag. 129
8. Publications	pag. 133

Introduction

The 2014 Activity Programme of Consorzio RFX was presented and evaluated at the 31st meeting of the RFX Scientific-Technical Committee on the 22nd November 2013 and afterward it was finally approved , with adaptation to the available resources, in the Consorzio RFX meeting, the 12th September 2014.

The 2014 was the first year with the new strong finalization (“goal oriented”) of the European fusion researches covered by the accompanying programme, managed by Eurofusion consortium, mainly focused to the success of the ITER project and to the preparation of the next step, the experimental reactor DEMO. As planned, Consorzio RFX has strongly contributed to this programme, finalizing to these priorities the 2014 RFX-mod experiments and increasing the involvement of physicist in the experimental activities of JET and AUG. All the activities in charge to Consorzio RFX, included into the 2014 Eurofusion programme, have been performed and the final reports have been delivered.

The most significant results related to the participation to the Eurofusion program are highlighted in the Section 1 - RFX-mod and RFP Physics, related to the RFP and Tokamak experiments in RFX-mod and to the theoretical studies on RFP configuration mainly included in the Enabling Research of Eurofusion, Sec. 2 with the results of Consorzio participation to the Eurofusion Tokamak and Stellarator Workprogramme, Sec. 4 with the NBI accompanying activities related to NIO1 experiment, Sec. 5 which report the activities and results related to PPPT and, finally, in Sec. 7 with the contribution to education and information to the public. The vastness of the activities for the Eurofusion Workprogramme which, as reported, was extended to all program lines of Consorzio RFX, accounts for the effort made to contribute adequately to the European program.

In order to maintain the excellence and the competitiveness of Consorzio RFX in physics research performed in the framework of the success of ITER, studies continued in order to identify the key RFX-mod enhancements, able to keep up-to-date the experiment and address key issues for fusion science.

The second pillar of the RFX researches was related to the activities for the development of the ITER NB injectors and the set-up of PRIMA facility. These activities were carried out, according to the signed Agreements, on the basis of the 2014 Workprogramme agreed with the various stockholders (ITER, F4E and the other Domestic Agencies) and endorsed in the Consorzio programme.

As reported in Sec. 4, the progress of the activity was relevant and in line with the main schedule; some uncertainties still open in the design have been fixed, because in the course of the year

some crucial aspects, such as the final layout of the facilities provided by the Japanese Domestic Agency, have been finalized. The year 2014 could be considered as the year in which there has been a transition from a phase in which the activities were primarily oriented to the design towards a phase where realizations are prevalent, with the Consorzio committed to the follow-up of the realization of the equipment and plants; a sign of this change could be considered the start, which took place at the end of the year, of the installation of the first experimental system, the cooling plant of SPIDER and MITICA and the completion of the design of the most complex component of MITICA, the beam source.

A success was the activity, reported in Sec. 3, related to the Broader Approach in charge to Consorzio RFX, with the shipment to Japan of the 13 Quench Protection Units for JT-60SA in September 2014 and the start of the installation activities in Naka.

Moreover, further activities are carried out by the Consorzio as direct contributions to ITER, related to some diagnostic systems and studies on disruption, and with some activities related to industrial applications of the technologies developed at RFX.

In the year 2014, 83 publications is the contribution on national and international journals (73 in 2013), 109 are the publications in conference proceedings (71 in 2013) and 29 communications in national and international workshops or conferences (46 in 2013).

1. RFX-MOD AND RFP PHYSICS

A significant part of physics studies at Consorzio RFX is related to the exploitation of the RFX-mod device. The program of the RFX-mod device is focused on two main lines: advancing the Reversed Field Pinch (RFP) fusion concept and contributing to key issues of the international Tokamak and Stellarator program. Indeed such two lines are not independent: the RFP shares with Tokamak and Stellarator several crucial open physical issues, including 3D nonlinear MHD modeling, MHD instability control, internal transport barriers, edge transport and turbulence, isotopic effect, high density limit, plasma-wall interaction studies, diagnostic development. The results and the competencies developed by a relatively large research group working together on these issues are naturally transferred to different magnetic configurations, also offering the added value of an original cross configuration view of the problems. In 2014, this strict relation between RFX-mod activity and the European program has manifested both in the fulfillment of the Enabling Research projects scored as relevant for the European roadmap (rated “A” or “B” by Eurofusion) and exploiting the RFX-mod experience in a direct contribution given to the Eurofusion Work Packages (section 2).

Peculiarity of RFX-mod is its flexibility: the device can be operated as a high current (up to 2MA) RFP, where advanced regimes featuring helical shape and opening a natural connection to the Stellarator geometry develop, and as a 0.2 MA ohmic circular Tokamak. As a RFP, mission of RFX-mod is the exploration of the high current regimes: this has been advanced in 2014 through an experimental and modelling effort to deepen the understanding of the single helical axis (SHAx) states [Escande 2000, Lorenzini 2009], in particular concentrating on the study of the electron transport barriers developing in such enhanced regimes [Carraro 2013] and of the isotope effect. As a Tokamak, though only low current plasmas can be produced due to the low available toroidal field, RFX-mod can extend the parameter space explored by the other devices and in 2014, thanks to its state-of-art control system, peculiar experiments have been performed, for example exploring the $q(a) < 2$ regime [Martin 2014, Piovesan 2014].

The topics where the 2014 activity was concentrated can be summarized, according to the 2014 Program Activity, as:

- 3D magnetic equilibria and internal transport barriers
- Isotopic effect studies
- Development of innovative MHD control techniques
- Plasma edge studies
- Plasma-wall interaction

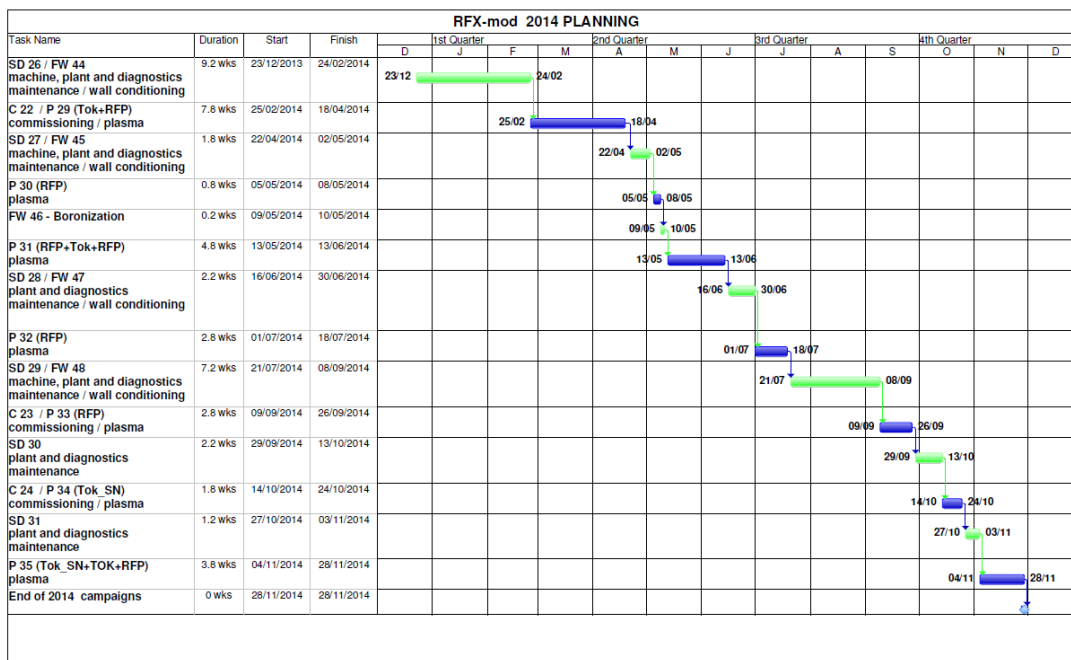
- Density limit studies
- Diagnostic developments

In the same time, studies for the conceptual design of machine improvements have proceeded.

The machine was operated along 25 weeks (4 days per week), shared between RFP and Tokamak experiments: 16 weeks as RFP and 8 weeks as Tokamak. In addition 1 week was spent to set-up and commission the coil configuration to produce Single-Null Tokamak equilibria.

During the year 6 saddle coils broke at different times and 2 of them (the only accessible have been repaired.

One boronisation treatment was performed in May, as shown in the 2014 general operation planning below.



1.1 3D magnetic equilibria and internal transport barriers

1.1.1 Transport studies. In RFX-mod, when operated as a Reversed Field Pinch, two different regimes are observed, the so called Multiple Helicity (MH) chaotic state and the Quasi-Single-Helicity (QSH) state, the latter developing as the result of a self-organization process from magnetic chaos to order.

In the MH state several $m=1$ MHD instabilities (with m/n poloidal/toroidal numbers) interact producing magnetic chaos and a large deformation of the last magnetic surface. The helical QSH state is instead spontaneously established at high plasma current, when a single $m=1$ mode dominates the other (secondary) modes and yields chaos healing in the core. When the amplitude of the dominant mode relative to the secondary ones is high enough, the separatrix of the associated island is expelled and its axis becomes the new helical axis of the plasma (Single Helical Axis, SHAx states). In SHAx, temperature and density in the core exhibit the same helicity as the dominant mode ($m=1, n=-7$ – the innermost resonant - in RFX-mod). The edge remains quasi symmetric, with reminiscences of the large core deformation. The global confinement is enhanced by a factor of $\approx 3-4$ with respect to MH. However, the improved helical states are observed at relatively low values of plasma density.

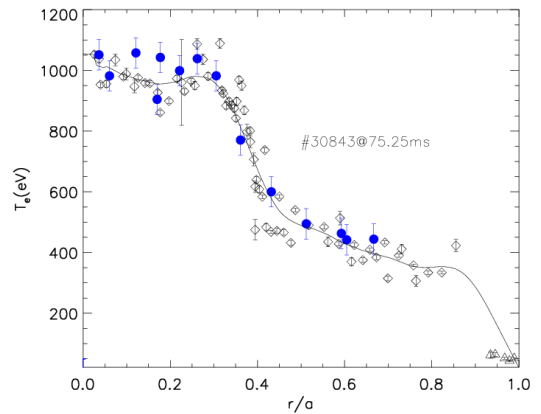


Fig. 1.1.1: Electron internal transport barrier in a SHAx state

SHAx states are characterized by strong temperature gradients (fig. 1.1.1). In 2014, studies on thermal transport across the temperature barrier have been favoured by the combination of data from a 84 points Thomson scattering diagnostic (10ms repetition rate) with a new multi-channel high frequency diagnostic (10kHz) based on double filter technique [Gobbin 2013]. In the barrier region, values of thermal conductivity χ_e ranging from ≈ 2 to ≈ 20 m^2/s have been found, to be compared to $\chi_e \approx 100$ m^2/s outside the barrier. In particular, the relation between χ_e and the secondary mode amplitude has been analyzed: fig. 1.1.2 shows the probability of achieving $\chi_e < 5$ m^2/s as a function of secondary mode amplitude (data refer to discharges with H as majority ion mass).

The decreasing tendency suggests that main contributors to the thermal transport at the barrier could be residual magnetic stochasticity and microtearing (MT) modes, as already suggested by GS2 gyrokinetic simulations in 2013 [Carraro 2013]. Recent simulations of particle transport in helical regimes showed that in the core diffusion coefficient is

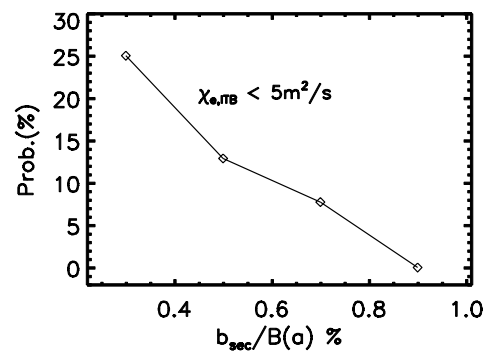


Fig. 1.1.2: Probability of achieving $\chi_e < 5$ m^2/s at the barrier location vs. secondary mode amplitude in SHAx plasmas

lower by about a factor of 10 at the lowest secondary mode amplitudes with respect to MH plasmas, reaching values of $\approx 1 \text{ m}^2/\text{s}$ [Auriemma 2014]

At the edge, the diffusion has been evaluated by a Gas Puffing Imaging and a Thermal Helium Beam diagnostic. Fig. 1.1.3a shows the edge diffusivity obtained as a result of the main gas influx ($D = -\Gamma_{in}/\text{grad}(n_e)$, black line) and the diffusivity related to blobs [Horton 1996], (green curve).

The Bohm diffusion coefficient is also shown for comparison. The time evolution of the edge electron pressure and of the local magnetic deformation are instead shown in fig. 1.1.3b and c, respectively. It can be seen that the diffusion related to coherent structures is of the same order as D , indicating that blobs are driving a significant portion of transport at the edge [Puiatti 2014].

In fig. 1.1.3 it is also shown that, though the helical ripple at the wall (of the order of 1%) is sufficient to modulate the edge kinetic properties, its effect on the diffusion is smaller. The blob diffusivity shows a good agreement with the result from ASTRA simulations (fig.1.1.4), reproducing the experimental density profile evolution.

Innovative genetic algorithms to study particle transport, based on analogies with bio systems according to the technique described in [Sattin 2012], have been developed and tested on RFX-mod data [Auriemma 2014]. An example is given in fig. 1.1.5, comparing the result of the calculation of the diffusion coefficient in a SHAx state from a traditional iterative approach with that from a direct calculation based on a genetic algorithms.

In principle, the advantage of the latter is that the function to optimize is not necessarily continuous and differentiable and can change in time; in addition, the whole parameter space is explored, with decreased risk of finding relative minima.

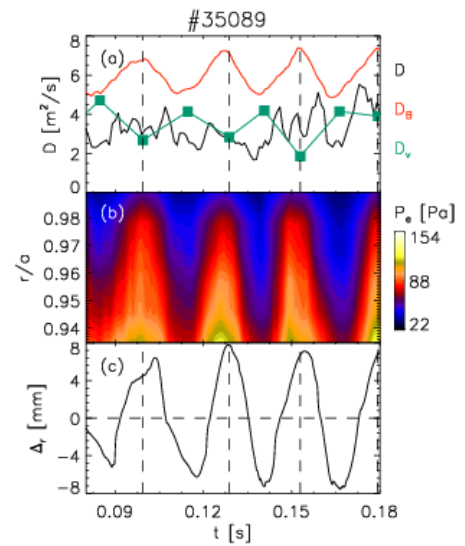


Fig. 1.1.3: (a) edge diffusivity from the main gas influx (black), contribution to diffusivity due to blobs (green), and Bohm diffusion (red); (b) edge pressure profiles from a thermal helium beam diagnostic; (c) magnetic deformation at the diagnostic location

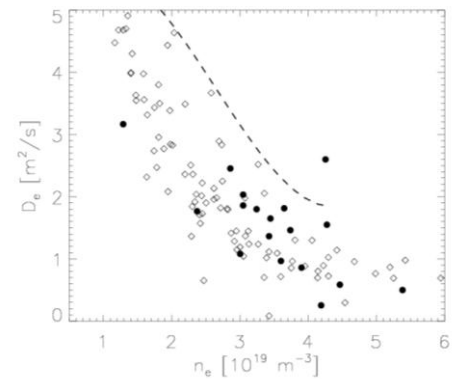


Fig.1.1.4: comparison of the edge diffusivity as obtained by ASTRA simulations (empty) and by thermal helium beam diagnostic (full). Bohm diffusivity is also shown (dashed)

1.1.2 3D reconstruction of magnetic equilibria.

In SHAXs states, 3D tools, originally developed for the Stellarator and adapted to the RFP are used to reconstruct the internal helical magnetic equilibria. In particular, for RFX a significant effort is in progress in advancing the capability of the reconstruction of the helical state by the VMEC+V3FIT code suite. The VMEC code is used as a non-linear equilibrium solver [Hirshman 1983] and coupled to V3FIT [Hanson 2009], where both magnetic and thermal measurements are taken into account in V3FIT [Terranova 2013]. In particular, in 2014 the Soft X-Ray -SXR- emissivities have been included in the reconstruction.

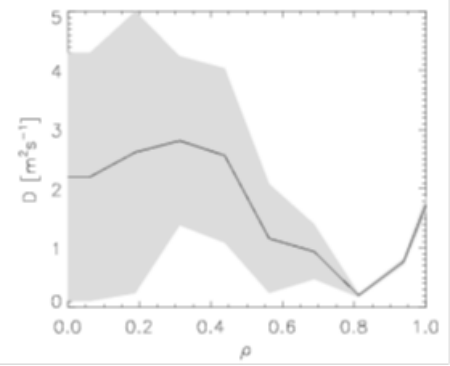


Fig.1.1.5: Comparison of the diffusivity in a RFX-mod helical state as obtained with a traditional iterative approach (plain line) and with a genetic algorithm (shadow)

1.1.3 Helical state dynamics.

Helical states are not stationary, as they undergo periodic back transitions to the chaotic state during the so called Discrete Relaxation Events (DRE), which can be described as events of toroidal flux self-generation by the action of discrete dynamo. In 2014 a large part of the modeling activity has been focused on the understanding of such intermittent behavior of QSHs, by applying the SPECYL and PIXI3D MHD codes [Bonfiglio 2013]. In particular, the experimental sawtoothing dynamical behavior of QSHs has been well reproduced by the SPECYL code introducing the effect of helical boundary conditions for the radial field, consisting in a $m=1, n=-7$ helical modulation of the plasma magnetic boundary. An example is shown in fig. 1.1.6, where SPECYL runs corresponding to subsequent time ranges with different amplitudes of the helical boundary are drawn. Quasi-periodic cycles with clear (1,-7) QSH phases interrupted by reconnections with enhanced MHD activity are obtained, remarkably similar to the experimental behavior in a RFX-mod plasma discharge, also shown in

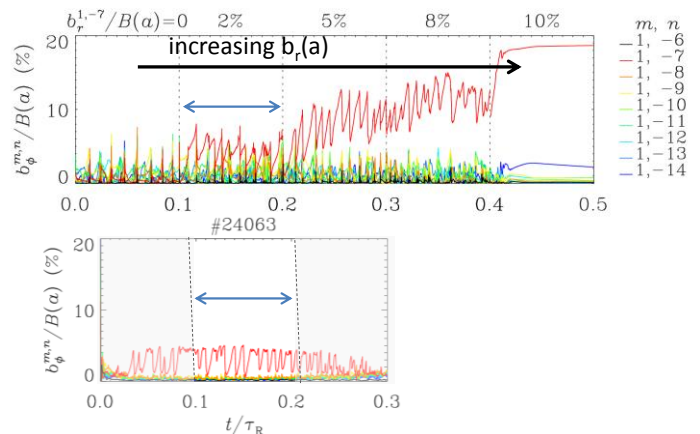


Fig. 1.1.6: (top) SPECYL simulation with an helical boundary of increasing amplitude compared with the experimental case (bottom)

the plot. Quantitatively, the main difference relies on the secondary mode amplitude, which in the simulation must be higher to quantitatively reproduce the experiment. This can be ascribed to a dependence on the viscosity ν , which is a parameter still matter of investigation in the RFP; in particular, a fixed Prandtl number $P=\nu/\eta$ turns out to provide a numerical scaling of secondary modes with the Lundquist number S close to the experimental one.

1.2 Isotopic effect studies

The first extensive campaign using deuterium as filling gas has been performed in 2014, after the licensing procedure. First objective of the experiments was to compare the effect of the majority ion mass in RFPs with the Tokamak and Stellarator. In fact, it is well known that in Tokamak the majority ion mass impacts on confinement and MHD properties, while no similar effect is observed in the Stellarator. However, the mechanism behind the different isotope effect in Tokamak and Stellarator is not yet well understood, so that the investigation of the dependence of plasma properties on majority ion mass in a magnetic configuration allowing the exploration of a new space of plasma parameters gives more insight into such physics.

In particular, in 2014 the investigation on the isotope effect was limited to high current discharges, aiming at its characterization in helical states. An interesting extension, planned in 2015, is the comparison between H and D in Multiple Helicity and in low current plasmas.

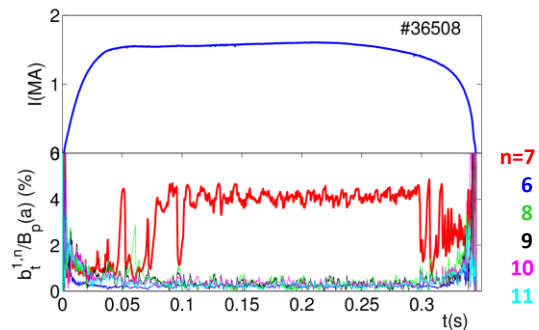


Fig. 1.2.1: amplitude of $m=1$ modes in a deuterium discharge showing a quasi-steady state QSH. Plasma density $n/n_G \leq 0.1$

1.2.1 Helical states in deuterium.

A first observation was that deuterium allows operation at lower density than H, suggesting a different plasma-wall interaction. In particular, high current discharges at $n/n_G < 0.1$ (n_G Greenwald density) have been sustained, which allowed the onset of quasi-stationary QSH phases, as for example shown

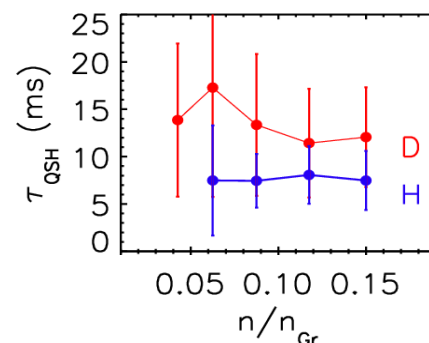


Fig. 1.2.2: comparison of QSH state average duration in D and in H

in fig. 1.2.1. However, D favours longer QSH persistence also at higher density: a statistical analysis comparing H and D discharges at the same density is shown in fig. 1.2.2. Indeed a statistical analysis shows that in deuterium QSHs are more resilient than in hydrogen to discrete reconnection events (DRE), related to back-transitions to Multiple Helicity states. The fraction of DREs resulting in a back transition to MH is found to be $\approx 55\%$ in D to be compared with $\approx 75\%$ in H. A more detailed study of the DRE physics in the RFP and its impact in the understanding of magnetic reconnection phenomena is part of the Eurofusion Enabling Research project WP14-ER-01/ENEA-RFX-02.

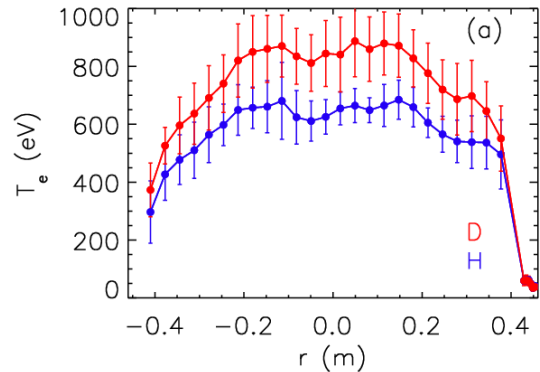


Fig. 1.2.3: comparison of electron temperature profile from Thomson scattering and Thermal Helium Beam diagnostics in D and in H

1.2.2 Majority ion mass effect on confinement. The longer lasting helical phases in deuterium can be also related to a difference in MHD. Deuterium shows a stabilizing effect on the secondary modes resonating at the edge, with a lower request for dynamo field [Lorenzini 2014]. In fact, in deuterium at the same density the saturation amplitude of secondary modes is lower than in H, so that the longer persistence is consistent with the relation between QSH duration and mode amplitude already documented in [Piovesan 2009]. The smaller saturation amplitude of secondary modes can be also related to a difference in the temperature, whose profile shows more pronounced gradients in D than in H, both in the core and at the edge (example in fig. 1.2.3, showing two temperature profiles obtained by the Thomson scattering diagnostic in similar D and H discharges). Though in D more pronounced gradients are present both in the core and at the edge, the main difference between the two relies in the higher pedestal in D, which suggests a mitigation of thermal transport at the edge. A more detailed study of edge behavior and transport, in particular with better experimental informations on density profiles and Long Range Correlations structures is expected in 2015. Since the input power does not change, the higher temperature leads to an improvement by $\approx 20\%$ of the energy confinement time, scaling as $\tau_E \sim M_i^{0.3}$. The scaling is less favourable than in Tokamak ($\tau_E \sim M_i^{0.5}$), but still significant and indication of an isotope effect in the RFP.

1.3 Development of innovative MHD control techniques

The skills growing in time at Consorzio RFX in the development and application of techniques to control MHD instabilities have been applied in 2014 both to RFP and Tokamak plasmas, with some preponderance for Tokamak. A large fraction of the results are included in the report of the WP14-ER-01/ENEA-RFX-05 Eurofusion Enabling Research project, where the results are fully described.

1.3.1 Studies on decoupling matrix in the RFP.

The RFX-mod actuator grid, wrapping the whole RFX torus, produces a Fourier spectrum that is influenced by geometrical aspects, such as the toroidicity of the boundary and the shape of actuators. When supplying a single harmonic in current references, the measured field resulting from the superposition of all the couplings contains undesired harmonics. Numerical simulations have been performed to compare different strategies for the reduction of distortion of the harmonics. In particular, two limiting cases of decoupling matrices have been tested: a static actuator-sensor decoupler and an infinite-frequency decoupler. Simulated and experimental data have shown that the mutual couplings can help in the task of producing monochromatic fields or, in general, in following as much as possible a given reference. The simulations have been presented in [Pigatto 2014a]. The same technique has been applied to partially compensate for missing coils due to broken contacts. The basic idea is to generate from the initial reference currents, through a Pseudo-Inversion based on a Singular Value Decomposition of the mutual coupling matrix, a new current distribution that allows the reconstruction of a desired field pattern. Initial encouraging results have been presented in [Pigatto 2014b] and further tests are foreseen in 2015.

1.3.2 RWM studies.

The RFX-mod control software can be modified in order to test the effect of different virtual coil configurations on RWM stability. This has been compared with the CarMa model [Albanese 2008], already used to predict RWM stability in presence of 3D passive structures and external fields in several Tokamaks, including ITER, and recently upgraded to account for several toroidal harmonics in addition to the multimodal poloidal capability. Such virtual reconfiguration can be applied both in RFP and in Tokamak [Bolzonella 2014]. Fig.1.3.1 shows the comparison of the effect of a $(1,-6)$ RWM in RFP plasmas as predicted by CarMa and as seen in the experiment configured with (1×16) actuators.

Theoretical studies on RWM stability, both in RFP (including shaping effects) and Tokamak, progressed in 2014 by means of a toroidal MHD kinetic hybrid stability code. The effect of the isotropic/anisotropic energetic particles on fishbone-like modes and RWM is studied, showing that such modes, despite their different nature, can coexist or even couple (one mode can change nature during plasma evolution) [Guo 2014].

1.3.3 Feedback controlled disruptions in Tokamak plasmas. It is well known that in Tokamaks the onset of an external kink sets a limit to the maximum current at a given amplitude of the toroidal field. In past years, in RFX-mod the possibility of operating above such limit by controlling the (2,1) RWM was already demonstrated (provided that the density does not exceed the Greenwald limit) [Zanca 2012], with experiments exported to DIII-D [Piron 2013].

At $q(a) > 2$, the (2,1) mode becomes a tearing mode (TM). When its amplitude grows up and its rotation frequency decreases, two situations may occur: if $q(a) \leq 2.5$ the feedback system can keep the mode in slow rotation, avoiding wall locking and disruption. Instead at $q(a) > 2.5$ if the (2,1) TM penetrates the vessel so that the more external conductive shell determines its saturation amplitude, a disruption always occurs, even if its rotation frequency is high. The idea was to exploit the efficiency of RFX-mod control system in mitigating the mode at lower $q(a)$ to investigate whether a controlled $q(a)$ decrease can avoid disruption by dynamically converting the (2,1) tearing mode to a (2,1) RWM. The experiment was successful with 100% rate, even at high densities. An example is shown in fig. 1.3.2, where a controlled $q(a)$ reduction at $t=370\text{ms}$ has quenched the strong growth of SXR and (2,1) mode.

It is worth noting that in the case of a large Tokamak, even if equipped with a feedback control system able to stabilize (2,1) RWM, a $q(a)$ control based on the increase of current is probably not realistic, due to the large amount of required loop voltage. This further motivates the RFX-mod shaped operation, in order to apply a similar disruption avoidance technique decreasing $q(a)$ by a

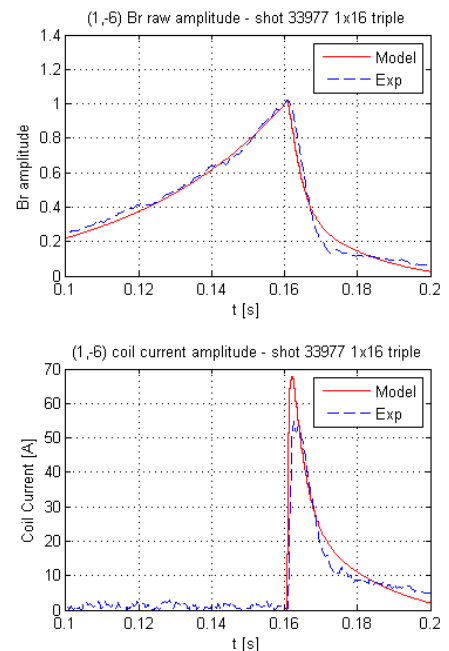


Fig.1.3.1: comparison of an experiment with a (1 x 16) coil reconfiguration and feedback control switched on at $t=0.16$ s (red, shot #33977) with CarMa (blue): (top) (1,-6) mode amplitude; (bottom) coil currents for the same harmonic

shape control, in particular through a decrease of the elongation, if the shape controller can be sufficiently fast.

1.3.4 Error field control by external 3D fields.

The effect of 3D fields in assessing and controlling error fields has been investigated both in RFP and in Tokamak configuration in collaboration with the EXTRAP-T2R (Sweden) group. The open loop rotation of a stable or marginally stable Resistive wall mode was developed first in EXTRAP-T2R and then applied to RFX-mod RFP plasmas

in the last part of 2014 campaign: the analysis is presently on-going. In Tokamak configuration, two techniques have been tested on RFX-mod, the dynamic error field correction and the so-called compass scan [Howell 2007]. The former has been applied to $q(a) < 2$ discharges, and is based on the combined application of direct feedback control and error field correction in a feed-forward scheme. The compass scan is instead applied in $q(a) > 2$ discharges, and is based on the scan of imposed perturbation with different phases up the locking. Phases corresponding to the mode locking are reported on a plane as real and imaginary components of the coil current and fitted by a circle. The intrinsic error is given by the displacement of the circle with respect to the origin. In both cases RFX-mod circular Tokamaks evidenced very low error fields; for example, fig. 1.3.3 shows a compass scan at $q(a)=2.4$. The small displacement of the circle from experiment would correspond to a field $B_r=0.2$ G. Such experiments are part of a MST2 project funded by Eurofusion

“Developing real-time control of error fields and MHD modes for RFX-mod, ASDEX Upgrade and MAST-U”, WP14-MST2-7); they have also been performed on ASDEX-Upgrade as part of the MST1 program (experiment): “Error field measurement/correction in

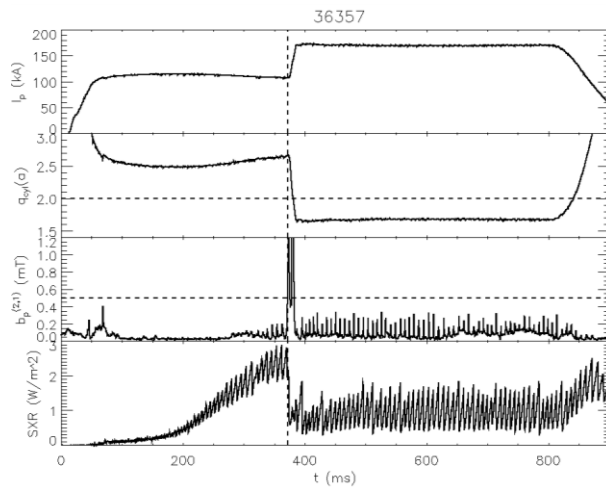


Fig. 1.3.2: disruption avoidance experiment in RFX-mod Tokamak. From top to bottom: plasma current; edge q ; $(2,1)$ mode amplitude; SXR emissivity

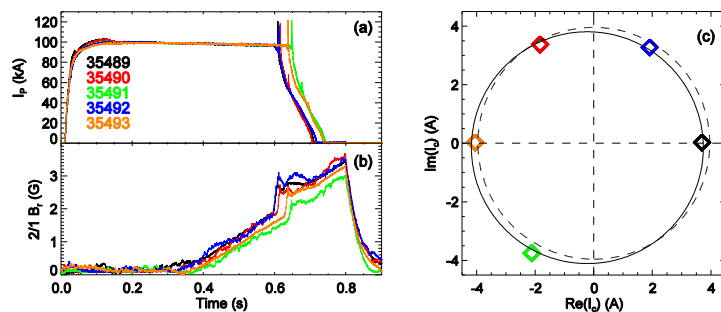


Fig. 1.3.3: example of compass scan in RFX-mod: (a) plasma current; (b) applied MP amplitude; (c) corresponding points on the $Im(I_0)$ and $Re(I_0)$ plane, showing a very small displacement

high-beta plasmas by a non-disruptive approach based on 3D plasma response”).

1.3.5 Runaway electron control by external perturbations.

In 2014, first indications of Runaway Electron (RE) mitigation by external Magnetic Perturbations (MP) have been obtained in the RFX-mod circular tokamak. Fast electrons are observed by NaI scintillators and SXR detectors in low density plasmas. A decorrelation effect by a non-resonant (2,1) MP has been observed and modelled by the ORBIT code. The application of the (2,1) mode

increases the edge stochasticity leading to increased RE losses, as only electrons in the region with well conserved magnetic surfaces can be accelerated to high energies. A parameter scan by ORBIT shows that the final energy and fraction of lost electrons depend on (2,1) amplitude and on q profile: as shown in fig. 1.3.4, the fraction of lost electrons increases with the perturbation amplitude, while the final energy decreases, and resonant perturbations are more effective in runaway decorrelation.

1.3.6 Non-circular Tokamak equilibria.

The flexible active control system of RFX-mod, allowing for the application of multiple and clean magnetic perturbations, induced the development of non-circular Tokamak equilibria, with the aim of obtaining an L-H transition and exploit the MHD control system in ELM mitigation studies. First single-null (SN) plasmas (following the double-null obtained in 2013) have been recently produced. Fig. 1.3.5 shows an example of single null tokamak equilibrium, with MAXFEA and V3FIT codes used for the equilibrium reconstruction.

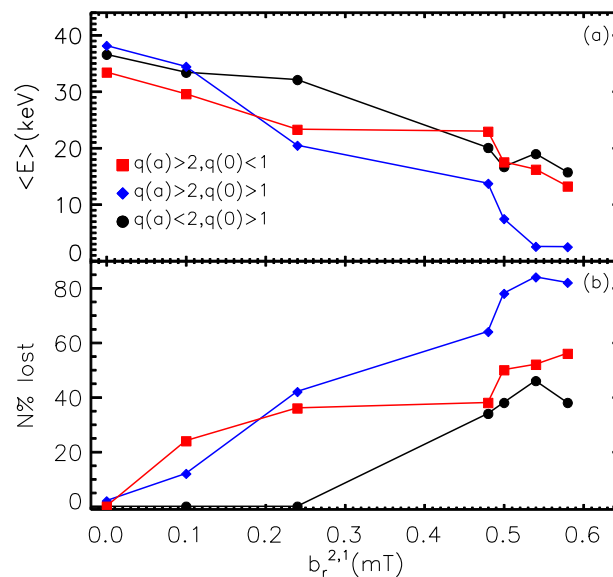


Fig. 1.3.4: final electron energy (a) and fraction of lost particles (b) as a function of the amplitude of the applied $m=2, n=1$ perturbation for three q profiles (ORBIT simulations)

During 2014 experimental campaigns with shaped plasmas a Linear Quadratic Gaussian (LQG) shape controller was designed and applied. This controller was derived by a new plasma response model provided by CREATE. In both Double or Single Null configurations, the controlled quantities are the 8 distances (gaps) of the plasma separatrix from the first wall along the radial direction corresponding to the flux loop position (or an inner one at 95% poloidal flux value). The first experiments with the LQG shape controller allowed a controlled variation of the gaps and consequently of the X-point position.

In order to optimize single-null plasmas, a particular care has been taken in the fuelling technique: indeed the equilibria produced up to now exhibits the SN on the top, just where the fuelling gas is injected, which makes difficult the density control. The inversion of the toroidal is planned for next campaigns, in order to produce the SN point on the bottom and improve the control of gas injection.

1.4 Plasma edge studies

Part of the results in this field are included in the report of the WP14-ER-01/ENEA-RFX-06 Eurofusion Enabling Research project.

1.4.1 Characterization of filamentary structures and microturbulence.

The EM features of filamentary structures detected in the RFX-mod (RFP and Tokamak) have been compared with L-mode plasmas in the TJ-II stellarator, and with the Simple Magnetized Torus TORPEX. Independently on the specific local magnetic topology, and on different drive mechanisms for the filaments formation, several common features have been found among the filaments detected in the explored configurations, both electrostatic, such as the presence of density and vorticity structures, and electromagnetic, such as the associated parallel current density. The inter-machine comparison indicates that the intensity of the vorticity associated to the filament exhibits a clear dependence on the local $E \times B$ shearing rate.

In collaboration with NanKai Univ. China, the physics of Trapped Electron Mode (TEM) in RFP plasmas has been studied by solving the gyrokinetic integral eigenmode equation. It has been found that the TEM instability in RFP requires much steeper density gradient than in tokamak, so that TEM turbulence is likely to appear mainly in the edge of RFP plasmas [Liu 2014]. The

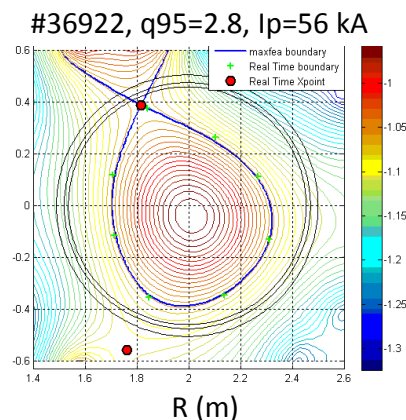


Fig.1.3.5: example of a Single-Null Tokamak equilibrium in RFX-mod

theory is being applied to the realistic RFP experimental data profiles, data analysis is in progress.

1.4.2 Effect of external perturbations on edge properties.

The effect of external magnetic perturbations on the edge properties has been analysed in RFX-mod comparing RFP and Tokamak plasmas. In both configurations and both with resonant and non resonant applied perturbations the parallel current density (see fig. 1.4.1) and the ExB flow have been found to be modulated according to the periodicity of the MP. In addition, MP also modulates the number of blobs and the thermal and particle fluxes, indicating a tight relationship between blobs and transport.

These observations hint at the challenging possibility of active control of filaments and their related transport by modulating the local magnetic topology [Spolaore2014, Vianello2014].

These observations hint at the challenging possibility of active control of filaments and their related transport by modulating the local magnetic topology [Spolaore2014, Vianello2014].

1.5 Plasma-wall interaction studies

Analyses of the graphite tiles and samples deposited with 10-20 μm W (CMSII, Combined Magnetron Sputtering Ion Implantation deposition technique) exposed to RFX-mod plasma discharges in the last campaign of 2013 and extracted

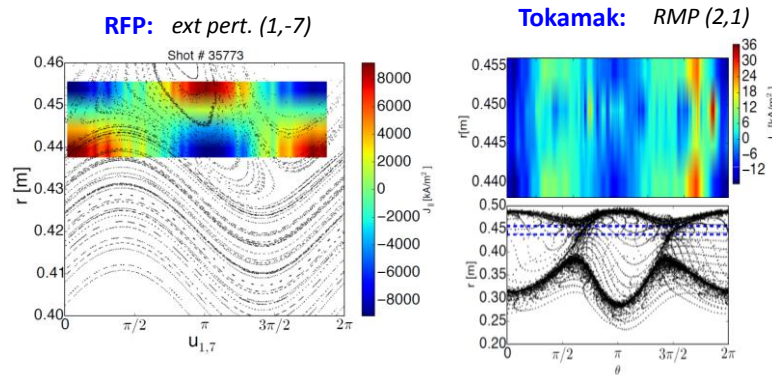


Fig.1.4.1: (left):in RFP, with (1,-7) applied perturbation, magnetic topology and parallel current density vs. the helical angle $u=m\theta-n\phi$; (right) in Tokamak, effect of (2,1) RMP on parallel current density

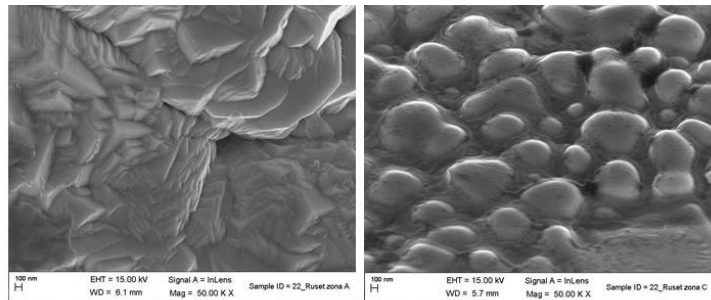


Fig. 1.5.1: SEM images (magnitude X 50K) of a sample with a 15 μm thick W deposition in a not damaged (left) and damaged (right) region after exposure to ≈ 10 RFP discharges

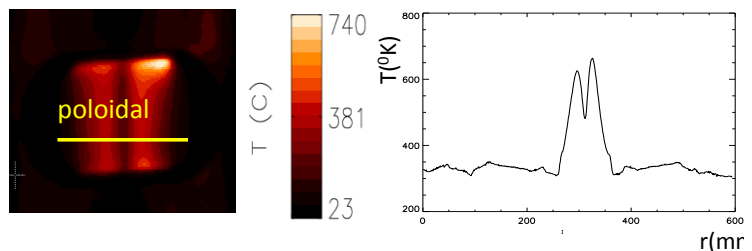


Fig. 1.5.2: example of temperature profile measurements by the IR camera on a sample exposed to a RFP plasma

in early 2014 showed large damaging; an example is shown in fig. 1.5.1, by the comparison of the SEM images obtained from a sample exposed to about 10 RFP discharges and inserted by 2 mm inside the first wall convolution: one of them refer to a not-damaged area, while in the other one blobs indicating material fusion are clearly visible. The idea is that the marked damaging observed on the W deposition is due on the one hand to the not-optimised shaping of the tiles and on the other hand (possibly mainly) to the morphology of the substrate, made by polycrystalline graphite, characterized by very low conductivity. The procurement of samples/tiles with a CFC graphite substrate will allow the confirmation of such hypothesis in 2015 campaign.

First measurements of sample temperature by an infrared camera have been obtained (example in fig. 1.5.2): the aim is to compare such results with the SOLEDGE2D code, developed for the Tokamak and under adaptation to the RFP.

1.6 High density limit

Studies on the RFP high density limit have been started in past year. In 2014, they proceeded with dedicated experiments and in tight comparison with Tokamak and Stellarator, thanks to the WP14-ER-01/ENEA-RFX-01 Eurofusion Enabling Research project.

In RFX-mod Tokamak, it has been found that the maximum achievable central density scales as $B^{1.5}$, similarly to what found in FTU. Instead, at the edge, a Greenwald-like scaling is found in Tokamak operation, $n_{e,edge} \sim 0.35 n_G$, fig.1.6.1. The same scaling holds for the

MHD stability of the edge-resonating $m=0, n=1$ island in the RFP, also corresponding to the maximum value of the density at which helical states develop. In the RFP, the 0/1 island induces a modification in edge transport, with the development of a convective cell, responsible of toroidally localized density accumulation ultimately leading to a MARFE-like radiating structure. During the 4-week dedicated campaign the 0/1 mode dependence on density has been characterized at different current levels (fig. 1.6.2); the active control system is able to control the mode amplitude up to $n/n_G \sim 0.35$. Above such threshold, the mode shows an explosive behavior, above which a MARFE-like structure develops, independently on plasma current level and on the injection of different gases (neon) to produce a symmetric radiative layer [Spizzo 2014].

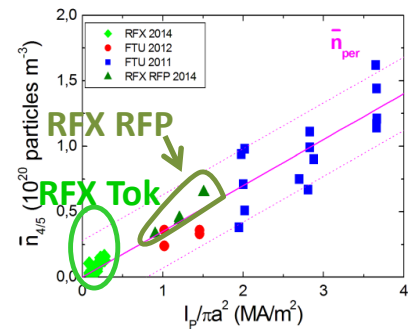


Fig. 1.6.1: Greenwald scaling of the edge density in RFX-mod (RFP and Tokamak), compared with the FTU Tokamak

1.7 Diagnostic developments

Although a remarkable capability in developing innovative diagnostics is present at Consorzio RFX, in the last years this kind of activities particularly suffered from budget limitations. Nevertheless, in 2014, such skills grown at RFX were exploited both in other Eurofusion Work Packages, as discussed in sec.2, and in some improvements of RFX-mod diagnostic systems.

1.7.1 New IR camera.

In 2014 a new IR camera, aiming at temperature measurements of plasma facing components has been installed, as mentioned in sec. 1.5 . The specific interest of such measurements relies in the fact that, thanks to the active control system, power loads as high as several tens of MW/m² can be driven by purpose on pre-determined locations in RFX-mod, where samples can be exposed allowing the observation of material behavior in presence of such high (transient) power loads.

1.7.2 REMIX diagnostic.

In 2014 a diagnostic aiming at a quantitative measurement of particle influx/outflux balance has been installed and tested. It includes two sets of Langmuir probes (one configured as a triple probe, to provide n_e , T_e and the other to measure the radial velocity), spectroscopic H α (or D α) measurements and a fast near infrared sensor to measure the surface temperature. However, during the test phase a series of issues emerged, which will be solved for next 2015 campaigns: first, the signal from the IR thermal sensor was polluted with hydrogen molecular emission (measurements on a different spectral band will be provided); second, unexpected electrical noise

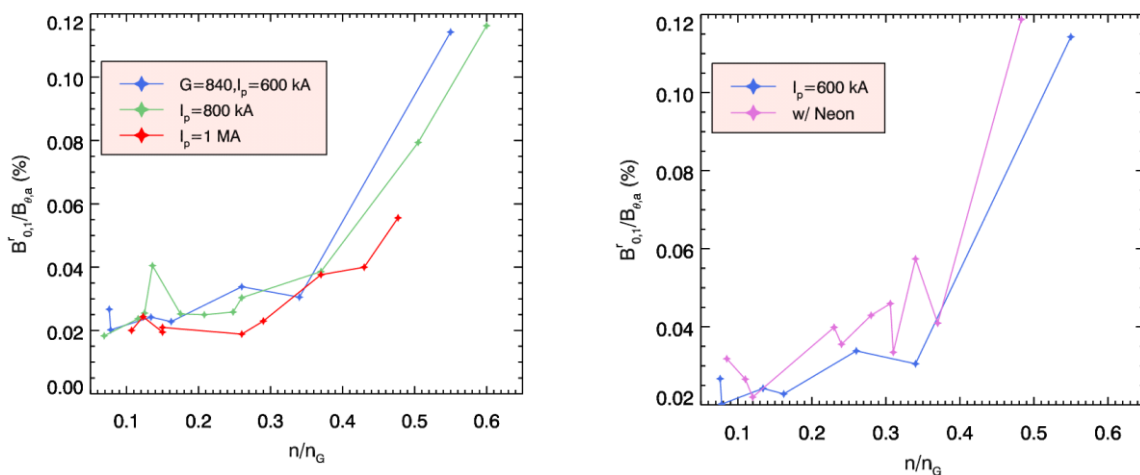


Fig. 1.6.2: amplitude of $m=0$ mode at different currents (left) and with and without Neon radiative layer (right)

problems, possibly dependent on the choice of extending the frequency band of the electrostatic probe up to 1 MHz.

1.7.3 Neutron detectors.

Following the possibility of deuterium operation, a neutron/ γ -rays spectrometer has been installed in collaboration with Padova University, Physics Department. The system is based on a liquid scintillator, a flat panel photomultiplier and an ad-hoc electronics discriminating neutrons and γ -rays. An example of neutron measurement is given in fig. 1.7.1. In addition, fast particles are measured by a NaI scintillator.

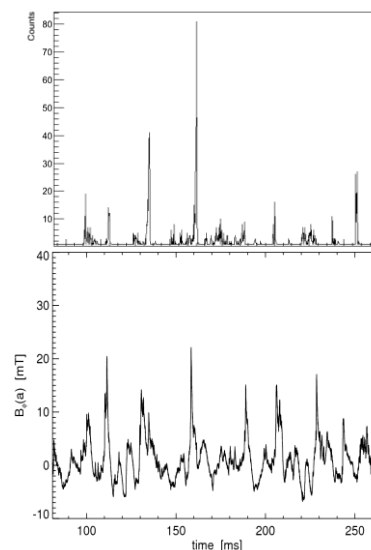


Fig. 1.7.1: (top) example of neutron emission in a deuterium discharge, compared with the magnetic reconnection events (bottom)

1.7.4 Additional Thermal Helium Beam systems.

Local edge temperature and density are provided in RFX by means of a Thermal Helium Beam (THB) diagnostic, based on the density and temperature dependence of He spectral line ratios. In order to relate the local T_e , n_e measurements to the edge magnetic topology, a second THB was installed in 2013 at a different toroidal angle. In 2014, a third system (copy of the other ones) has been added, at a different poloidal location, allowing the characterisation of 3D effects in edge T_e, n_e .

1.7.5 Modification of Li multipellet injector.

In 2014, the Li multipellet injector, developed in collaboration with PPPL already tested on RFX-mod in 2013, has been modified in order to inject faster and larger pellets, to improve the penetration (therefore the uniformity of deposition) and the amount of deposited Lithium. The technique to produce Li pellet with a diameter of 1mm has been debugged. The limited experimental time did not allow to test the new injector on high current plasmas in 2014, the system is ready to be applied in 2015.

1.8 Conceptual design of machine improvements

The proposal of machine improvements to increase the RFX-mod effectiveness in addressing key issues for fusion science, in particular related to MHD control system capabilities and potentialities, started in 2013, has progressed in 2014. A specific document, motivating in detail the proposed

upgrades, is being prepared and will be available in early 2015. Here only a short summary of the main considerations at the basis of the proposed modifications is given.

RFX-mod achieved its mission of operating at plasma current level as high as 2MA, thanks to an efficient tailoring of the magnetic boundary through its powerful active control system. The limits of the present system have now been explored, but a further improvement of the magnetic boundary control would allow the advancement of the RFP performance and the increase of the relevance of the experiments in Tokamak configuration. Some upgrade of the device, of relatively low impact, are necessary to extend the capability of exploring the potentiality of the RFP configuration while increasing the effectiveness of the contribution to cross-configuration critical issues for fusion science, including three-dimensional physics, MHD stability control, high density limit and turbulence physics, impurity behavior, plasma-wall interaction in presence of transient high power loads, 3D non-linear MHD modeling, disruption mitigation studies.

The proposed improvements are thought in order to achieve the following main deliverables:

- RFP – Achieve stationary SHAx helical states, thus allowing not only improved RFP performance, but also synergic studies with the Tokamak and Stellarator (3D magnetic equilibria, transport barriers, impurity transport, effect of 3D boundary, microturbulence and zonal flows studies). Explore RFP performance in QSH mode at High Current *and* high density (the Greenwald limit is $2 \cdot 10^{20} \text{ m}^{-3}$ in RFX-mod at 2MA). Increase the mobility of the modes and the current threshold for spontaneous mode rotation (presently observed only at low plasma current $\leq 100 \text{ kA}$).
- TOKAMAK – Improve the control of shaped equilibria. Achieve the L-H transition. In H-mode, error field assessment and control, tearing mode mitigation techniques, edge turbulence characterization, runaway electron decorrelation and ELM suppression/mitigation using *advanced active MHD control* in operating conditions relevant for the Fusion Roadmap.

The achievement of such objectives will be reached through the following modifications.

1.8.1 Improvement of the magnetic front-end

Although the sophisticated active control system of MHD instabilities, upgraded in 2013 with a new architecture based on a Linux multi-core server and supervised by MARTe [Neto 2010], has allowed a progressive reduction of the field error and a milder plasma-wall interaction, the achievement of an even smoother magnetic boundary remains a crucial issue for the RFP performance. With this aim, an improvement in the mitigation of tearing modes can be obtained by

changing the distance of the stabilizing shell. This has been predicted by performing simulations with the RFXLOCKING code which has been benchmarked against experimental data. It has been conservatively assumed that the nonlinear saturation amplitude of Tearing Modes will be the same as the present RFX-mod, even if it is expected that the reduction of the shell-plasma distance will reduce such value. A significant reduction of the edge radial field magnetic due to resonating tearing modes is expected by removing the present vacuum vessel and applying the graphite tiles (or, eventually, graphite tiles covered by a metal layer) directly on the stabilizing copper shell (fig. 1.8.1). The details of the calculations are reported in the internal notes [Zanca 2013]. This upgrade implies a modification of the present support structure, which must become vacuum tight, while maintaining one toroidal and one poloidal gap. In addition, an active correction of the

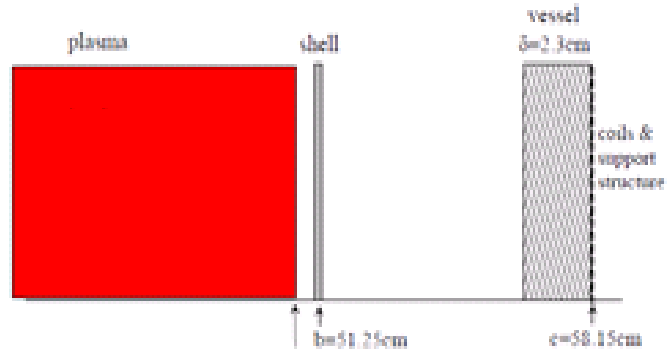


Fig. 1.8.1: proposed new magnetic boundary for RFX-mod, with the vacuum vessel removed

error field at the insulated gaps becomes necessary. Two new gap configurations (Butt-Joint Gap, Small Overlap Gap) have been compared to present RFX-mod solution (Overlap Gap): while the present design of the gap minimizes error fields without correction measures, active correction allows reaching similar results with a simpler gap geometry, should either constructive or assembly reason require it [Marchiori 2014]. Further improvement could come from studies to reduce the latency of the present power supply system for the MHD control, reported at the last SOFT conference [Recchia 2014].

1.8.2 Control of $m=0$ modes

RFXLOCKING simulations also revealed that improving the control of $m=0$, low n modes leads to faster slinky mode rotation [Zanca 2014]. Three possible actuators have been considered: upgrade of the present power supply of the Toroidal Field coils, the present saddle coils for $m=0$ modes generation and the introduction of new dedicated coils; but only the last solution produces significantly different behaviour of the slinky mode from the present experimental condition. RFXLOCKING predictions of $m=0$ control coils through the present saddle coils has been experimentally verified. Based on these results, the implementation of a scaled test experiment in EXTRAP-T2R is proposed.

1.8.3 Increase of the number of poloidal sensors and local field coils

In Tokamak configuration, first preliminary shaped plasmas experiments highlighted the need to increase both the diagnostic coverage and the actuator coils. Such improvements should include an increase of the number of poloidal sensors in the poloidal direction (the 192 coils are presently distributed in 48(toroidal) x 4 (poloidal) arrays with 48 x 4 sensors (radial, toroidal, poloidal) and the addition of a new reduced set of control coils with a geometry similar to DIII-D I-coils or ASDEX B-coils, in order to produce magnetic spectra more relevant for shaped tokamaks. In 2014 the analysis of the behavior of the actual magnetic sensors (located in air) to assess the compatibility with the vacuum environment has been performed. The assessment will be completed in the first part of the year to allow the finalization of the design of the sensors.

1.8.4 Improvement of density control

As an additional upgrade for RFX-mod, the possibility of improving density control through a reduction of wall gas retention is under consideration. As mentioned in sec.1.5, dedicated studies and experiments with different plasma-facing components have been done in 2014 and will be continued in 2015 campaigns. At the same time designing improvements for the wall conditioning techniques have been proposed and analyzed in 2014:

- increase of the Glow Discharge Cleaning (GDC) plant efficiency by adopting a higher number of toroidally equispaced electrodes (six or twelve instead of the present two) placed at the first wall radius, thus producing a more uniform plasma during GDCs
- Revamp the Pulse Discharge Cleaning system originally foreseen for RFX, which will be used not only for conditioning purposes but also for the baking of the first wall, given that the mean power released by the plasma to the wall is of the same order of the power required for baking up to 200 °C..
- optimization of a lithisation procedure suitable for RFX, in terms of uniformity of deposition and avoidance of lithium carbide Li_2CO_3 formation during the maintenance openings of the machine.

1.8.5 Additional heating for Tokamak configuration

Specific to Tokamak experiments, the possibility of applying an additional heating system (~100 kW, given the predicted power necessary to get L-H transition in RFX-mod according to multi-machine scaling) is being considered, either by applying a NBI already available at RFX (25 keV,

50 A), which, due to layout reasons, can be applied only radially and whose duration is limited to 30ms, or (preferred solution) by an ECRH system (28 GHz).

1.8.6 Technical solutions for the modification of the torus assembly

The most relevant modification of the torus assembly is the removal of the metallic vessel. The main consequences of this choice are:

1. The braking torque to the MHD mode plasma rotation produced by the vessel is eliminated
2. The toroidal support structure becomes the new vacuum boundary.
3. The toroidal copper shell 3 mm thick becomes the new support for the 2016 first wall tiles, with a small increase of the plasma minor radius but a significant decrease of the distance of the plasma last closed flux surface to the stabilizing shell (from $b/a \sim 1.11$ to ~ 1.05)
4. The copper shell requires a new system of stiffening rings based on insulated material compatible with the vacuum environment and with the expected temperature (200°C maximum baking temperature). The material presently under consideration is the TORLON 5030[®] because it has a temperature expansion coefficient very close to the copper of the shell.

The new vacuum boundary placed at the toroidal support structure requires a gap geometry different from the present one. The identified technical solution foresees completely welded toroidal and poloidal gaps.

In fig.1.8.2 the conceptual design of the gaps is shown.

The adopted joint solutions require a completely different assembly procedure for the torus that is now pre-assembled in two 180° toroidal half and then welded together at the last poloidal lips on two sections. The new solution has required, as above mentioned, to

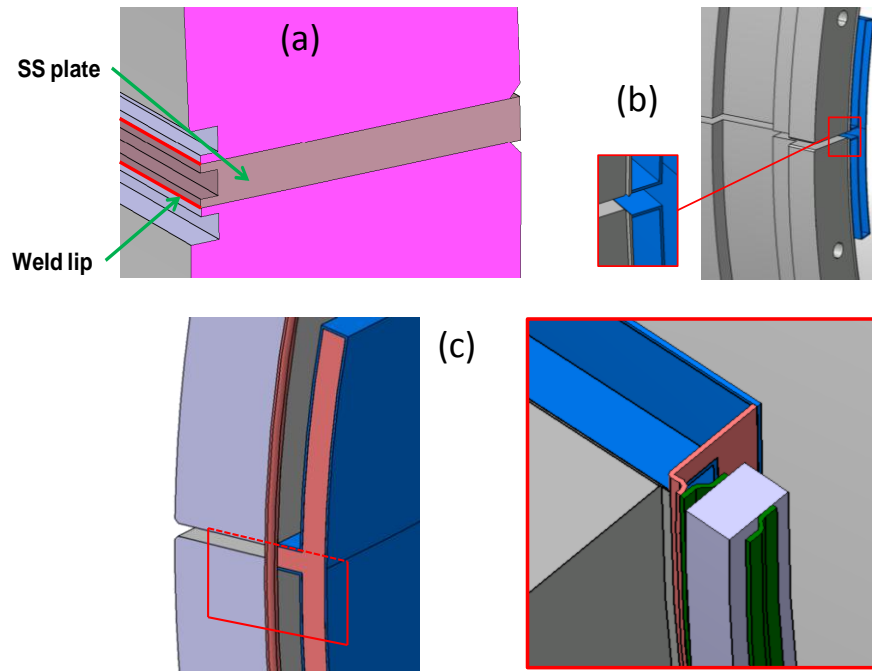


Fig. 1.8.2 (a) external toroidal gap; (b) internal high resistance toroidal joint; (c) Poloidal joint detail at the equatorial gap (the blue plate is in Inconel 625[®] 1 mm thick and the grey material is Alumina)

reassess the field errors at the gaps (see sec. 1.8.1) and, in order to reduce their value, introduce a new saddle coil system at the two poloidal gaps as shown in fig. 1.8.3.

Different solutions for the poloidal gap of the copper shell, not visible in the figure, has been proposed in and the results have been compared to identify the best one taking into account the active control performed by the local gap coils and in the uniformly distributed saddle coils.

REFERENCES

[Albanese 2008] R. ALBANESE et al. 2008, IEEE Trans. Magn. 44, 1654

[Auriemma 2014] F. AURIEMMA et al. 2014, 41st EPS Conference on Plasma Physics, Berlin, P5.079

[Bolzonella 2014] T. BOLZONELLA et al. 2014, Plasma and Fusion Res. 9, 3402081

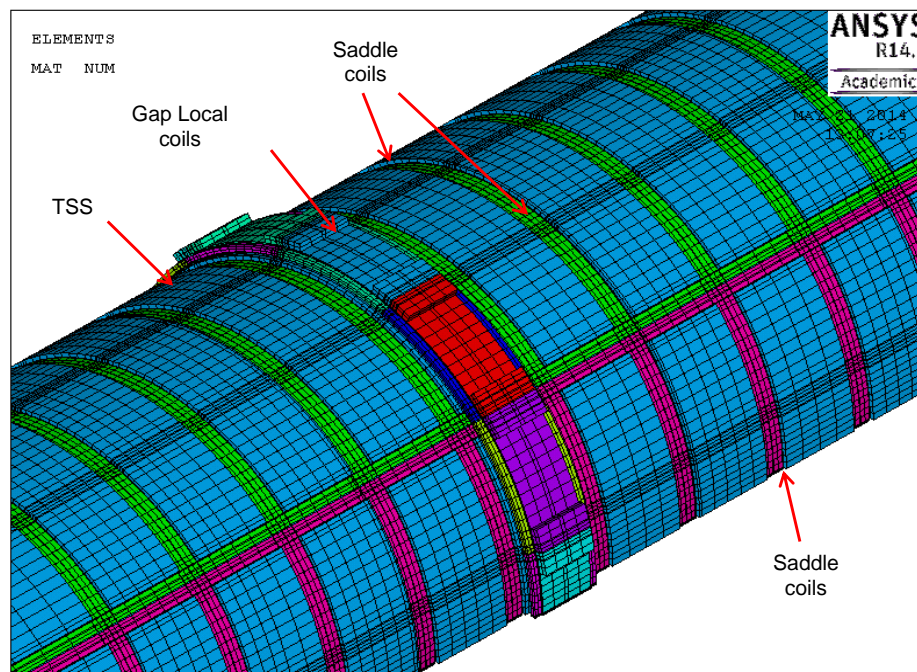


Fig. 1.8.3: layout of saddle coils at the poloidal gap

[Bonfiglio 2013] D. BONFIGLIO et al. 2013, Phys. Rev. Lett. 111 085002 DOI: 10.1103/PhysRevLett.111.085002

[Carraro 2013] L. CARRARO et al. 2013 Nucl. Fusion 53 073048 doi:10.1088/0029-5515/53/7/073048

[Escande 2000] D. ESCANDE et al. 2000 Phys. Rev. Lett. 85 3169, doi: 10.1103/PhysRevLett.85.3169

[Gobbin 2013] M. GOBBIN et al. 2013 Plasma Phys. Control. Fusion 55 105010 doi:10.1088/0741-3335/55/10/105010

[Guo 2014] S.C. GUO et al. 2014 “Progress in theoretical study of Resistive Wall Mode for RFP plasmas and comparison with Tokamaks” , 25th IAEA Fusion Energy Conference , St Petersburg 13-18 October 2014, paper TH/P5-10

[Hanson 2009] J.D. HANSON et al. 2009 Nucl. Fusion 49 075031 doi:10.1088/0029-5515/49/7/075031

[Hirshman 1983] S.P. HIRSHMAN and J.C. WHITSON J.C. 1983 Phys. Fluids 26 3554 <http://dx.doi.org/10.1063/1.864116>

[Horton 1996] W. HORTON and Y.-H. ICHIKAWA 1996, “Chaos and Structures in Nonlinear Plasmas” (World Scientific, Singapore, 1996)

[Howell 2007] D.F. HOWELL et al. 2007 Nucl. Fusion 47 133

[Liu 2014] S.F. LIU, S.C. GUO, et al. 2014, Nucl. Fusion 54 (2014) 043006

[Lorenzini 2009] R. LORENZINI et al 2009 Nature Phys. 5 570–4

[Lorenzini 2014] R. LORENZINI et al. 2014 “The isotope effect in the RFX-mod experiment”, 25th IAEA Fusion Energy Conference , St Petersburg 13-18 October 2014, paper EX/P1-41, submitted to Nucl. Fus.

[Marchiori 2014] G. MARCHIORI et al. 2014, “Feasibility study of a local active correction system of magnetic field errors in RFX-mod”, G. Marchiori, et al., 28th Symposium on Fusion Technology (SOFT), 29/9 - 3/10 2014, San Sebastián, Spain

[Martin 2014] P. MARTIN et al. 2014 “Extreme low-safety factor tokamak scenarios via active control of three-dimensional magnetic field”, 25th IAEA Fusion Energy Conference , St Petersburg 13-18 October 2014, paper EX/P2-41

[Neto 2010] A. Neto et al. 2010, IEEE Trans. Nucl. Sci. 57

[Pigatto2014a] L. PIGATTO et al 2014, “MHD control system optimization to RFX-mod real passive boundary”, L. Pigatto, et al., 41st EPS Conference on Plasma Physics, Berlin, 23-27/6/2014

[Pigatto 2014 b] L. PIGATTO et al 2014, “Strategies for real-time actuator decoupling in closed-loop MHD control operations”, L. Pigatto, et al., 28th Symposium on Fusion Technology (SOFT), 29/9 - 3/10 2014, San Sebastián, Spain

[Piovesan 2009] P. PIOVESAN et al. 2009 Nucl. Fusion 49 085036 doi:10.1088/0029-5515/49/8/085036

[Piovesan 2014] P. PIOVESAN et al. 2014 Phys. Rev. Lett. 113, 045003 DOI: 10.1103/PhysRevLett.113.045003

[Piron 2013] L. PIRON et al. 2013 Nucl. Fusion 53 113022 doi:10.1088/0029-5515/53/11/113022

[Puiatti 2014] M.E. PUIATTI et al. 2014 “Overview of the RFX-mod contribution to the international Fusion Science Program”, 25th IAEA Fusion Energy Conference , St Petersburg 13-18 October 2014, paper OV/5-2, submitted to Nucl. Fus.

[Recchia 2014] M. RECCHIA et al. 2014 “Improvement of the RFX-mod power supply system for MHD control”, 28th Symposium on Fusion Technology (SOFT), 29/9 - 3/10 2014, San Sebastián, Spain

[Sattin 2012] SATTIN F et al 2012, Plasma Phys. Control. Fusion 54 (2012) 124025, doi:10.1088/0741-3335/54/12/124025

[Spizzo 2014] G. SPIZZO et al. 2014, " Density Limit Studies in the Tokamak and the Reversed-Field Pinch", 25th IAEA Fusion Energy Conference , St Petersburg 13-18 October 2014, paper EXD/P1-42, submitted to Nucl. Fus.

[Spolaore 2014] M. SPOLAORE and al. 2014 "Turbulent electromagnetic filaments in toroidal plasma edge", 25th IAEA Fusion Energy Conference , St Petersburg 13-18 October 2014, paper EX/P1-40

[Terranova 2013] D. TERRANOVA et al. 2013 Nucl. Fusion 53 113014 doi:10.1088/0029-5515/53/11/113014

[Vianello 2014] N. VIANELLO et al. 2014, " Magnetic perturbations as a viable tool for edge turbulence modification », invited talk at 41st EPS Conference on Plasma Physics, Berlin, submitted to Plasma Phys. Control. Fusion

[Zanca 2012] P. ZANCA et al. 2012 Plasma Phys. Control. Fusion 54 094004 doi:10.1088/0741-3335/54/9/094004

[Zanca 2013] P. ZANCA. 2013 internal note FC/85

[Zanca 2014] P. ZANCA. 2014 internal note FC/88

2. EUROFUSION TOKAMAK AND STELLARATOR WORKPROGRAMMES

Following the new Eurofusion organization of research, in 2014 Consorzio RFX has shifted a substantial portion of its resources in order to significantly contribute to the European workprograms JET1, MST1, WPSA and WPS1. Besides the MST1 leadership (P. Martin) and JET1 organisation responsibilities (A. Murari), RFX has contributed to the experimental activity of JET1 and MST1 with Scientific Coordination of several experiments and tasks (M Valisa JET1 and MST1, Piovesan MST1, N Vianello Jet1 and MST1, T Bolzonella MST1 MHD modelling); care was paid to group the resources grouped in the attempt of approximating as much as possible critical masses and avoiding excessive dispersion throughout small activities. Additionally, in this chapter are summarize also the activities carried out on other Tokamak laboratories with funds assigned to the Enabling Research.

2.1 MST1

2.1.1 MHD AUG14-1.4-5: Beta-limit with conducting structures

This MST1 experiment was coordinated by a scientist from Consorzio RFX. The no-wall beta limit was probed in NBI heated hybrid discharges measuring the plasma response to rotating $n=1$ external fields, taking advantage of the availability since 2014 of new AC power supplies for the non-axisymmetric coils. The $n=1$ helical distortion increases with beta, as expected when the no-wall beta limit is approached, and was measured with a suite of high-resolution diagnostics, from magnetics to soft x-ray, ECE-Imaging, Lithium beam and others. In particular, analysis of multi-chord soft x-ray data allowed to measure the entire $n=1$ response profile from HFS to LFS, revealing a significant $m=1/n=1$ distortion of the core (see Fig. 2.1.1.1).

This is likely due to the flat q -profile just above 1, typical of these hybrid plasmas and it is associated to significant braking of core rotation. Both the spatial structure of the 3D response and the effects on rotation have being modelled with various codes, such as the linear MHD code MARS-K, which can include the effects of rotation, resistivity, and drift-kinetic. Preliminary results have been presented at the ITPA-MHD Meeting in Padova , the APS meeting 2014 and the MHD Workshop 2014.

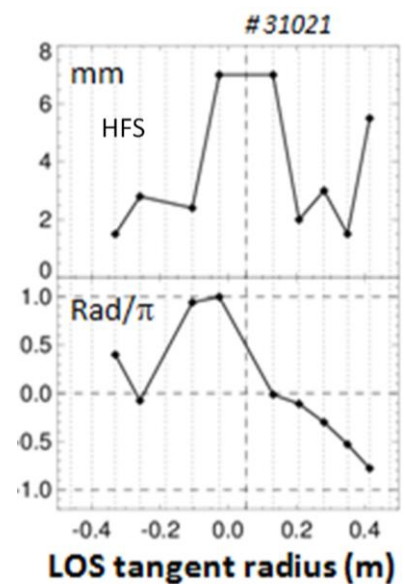


Fig.2.1.1.1: Line averaged plasma (1,1) displacement (top) and phase (bottom) from the vertical SXR camera.

Implementation and validation of 3D modeling tools for MHD active stability studies

In the framework of MST1 experiments aiming at studying the AUG plasma behavior at high β_N values, Consorzio RFX participated also in a related collaborative modeling effort. Main subject of this multi-annual activity is the implementation of AUG description in numerical tools for a dynamical fully 3D reconstruction of magnetic fields generated by external coils under realistic geometries of walls and

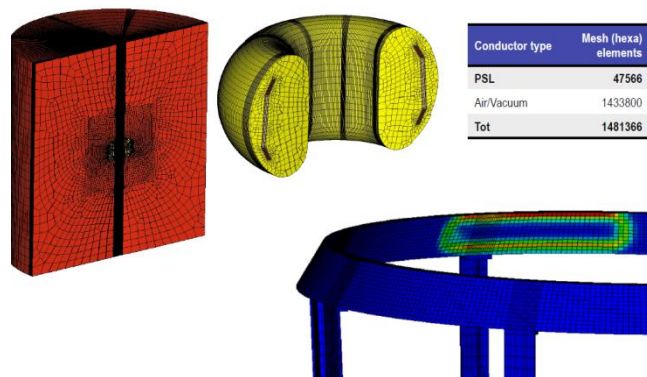


Fig.2.1.1.2: 3D AUG model as used in CAFE code. Note the high number of elements that can be handled by this codes and the fact that, being based on a discrete geometric formulation, needs the additional effort of producing the mesh also of air/vacuum (plasma included) regions.

actuators; codes of interest are CARIDDI, CAFE, CarMa. This kind of modeling is of paramount importance for a correct and quantitative interpretation of any experiment making use of external active coils (named B-coils in AUG). Consorzio RFX researchers gave an essential contribution to this collaboration that involves also colleagues from Consorzio CREATE, IPP-Garching and CCFE. In 2014 the numerical 3D model of the device has been ported to CARIDDI and CAFE starting from CAD data obtained by IPP. In Fig. 2.1.1.2 some details of the CAFE model are shown together with the number of elements used to solve the e.m. problem. This allowed a first benchmark between the two codes for some vacuum test cases. The relevant information that can already be extracted from this preparatory work is that AC fields produced by the B-coils (e.g. during rotating perturbation experiments) are strongly influenced by the presence of passive structures in terms of both amplitude and phase and that any plasma response estimate should take these affects into account.

2.1.2 MHD AUG14-2.2-3 Filamentary transport in high density regimes L-Mode studies

A great effort has been devoted in the framework of the MST1-ASDEX-Upgrade campaign to evaluate the modification of SOL and far SOL transport at different density regimes. The interest in the argument is driven by the observation that, with the increasing of the Greenwald density fraction, a shoulder in the SOL density profile builds up: these observations are relatively old [LaBombar01, Rudakov05] and this was ascribed to a different ratio between parallel and perpendicular transport or, equivalently, to an enhancement of filamentary induced perpendicular

transport: the transition is governed by a normalized parameter, named effective collisionality $\Lambda = L_c v_{ei} \Omega_i / c_s \Omega_e$, and it is associated to a flattening of the density profile at the midplane, establishment of detachment at the LFS divertor plane (Degree of Detachment DoD >1) and to an increase of the filaments size [Carralero14].

The experiment has been conceived to discriminate which, between midplane and divertor effective collisionality, plays the major role and to establish a possible heating power dependence. The result of this L-Mode investigation is summarized in Figure 2.1.2.1 where the parameter Λ computed at the midplane and at the divertor plate and the DoD are shown as a function of edge density during density scan experiments performed at different heating power. Transitions, observed for DoD >1, are clearly governed by divertor parameter whereas midplane effective collisionality remains substantially unaffected. Computing the increasing of λ_n as a function of Λ_{div} as shown in Fig 2.1.2.2 reveals that threshold actually occurs for DoD greater than 1.

H-Mode studies

Based on the experience collected in L-mode studies, the mechanism of SOL saturation at high density has also been investigated in high density, ITER relevant scenario. In particular discharges with $P_{sep}/R = 7.3$ MW/m and Greenwald fraction $f_g=0.8$ have been obtained, investigating SOL and far SOL transport properties. As shown in Fig 2.1.2.3 also in these extreme plasma condition SOL density shoulder appears at higher values of Greenwald fraction. It has been shown [Müller14] that the increase of density is actually associated to an increase of the filamentary cross -field transport

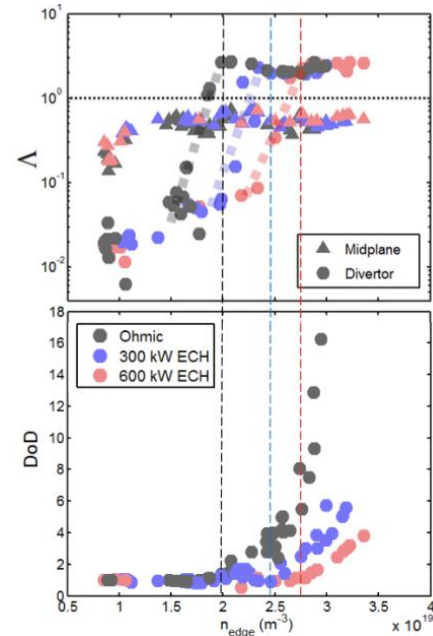


Fig.2.1.2.1: Top: Effective collisionality determined at the midplane and at the target as a function of edge density. Bottom: Degree of Detachment as a function of edge density. Both the panels show results obtained at different heating power

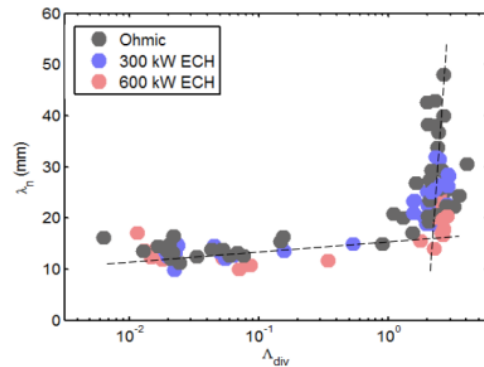


Fig.2.1.2.2: Density scale length as a function of divertor effective collisionality

obtained beyond the value $\Lambda_{\delta_{i\omega}} > 1$, but

differently from the L-mode case the divertor is still attached in these condition (highly recycling regime). Additional ingredient seems to play a role in these regime, namely the neutral pressure at the divertor and the Power at the separatrix. These studies actually deserve further experimental investigations which have been proposed for the forthcoming MST1 campaign.

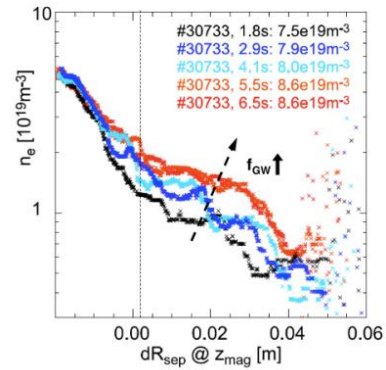


Fig.2.1.2.3: Edge density as a function of minor radius in ITER relevant condition at different values of on-axis density

2.1.3 AUG14-2.2-4 “Ion Cyclotron Wall Conditioning”

RFX participated to the study of N2 removal from the Asdex first wall by He cold plasmas sustained by Ion Cyclotron antennas only. In that experiment, the RFX team concentrated in the characterization of the edge cold plasma by means of the available electrostatic probes. They also contributed to the determination of ion density profiles. The analysis of the collected data is now under way.

2.1.4 AUG14-1.5-3 W transport and accumulation in presence of MHD instabilities in H-mode plasmas

This experiment aimed in particular at the determination of the impact of the $m=1, n=1$ mode that often develops when ECRH heating is applied to the AUG H mode plasmas. More specifically, the intent was to investigate the possibility that it is just the MHD mode that produces the well known impurity pump out in presence of extra central electron heating. RFX participated to the scientific coordination of the wide experimental team, contributing with its long lasting experience on impurity transport studies on RFX, AUG, FTU, and JET. In the allocated discharges, the impact of ECRH power deposited inside and outside the $m=1$ surface has been compared with NBI only and ICRH heating cases. The analysis of the data is now ongoing.

2.2 JET1

2.2.1 Investigation on the M-Mode

During 2014 the investigation of the M-Mode has continued. The M-Mode is a medium confinement regime observed in JET tokamak at power levels close to the L-H power threshold

and is accompanied by a medium increase of the performance with a pedestal in density but not in temperature. It is typically associated to a low-frequency mode, detected both in pedestal and in SOL signals [Solano13]. As to the nature of the observed oscillations, there have been already speculations that their frequency could scale with the poloidal Alfvén velocity. In such a

case, an isotope effect should appear in the mode frequency. Fig. 2.2.1 is an example of the frequency scaling of the mode, as a function of poloidal Alfvén velocity [Delabie14], for a series of shots in H and D. The frequency of the mode does increase by decreasing the mass but the scaling is not linear. Now, the fluctuations in magnetic field associated to the M-Mode revealed a more complicated pattern. In figure 1.1.2 the low frequency oscillations seem to have a high frequency counterpart as a broad band oscillations around 70 kHz. A mode analysis confirms that both the high frequency broad band and the low frequency mode have the same toroidal mode spectrum $n=0$. It has been observed that, the power spectrum integrated over the broad-band region exhibits pulsation at the frequency corresponding to the low frequency band. Further analysis is now in progress to relate the described phenomena to other plasma parameters.

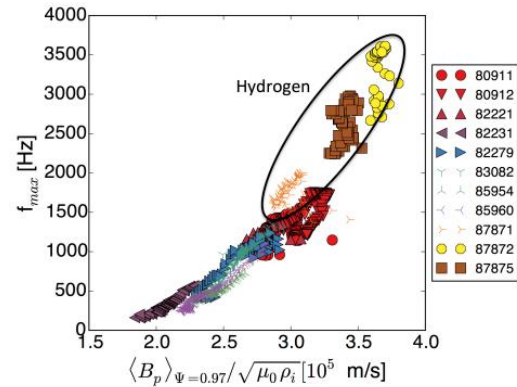


Fig.2.2.1: Scaling of the mode frequency associated to the M-Mode as a function of the poloidal Alfvén velocity, where the magnetic field is computed at $\rho=0.97$

2.2.2 Experimental evaluation of the q minimum evolution by Alfvén Cascades analysis

Alfvén Cascades (AC) were observed to arise in reversed magnetic shear plasmas, during "advanced regimes" in JET experiment [Sharapov, 2002]. As well known, these instabilities can be used to gain information about the minimum of the safety factor radial profile, since they appear when q crosses resonant values. While the toroidal mode number n associated to the AC is measured by magnetic sensors located at different toroidal positions, their poloidal mode number m is not experimentally available. Thus, the resonances cannot be univocally defined.

With the aim to trace the time evolution of the q minimum, we can overcome the problem recognizing the resonance where $q=1$, by the sawtooth appearance in the ECE signal.

Nevertheless, in discharges where q does not reach this value, we can try to evaluate the m number associated to the modes, by the analysis of the AC linear phases, where the evolution is not affected by the coupling with other Alfvén components. The slope of the linear phase is indeed directly proportional to m . A semi-automatic program provides this estimation and thus the evolution of the $q(t)$ in discharges where magnetic or interferometric spectrograms are rich of modes. A paper on this topic is under development.

2.2.3 Quasi-coherent fluctuations

While progressing in the understanding the role of the edge turbulence in the LH transition physics (M13-23 experimental campaign), the analysis effort focused on the characterization of special edge fluctuations (see also 2013 activity report) detected through the correlation reflectometer KG8c operating on the JET experiment. These fluctuations are characterized by a frequency range of about [40-100] kHz and are well localized on the pedestal top. They are found to be linked with the pedestal dynamics and their amplitude linked with the inter-ELM phase. Analysis is still ongoing to understand the global parameters (density, temperature, collisionality, etc.) enabling the destabilization of those fluctuations and a closer correlation with the pedestal pressure gradient (to be evaluated with sufficient time resolution through different diagnostic systems). In order to gain a better insight on their intimate nature, a collaboration with PPPL (Diallo) and CEA (Arnichand) laboratories started in 2014. With the same goal a specific experimental proposal has been submitted for the 2015 JET experimental campaign.

2.2.4 Support in Preparation of H14-03 experiment "Pedestal and confinement in H vs D plasmas" in C34 JET campaign

The activity has been carried out within the preparation of the H14-03 experiment "Pedestal and confinement in H vs D plasmas" (Scientific Coordinator: Costanza Maggi) of C34 hydrogen JET campaign. The aim has been to support the preparation of the experiments with core modeling, providing detailed analyses of NBI-plasma interaction for D and H plasmas in order to estimate the possible differences.

In particular interpretative analyses have been performed to investigate the different neutral beam absorption and fast ion behavior in D and H plasmas. NBI has been simulated with ASCOT Monte Carlo code [Hirvijoki14] in JINTRAC transport suite of codes [Romanelli14]. As first approximation, the comparison for D and H cases has been done fixing the plasma scenario and changing the NBI from H case (90keV, H injection in H plasma) to D case (100 keV, D injection in D plasma).

Due to the expected decreased confinement properties in H plasma [Cordey00] [Urano08] [Urano12], a lower stored fast ion energy has been found in H case as depicted in figure 2.2.4.1(b). H case showed also enhanced shine through losses, as found also in [Urano12] for JT-60U. This is shown in figure 2.2.4.2. A comparison between ASCOT code and PENCIL code [Challis89] has been also provided, showing some differences due to the different physics model approach, which can be useful in understanding the simulation outputs. The work has unfortunately terminated due to the JET water leak that cancelled the scheduled H14-03 experiment.

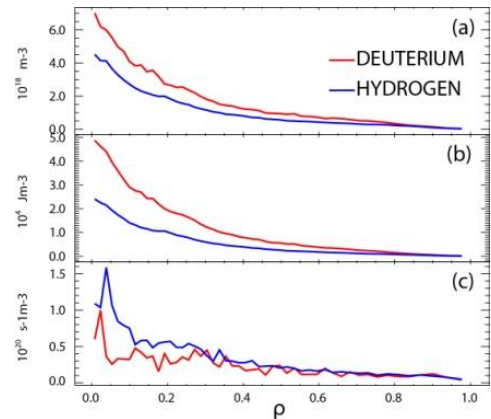


Fig.2.2.4.1(a): Comparison of fast ion density profiles between D-red- and H-blue- cases.(b):Fast ion energy density profiles for D and H. (c):Fast ion birth profiles for and H.

2.2.5 Exp M13-25 .Investigation of impurity transport via Laser Blow Off technique

Evidence of heavy impurity flow reversal from inward to outward due to the application of central Ion Cyclotron Resonance Heating (ICRH) in JET standard H-mode discharges has been found by injecting Mo and analyzing the transient behavior of the impurity. The use of recently developed theory-based models of heavy impurities transport [Angioni14, Casson15, Valisa14, Mantica14] has led to the comprehension of the complex mechanism behind the ICRH effect. A key aspect of the model, based on neoclassical and linear gyro-kinetic calculations of impurity transport and the comparison with experimental data and interpretive simulations, is that it incorporates the two dimensional nature of the problem. The extreme sensitivity to neoclassical transport, appears in fact to be strongly enhanced by any types of poloidal asymmetries in the electrostatic field, and makes large mass and charge elements, such as W and Mo, prone to core accumulation in presence of peaked density profiles. ICRH on minority species (H) counteracts tungsten and Mo accumulation in the core first of all by flattening the density profile. The minority species temperature gradient introduces an additional screening mechanism, which has been shown to strongly depend on the centrality of the deposition layer of the RF power. The anisotropy of the radiofrequency heating ($T_{\text{perp}} \gg T_{\text{par}}$) also affects impurity

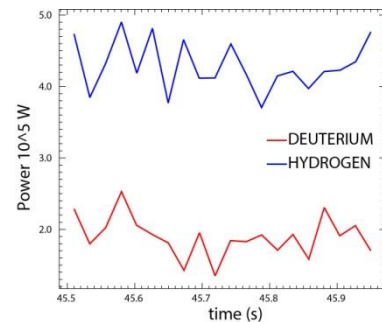


Fig.2.2.4.2: Shine through losses in D-red- and H-blue- cases.

transport. The extreme sensitivity to neoclassical transport, appears in fact to be strongly enhanced by any types of poloidal asymmetries in the electrostatic field, and makes large mass and charge elements, such as W and Mo, prone to core accumulation in presence of peaked density profiles. ICRH on minority species (H) counteracts tungsten and Mo accumulation in the core first of all by flattening the density profile. The minority species temperature gradient introduces an additional screening mechanism, which has been shown to strongly depend on the centrality of the deposition layer of the RF power. The anisotropy of the radiofrequency heating ($T_{\text{perp}} \gg T_{\text{par}}$) also affects impurity

transport. Analysis of impurity transport has been extended to the hybrid scenarios where, in particular, the effect of the position of the radiofrequency resonance layer in the plasma has been investigated. In the still ongoing analysis, the role of the NBI contribution to central fuelling and thus to the main plasma density peaking, which appears to be the main cause of the central impurity accumulation driven by neoclassical transport, has been highlighted.

2.3 WPS1 and WPS2

2.3.1 Assessment of the impact of the finite transverse size of the viewing pyramids on the brightness simulations of localized islands chains

This project is a collaboration between RFX-Mod and W7-X on XMCTS diagnostic based on the common interest of studying soft x-ray (SXR) features in flux coordinates. The aim of the project is the investigation of the impact of the finite transverse size of the viewing pyramids on brightness simulations. The SXR brightnesses of the W7-X tomography have been calculated over synthetic x-ray emissivities of various type (unperturbed, with localized islands chains and others). Two different methods have been described and used: the line and the area-integral approximation. In the first one variations of SXR emissivity inside the cones of sight (the volume defined by the detector and pinhole) are neglected and the brightness is simply the line integral along each chord. In the second case the finite size of the detectors and pinholes are considered and each chord becomes the area delimited by the lines at the edges of the photodiode and pinhole. Dividing the detector and pinhole in smaller parts a set of lines are identified; for a sufficient number of lines of sight, the integral of the emissivity in the area can be calculated as the sum of the integrals along the new lines. This area integral will be the simulation of the brightness for that chord. The difference between the two approaches becomes relevant for consistent variations inside the area of sight, i.e. in the presence of marked gradients. If the size of a hotter structure in the emissivity is smaller than the width of the area of sight, the line and area integrals can be different. In any case, the study has showed that the amplitude of the localized structure must be very large to have an effect on the brightness profiles. This can be summarized defining the limit of the line-integral approximation as the width of the area of sight associated to the detector and pinhole, for example the width in the middle of the line; typical values are of the order of 2-2.5 cm for W7-X tomography. If the structure size is larger than this limit and covers several areas of sight, the area and line integrals are the same.

This is a preliminary study that can be integrated with additional analysis. Now that the software tools to perform line and area integral calculations are available, the introduction of errors in the

data can improve the simulations. The area integrals can also be used in inversion algorithms to reconstruct the emissivity and study the impact of large gradients in the results.

2.3.2 WPS2.2.4 turbulence optimization in stellarators

Activity has been focused on the role of a class of geometric coefficients on the ion-temperature-gradient (a.e.) modes in W7X-like configurations, in particular on the minimization of the driving effect of certain parameters, e.g., curvature and g_{11} . The numerical tools used for this study are GENE (gyrokinetic), VMEC (for the equilibrium computation), and GIST (geometric interface).

2.4 WPSA

2.4.1 Study of RWM evolution in JT-60SA and requirements for stabilization

The study of RWM evolution in JT-60SA evolved in 2014 following two main lines: 2D stability studies including resistive wall and flow effects and 3D passive boundary modeling.

For the first subject the numerical tool used is the MARS code. The identification of an effective 2D wall geometry (to be considered as having a uniform resistivity) agreed with the JAEA colleagues was the first essential step. The first result was the evaluation of the ideal-wall limit for a reference equilibrium to be used in comparative studies with Japanese codes; the sensitivity of this result on the effective 2D wall shape is presently under investigation. By using this wall shape, first studies on the role of fluid rotation were also performed. MARS code solved MHD equations including fluid acoustic damping (parallel sound wave damping); in the momentum equation, the parallel acoustic damping is multiplied by a strength parameter $k_{||}$ that allows parametric studies of the effect of viscous damping on RWM stability.

At the same time, while keeping a fixed value of the strength parameter, the influence of different rotation speeds can be investigated. This is indeed an important study for JT-60SA given its flexibility in modulating the momentum input to the plasma by choosing different combinations of P-NBI and N-NBI systems. An overview of these effects can be seen in Fig.2.4.1.1: the opening of a stability window clearly appears and is enlarged by increasing normalized plasma rotation frequency Ω/ω_A . At the same time the positive effect of moderately increasing the relative position of the effective wall is highlighted in the figure. It has to be finally noted that the rotation frequency required for entering the stability windows is very sensitive to the shape of the rotation profile itself. As for 3D stability studies, in 2014 the main efforts were devoted to the development of a detailed electromagnetic 3D modelling of JT-60SA. Different computational tools have been used, ranging from a purely electromagnetic description to models including the plasma response.

Detailed 3D finite elements meshes have been developed, including key conducting structures (both passive and active). A positive comparison of results produced with different assumptions and independent codes allows confidence in results (see e.g. Fig. 2.4.1.2). Frequency-domain electromagnetic characterization of active coils has been achieved, as well as first Resistive Wall Modes growth rate computation. Results of this activity have been presented at international conferences (CEFC and SOFT 2014) and open the way to their future inclusion in a state-space model, including the plasma response, for RWM feedback controller design and performance evaluation.

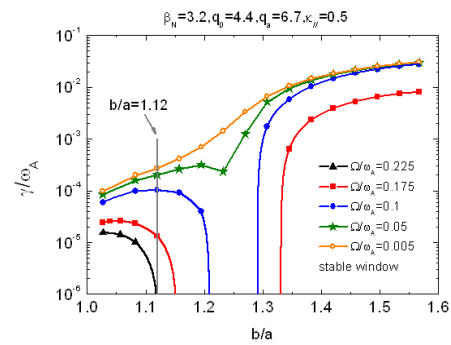


Fig.2.4.1.1: $n=1$ RWM growth rate γ/ω_A versus wall position b/a for different plasma rotation frequencies

2.4.2 Polarimeter JT-60SA and requirements for stabilization

Some issues in the design of the polarimeter for JT-60SA were addressed using the V3FIT code. In particular starting from modeled equilibria obtained with Chronos, V3FIT was used to solve the inverse problem of equilibrium solution assuming different layouts of polarimetric chords. The aim in this work was to assess the limit in the determination of q on axis using only horizontal chords and the possible need of vertical chords. A limited set of diagnostics was used for the modeling (in particular no magnetic diagnostic was implemented). The result is that vertical chords are indeed needed in order to discriminate between different q profiles in the plasma core. Future work will consider a more realistic scenario and diagnostics layout.

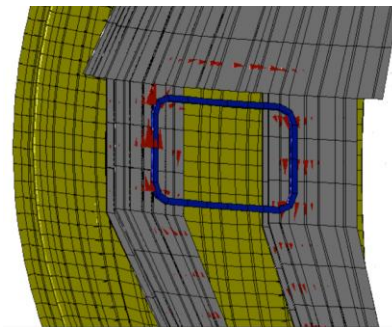


Fig.2.4.1.2: Eddy Current pattern (red cones) along Stabilizing Plate (grey) and Vacuum Vessel (yellow) elements. Active coil: RWMC nr.8 (blue), 100 Hz.

2.4.3 JT-60SA data analysis and remote participation

Within the Operation area some activities have been performed for the definition of the requirements and preliminary feasibility analysis for the JT-60SA remote participation and remote control room. In particular, requirements have been revised for data model, data archiving and architecture; remote computers and data access; support tools and remote control room. In terms

of remote participation and remote control room feasibility, activities have started in the following subjects: desktop sharing and file transfer. A survey of the commercially and freely available desktop sharing application has been performed; a test of two applications which provide the best features is planned at the beginning of 2015. Collaboration with F4E and Japanese National Institute for Fusion Science has been arranged to participate in file transfer test using Massively Multi-Connection FTP (MMCFTP). Results will be compared to previous tests performed using standard techniques.

2.5 MST2

WP14-MST2-10- "Implementation of multichannel edge density profile reflectometer for ICRF antenna on AUG". Analysis software implementation.

This MST2 project involved the setting-up of the new reflectometer on AUG. The activity in 2014 concerned the implementation of the analysis code to produce the edge density profile starting by the raw data. The code has been written in IDL in collaboration with Dr. Fattorini from IFP-CNR of Milan. At present, the code is able to read the raw signals, the magnetic field and to evaluate the first reflected frequency by the plasma (needed to initialize the profile) through different technique and the group delay. In January 2015, the code will be completed by implementing the profile inversion.

2.6 Collaborations under enabling research

2.7.1 WP14-ER-01/ENEA_RFX-06 Investigation of edge plasma electromagnetic filaments and associated transport: from ELMs to turbulent structures

This enabling project included a collaboration with COMPASS, Simple Magnetized Torus TORPEX and TJII. In particular in the COMPASS tokamak the commissioning of the U-probe allowing the simultaneous measurements of electrostatic and magnetic fluctuations with high time resolution suitable for the identification of EM features of the ELMs filaments, similar to the one operating in RFXmod, was completed [Kovacic2014]. In TJ-II stellarator both EM and ES high frequency fluctuations were monitored in the H-mode phase was achieved during NBI powered discharges; data analysis is in progress. Several common features are shared among the filaments detected in the different configurations explored, including RFX-mod [Spolaore, PoP], both electrostatic, such as the presence of density and vorticity structures, and electromagnetic, with a parallel current density associated. One can conclude that local plasma

parameters seem to rule the intensity of some specific quantities and in particular the intensity of the vorticity associated to the filament exhibits a clear dependence on the local ExB shearing rate. Furthermore the wide range local beta explored, about four orders of magnitude, allows concluding that this parameter play a fundamental role in the appearing of the EM features of the filaments.

2.6.2 WP14-ER-01/ENEA_RFX-01 – Density Limit Studies

For this research project a collaboration with FTU and TJII was established.

The known scaling [Pucella2013] of the maximum achievable central density in the tokamak that scales as $B^{3/2}$ has been extended to the range from 0.5 to 8 T with the inclusion of RFX tokamak results. The central density, thus, does not follow a Greenwald scaling. Additionally, in both FTU and RFX a Greenwald-like scaling $n=0.35 n_G$ has been found for the peripheral line averaged density at $r/a=0.8$, (n_G is the Greenwald density). A similar scaling holds for the MHD stability of the edge-resonating $m/n=0/1$ island in the RFP. This suggests a common MHD precursor for the density limit, the 0/1 mode in the RFP, and the 2/1 tearing mode in the FTU tokamak. Experiments in FTU to stabilize the 2/1 mode resonance via electron cyclotron heating (ECRH) showed a reduction of the 2/1 amplitude, without exceeding the Greenwald limit. Regarding TJII the record densities are obtained in NBI heated discharges that restart after suffering an early radiative collapse at relatively low density. In the reheated phase both the impurity content and the MHD activity are reduced and in particular the radial electric field at the plasma periphery field is positive, despite of the high density. The result is consistent with the picture of the edge density limit in FTU and RFX, where the edge radial electric field plays an important role in the development of the MARFE.

REFERENCES

- [Angioni14] C Angioni et al Nucl. Fusion 54 083028 (2014)
- [Challis89] C D Challis et al 1989 Nucl. Fusion 29 563
- [Carralero14] D Carralero et al. (2014). Nuclear Fusion, 54(12), 123005 (2014)
- [Casson15] F Casson et al Plasma Phys. Contr. Fusion 57 014031 (2015) [LaBombard01]
- [Cordey00] J. G. Cordey et al., Plasma Phys. Control. Fusion 42 (2000) A127-A132
- [Delabie14] E Delabie et al., Presented at the 25th IAEA FEC, St. Petesburb, (2014)
- [Kovacic14] K. Kovacic et al EPS Berlin, 41st Conf Plasma Phys COntr. Fus. (2014) P5.025
- [Hirvijoki14] E. Hirvijoki et al 2014 Computer Physics Communications 185 4
- [LaBombard05] B. LaBombard et al. Physics of Plasmas, 8(5), 2107. (2005)

-
- [Mantica 14] P. Mantica EPS Berlin, 41st Conf Plasma Phys COntr. Fus. (2014) P1.017
- [Müller14] H W. Müller et al., PSI 2014
- [Pucela 2013] Pucella G et al, Nucl. Fusion 53 023007 (2013) and Nucl Fus.53 083002 (2013)
- [Romanelli14] M Romanelli et al 2014 Plasma and Fusion Research **9** 3403023
- [Rudakov05] D. L. Rudakov, et al. Nuclear Fusion, 45(12), 1589–1599. (2005).
- [Sharapov02] S.E. Sharapov, et al., Phys. Plasmas **9**, 2027 (2002)
- [Solano13] E. R Solano, Vianello, N., et al. 40th EPS Conf Pl. Phys. p 4.111 (2013)
- [Solaorepop] M Spolaore et al. Submitted to Phys of Plasmas
- [Urano08] H. Urano et al., Nucl. Fusion 48 (2008) 045008
- [Urano12] H. Urano et al., Nucl. Fusion 52 (2012) 114021
- [Valisa14] M Valisa et al Proc. of FEC IAEA (2014) St Petersburg, EX6-1

3. Broader Approach

The work of Consorzio RFX team in the framework of the Broader Approach agreement was addressed to continue the fulfilment of the commitments for the JT-60SA project: the procurement of the “Quench Protection Circuits” and of the “Power Supplies for the in-vessel sector coils for RWM control”. An additional contribution has also started in 2014 in the frame of the IFERC project for the development of the Remote Experimentation Centre.

Moreover, Consorzio RFX participated in the JT-60SA physics studies and in the preparation and update of the Research Plan. These activities are described in section 2.4.

3.1 Quench Protection Circuits

The Quench Protection Circuits (QPC) of the JT60-SA poloidal and toroidal superconducting magnets are provided by a contract awarded by Consorzio RFX to the company Nidec ASI (formerly Ansaldo Sistemi Industriali) in December 2010. The ratings of the QPC units are summarized in Table 1

Table 1 – Ratings of QPC units

Coils	Number of units	Rated value (assumption)
Toroidal	3 units	25.7 kA / 2.8 kV
Central Solenoid	4 units	20kA / 4.2 kV
Equilibrium Field	6 units	20kA / 4.2 kV

After the completion of the detailed design in Summer 2011, two full scale prototypes were developed by Nidec ASI to verify the performances of the innovative design solution based on a hybrid mechanical-static circuit breaker. In 2013, the manufacturing and routine tests of two QPC pre-series units were successfully completed giving the green light for the manufacturing of the remaining QPC units.

The main activities and achievements in 2014 can be summarized as follows:

- the completion of the manufacturing and routine tests of all the QPC component carried out from summer 2013 to July 2014.
- the completion of the new pyrobreaker actuation system, composed of explosive charges, detonators and firing circuit, which was launched in 2011 to reduce the risks of significant delays due to the difficulties related to the exportation of the explosive from Russia. The last routine tests on the triggering boards of the pyrobreakers were carried out in July and in the same month was also completed the report on this development which was evaluated during the Design Review Meeting (DRM), held on July 22th.

-
- the completion of the III deliverable: “Factory Routine Test Report”, which was evaluated during the DRM held on July 24th and approved on August 13th, thus allowing the achievement of the III PA milestone
 - the packaging, shipping and delivery of the QPC components, thus allowing the achievement of the IV PA milestone
 - the assessment of the procedures to export the “dual use items”: pyrobreaker explosive charges and firing circuits
 - the start of the installation activities in December

The contract follow-up activities proceeded in parallel to the company activities on all the topics in progress.

As for the routine tests, specific analyses were necessary to understand the reason why the test results on BPS series units showed a delay time from the command to the contact opening longer than that of the prototype (239 ± 15 ms). A bouncing of the main contacts due to an oscillation between the two systems of springs was identified as the major cause of the higher delay. The problem was solved using laminated springs only, adjusted to apply the same force as before. One BPS was modified with the new spring system and type tests were performed to qualify the operation. Additional measures were carried out on all the units to measure the distance of the contacts at 350 ms to quantify the margin in terms of voltage holding capability, with successful results.

In July, the components of the 13 QPC units were packaged in big moisture barrier antistatic bags, to prevent damages to electronic devices during the trans-oceanic shipment, then closed in 72 wooden boxes and stored in 17 containers; the total weight was about 137 tons. The containers were shipped from the Genova Port on August 11th, and were delivered at the Yokohama port on September 19th and 26th. After the joint check of the packages, they were transported on trucks to Naka site, where they were moved close to the final installation place in the Rectifier building and in the Toroidal PS Hall. The QPC installation started in December; this phase represents the first instance of activities directly performed by European personnel at Naka Site; the related organization required the assessment of several unprecedented issues; the aspects related to the safety were analyzed in deep detail. Fig. 3.1 summarizes the phases of packaging, transportation, movement at Naka site and start of the installation activities.



Fig.3.1 summary of the phases of packaging, shipping, transportation and movimentation at Naka site and start of the installation activities.

The specific analysis of the transient voltage across the TF coils at the pyrobreaker intervention for toroidal QPC continued in 2014. The proposal of modification of the busbar route to reduce the peak value of the transient voltage was endorsed and further verification of the expected transient voltage were carried out in parallel to the definition of the final assessment of the power connections at Naka site, utilizing the QPC models validated against the experimental results.

3.2 Power supplies for in-vessel sector coils for RWM control

In JT-60SA, a set of 18 in-vessel coils are foreseen to control a particular type of plasma instabilities called Resistive Wall Modes (RWM); Consorzio RFX is in charge to provide the power supplies to feed these coils. After joint studies between Consorzio RFX and JAEA to improve the design of the whole system for RWM control, the coil design was finalized by JAEA in 2012 and the final set of power supplies requirements was agreed. Each coil will be fed by a dedicated inverter (300 A, 240 V), which has to guarantee very high dynamic performance. In particular, a current bandwidth of 3 kHz and latency between output voltage and reference lower than 50 μ s are necessary. To prove the feasibility of the specifications and the availability of suitable power switches at reasonable cost, Consorzio RFX proposed to develop an inverter prototype.

A call for tender was placed and won by the Italian company Equipaggiamenti Elettronici Industriali (E.E.I.) in May 2013 and the design phase was completed in autumn 2013. The inverter prototype design was based on very fast and innovative hybrid Silicon-IGBT / Silicon-Carbide-Diode modules, switching at 30 kHz; a picture is shown in Fig. 3.2. A sophisticated control board was developed to

satisfy the stringent dynamic requirements; it is based on the combination of a fast microcontroller and a FPGA running optimized firmware.

The inverter prototype was tested in depth to verify the compliance with the specifications. The stringent dynamic requirements are satisfied; in particular, the average latency is about 30 μs and the maximum value is always lower than 40 μs (Fig. 3.3); the current attenuation in CCM is -3dB at 3 kHz, as required.

The results of the test carried out confirmed the feasibility of adopting the reference scheme

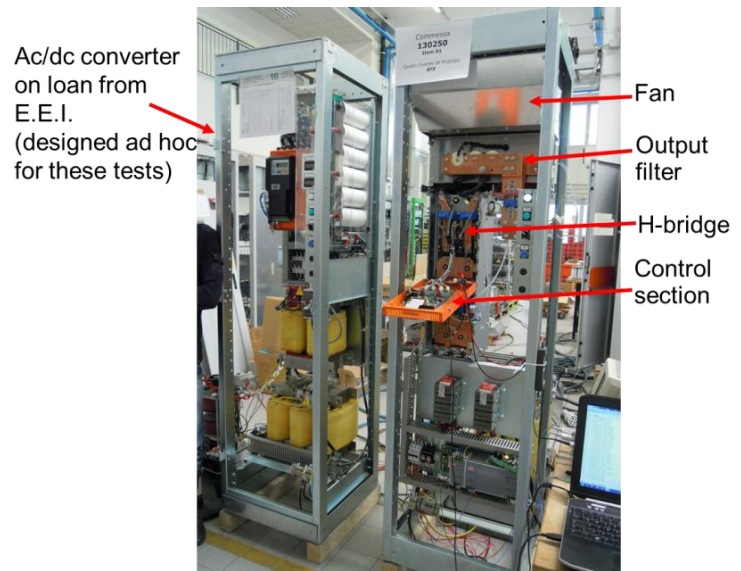


Fig. 3.2 Inverter prototype

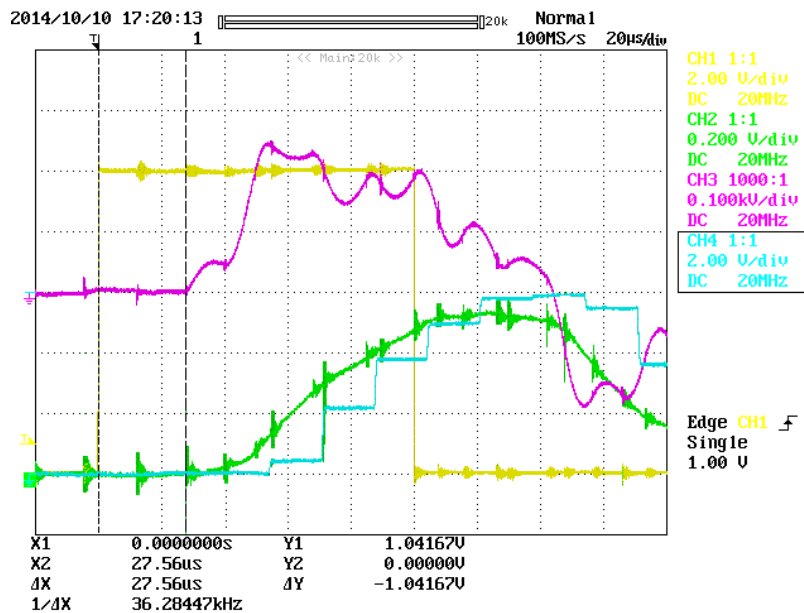


Fig. 3.3 - Voltage and current waveforms in CCM, with step reference with amplitude +10 V (corresponding to +300 A) and duration 100 μs . CH 1: reference (1 V/V); CH2: instantaneous load current (450 A/V); CH3: instantaneous load voltage (1 V/V); CH4: average load current (40 A/V, averaged every 16.7 μs)

selected for the inverters, based on the H-bridge topology, thus benefiting of its higher simplicity and reliability and gave confidence enough to proceed with the procurement of the whole system. The Agreement of Collaboration and Procurement Arrangement documents were prepared and are presently under the signature process.

REFERENCES

[Maistrello 2014] A.Maistrello, E. Gaio, A. Ferro, M.Perna, A. Coffetti, L. Novello, M. Matsukawa, K. Yamauchi: "Experimental qualification of the Hybrid Circuit Breaker developed for JT-60SA Quench Protection Circuit", IEEE Transactions on Applied Superconductivity, Volume: 24 , Issue: 3, 2014

[Maistrello1 2014] Alberto Maistrello^a, Elena Gaio^a, Luca Novello^b, Makoto Matsukawa^c, Kunihiro Yamauchi^c "Analyses of the impact of connections' layout on the coil transient voltage at the Quench Protection Circuit intervention in JT-60SA", presented at the 28th SOFT and submitted for publication in Fusion Engineering and Design

[Novello 2014] Luca Novello^a, Olivier Baulaigue^b, Alberto Coletti^a, Nicolas Dumas^b, Alberto Ferro^c, Elena Gaio^c, Alessandro Lampasi^d, Alberto Maistrello^c, Makoto Matsukawa^e, Katsuhiko Shimada^e, Kunihiro Yamauchi^e, Pietro Zito^d "Present Status of the new Magnet Power Supply Systems of JT-60SA procured by EU" presented at the 28th SOFT and submitted for publication in Fusion Engineering and Design

[Gaio 2014] E. Gaio¹, A. Maistrello¹, L. Novello², M. Matsukawa³, A. Ferro¹, K. Yamauchi³ and R. Piovan¹ "Protection of superconducting magnets in fusion experiments: the new technological solution for JT-60SA", presented at the 25th IAEA FEC

[Ferro 2014] Alberto Ferro^a, Elena Gaio^a, Luca Novello^b, Makoto Matsukawa^c, Katsuhiko Shimada^c, Yoichi Kawamata^c, Manabu Takechi^c "Reference design of the Power Supply system for the Resistive-Wall-Mode control in JT-60SA" presented at the 28th SOFT and submitted for publication in Fusion Engineering and Design

4. ITER

4.1 NBI development

This section reports the status of the activities performed by the NBTF Team, including the Third parties, as foreseen by the agreements existing among ITER, Fusion for Energy and Consorzio RFX mainly devoted to realize the PRIMA Test facility at Padova [Toigo1].

In 2014, the main areas of activity performed by NBTF Team and third parties have been:

1. Construction of PRIMA buildings and auxiliaries and delivery of some areas for the installation on the first SPIDER plant systems.
2. Design of MITICA components, diagnostics, control, protection and safety systems towards the preparation of the documentation for the procurement activities.
3. Technical follow up of procurements from Call for Tender (CfT) issued by F4E up to the installation phase, including factory acceptance tests of some plant systems.
4. Completion of R&D on prototypes of components to confirm the design choices, to assess the reliability of the chosen technologies and to identify correct manufacturing processes.
5. Plant integration between experimental plants and PRIMA buildings by using 3D Cad model [Fellin1].
6. Interface management between buildings-plant systems-components to guarantee the coherence of the overall design.
7. Support to JADA and INDA DAs in the integration of their procurements with different NB components and buildings to ensure overall performance of test beds.
8. Modelling and experimental validation on existing facilities to support the design work of the ITER test beds in close collaboration with the Accompanying Programme.
9. Support to the Host Site activities required during construction, supervision and coordination of the Facility.

During 2014 there was a considerable commitment of resources for carrying out activities of finalization of MITICA BS design, procurement follow-ups, support to JADA procurement and support to Host Site Activities and plant integrations. About 290 meetings have been held with participation of NBFT personnel; 150 documents uploaded on F4E IDM as deliverables of WP2014 and Framework Programmes.

In February 2014 the Framework Contract for the procurement of the Central Control and Data Acquisition System (CODAS), as well as Interlock and Safety systems has been signed and the first specific contract for the procurement of the SPIDER CODAS and Interlock system signed in

July. After signature of the specific contract, activities of design and procurement of components and plant systems for the realization of the SPIDER control and protection systems have started; at the same time activities relevant for the finalization of the interfaces between CODAS, Interlock and plant units have continued.

Activities on the development of diagnostics continued both maintaining support for the definition of interfaces with other systems and the development of prototypes. Moreover, during 2014 the Framework Contract for the procurement of both SPIDER and MITICA diagnostics has been prepared and the contract has been signed in December.

Difficulties have been encountered in the follow-up of SPIDER Beam Source. Many issues were arisen during design and manufacturing of components and extra work of NBTF Team was necessary to perform additional design and CAD activities or R&D.

Progress on the procurement activities with the support of the NBTF Team has been made. In particular all SPIDER plant systems and components are under procurement: the manufacturing of the Ion Source and Extraction Grid Power Supply system has been completed and factory tests successfully performed by May 2014: the design and manufacturing of the HV Deck has been completed and the system ready to be installed; the design of the Transmission Line is completed and the mock-up under construction; the installation of the Cooling plant system has been started in November and the Vacuum and Gas Injection and storage system ready to be installed; finally, Factory tests of SPIDER Vessel were passed and in February 2015 the component will be installed inside the SPIDER bio-shield.

Regarding MITICA experiment: the design of the injector mechanical components has been almost completed, CfT for the procurement of some plant systems have been lunched; other CfT's will be lunched during 2015. In particular, contracts for the procurement of the MITICA Vessel and HVD1 and HVD1-TL2 bushing have been signed by the end of 2014; instead CfT process for the procurement of the AGPS & GRPS has been launched in October 2014 and the process will be concluded in 2015. All these activities have been performed directly by or with the support of the NBTF Team.

During 2014 NBTF Team has continued to update the sequence of installation and commissioning relevant to both SPIDER and MITICA. These sequences have been presented and discussed in several meetings among RFX, IO, F4E and the DAs and updated according to the agreements reached.

Training of personnel and test on diagnostic prototypes has continued mainly at IPP but also in other laboratories.

Some thermo-mechanical R&D has been performed with the support of an external company, mainly as a completion of activities previously started and focussed to support the design of MITICA BS and BLCs.

Finally, vacuum HV R&D using HVPTF facility and RF R&D activities have been made with the aim of supporting the BS design and of training the NBTF staff to work with the RF and with high voltage in vacuum. In particular HV tests of MITICA post insulator prototypes have been performed and the full voltage performances of 240kV for some hours reached with some of them. The status of the project and the main achievements of the year are described in detail in the following sections.

4.1.1 PRIMA

4.1.1.1 Buildings

The NBTF building construction started in September 2012; during 2013 all foundation and basement have been realized and the erection of the buildings has been started and well advanced, completing the realization of almost all of the buildings, including installation of cranes and some auxiliaries.

During 2014 the activities have continued; in particular:

- All buildings have been erected, including Building 12 hosting experiment control rooms;
- SPIDER bio-shield has been completed including removable concrete beams;
- The pit and fixed structural parts of MITICA bio-shield have been completed;
- Pit and tranches hosting MITICA transmission line and other HV components have been started;
- Concrete slabs and other external civil structures to host gas storage tanks have been started and well advanced;
- All auxiliary plant systems have been progressed;

Some buildings have been released to F4E for the installation of the first plant systems and components; in particular:

- Building 2 for the installation of the Cooling Plant system;
- Building 6 for the installation of the SPIDER power supply system



Fig. 4.1: PRIMA Site: areal view of PRIMA buildings

Taking into account the criticality of the EMI immunity for the correct operation of the experiments, particular attention has been paid to the design and realization of the ground system, including verification and measurements during its realisation [Pomaro1].

Finally, SPIDER bio-shield has been completed and cleaned and will be released to F4E at the beginning of 2015 for the installation of SPIDER vessel.

4.1.1.2 Cooling Plant for SPIDER and MITICA

The procurement for PRIMA Cooling Plant [Fellin2, Fellin3] advanced regularly during 2014 under F4E contract OPE-351. RFX performed the foreseen follow up activities verifying the documents



Fig. 4.2: SPIDER bio-shield: installation of the removable concrete beams

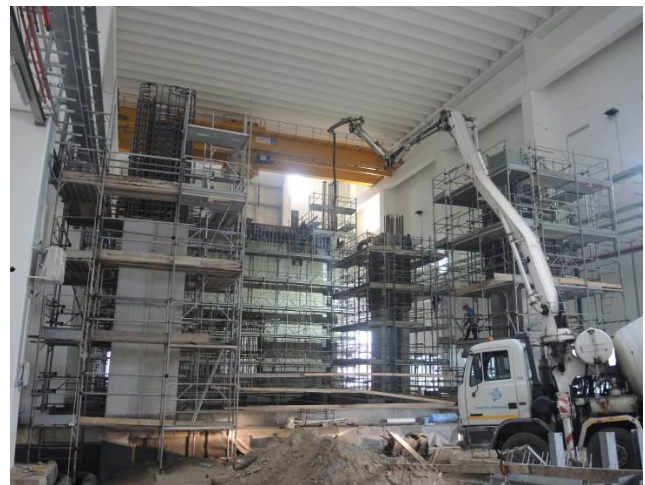


Fig. 4.3: MITICA bio-shield: realization of the fixed structural parts



Fig. 4.4: Concrete basement of the TL2 tower



Fig. 4.5: Building 6 ground floor: internal view of the pit hosting the post-insulators of the HVD

produced by the Supplier (Delta-Ti Impianti) and sub-suppliers, giving technical information to the Supplier for plant integration on Site, performing visits at sub-suppliers' sites for intermediate tests on components (pumps, cooling towers) and checking and solving the integration issues arisen for plant assembly on-site.

The on-site activities started on 3rd November 2014. Most of the pipes for Secondary circuits have been delivered at PRIMA site and are now under installation inside Building 2. The cooling towers have been also delivered at PRIMA site on the 16th and 17th December 2014.

Assembly and tests of SPIDER Cooling Plant (pipes, valves, heat exchangers, pumps, sensors, electrical plant and local control system) and the relevant part of Shared Cooling Plant will be completed during 2015 and in parallel the



Fig. 4.6: Tests of cooling plant pumps at manufacturer premises (Garbarino Spa, Acqui Terme, Italy, the 9/10/2014)



Fig. 4.7: Particular of a cooling tower basin at the manufacturer premises (Evapco Europe srl, Passirana di Rho, Italy, the 29/10/2014)



Fig. 4.8: Cooling pipes installation inside Building 2 at level -2.0 m

MITICA Cooling Plant design and procurement will be completed defining in particular details for pipes layout and supports for MITICA Primary Circuits.

4.1.1.3 Vacuum, gas injection and gas storage for SPIDER and MITICA

The procurement contract for the PRIMA Gas and Vacuum System (GVS), signed by the end of 2012 as F4E contract OPE-279, continued regularly and intensively during 2014 and some important milestones have been achieved. In particular the Factory Acceptance Test (FAT) for the SPIDER part of the procurement has been performed successfully and the PSC (Plan for Safety and Coordination) issued by the CSP.

The start of assembly on Site is foreseen by February 2015.

4.1.2 SPIDER

4.1.2.1 SPIDER Vacuum Vessel

The construction of SPIDER Vacuum Vessel has been completed during 2014 and all the foreseen factory acceptance tests have been carried out. RFX performed the technical follow up of the contract, with frequent meetings and visits at the Supplier's premises (E. Zanon) and relevant sub-suppliers, verifying documents submitted by the Supplier and advising for integration, test and assembly at PRIMA site [Zaccaria1].



Fig. 4.9: Delivery of Cooling Towers at CNR Research Area, to be then installed on the roof of PRIMA Buildings

The Vessel is presently at the Supplier's factory to apply some minor corrections to the interface with Transmission Line before delivery to PRIMA Site, presently foreseen by February 2015.

The acceptance tests were completed with general positive results. Some non-conformities have been identified on the positions of service and diagnostic ports. Some of them are accepted without problems, being the interface less critical, some others, as the ones on the Beam Source Module, will require careful operations and checks during assembly and in-vessel installation of the Beam Source.

Assembly, alignment and opening/closing activities were correctly performed at the factory and correct positions of Vessel components have been obtained.

The Vacuum tests at the factory were passed positively achieving the foreseen level of pressure and leak rate values (localized leakages lower than 10^{-9} mbar l/s). Despite the careful and repeated cleaning of Vessel internal surfaces, the Residual Gas Analysis (RGA) tests showed unsatisfactory results, so a baking cycle at a temperature around 150°C is considered necessary. This outgassing process will be performed on site after Vessel delivery and assembly inside the SPIDER Neutron Shield.

The full assembly and acceptance tests of the SPIDER Vacuum Vessel at PRIMA Site are foreseen during the first half of 2015.

Some images of the Vessel during factory tests at Zanon premises are shown in the following figures 4.10 and 4.11.



Fig. 4.10: SPIDER VV during assembly at Zanon for factory tests



Fig. 4.11: SPIDER Vacuum Vessel during global He leak tests (vacuum inside, He inside plastic bag)

4.1.2.2 SPIDER Beam Source

SPIDER Beam Source manufacturing progressed during 2014 under F4E contract OPE-081, with continuous and strong effort on RFX side for technical follow-up [Pavei1].

The First Design Report for Beam Source (regarding the core components) was submitted and approved on 8th April 2014. Hundredths of manufacturing drawings and documents have been uploaded by the Supplier in F4E-IDM during 2014, checked by RFX, revised and finally approved. Other technical documents as Control or Manufacturing Plans have been also produced, checked and approved.

Manufacturing of the main components of the beam source is going on at Cecom (I), Galvano-T (D) and relevant sub-contractors, while parallel activities have been carried out at Zanon (for manufacturing of BS support structure, electrical and hydraulic feedthroughs flanges and BS Handling Tool), Fives Nordon (sub-supplier for cooling circuits) and Spinner (sub-supplier for RF line). The ceramic insulator prototypes have been manufactured by Wesgo Ceramics.

Fives Nordon will be the Thales sub-supplier for BS assembly and tests at the factory.

A scheme of the different companies involved for SPIDER BS manufacturing is shown in figure 4.12.



Fig. 4.12: Sites of main Companies involved for SPIDER BS manufacturing

A first segment of grounded grid, see figure 4.13, has been manufactured and positively tested at Cecom; the other GG segments are under manufacturing.

Fabrication of lateral walls, see figure 4.14, quarters is going on at Cecom and Galvano-T respectively for specific manufacturing steps, revealing problems in achieving the foreseen tolerances. Actions to control and reduce deformations during intermediate manufacturing phases have been identified and implemented. Final results will be checked and a suitable assembly process will be developed by the Supplier. A first Faraday Shield Back-plate (FSBP) and Plasma Drivers Plate Quarter (PDPQ) have been also completed and tested at Cecom (see figures 4.15 and 4.16).

The Plasma grid segments are under final machining phase at the sub-supplier Research Instruments (RI), see Figure 4.17, after complete Cu electrodeposition at Galvano-T. Machining of extraction grid segments just started at RI factory after problems with a previous sub-supplier and excessive

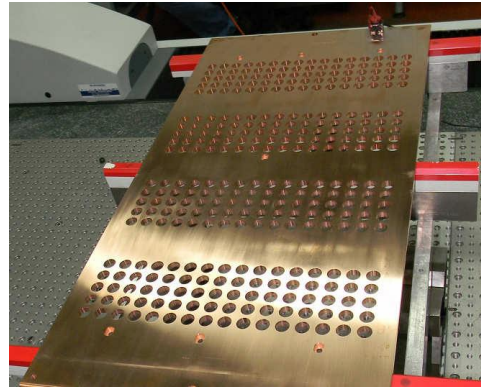


Fig. 4.13: First segment of SPIDER GG at Cecom during dimensional check



Fig. 4.14: The Lateral Wall Quarter at Cecom during intermediate dimensional checks

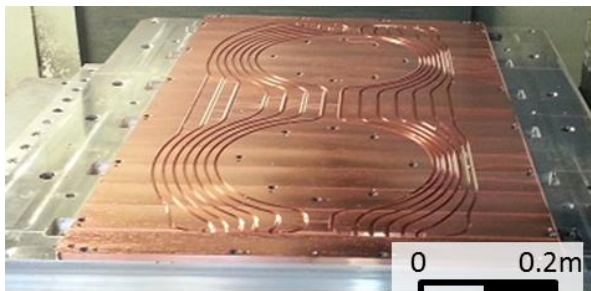


Fig. 4.16: PDPQ during dimensional control, after machining of the embedded cooling channels

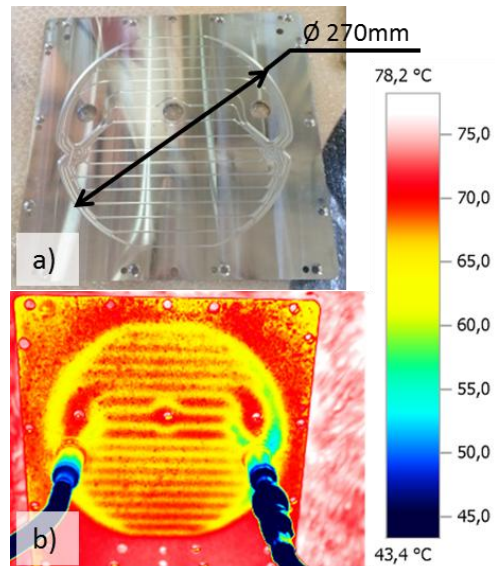


Fig. 4.15: FSBP during manufacturing control (a) and during flow rate thermographic tests (b)

deformations occurred on a first piece after electrodeposition.

Thermal sensors produced and tested at sub-supplier Thermo-coax have been delivered to Fives Nordon (F) sub-supplier, ready for Beam Source assembly.

Electrical tests on PG-EG and EG-GG post insulators have been passed at Thales, achieving a voltage up to 140 kV in vacuum (see Figure 4.18). The ones on BS-VV support insulators are still on-going with some

problems in achieving the required parameters. Mechanical tests on EG-GG and PG-EG post insulators have been also passed in December 2014 (see Figure 4.19), with target values obtained as a consequence of all foreseen load cases [Sartori1].

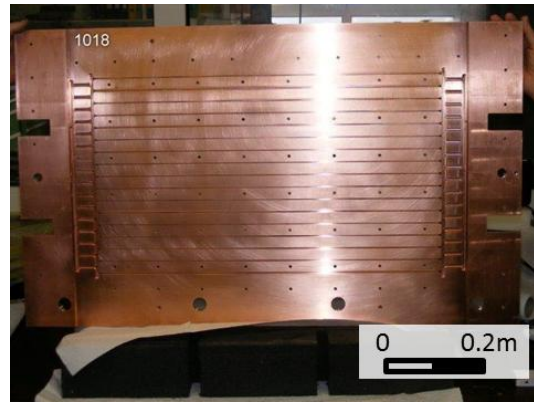


Fig. 4.17: One of the four PG segments after machining of the embedded cooling channels

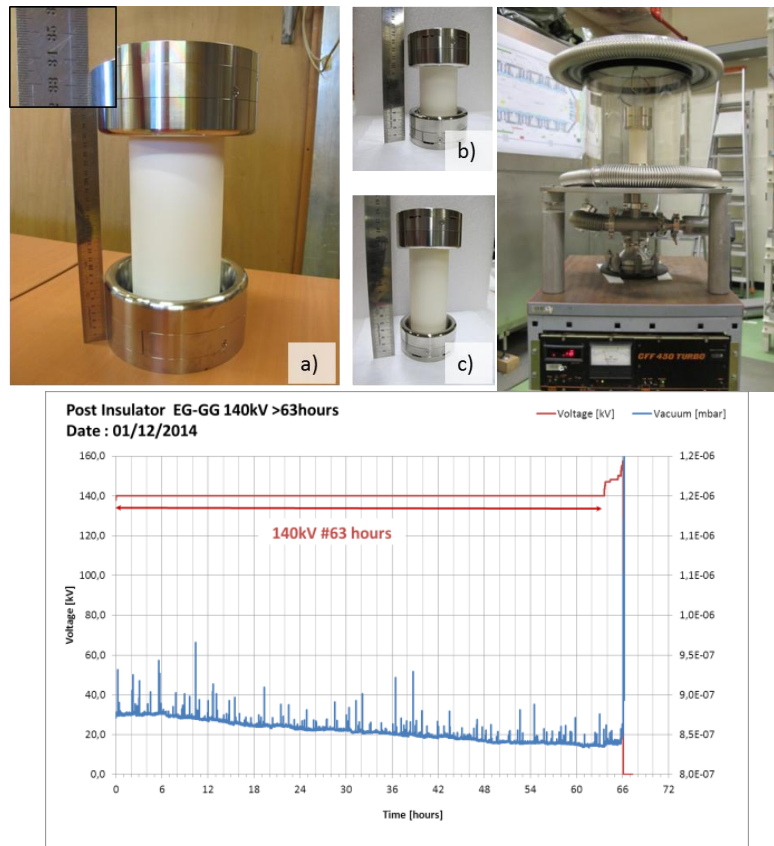


Fig. 4.18: Views of: 112kV BS ceramic supports (a), 12kV PG-EG post insulators (b), 100kV EG-GG post insulators (c), the test set-up for electrical tests at Thales premises and one test record

The present manufacturing plan foresees the completion of source components within May 2015 and the start of Beam Source assembly at Fives Nordon in June 2015. Final delivery of the Beam Source to PRIMA site is foreseen by the end of 2015.

4.1.2.3 SPIDER Beam Dump

Manufacturing, assembly and factory tests of SPIDER Beam Dump (Figure 4.20) have been completed during 2014 by the Supplier PVA TePla (D) under ITER India procurement contract.

RFX Team was mainly involved to verify and evaluate some non-conformities on thermocouples locations and other minor changes to the high heat flux components proposed by ITER India and the Supplier for assembly reasons, to guarantee the final opacity needed to avoid any beam shine-through.

The factory tests have been performed from 15th to 18th December 2014 at PVA TePla premises at the presence of IO, ITER India and RFX representatives.

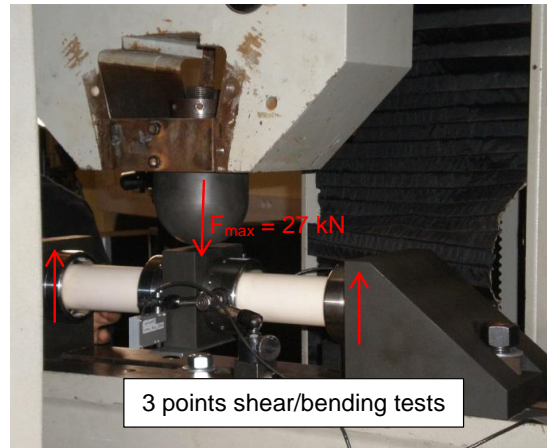


Fig. 4.19: Test set-up for mechanical tests of SPIDER BS post-insulators – F_{max} at rupture 27 kN



Fig. 4.20: Rear and front views of the SPIDER Beam Dump assembled at the Supplier's factory (PVA TePla)

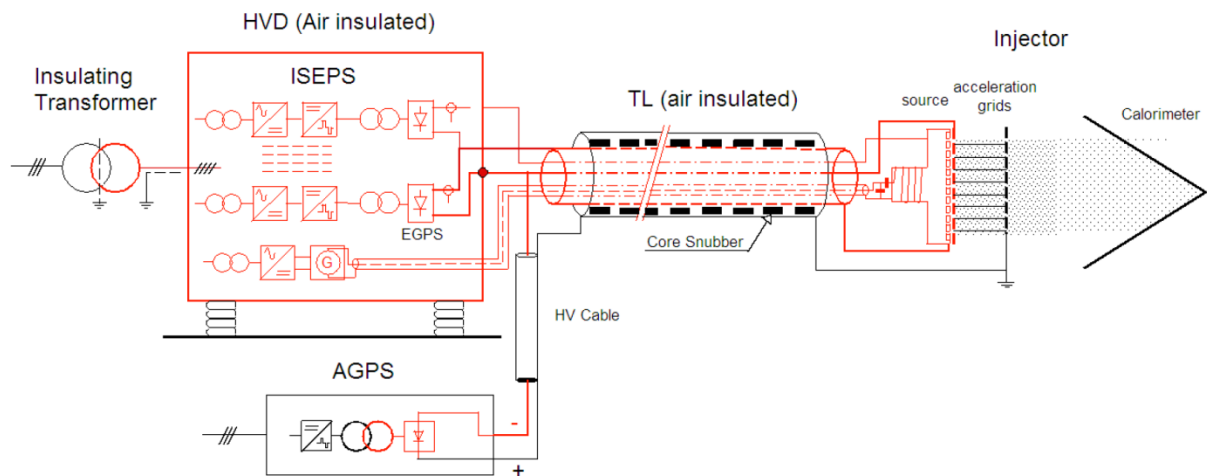


Fig. 4.21: Conceptual scheme of the SPIDER power supply system

Visual and dimensional controls, pressure test, He leak tests, high voltage tests and electrical tests on sensors were executed and the whole technical documentation was checked. RFX personnel witnessed the final tests during the four days meeting and carefully verified the interfaces and component condition before packing and delivery to PRIMA site.

The component was finally delivered to PRIMA Site on 22nd December 2014. It is now stored waiting for some adjustments to solve some minor problems detected during factory tests. The installation of thermocouples on the back side of high heat flux components and the final installation of the Beam Dump inside the SPIDER Vacuum Vessel are foreseen during the second half of 2015.

4.1.2.4 SPIDER power supplies: ISEPS, 100 kV accelerator power supplies, High Voltage Deck and Transmission line

The circuit diagram of the SPIDER power supply system is shown Fig. 4.21.

The High Voltage Deck (HVD), insulated for -100 kV, hosts the Ion Source and Extraction Power Supplies (ISEPS), electrically connected through the air insulated Transmission Line (TL) to the beam source, which is polarised at -100 kV by the Acceleration Grid Power Supply (AGPS). In Fig. 4.22 the layout inside the buildings is shown of the HVD (yellow box), of the TL (square shaped grey coloured) and of the AGPS (three racks with red conversion modules, INDA procurement).

The procurement of the Ion Source and Extraction Power Supplies (F4E OPE-046 with OCEM-Energy Technology) saw in 2014 completion of manufacturing and of the factory acceptance tests, including testing at full power of all power supplies. The second part of the in kind contribution of

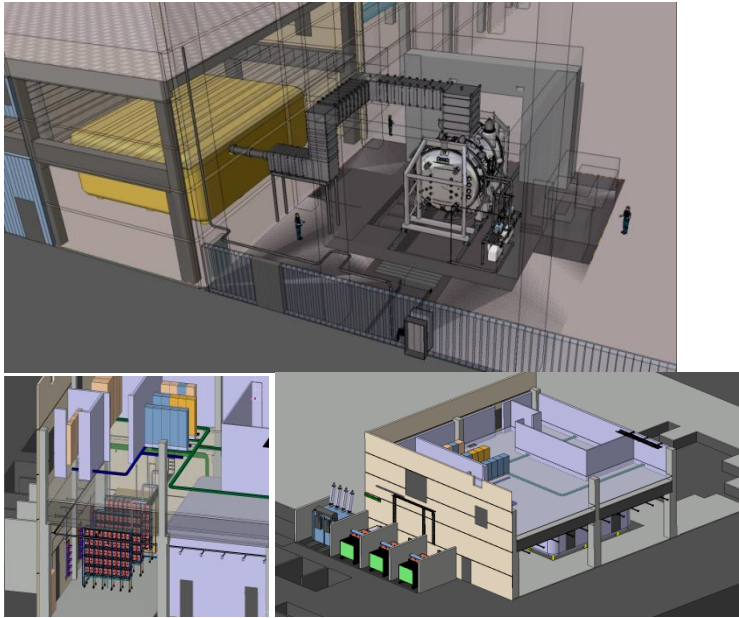


Fig. 4.22: SPIDER air insulated High Voltage Deck (HVD) and Transmission line (TL)

the Indian Domestic, the SPIDER AGPS (Acceleration Grid Power Supply) completed most of manufacturing.

The High Voltage Deck & Transmission Line (HVD & TL, procurement contract OPE-396 with COELME - Italy) design was reviewed, finally approved and manufacture launched. HVD factory testing was completed and preparation for start of installation on site too.

In 2014 ISEPS manufacture and factory acceptance testing has been followed closely. Significant manpower, both engineers and technicians, has been deployed to witness all phases of factory acceptance test (see fig. 4.23 and [Bigi1]). The equipment passed all tests and was declared fit for delivery to site. Nonetheless, a number of system improvements and minor modifications were identified and followed-up with the Supplier. In addition testing at the factory of the ISEPS Medium Voltage distribution board (not part of the factory acceptance tests) has been witnessed and resulting issues discussed. An important activity was the support to the ISEPS Supplier in the discussion and definition of the interfaces with the HVD, object of a separate F4E procurement as mentioned above. This aspect has been especially critical and demanding, because the ISEPS design had been closed in 2011 before the HVD contract was even signed. This meant that a number of constraints resulting from the HVD and TL design had to be discussed and agreed with OCEM-ET at a late stage of the SPIDER ISEPS procurement. Another activity was the support to the Supplier in the preparation of the documentation and in the site inspections



Fig. 4.23: Attendance on the last day of SPIDER ISEPS factory acceptance tests at OCEM-ET premises (Bologna, Italy) in May 2014

for installation work on site, due to start in 2015 upon availability of the HVD. Work has also been devoted to update the interfaces with the control and data acquisition system, also in the light of the factory acceptance tests, including hardware specifications, signal lists and mimics.

With respect to the work with INDA for the procurement of the SPIDER AGPS, information and requirements were exchanged on the interfaces with buildings and their electrical services, with the Control and Data Acquisition System and with PRIMA Cooling Plant. A layout conflict with the buildings was identified during a site inspection as part of the SPIDER Power Supply interface management meeting held in Padua in June. The conflict was subsequently discussed in dedicated meetings and exchanges and a solution finally identified. An important effort has been devoted to supporting INDA in the identification and discussion with potential suppliers of services for their electrical installation on site and in person meetings between INDA and four suitable companies arranged in July. Though not involved in the commercial aspects, RFX continued to support the technical exchange and clarifications between the local companies and INDA.

The 2014 activity in support to F4E procurement of SPIDER HVD&TL was significant [Boldrin1]. At the beginning of the year the review was carried out of the Supplier design first submitted at the end of 2013. The activity involved a number of exchanges and iterations, in particular on few critical aspects (e.g. the HVD ventilation system). A consolidated HVD design was finally submitted by the Supplier and approved. On this basis the Supplier started manufacture, which in the case of the HVD was completed in July with successful factory tests witnessed by RFX staff on behalf of F4E, see Fig. 4.24. To the interface aspects with ISEPS (mostly for the HVD), SPIDER Beam Source (mainly for the TL) and buildings was committed a large fraction of the follow-up effort. The interface with ISEPS was fully defined, whereas on the side of the SPIDER



Fig. 4.24: Some pictures of HVD components taken in July during inspection at the COELME sub-contractor premises

Beam Source (supplied by THALES under F4E procurement OPE-081) a number of open issues still exist. Many exchanges and discussions with F4E were held to define the mutual sequence of HVD and ISEPS installation, with several technical implications and also linked to contractual aspects like acceptance of the supply. Eventually it was decided that ISEPS installation would only start upon full acceptance of the HVD by F4E. Another important activity was the support to the HVD Supplier in the preparation of the documentation and in the site inspections for installation work on site, due to start early 2015. This involved safety documentation on the one hand and administrative and technical documentation for the Padua town council, associated to the nature of “structure” of the HVD which carries with it a number of regulatory requirements.

4.1.2.5 SPIDER & MITICA diagnostics

Procurement follow up of diagnostics embedded in SPIDER components (F4E contracts for source & vacuum vessel and transmission line), further design optimization and continuation of R&D on diagnostic concepts and components have been the main tasks in 2014, together with the production of an offer for the framework procurement contract (FPC) for diagnostics, the consequent negotiation and award in December 2014.

The FPC, awarded by F4E to Consorzio RFX, comprises the final design, procurement, assembly,

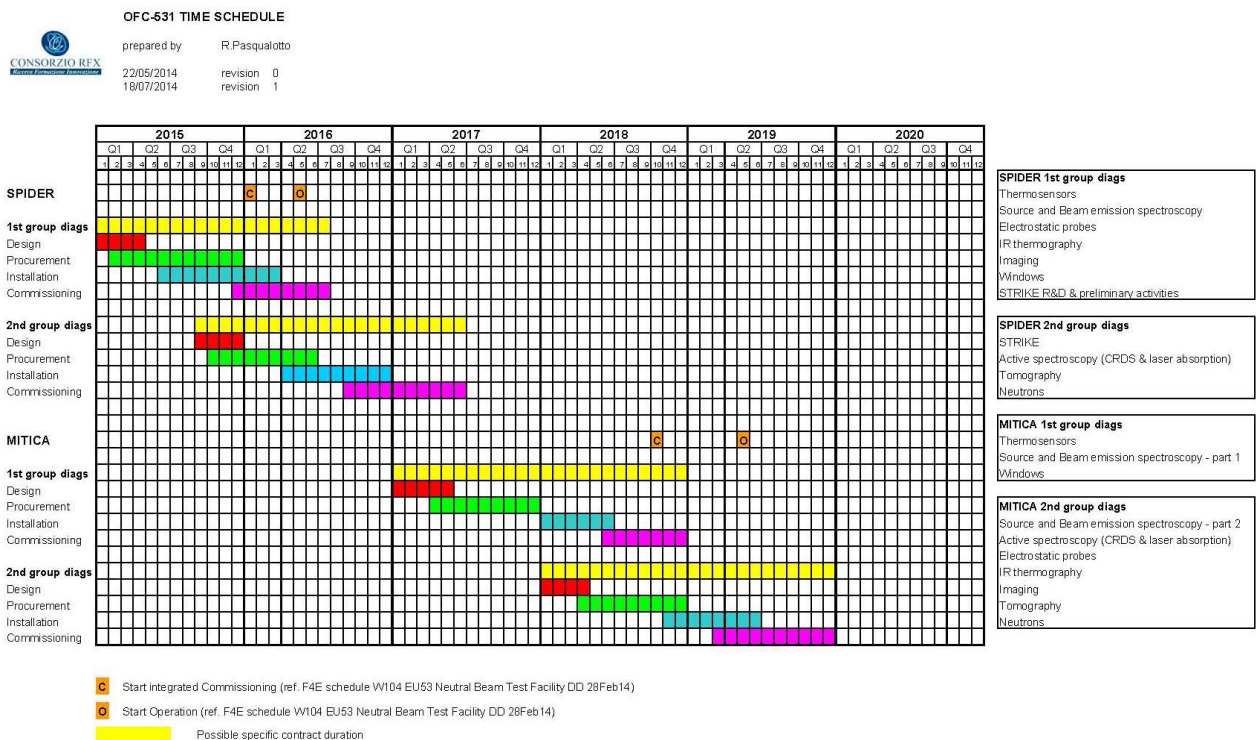


Fig. 4.25: Schedule of the four Task Orders in the Framework Procurement Contract for Diagnostics

installation and commissioning of all diagnostics of SPIDER and MITICA that are not embedded in other NBTF components, for which the procurement contract is managed directly by F4E. For the FPC instead the procurement of diagnostic components will be managed directly by RFX, following the internal Quality and Purchase procedures, and RFX will be responsible for the final performance of the integrated systems. The offer comprised a detailed documentation set, including a Quality Plan with description of the project team, project management and procurement schedule, an Execution Plan and proof of experience and of compliance with the technical specifications. The first Task Order is for SPIDER diagnostics to be available on the first day of operation (2016 Q3) and its call is expected in January 2015, while its signature is planned in March 2015.

Thermocouples (TC) and electrostatic probes (EP) are embedded in the SPIDER source and their cabling comprise feedthroughs on the vacuum vessel and cables in the transmission line. Their procurement and installation is being followed up as part of two F4E contract with the companies Thales for source and vessel and COELME for the transmission line. Frequent interactions of RFX experts with F4E and the two companies helped to finalise the details of the design, in particular the fixing methods of the sensors, types and layout of cables, connectors and feedthroughs, screening and grounding and interfaces between the different contracts. This has not been a straightforward task, as RFX was providing technical expert support to a contract run by F4E with several penalizing conditions, among which the fact that, despite it was to be based on built-to-print-design, actually several designs required finalization by the company in the manufacturing phase. This resulted in accepting several downgrades and technical compromises to avoid excessive cost increases. So far the design has been fully detailed, components are being procured and production is starting. The production of TC based on mineral insulated cables has been successfully completed in December 2014 by Thermocoax, which proved as a reliable supplier. EP sensor prototypes are going to be manufactured again with a revised design after a first failure; EP cabling layout has been improved on the basis of the experience gained during the tests at IPP, with the insertion of some conditioning electronics in vacuum, nearer to the sensors. The tests of the EP on BATMAN at IPP, started in 2012 and progressed in 2013 [Brombin1, Brombin2], have been completed in 2014 with an experimental campaign featuring both cesium evaporation and beam extraction (i.e. source at HV). To withstand the potentially severe EMI from RF lines and from HV breakdowns, the layout was further improved with respect to the previous tests and the entire conditioning electronic and acquisition system was enclosed in custom built

copper cabinet which proved successful. Probe measurements on different plasma conditions were performed, which were affected by tolerable noise levels.

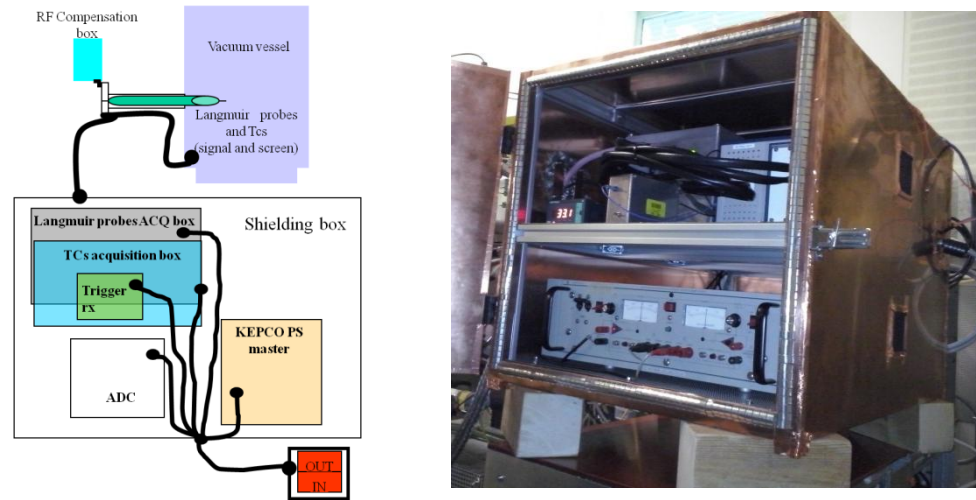


Fig. 4.26: Layout of the EP measurements in BATMAN and shielded cabinet with all electronics

During this campaign, also the latest version of the thermocouples conditioning and acquisition system, similar to that for the SPIDER source, was successfully commissioned at HV.

A different custom built circuit for TC, also for use in SPIDER and NIO1, was instead tested in the mini-STRIKE measurements in BATMAN, see Fig. 4.26.

Another important follow up was the installation of calorimetry TC on the cooling pipes of the SPIDER beam dump and the holes drilling on cooled plates, for installation of TC by RFX. Several interactions with IO and ITER India brought both better definition of the calorimetry TC cabling layout and fixing method, and more effective distribution of the holes, supported by a simple simulation of the heat load distribution.

Spectroscopy diagnostics advanced with progress in the layout [Delogu1] and with a new design of the optical heads, based on the experience on NIO1, now interfaced to optical fibres through a more robust and reliable standard connector, rather than with a custom support of the fiber optic end as before. Also the simulation and analysis code of the beam emission spectroscopy, dBES, was further improved and benchmarked against the corresponding code in use at IPP, BBC-NI, and the experimental spectra measured on ELISE.

Investigation of a suitable linear CCD camera for tomography continued with additional market surveys, purchase and test of a new camera which gave poor results, and with exploration of a more efficient way to control the Hamamatsu camera, so far only suitable detector, but with too primitive and unreliable control features. Work on tomographic inversion codes progressed [Fonnesu1].

Work on instrumented calorimeter for SPIDER, STRIKE, was mainly focused on continuation of the experiments with mini-STRIKE (a reduced size version of the full diagnostic) on BATMAN [Serianni1] and at NIFS, reported in section 4.2.6.

R&D on CFC-1D tiles stopped after mechanical failure of some small scale prototypes on the GLADIS high power beam [DeMuri1]: it has been decided to insert in the first Task Order the procurement of a full size CFC tile prototype, whose result will show if a qualified manufacturer exists.

Meanwhile alternative approaches with lower performance, especially in terms of spatial resolution, are being considered. Small scale graphite tiles were machined by both electro-erosion and saw disk machining, into a 2D array of 2.5mm x 2.5mm pillars, with 0.5 mm separation, 8mm high out of a 10mm thick tile, see Fig. 4.27. The manufacture process seems reliable, but it should be tested on a full scale tile and the machined tile should withstand the mechanical stresses induced by a high power beam like on GLADIS, similarly to what done with the CFC prototypes. The latter will be done in 2015, the former will be considered if the CFC prototypes will give negative results. So far heat conduction experiments have been performed with a focused CO₂ laser beam, like previously done with CFC tiles, and preliminary results indicate heat conduction preferentially in the perpendicular direction, as shown also by numerical simulations.

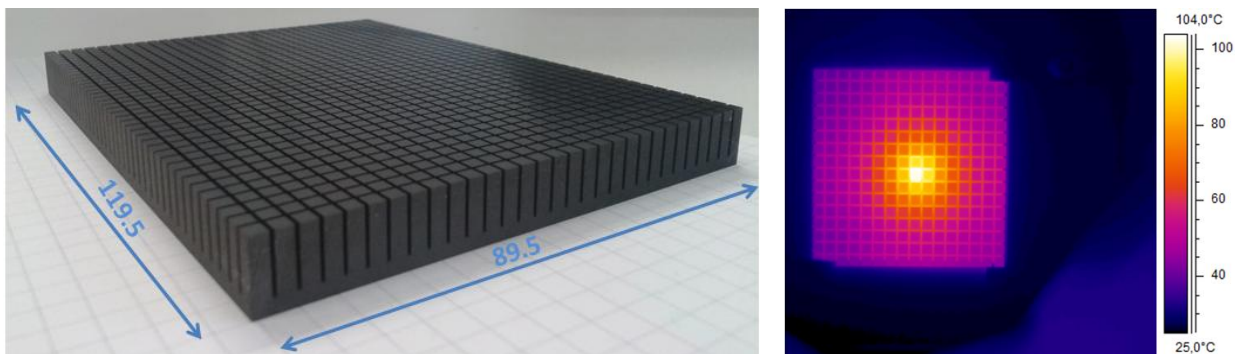


Fig. 4.27: Graphite tile machined into a 2D array of 2.5mm x 2.5mm pillars, 8mm high (left); thermal footprint on the rear side of a CO₂ laser beam focused to a 2 mm diameter spot on the front side, on a smaller prototype (right)

A different low performance alternative is a wire calorimeter, already in use on BATMAN and ELISE at IPP: a grid of tungsten wires intercepting the beam, emits visible radiation when heated at high enough temperature by the beam. So far this diagnostic has been used only for qualitative imaging. At RFX we have shown with a test bench experiment and through simulations, see Fig. 4.28, that a tungsten wire exposed to the SPIDER beam emits blackbody radiation with a spatial profile sufficiently resolved to distinguish the single beamlet and to provide information on the

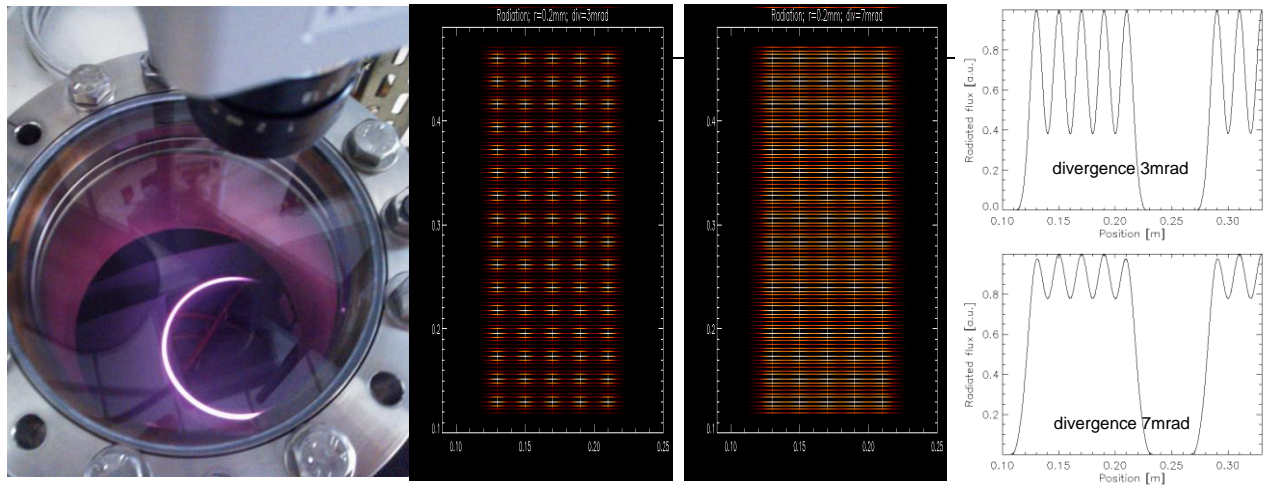


Fig. 4.28: Setup for emitted radiation calibration of electrically heated tungsten wires (left); simulation of the emitted radiation modulation along a vertical array of wires (centre) and on a single wire (right) for both 3mrad and 7 mrad divergence

beam parameters, provided the diagnostic is calibrated by heating the wires with electric current and measuring the emitted radiation with the same setup [Pasqualotto1].

An IR camera similar to that foreseen on SPIDER has been installed in ELISE to measure the H/D beam profile by observing the front side hit by the particle beam of the new instrumented calorimeter, painted by a black coating chosen after the experience on the simpler calorimeter in operation in 2013. From the analysis of the IR thermography data, based on fitting the power density matrix with 8 gaussian sub-beams, one for each beamlet group, beam divergence and homogeneity are obtained, see Fig. 4.29. The gained experience will be useful for the application of infrared thermography on SPIDER.

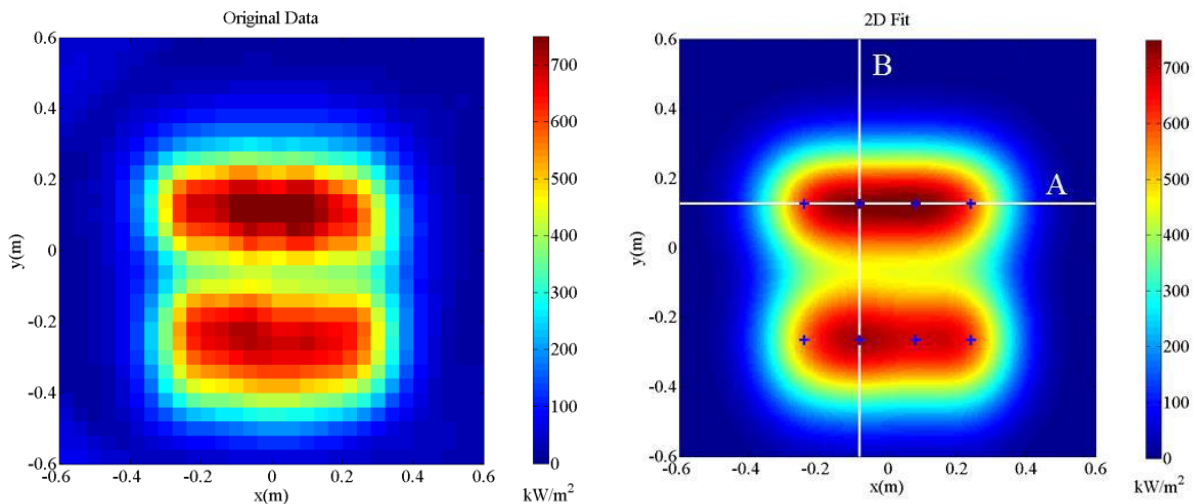


Fig.4.29: Example of power deposition on ELISE diagnostic calorimeter (left) and corresponding gaussian fit (right)

The neutron imaging diagnostic progressed with the final design and commercial investigation of the in-vacuum detector box, the cabling layout from the detector to the acquisition cabinet, with intermediate neutron shielded box for acquisition electronics just outside the exit from the vacuum vessel and further R&D on the nGEM detector [Muraro1]. In particular a second improved full size nGEM prototype was manufactured and tested both with an X-rays source and on a fast neutron beam at ISIS spallation source (UK), showing a much better and now suitable uniformity ($< 20\%$), good temporal stability and vibration immunity. Also another detector with different pixel sizes has been manufactured and tested, see Fig. 4.30, showing that larger pixels are affected by higher noise, but a much reduced noise is achieved when separating the acquisition electronics from the detector, so that even for the larger nGEM pixels of MITICA the expected noise is acceptable.

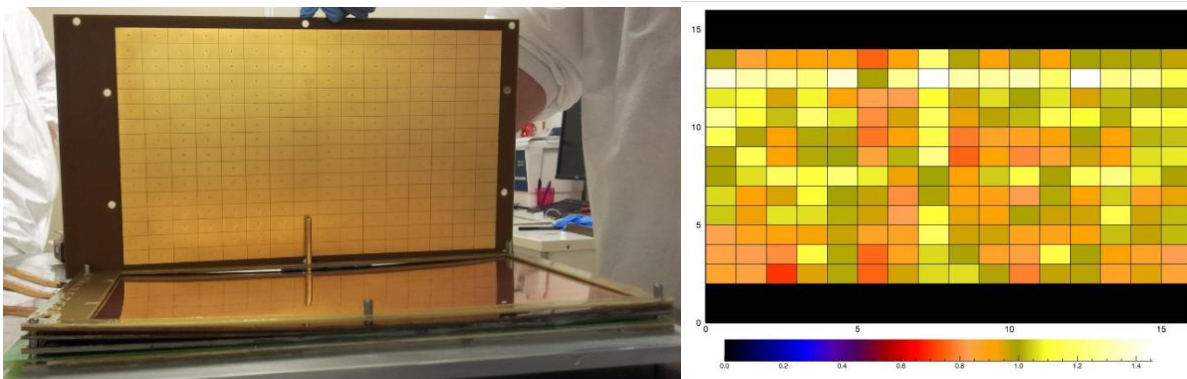


Fig. 4.30: Assembly of the second full-size nGEM prototype for SPIDER (left) and nGEM uniformity map (right)

Work on MITICA embedded diagnostics was limited to a preliminary design of the spectroscopy lines of sight and of the thermocouples layout in the source, together with a progress in the design of the thermal and other sensors integrated in the beam line components.

4.1.2.6 NBTF Control and Interlock

F4E Framework Contract for the Procurement of the NBTF Control, Interlock and Safety Systems

In the last quarter of 2013, on reply to the call for offer received from Fusion for Energy, an offer was prepared for the Framework Contract (FC) to develop the Control, Interlock and Safety systems of the NBTF [Luchetta1]. The FC will cover seven years of activity with a total manpower associated of about 50 PY. During the first months of 2014, the framework contract was finalized. In February 2014 it was awarded to Consorzio RFX and finally signed on 9 April 2014.

The first specific contract was then prepared in the second quarter of the year. It includes the construction, installation and commissioning of the SPIDER Central CODAS, part of plant system CODAS (interface to Plant Systems) and the Central Interlock System. The Specific Contract no. 1 was signed on 30 July 2014. It is expected to be completed by autumn 2015.

The first order for the procurement of the data acquisition hardware for the SPIDER power supply systems, thermocouples and miniCODAS has been issued at the end of the year.

SPIDER Control and Data Acquisition System

In the first part of the year the design of the CODAS was completed with the definition of the technical specifications of the computers and data storage system and of the plant operation, streaming data and offline networks [Barbato1].

In parallel the definition of the SPIDER CODAS interface to ISEPS, AGPS, Cooling Plant and Gas and Vacuum System was progressed. In details, the ISEPS human machine interface was developed and commissioned and tests were carried out at RFX, with the collaboration and presence of colleagues from ITER India, to exchange data between CODAS and AGPS.

Fast control for power supply and fast data acquisition was implemented and tested. [Luchetta2]

SPIDER Central Interlock System

The Technical Specifications for the SPIDER Central Interlock (CIS) were completed and the system is now ready for subcontracting [Pomaro2]. CIS is based on three components linked with a loose interface as shown in Fig. 4.31: i) the slow interlock subsystem provides interlock functions with a total reaction time (from fault detection to emission of protection commands) of 10 ms; ii) the fast interlock subsystem is devoted to the protection of the power supply systems and its reaction time is faster than 10 μ s; iii) the thermal protection subsystem is devoted to acquire temperature signals from SPIDER critical components (source and beam dump).

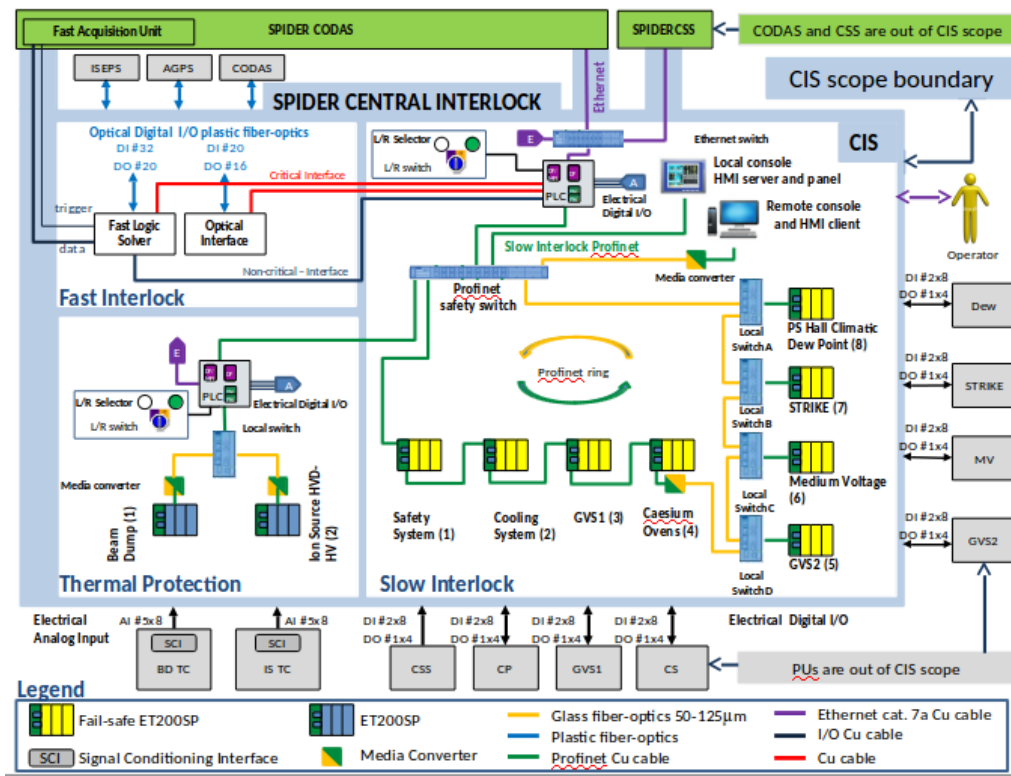


Fig. 4.31: Architecture of the SPIDER Central Interlock System

MITICA CODAS and Central Interlock Systems Central Interlock System

The requirements for architecture of MITICA CODAS were finalized and the conceptual architectures of MITICA CODAS and Interlock were defined [Luchetta3, Pomaro3].

4.1.3.7 NBTf Safety

The aim of the PRIMA Safety System is to deal with all the safety hazards and manage safety risks in a coordinated way, adopting all the prevention and protection measures necessary to grant health and safety of people doing any kind of working activity in the PRIMA facility.

During 2014, the architecture of the PRIMA Safety System has been defined in order to satisfy the risk assessment. Moreover, according to IEC/EN 61508 - IEC/EN 62061, the Safety Integrity Level (SIL) of the protection functions of the Central Safety System (CSS) has been determined.

Fig. 4.32 shows the proposed architecture of the the Central Safety System (CSS). , The requirements concerning protection, functional, general design, hardware and software aspects have been defined also. During the design phase, interfaces and signals among CSS, its subsystems, experimental and conventional Plant Units have been developed.

The general architecture of the PRIMA Safety System, see Fig. 4.32, is divided into two integrated subsystems:

- Organizational safety;
- Personnel Protective Equipment: to be adopted for collective and personnel protection of workers during activities;
- Notices: measures to point out potential risks for the safety of the human health;
- Procedures: measures to carry out operational activities in safe conditions;
- Central Safety System: CSS is a fail-safe system devoted to the personnel protection. Its main purposes are to manage, by means of a CSS supervisor, dangerous events occurring in one or more Plant Units (PU) minimizing adverse consequences for the personnel, and to permit a safe human intervention putting the Plant Systems (SPIDER and MITICA) in safe conditions/configurations by mean of a sequence of operations.

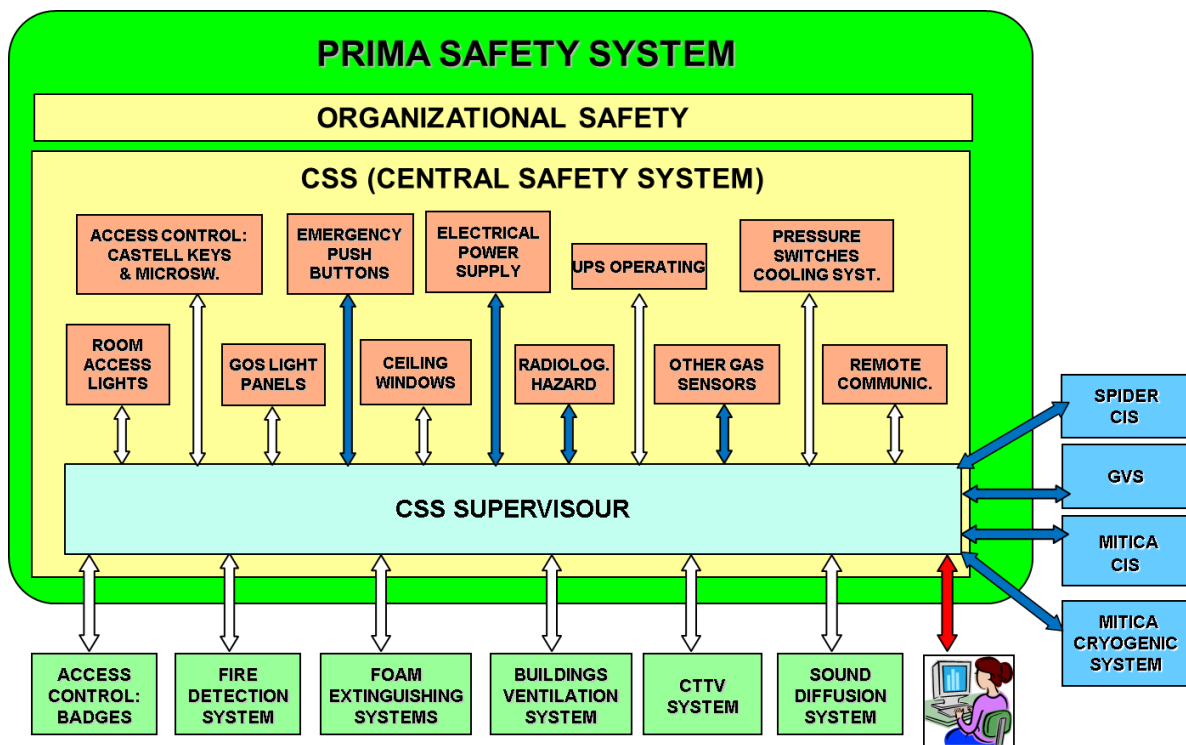


Fig. 4.32: Architecture of PRIMA Safety System

4.1.3 MITICA

4.1.3.1 Introduction

During 2014 the work has been focused on:

-
- Support to F4E in the CfT activities relevant for the procurement of the MITICA Vessel, HVD1 and HVD1-TL2 Bushing, AGPS&GRPS and cryo-plant
 - Finalization of the design of the Beam Source and Handling tool up to release of the tech spec documentations
 - Completion of the design of beam line components and preparation of drafts of tech spec documents
 - R&D activities in support of the design developments of Beam Source and Beam Line Components [Dalla Palma1, DallaPalma2, Agostinetti1, Agostinetti2, Pilan1, DallaPalma3].
 - Support to F4E in the preparation of the tech spec documentation for the procurement of the SF6 Gas Storage and Handling Plant

Moreover during this year the integration of the HV components to be delivered by the Japanese Domestic Agency has progressed including the finalization of the interfaces of the AGPS overall system and Transmission Line with buildings and auxiliaries.

The procurement contracts of the MITICA Vessel and HVD1 and HVD1-TL2 Bushing have been signed by the end of 2014, while the signature of the procurement contracts of AGPS&GRPS, Beam Source and cryo plant will be done during 2015.

4.1.3.2 MITICA Vacuum Vessel

The procurement contract for manufacturing of MITICA Vacuum Vessel was launched and awarded during 2014. Drawings and Technical Specification for launch of Call for Tender by F4E were completed and finally revised by RFX after comments and verifications by IO and F4E.

The Call for Tender was launched on 25th April 2014 and the period for preparation of offers was extended up to 8th August 2014. The Tender evaluation process took place from August to October 2014. Finally the contract was awarded by F4E to the winner (De Pretto Industrie (I)) on 5th December 2014.

RFX gave support to F4E during the whole year preparing technical documents (Technical Specification, CAD model and 2D drawings), answering the bidders' technical questions and participating to technical evaluation of the offers.

The contract is now signed and the kick-off meeting is foreseen at F4E in Barcelona on 21st - 22nd January 2015.

An overall view of the MITICA Vessel is shown in Fig. 4.33. The procurement includes manufacturing, pre-assembly and tests at the factory and the final assembly at PRIMA Site.

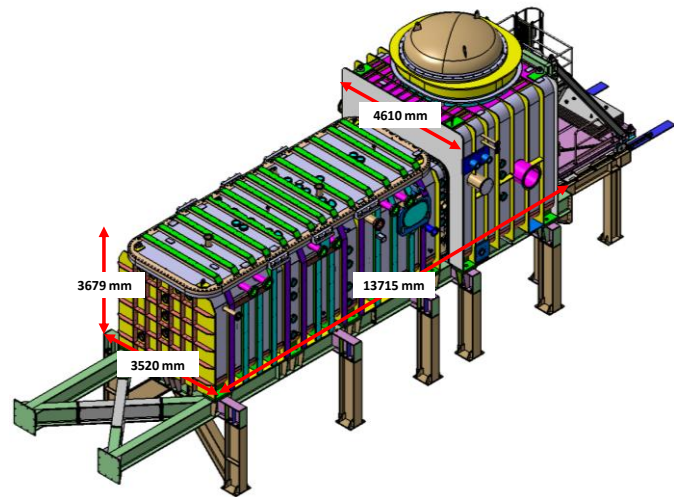


Fig. 4.33: The MITICA Vacuum Vessel

4.1.3.3 MITICA beam source

The MITICA beam source design has been finalised in 2014 and the preparation of the set of drawings for the completion of the procurement technical specification is expected during January 2015.

In Fig. 4.34 the present status of the design of the whole source is shown.

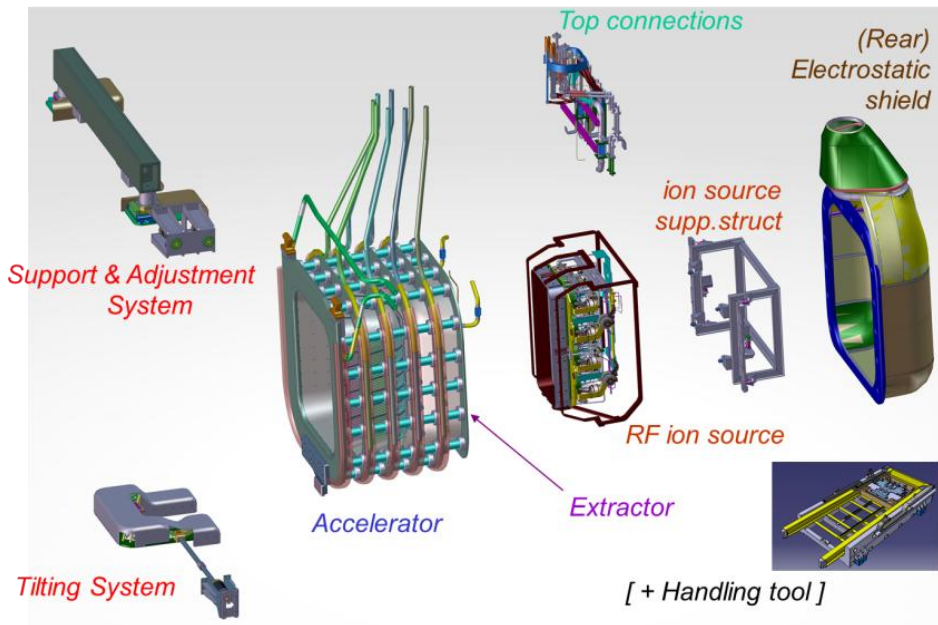


Fig. 4.34: MITICA beam source – exploded view

R&D activities (Fig. 4.35) initiated in 2012 were continued during 2014.

Manufacture of post-insulator prototypes with solid cylindrical geometry started during 2013 led to the completion of the first set of tests. Mechanical tensile tests showed strength results of the component in the chosen configuration, representative of the most loaded element, in the order of

30-35 kN, while a target of 50 kN had been identified and much higher values were expected from numerical calculations. (Fig.4.35)

On the other hand, electrical tests carried out in the HVPTF facility gave immediately positive results: voltage was brought gradually up to 240 kV and kept for several hours without issues [Pilan]. Additional tests in parallel helped the understanding of possible influence of magnetic field on the voltage holding [Pilan2]

Thorough discussion with the involved company allowed to identify the cause in a manufacturing issue for such a big solid ceramic part leading to a non-perfect sinterization and to define two revised solutions (completely or partially hollow). Manufacturing of new prototypes was completed with no issues and first tests are very promising, as the completely hollow geometry reached unharmed 80 kN.

Heterogeneous joint samples manufactured with the VTTJ technique patented by RFX were subjected to a set of tests dedicated to qualify finally and formally the solution for ITER environment (Fig.4.35). Heterogeneous joint samples including Electron Beam Weld technique were finally manufactured and pressure-vacuum tested, giving positive results for the configurations relevant for the grids [Agostinetti2].

A major design effort has been dedicated to finalize the source design. After FDR taken place in January, an extensive effort to develop all the mechanical details was paid, in parallel to the solution of the outstanding issues, some of which are described hereafter.

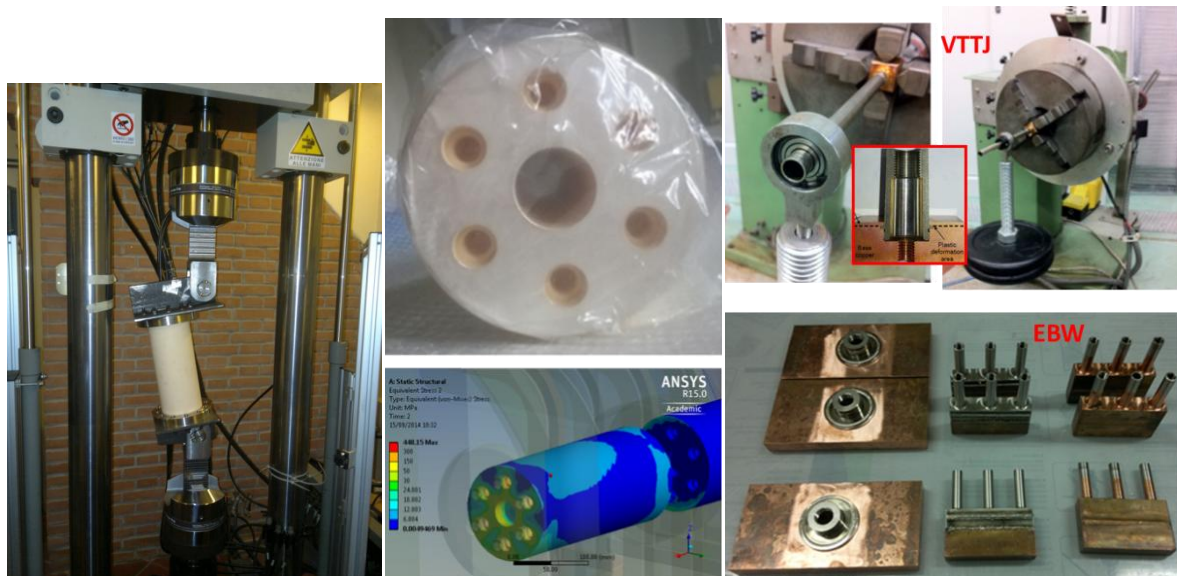


Fig. 4.35: R&D main results in 2014 – (a) numerical simulations and mechanical test on accelerator ceramic insulators, (b) tests on heterogeneous joints obtained by VTTJ and EBW techniques

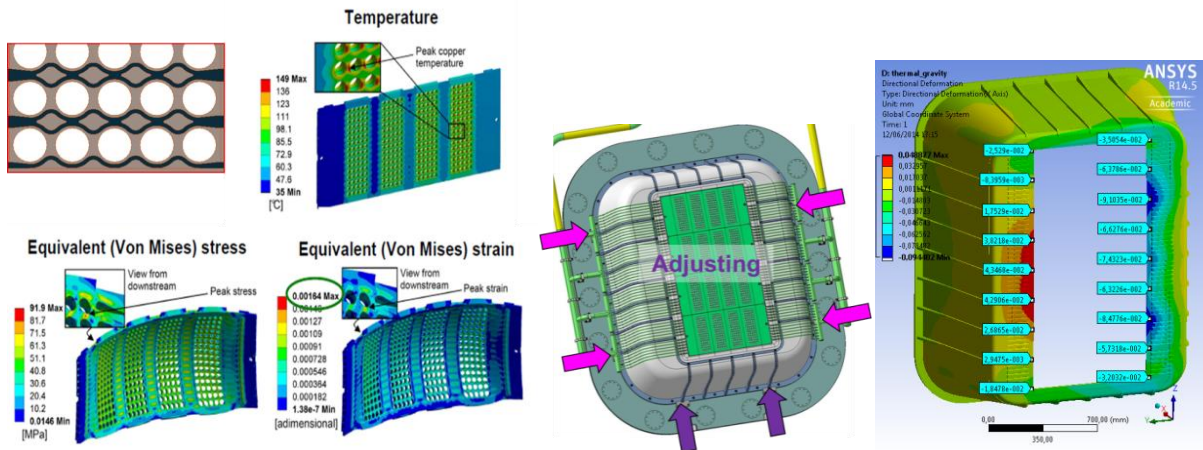


Fig. 4.36: Accelerator design revision – (a) optimization of cooling channels and thermo-mechanical behavior, (b) development of assembly and alignment procedures and related verifications

An integrated mechanical design was developed to optimize the demanding assembly and alignment procedure of the accelerator structure, including adjusting elements that will allow final precise positioning of the grids after final assembly, also taking into account the different operation temperature of the various parts (Fig. 4.36).

Revised geometry of the cooling circuit of the grids allowed satisfying all the requirements and verification according to ITER SDC-IC norm (Fig. 4.36), with relation to the latest power loads from the beam particles [Sartori2][Sartori3][Sartori4][Marconato1]. A brand new electron dump was added on the inside of the Grounded Grid support frame in order to exhaust the heat from electrons leaking out of the accelerator and to prevent a thermal deformation of the support frame, detrimental for grid alignment. (Fig. 4.37)

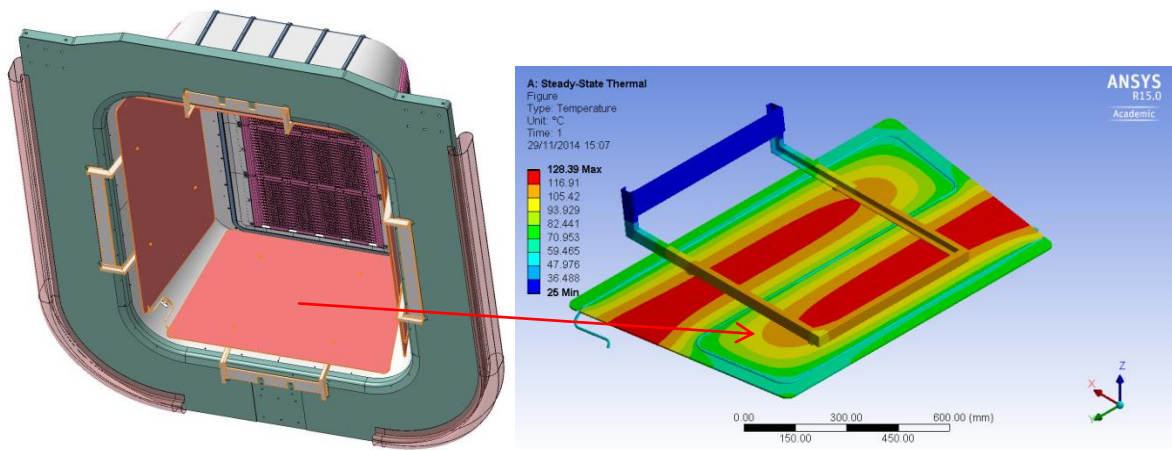


Fig. 4.37: Electron Dump on GG support frame and related thermo-mechanical verifications

Complex interfaces with HV Bushing, including -1 MV screen, were finally completed, including interfaces with RH tools and related procedures to (dis-)install the source body inside the vessel and thermal analysis to verify compatibility of temperature behaviour of the service line set to the manufacturing and operational requirements (Fig. 4.38).

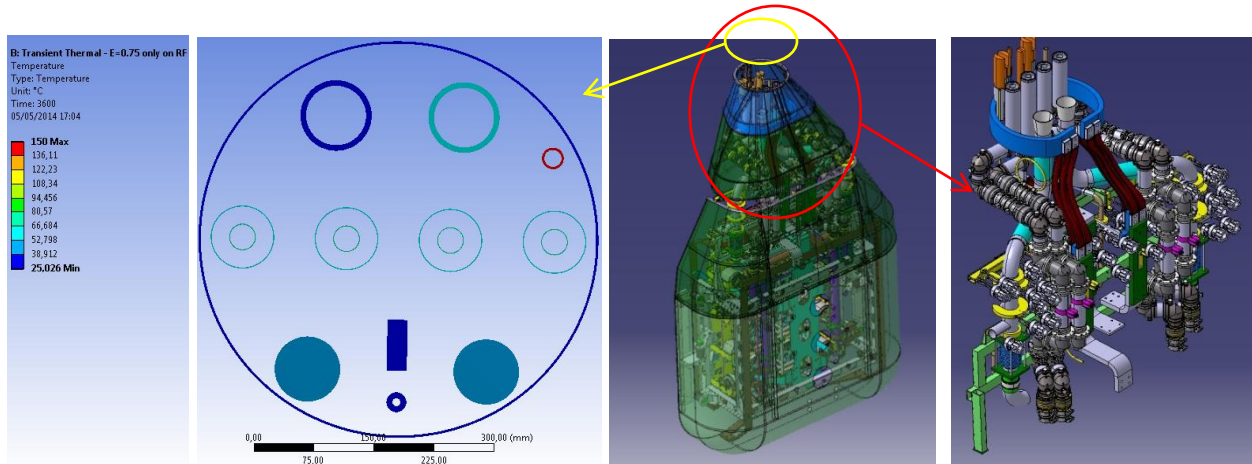


Fig. 4.38: Connections with HV Bushing – thermal simulation of in-vacuum radiation heat exchange and final detailed design

Further developments and verifications were carried out also on critical parts like the rear vertical plate of the source case, featuring explosion bonding of Mo on copper in order to resist to the highly focused beamlets of back-streaming positive ions (Fig. 4.39).

Also other measures were taken in order to minimize the loads on the ceramic insulators, like the revision of the design of the GG flange next to the support beam interface and of the tilting system (Fig. 4.40).

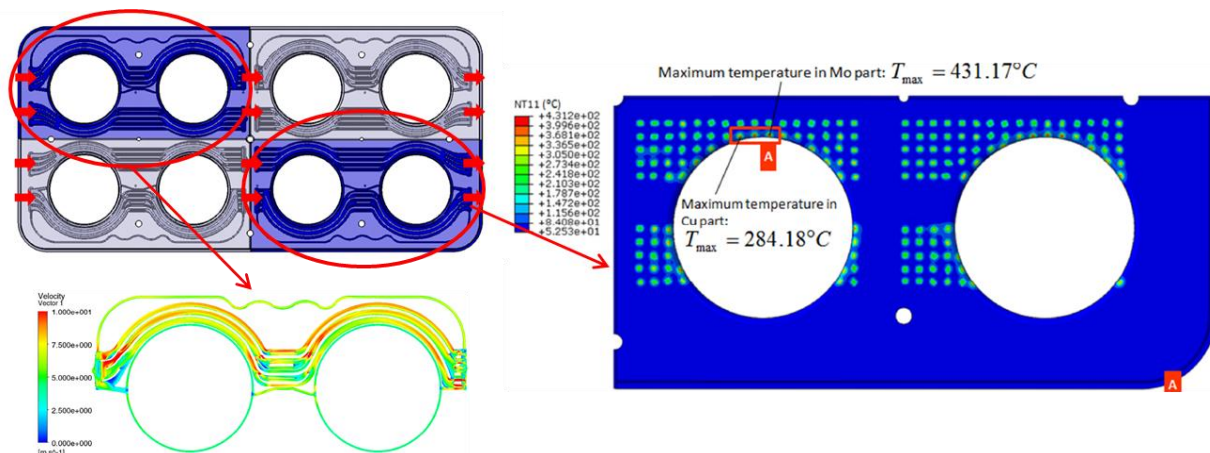


Fig. 4.39: Fluido-dynamic and thermo-structural final verifications of source case vertical plate

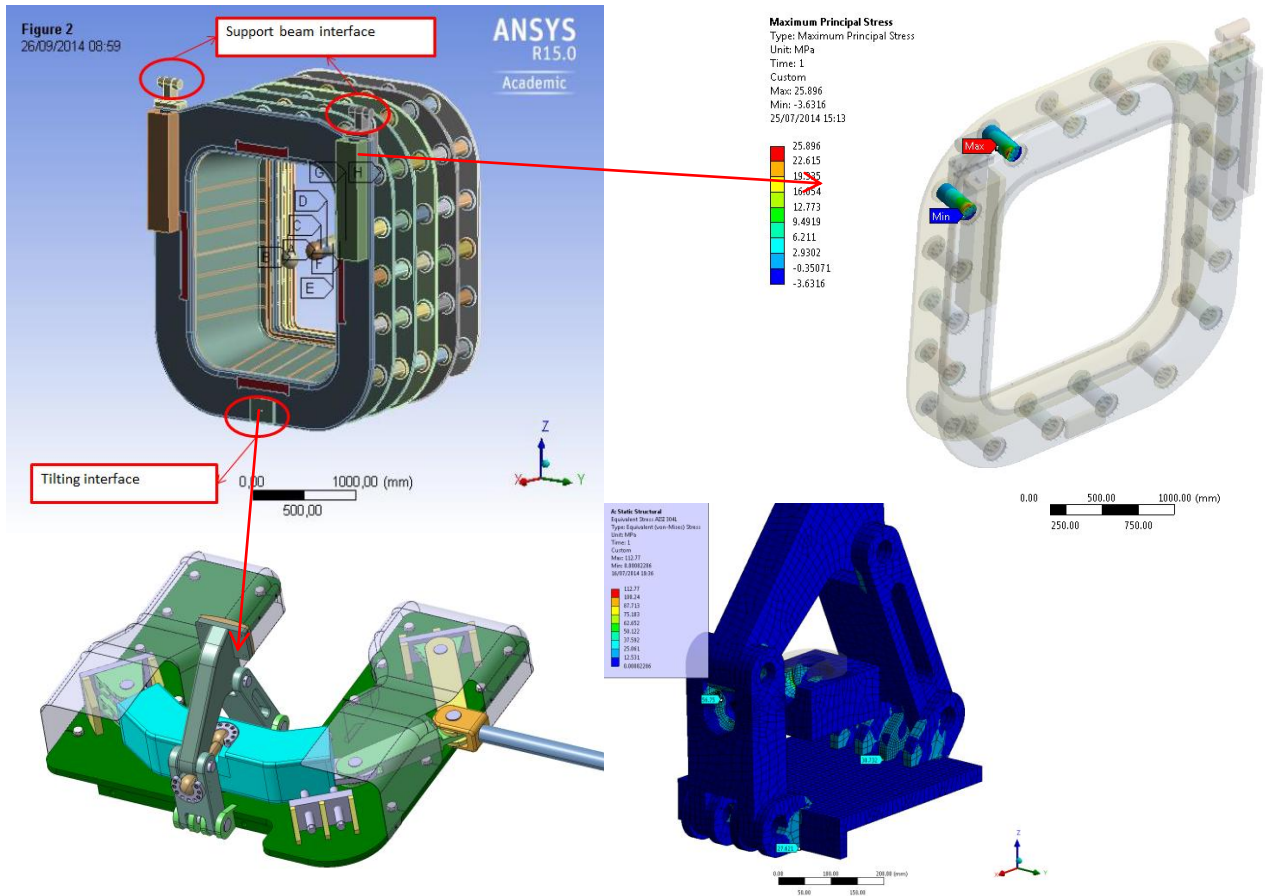


Fig. 4.40: Design optimization related to GG flange and tilting system for stress minimization on ceramic insulators, and related numerical verifications

The Handling Tool to (dis-) install the Beam Source in MITICA vessel was completely designed and verified (Fig. 4.41).

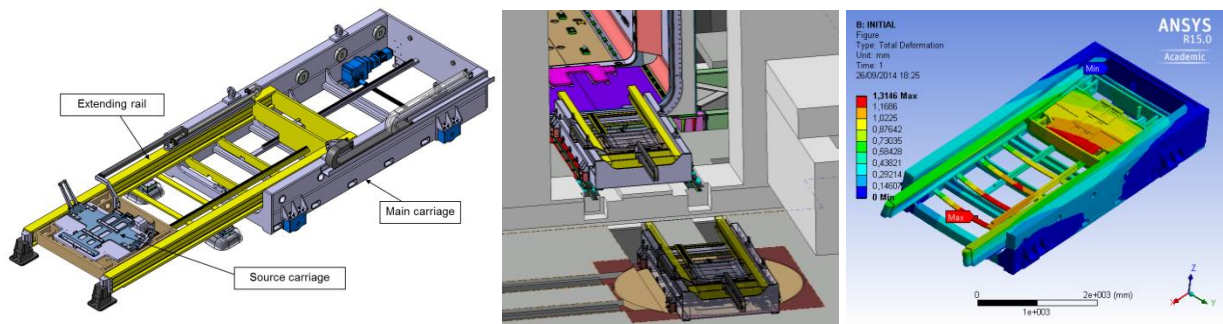
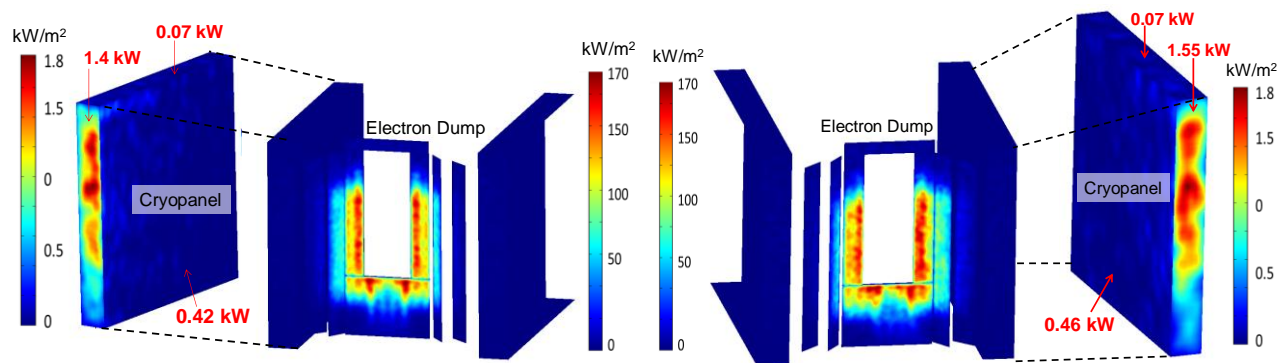


Fig. 4.41: Beam Source Handling Tool - final detailed design, integration in the buildings and numerical verifications

4.1.3.4 MITICA Beam Line Components

The design of the MITICA Beamline Components (Neutraliser, RID, Calorimeter) was progressed during the 2014 towards the finalisation [DALLAPALMA4]. The design developments were addressed considering the actions agreed with IO and F4E during the Final Design Review (FDR) meeting held on January the 28th in order to evaluate recommendations and observations collected as FDR chits.

Simulations of the optimized MITICA accelerator design estimate 450 kW carried by co-accelerated stray electrons. The trajectories of these electrons in regions far from the beam were simulated with the Monte Carlo BACKSCAT code which considers local electro-magnetic fields, electron reflections at walls, and secondary emission. Results were used to improve the design of the Electron Dump (ED), protecting the cryopump from electrons, and to estimate thermal loads on Neutraliser leading edges and on the vessel surfaces. The magnetic fields considered are: 0.6mT average horizontal due to plasma grid filter and 0.1mT vertical as in ITER NBIs. With the improved ED design, the total power transmitted to the cryopump was minimized as shown in Fig. 4.42. Analyses to approach coherently the production of secondary particles originated from the interaction of the beam with background gas were undertaken with the Samantha code to obtain: a) the optimised stray field at the RID avoiding acceleration of electrons towards the cryopump; b) 58 A coming from particles deposited on the RID walls and drawn to the feedthrough providing the biasing voltage.



a) MITICA configuration (without vertical magnetic field) b) ITER NBI configuration (0.3mT vertical magnetic field)

Fig. 4.42: Electron power density contour [kW/m²] and power [kW] on each panel

Beside the beam neutralisation efficiency, the gas density distribution plays an important role in stripping re-ionisation, additional thermal loads, beam diagnostics and in voltage holding for possible breakdowns at the accelerator and RID regarding the Paschen law. While in the past the gas density profile was studied as averaged values along the beam line, three-dimensional

distributions were evaluated modelling the geometrical details and dimensions of in-vacuum components with Avocado code. The geometry of the ED was optimised with Avocado as a trade-off among different aspects: the reduction of gas conductance from the Beam Source to the cryopump, the protection of cryopanel against co-accelerated electrons, and the possibility to remove from the vessel the ED with the Neutraliser during maintenance operations. By adding the ED, the gas pressure in the Beam Source region is expected to rise from 0.019 Pa to 0.025 Pa (see Fig. 4.43).

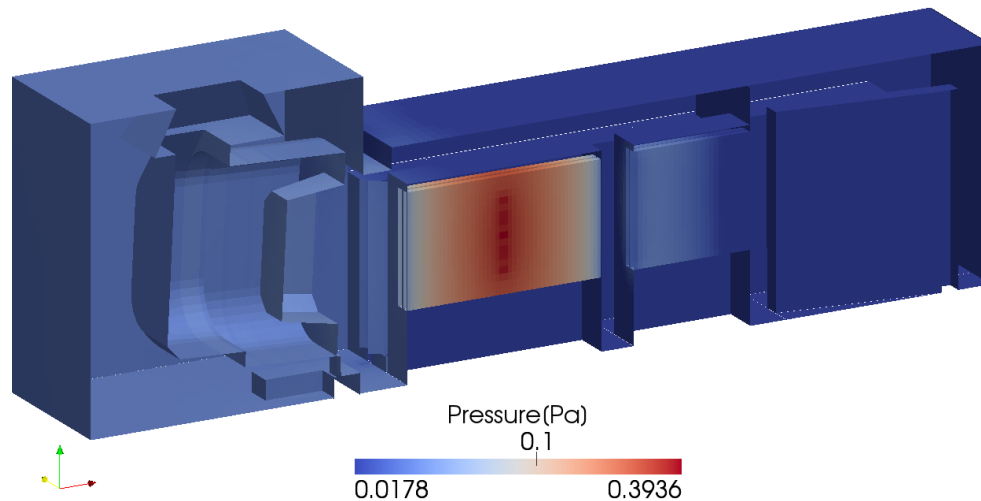


Fig. 4.43: Simulation of gas density spatial distribution

The high voltage walls of the RID will be electrically insulated by two cooling breaks at the main cooling manifolds and by standoff insulators at the supporting structure. The geometrical optimization of standoff insulators at the RID walls was constrained by considerations on machinability, metal-ceramic joining, and minimization of the ceramic volume. The surfaces of ceramic will be protected from deposition of sputtered particles by screens deforming the spatial electric field. Electrostatic analyses were carried out for the cooling breaks considering for the ceramic an internal diameter of 100mm and a length of 230mm; the field intensities resulted below the limits. Considering an electric current drawn throughout the demineralised water (grade 2 as for ISO 3696) flowing inside the cooling breaks, any substantial difference in the potential distribution can be observed (see Fig. 4.44). With the average biasing voltage of 20 kV, a leakage current through the inlet and outlet cooling breaks of 0.11A (25°C) and 1.1A (80°C) respectively will occur, corresponding to an additional current of 1.2A to be sustained by the power supplies. The breakdown voltage was verified for planar surfaces as all significant edges will be rounded

and the minimum distance will be 50 mm whereas the allowable distance is 8.4 mm for maximum 25 kV.

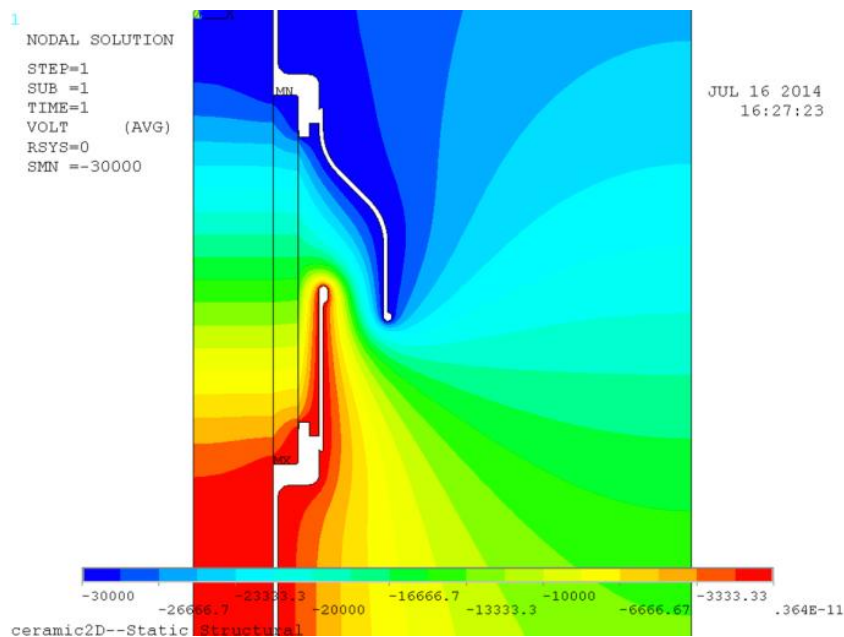


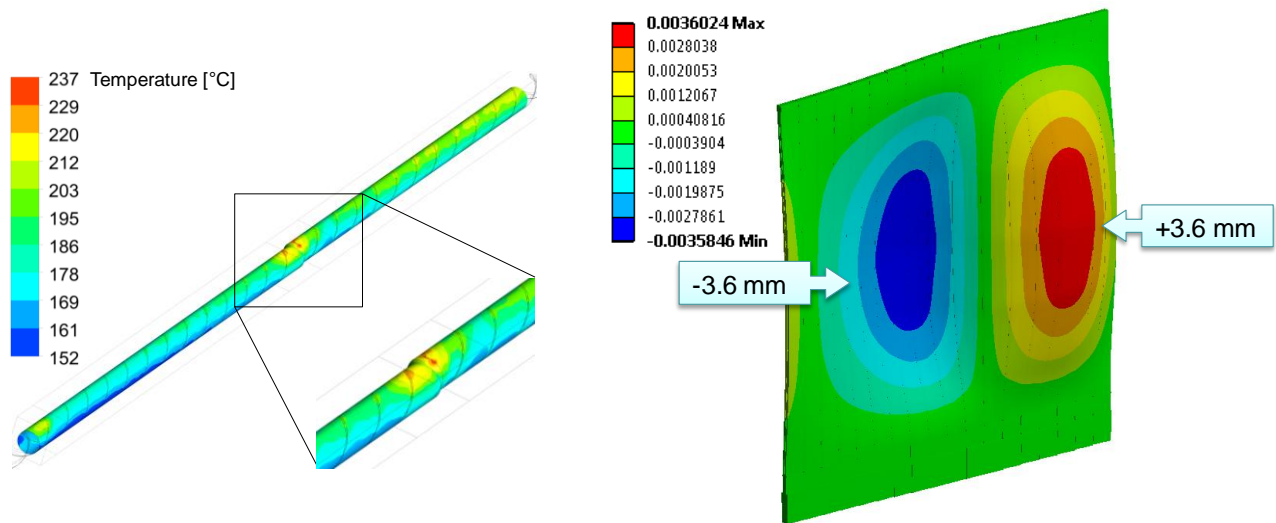
Fig. 4.44: Voltage contour [V] of resistive analysis of cooling breaks

All panels exposed to the particle beam are actively cooled with demineralised water and thermally controlled carrying out protection and calorimetry measurements with thermal sensors that were properly located. The penetration of signal conductors through the confinement boundary of the vacuum vessel was designed developing double and single barrier feedthroughs [DALLAPALMA4]. The demanding heat transfer conditions are sustained by twisted tape inserts that induce convective flow modes moving the vapour bubbles nucleated at the channel inner wall into the subcooled bulk; turbulence is promoted realising a proper twist ratio defined as $k=\pi \cdot D / p t$, where D is the cooling channel diameter and $p t$ is the pitch of the twisted tape. Customised routines were linked with the Finite Element (FE) code ANSYS and used to simulate this subcooled boiling condition in the cooling channels to obtain distributions of thermo-mechanical parameters. The water flow rate to the Beamline Components was verified and fixed considering the deposited beam power and the maximum water temperature: 55kg/s to exhaust the 6MW at the Neutraliser, 100kg/s for the 18MW at the RID, and 100kg/s for the 18MW at the Calorimeter. The flow rate partitioning among cooling channels was verified carrying out mono-dimensional FE analyses of the fluid field supported by CFD analyses to characterise the flow behaviour in fittings and complicated local geometries. The flow parameters at the double side drilled cooling channels of the Beam Stopping Elements (BSEs) were investigated and optimized; the flow temperature

distribution in convective conditions is shown in Fig. 4.45 a). A summary of hydraulic parameters is presented in Table 4.1 considering 35°C inlet temperature and 20 barA inlet pressure provided by the ITER cooling system.

Table 4.1: Hydraulic parameters for the Beamline Components of MITICA and ITER NBI

Cooling circuit	Max power density [MW/m ²]	Water flow rate [kg/s]	Water velocity [m/s]	k	Max heat transfer coeff. [kW/(m ² K)]	Max channel wall temp. [°C]	Flow non-uniformity	Max water temp. [°C]
Neutraliser leading edges	5	1.2	6.5	0.8	60	210	0.6%	100
RID beam stopping elements	6	1.34	5.4	0.9	50	227	1.6%	130
Calorimeter swirl tubes	13	1.04	6.0	1	100	312	2%	138



a) Flow temperature distribution in the RID b) Displacements [mm] of the RID middle wall cooling channel with swirled tape under beam-on thermal loads

Fig. 4.45: Thermo-mechanical analyses of the RID middle wall under beam-on thermal loads

As the ITER NBIs will operate 5-10⁴ beam-on/off cycles, the Beamline Components have been verified according to Structural Design Criteria for ITER In-Vessel Components for fatigue and

ratcheting damage. The fatigue life consumptions were calculated: 9% at the Neutraliser leading edges, 90% at the BSEs, 66% at the Calorimeter swirl tubes. The corresponding deformation plot of a RID middle wall is shown in Fig. 4.45 b). Furthermore, $4.5 \cdot 10^5$ thermal cycles are expected for breakdowns at the accelerator grids. The strain ranges corresponding to breakdowns are considerable only at the swirl tubes with a maximum fatigue life consumption of 9%.

The design of the ceramic elements depends strongly on the production process and is not covered by any standard; thus, proof testing is required to qualify the products. FE modelling was used to: a) obtain the stress distribution to quantify the probability of failure and so defining the required allowable properties of the ceramic material, b) estimate the forces acting at the boundaries and produced by the complex operational conditions; these forces will be properly amplified to determine proof testing conditions. The survival of the component to proof testing will exclude the occurrence of damage due to lesser loads experienced during the required life. On the other hand, too high and prolonged test levels can cause unnecessary damage.

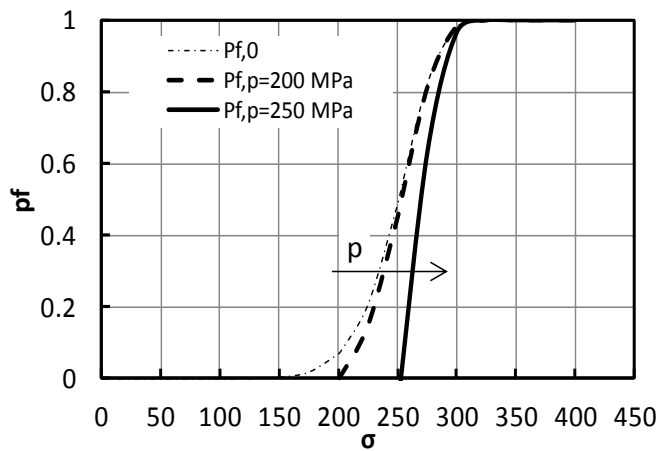


Fig. 4.46: Failure probability during life of cooling breaks depending on proof test levels

The two cooling breaks at the main cooling manifolds and the standoff insulators at the supporting structure of the RID will be produced by metal-ceramic joining of Kovar to polycrystalline alumina, the latter with a high purity level compatible with the radiation environment, small average defect dimension with reduced variability in size (Weibull modulus $m > 10$), negligible corrosion and creep below 800 °C, and limited susceptibility to slow thermal cycles. The maximum force results 4.5 kN (compressive) due to the sole weight, with an increase of 0.5 kN and a transverse force of 0.6 kN when thermal deformations of wall panels and piping assembly are considered. These forces produce maximum principal stresses σ_1 below 10 MPa. The cooling breaks are subjected to water pressure and displacements caused by thermal deformations transmitted by the cooling tubes.

These loads increase the stress levels from $\sigma_1 \approx 10 \text{ MPa}$ to 100 MPa . The failure probability versus operational stress with different proof test levels is represented in Fig. 4.46.

Special Research & Development (R&D) and Return On eXperience (ROX) investigations were undertaken to support the design of the Beamline Components, especially regarding the water-vacuum barriers of tubing and actively cooled elements made of Stainless Steel (SS) TP316L, Oxygen Free (OF) copper, and CuCr1Zr alloy. Butt welding is identified consistently with the ITER vacuum requirements as the main technique to implement as much as possible using automated welding heads. The technique was investigated for similar and dissimilar metal welds (SS to OF copper and SS to CuCr1Zr) with the interposition of an Inconel element in order to adjoin mutually soluble metals.

Liquid state diffusion bonding was investigated for the RID cooling breaks, being the most common method of manufacturing long term stable joints ensuring leak tightness ($10^{-10} \text{ Pa}\cdot\text{m}^3/\text{s}$ helium leak rate) and high integrity joints with tensile strength around 100 MPa . Metal ends are Ni-plated and the alumina part is metalized with Ag-Cu-Ti to resist to water corrosion. In the metal to ceramic joint a foil of filler metal (high-purity silver-copper eutectic for vacuum bonding, Cusil™) is used as an interlayer to aid the bonding process and to uniform post-bond stress distribution. The process produces coalescence of metals and forms intermetallic compounds in a diffusion zone by heating to $780 \text{ }^\circ\text{C}$.

The thickness of the cooling pipework was optimised considering the applied loads (mainly the water pressure of 20 barA) and avoiding the transmission of displacements on the ceramic insulators during beam-on operations, installation, and seismic events.

4.1.3.5 MITICA Cryopumps and Cryoplant

The design and preparation of technical documents for MITICA Cryopump Call for Tender was in charge of ITER Vacuum Group during 2014. The final Technical Specifications, drawings and CAD model are expected by January-February 2015 for following verifications and integrations by RFX and F4E. Call for Tender is presently foreseen by F4E within the end of 2015.

However all interfaces of Cryopumps have been passed by IO during 2014 to F4E/RFX to allow the necessary integration checks and adaptations of MITICA Vessel interfaces.

As regards the MITICA Cryogenic Plant the final Technical Specification have been deeply integrated and checked by RFX during March-June 2014 and finally delivered to F4E on 30th June 2014.

F4E is presently preparing all documentation necessary for the Competitive Dialogue Procedure for the procurement of MITICA Cryogenic Plant. The Dialogue Phase is foreseen to start on March

2015. Then the Technical Specification are foreseen to be finalized basing on the feedback coming from the Companies at the end of July 2015. The launch of Call for Tender by F4E is expected in August 2015.

4.1.3.6 MITICA Power supply systems

Fig. 4.47 shows the circuit diagram of the MITICA power supply system.

The power supply system of MITICA includes, similarly to SPIDER, a set of power supplies feeding the active components of the ion source (MITICA Ion Source and Extraction Power Supplies, MP-ISEPS) at a potential of approximately -1MV , a Ground Related Power Supply (GRPS) for the Residual Ion Dump and a further system, the largest in terms of power, supplying the beam accelerator composed of five stages of -200 kV each (MITICA Acceleration

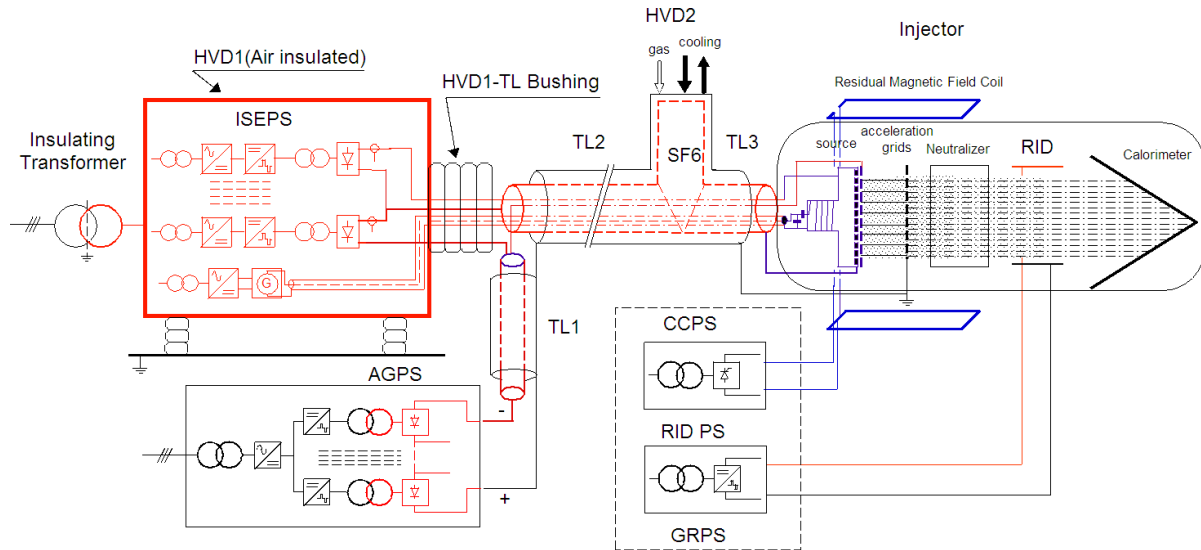


Fig. 4.47: circuit diagram of MITICA power supplies

Grid Power Supply, MP-AGPS). The procurement of the latter system is split between JADA and F4E. In particular, the MP-AGPS DC Generation system (AGPS_DCG) including high voltage transformers with the rectifier diodes on top fall within JADA scope of procurement, as well as the SF₆ (6 bar) insulated transmission line; instead, the AGPS Conversion system (AGPS-CS) is part of the F4E procurement. The MITICA power supply system includes two High Voltage Decks:

- HVD1 and the associated HVD1-TL bushing for connection to the Japanese transmission line, procured by F4E and hosting MP-ISEPS
- HVD2, procured by JADA, feeding the ion source and the intermediate voltage stages with cooling water and operating gases

A 3D view of the MITICA power supply HV components is shown in Fig. 4.48.

The European components are procured by means of four contracts:

- AGPS-CS & GRPS
- HVD1 and HVD1&TL Bushing
- MP-ISEPS
- SF6 Gas Storage and Handling Plant (GSHP)

On the AGPS-CS and GRPS [Zanotto1], in the first part of 2014 support has been given to the F4E review of the technical specifications previously delivered by RFX. RFX also supported F4E in the definition of the technical contents for other Call for Tender documents. After the launch of the Call for Tender in October, assistance has been given in answering technical queries from companies and in attending the information day organised by F4E at the beginning of December in Barcelona.

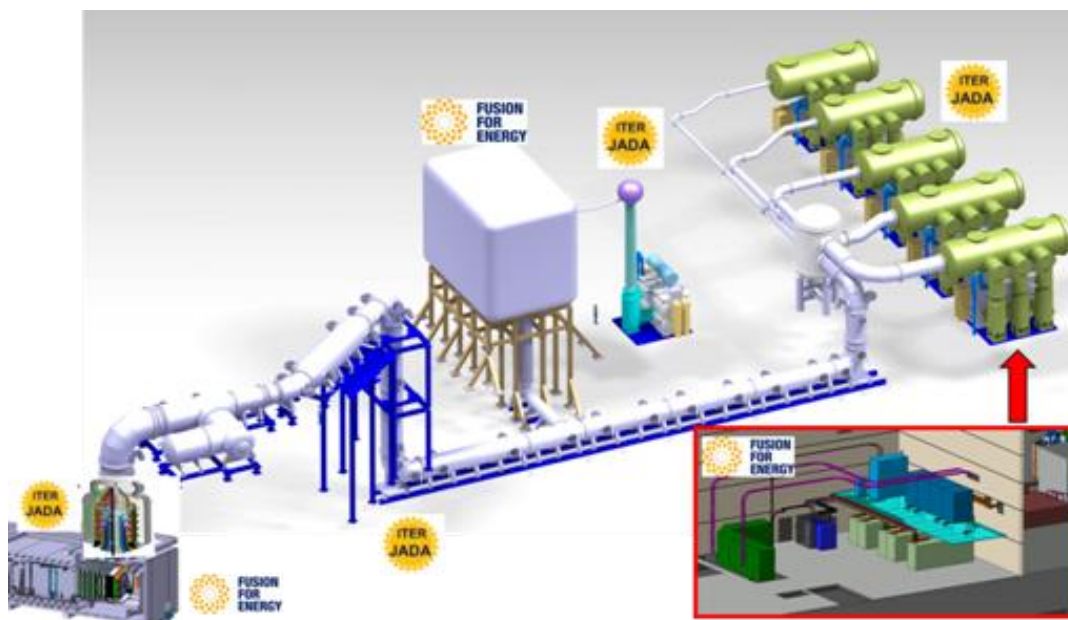


Fig. 4.48: 3D view of the MITICA power supply HV components

Regarding HVD1 and HVD1-TL bushing procurement, the associated contract was signed at the end of 2014 and the 2014 activities, lighter than anticipated, are summarised below:

- Review with F4E of the tech spec, also in the light of the experience with ISEPS and HVD of SPIDER regarding the requirements associated to ISEPS positioning

-
- Answers to comments received by F4E from the Supplier in advance of the signature of the contract

On MITICA ISEPS (MP-ISEPS), although the associated contractual stage was released by F4E at the end of 2014, some activity was carried out during the year as listed below:

- Identification of design changes (deviations) implemented on SP-ISEPS and applicable also to MP-ISEPS
- Identification of design changes not implemented on SP-ISEPS but applicable to MP-ISEPS. The most significant of these is the investigation of the feasibility of a RF generator with solid state technology. The activity was carried out by the Supplier and has been supported by RFX with response to technical queries related to performance specifications, behaviour of the RF load, site conditions and constraints etc.

The launch of the CfT of the SF6 GSHP system is foreseen around the middle of 2015. The Technical Specification documents will be prepared directly by F4E with the support of RFX. During 2014, RFX staff has contributed to work on this topic revising the conceptual design of the GSHP system, including volume and quantity of SF6 gas necessary for the operation, layout, interfaces with the HV components, with the auxiliaries, etc.

In 2014 the work for coordination and integration with the Japanese scope of procurement has been very significant. Three main goals have been pursued:

- to finalize the interfaces between JADA components and buildings and auxiliaries;
- to finalize the interfaces between JADA components and other plant systems procured by F4E; i.e. cooling plant, AGPS-CS, HVD1-TL Bushing, Vessel, Beams Source, SF6 GHSP, etc.
- to organize the JADA on-site installation activities the beginning of which is expected in December 2015

The more significant events have been:

- 3 Interface Management Meeting (IMM) each of three days of duration, managed by IO, of which one hosted in Naka and two at Consorzio RFX;
- 4 visits of one week each of JAEA members to Consorzio RFX to discuss in particular the organization of the installation activities and possible support by EU members (F4E, Consorzio RFX). During these events, meetings with potential Italian installation companies have been organized by NBTF Team;

-
- weekly meetings and exchanges with JADA, F4E and the IO in order to address many interface open points, the main ones being:
 - buildings re-design associated to the new layout for the 1-MV Insulating Transformer from JADA (structural design, layout, safety etc.);
 - readjustment of drawings of the pits, tranches and concrete slabs supporting DCG's components and Transmission Line components on the basis of the detailed design of these components;
 - Safety file update and other checks in relation to new location of the Testing Power Supply
 - definition of the layout of the auxiliary plant systems and updated of auxiliary loads required by JADA components;
 - Support to JAEA in the interpretation of the Italian rules to be applied to electrical and mechanical components installed in Italy;
 - Preparation (review of documentation) and participation to the FDR of the DCGs and -1MV insulating transformer
 - Work in progress on the finalization of a number of interfaces including TL supports, DCG supports, Testing PS, gas supply system, compressed air, etc.;
 - Progress in the definition of the interface parameters listed in the so-called "Confirmation table", including auxiliary power from site, JADA signal to be routed to and managed by the AGPS-CS control and others

4.1.4 SPIDER & MITICA electric fast transient modellings

SPIDER and MITICA electrical models have been developed during previous contracts, mainly for the study of breakdown events and optimization of passive protection. During 2014, both models underwent a series of optimizations aimed to improve computational performance in terms of system stability and speed. In particular, several improvements were introduced to speed up the initial state computation.

With Reference to the SPIDER electrical model, three specific activities have been carried out:

- Upgrade of ground connections: in the previous versions of the model, the connection between the outer screen (OS) conductor of the Transmission Line and the ground potential was direct. A more realistic model with a LR network has been added between the two potentials.

- Analysis of breakdown effects on signal conductors: electrical models for source sensors cables have been added, considering the different position of sensors inside the source (backplate, Bias Plate, Plasma Grid, Extraction Grid) and different connections schemes for in-vessel and Transmission Line cable screens have been simulated in order to check the present scenario and to evaluate alternative solutions.
- Analysis of breakdown effects on Core Snubber power supply: The Core Snubber power supply has the role to improve the flux swing performance of this component. Overvoltages during breakdown have been simulated, evidencing the need of passive protections.

4.1.5 HV Holding R&D

4.1.5.1 Surface treatment on Stainless Steel electrodes at the anode side

The activities were focused on the surface treatments to improve the voltage holding in vacuum at pressures lower than 10^{-6} mbar. Some different treatments have been compared to identify a suitable procedure to treat the inner wall of the vacuum vessel of MITICA. The electrode material is AISI 304L and the raw material surface correspond to grade 1D according to EN 10088-4 (hot rolled, solution heat-treated and pickled surface).

The results obtained from a surface treated by micro shot peening (test #2) have been compared with the ones obtained from a raw surface which has been cleaned only by acetone (test #1).

The results are reported in fig. 4.49 in term of breakdown voltage vs. breakdown progressive

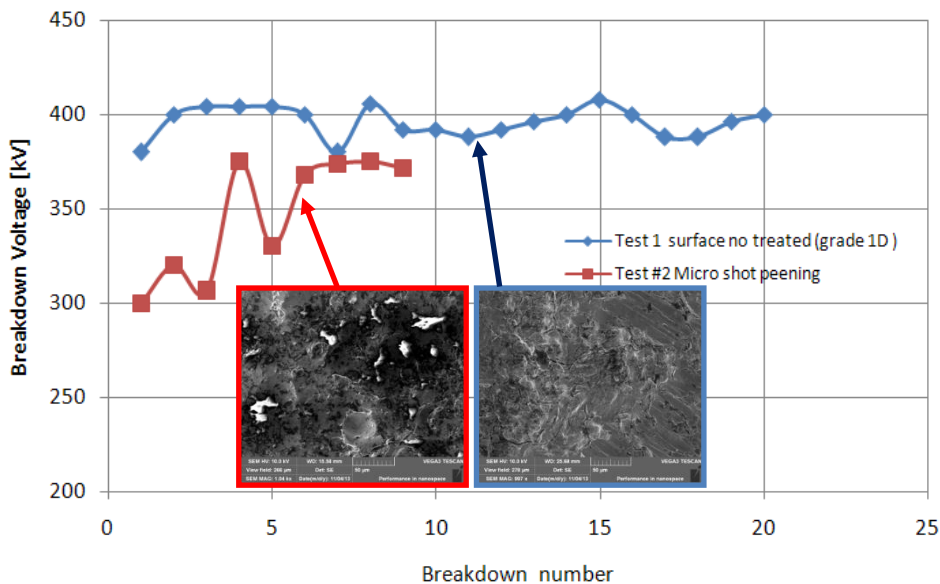


Fig.4.49: Conditioning histories, breakdown voltages vs. breakdown progressive number for test #1 and #2

number. Micro shot peening on the anodic surfaces seems a treatment not suitable to improve the voltage holding.

4.1.5.2 R&D on prototypes of MITICA post-insulators

Some experimental campaigns have been dedicated to study the voltage holding performances of some prototypes of the MITICA standoff insulators made by high purity alumina.

The target of 240 kVdc was reached only for the first kind of prototype after 140 h of high voltage conditioning; such voltage was withstood without any breakdown for 6.5 hours, no gases were injected during the test.

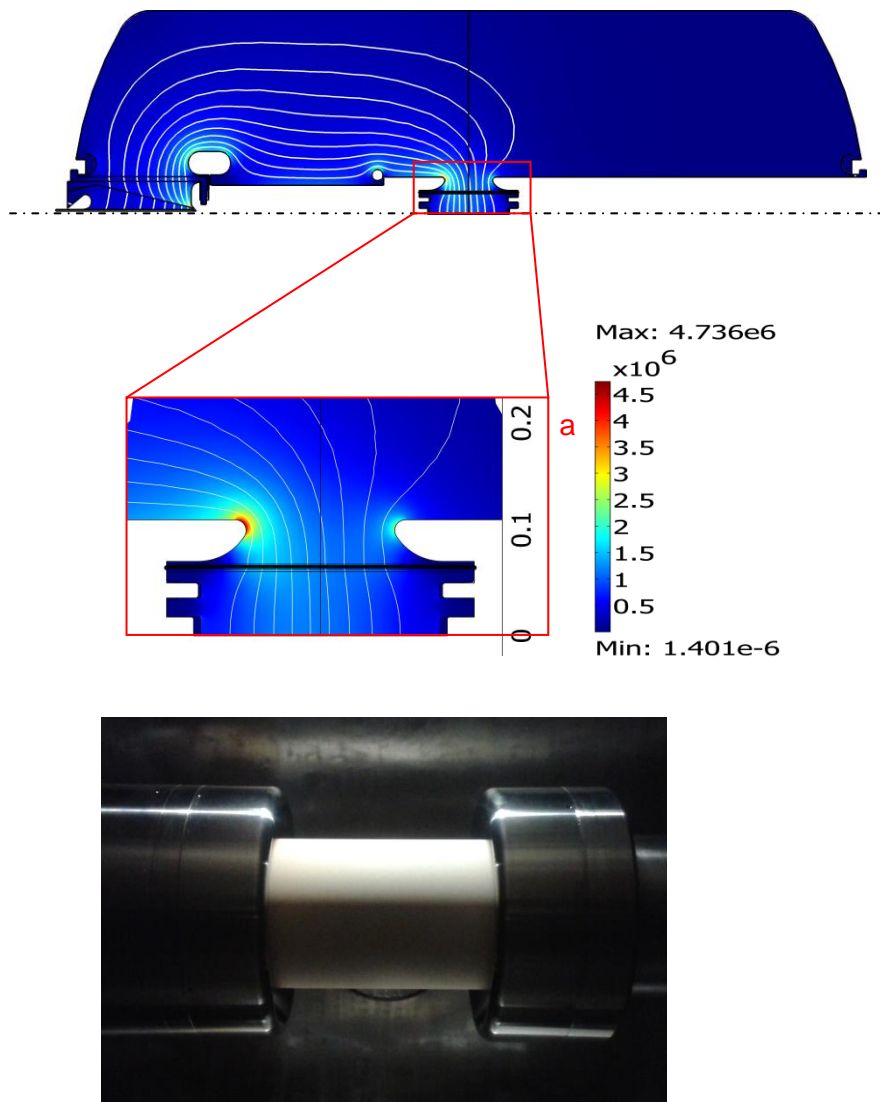


Fig. 4.50: Ceramic insulator and electrostatic field map distribution during the high voltage test at the HVPTF at +240kVdc.

The R&D activity is not concluded yet because a configuration fulfilling both electrical and structural aspects has not yet been found.

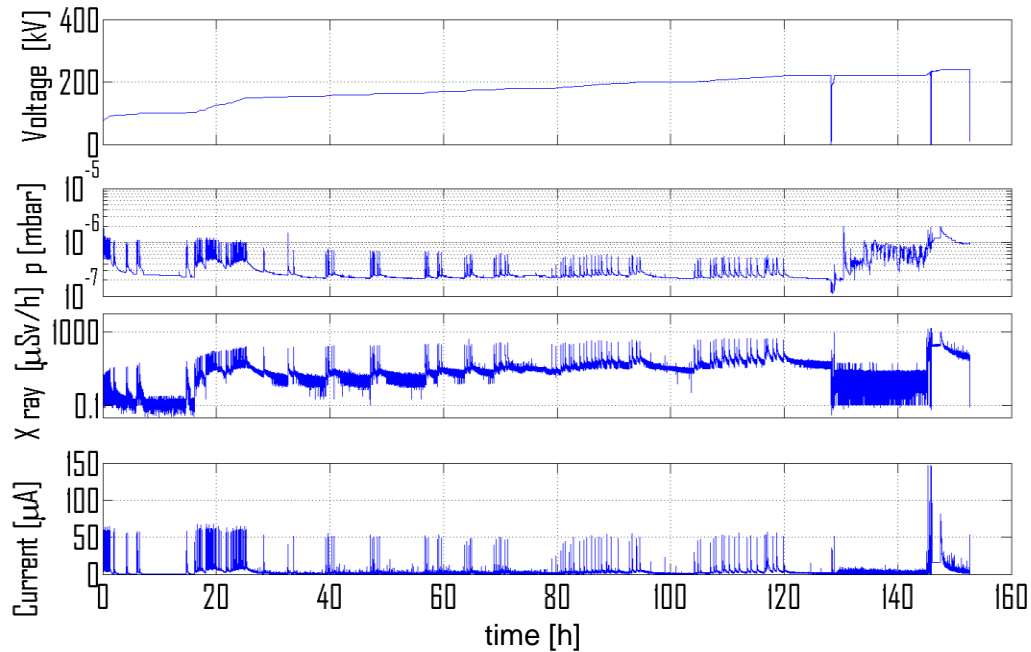


Fig. 4.51: Voltage, pressure, X-ray and current signals vs. time during the first HV test on the ceramic insulator prototype

4.1.5.3 Preliminary test on additional diagnostic systems

Preliminary investigations by using a Residual Gas Analyser (RGA) and X-ray scintillators were carried out during the 2014, some experimental evidences have been found concerning the gas released during the high voltage conditioning procedure. Application of voltage steps during the conditioning phase, usually corresponds to occurrence of micro discharges (not breakdowns) with production of X-rays and gas emission. The phenomenon seems associated to a selective emission of light species e.g. Helium desorbed from the anodic surfaces.

Fig. 4.52 represents the RGA normalized signals (100 channels) vs. time, two consecutive voltage steps of +1kV were applied starting from 200kV. The voltage was applied on a couple of stainless steel electrodes insulated by a vacuum gap of 120 mm.

4.1.6 On Site Activities

During 2014 a very intensive support has been given to designers for building design changes and big effort put on the activities for construction supervision coordination, mainly between buildings and power plant but also between buildings and all the other plants. Particular effort has

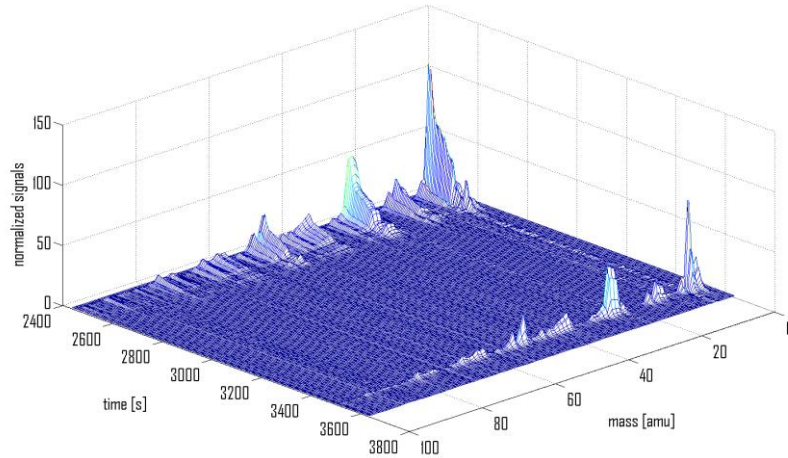


Fig. 4.52: RGA normalized current signals, mass scan in range 1-100 a.m.u., refresh time 5 s, $t > 2440$ s.

been required for management of interfaces between buildings and the experimental plants in advanced procurement phase.

The support to F4E for the procurement of the Construction/Erection All Risks insurance contract for the NBTF, managed by Consorzio RFX, has continued. The tender has been prepared by RFX and the contract placed. The “All Risks” insurance has been activated around middle of 2014 well in advance against the beginning of the installation on site of the first experimental plants.

The On-Site (yard) organization, with reference to D.Lgs. 81/08 (Health and Safety), has been finalized and put in place through the Implementing Agreement and the subsequent appointments of F4E and Consorzio RFX representatives and of the Responsible of the Work.

Support for the definition of the F4E on-site organization and more in general for the definition of the work-on-site rules has been also given.

The appointments (and the two related contracts) of the CSP (Coordinator for Safety in the Design phase) and the CSE (Coordinator for Safety in the Execution phase) for the NBTF yard have been done: CSP/CSE Coordinator, has been appointed the same person for both the roles, started the collaborations with the different companies in order to prepare all the documents foreseen by the Italian Law to start the work on-site (mainly the PSC – Plan for Safety and Coordination). By the end of the 2014 four PSCs have been issued enabling the amendment of the F4E procurement contracts for the costs of the safety (not fully considered before).

The first Supplier (Delta-Ti, for the Cooling Plant) entered the yard in the first days of November starting the installation works in buildings 2, after the signature of the area handover document.

A lot of site-yard inspections have been performed by almost all the Companies that will start the works in the next future (Coelme, ATT, Zanon, Thales, Ocem).

As for the Licence to operate the two experiments, a new contract with the same radioprotection Qualified Expert (Esperto Qualificato liv.III) has been signed, and:

- for SPIDER all the documentation has been sent to the proper Italian Authorities aimed at obtaining the Nulla Osta cat.A (art.28 D.Lgs.230/95 e s.m.i.); some Authorities have already given positive answer but some others, as ISPRA and Ministero dell'Interno (VVF), not yet. Concerning ISPRA in particular, a document with replies to specific questions given by ISPRA people in charge for SPIDER Nulla Osta has been sent at the end of the year.
- for MITICA the preparation of all the necessary documents to be sent to the Italian Authorities has started with priority to the radioprotection technical report.

Furthermore, metrology on-site activities have been performed mainly devoted to the definition of the SPIDER metrology network. CAD-related metrological activities, complementary to the on-site ones, have been also carried out. The full metrology survey of the SPIDER experiment area has been completed preparing, in example, the information to be given as reference for the installation/positioning of Vessel and Transmission Line.

4.2 NBI accompanying activities

4.2.1 HV holding Modeling

High Voltage Holding is a key requirement for neutral beam Injectors for ITER which will operate at 1 MV acceleration voltage. In order to ensure this requirement, HV conditioning is a key aspect to be carefully assessed and tested in the Neutral Beam Test facility in Padova. For this purpose a theoretical modelling of the processes involved and to identify and describe the underlying has been carried out.

A Breakdown modelling has been developed to describe the effect of a dielectric (oxide) layer deposited on one of the electrodes. The main aspect of the BIRD model (Breakdown Induced by Rupture of Dielectric layer) is that the cathode is considered as the starter of burst processes and its main advantage lies in being able to describe the appearance of bursts, during conditioning of electrodes, at constant voltage. Currently an investigation is in progress to compare experimental burst frequency with model predictions and to verify the applicability of the model to bursts originating at voltage steps. Data analysis will be extended to subsequent campaigns, one with the anode electrically powered and the cathode to ground and the other with both cathode and anode electrically powered. These configurations present particular features which could highlight the validity of the model. Nevertheless, a full experimental validation requires a more accurate time

resolved measure of Negative and Positive power supply Current bursts. In addition further analysis of X-ray spectra is planned to identify the presence of primary electron emitted from the cathode from those produced by the ionization of the desorbed gas so to clarify the underlying physical mechanisms.

4.2.2 NIO1 experiment

In 2014 several components of the NIO1 experiment were completed and commissioned so that operation of the RF source started [Cavenago_2014]. Other activities were performed to prepare for the operations of 2015. Here is a list of the main components installed in 2014:

- the lead X-ray shield, composed by a supporting structure and the lead proper, sandwiched between two aluminium layers (see Fig. 4.53)
- the insulation 40kVA transformer (see Fig. 4.53)
- the high voltage deck (see Fig. 4.53)
- the RF transmission line, made of two copper plates at a distance of 15mm (**Error! Reference source not found.**)
- the cooling system (**Error! Reference source not found.**)
- the gas injection line
- the first version of the Labview[®] control system for all power supplies and gas injection

Several components of NIO1 were commissioned in 2014:

- the gas injection line and its components (like the ceramic insulators; between them a custom gasket was inserted to prevent gas breakdown all the way from ground to 60kV)
- the cooling system: the primary circuit, where de-ionised water flows, was found to meet it requirements, whereas the secondary circuit, where glycol water flows, was insufficient for



Fig. 4.53: left: X-ray shield after installation; centre: insulation transformer; right: high voltage deck



Fig. 4.54: left: RF transmission line; centre and right: components of the cooling system

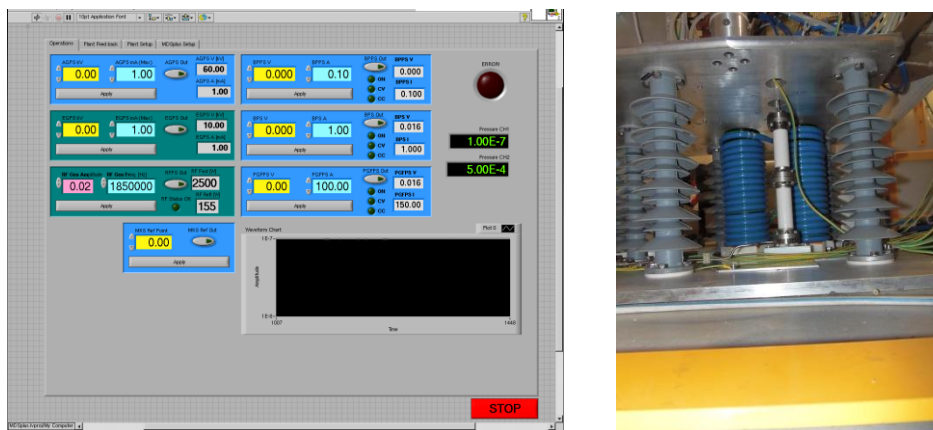


Fig.4.55: left: computer-based control system; right: ceramic insulators in the gas injection line

full power operations of NIO1 and alternatives are begin implemented

- the components of the high voltage circuits: the resistors to be used in parallel to the high voltage power supplies were tested for continuous high voltage holding; the series resistors, dedicated to mitigate the effect of accelerator breakdowns, where tested for transient high voltage holding.

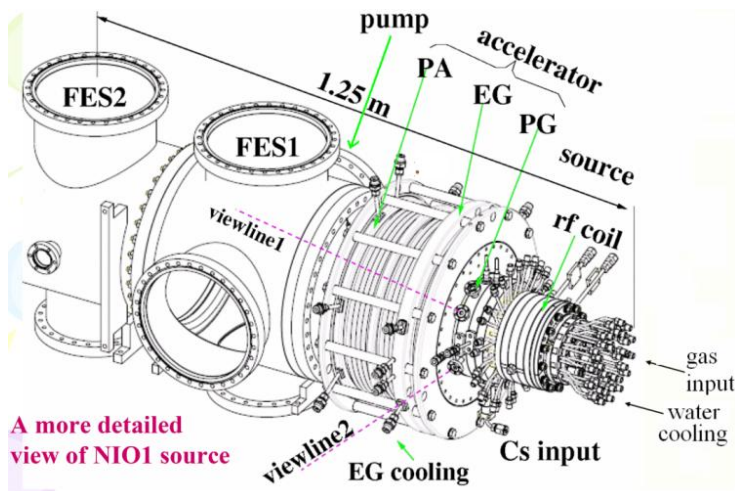
In 2014 the first experimental campaigns were carried out to characterise the RF source. In correspondence a calibration of the pressures measured in the source and in the vessel was performed (fig.4.56). Several diagnostic systems were operating arranged as in fig.4.56.

4.2.3 Spectroscopic Diagnostics

NIO1 diagnostics comprise a standard set of techniques required to characterize the plasma in the source and the extracted beam [Zaniol_2014]. Thermocouples are used for calorimetry in water cooling circuits, to measure the dissipated power in the source, on the grids and on the calorimeter, where they are also used to characterize the spatial profile of the power load. The

source plasma will be investigated with laser absorption spectroscopy for cesium density, Cavity Ring Down Spectroscopy (CRDS) for negative ion density, and Source Optical Emission Spectroscopy (OES) for information on electron temperature and density, negative ions, neutral hydrogen and cesium density, and finally to monitor the amount of impurities. The accelerated beam will be measured in terms of uniformity (intensity profile) and divergence by Beam Emission Spectroscopy (BES), Fast Emittance Scanner (FES), visible tomography and a carbon fiber calorimeter looked from behind with a thermal camera. So far Source OES is the only installed diagnostic, used during operation, while BES, tomography and carbon calorimeter are under development, and other diagnostics are still in the design phase.

The spectroscopic diagnostics ready to assist the NIO1 first operations were: the Plasma Light Detector (PLD) with a Line Of Sight (LOS) through one of the ports on the back of the driver, and



A more detailed view of NIO1 source

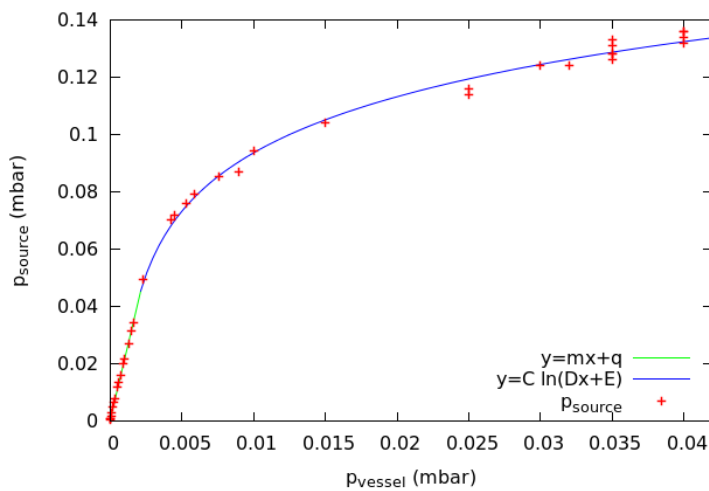


Fig. 4.56: top - arrangement of some NIO1 diagnostic systems; bottom: source vs vessel pressure

the Optical Emission Spectroscopy (OES) with two LOSs parallel to the plasma grid, one connected to a low, the other to a high resolution spectrometer. Air has been used instead of hydrogen as working gas: a choice suggested by the need to obtain a negative ion beam intense enough even without caesium evaporation, because of the high electronegativity of oxygen atoms.

Data and samples of spectra have been acquired during the three power scans up to 300 W at the pressure values of 1.1, 6 and 10.5 Pa, and a pressure scan from 0.1 to 10 Pa at the fixed power of 170 W. The source was operated with a long single pulse often lasting several minutes, during which the different pulse conditions were explored, see fig. 4.57.

Source emission spectra are dominated by the roto-vibrational bands of N_2 , being the source filled by air. The 1st and the 2nd positive systems are clearly visible on the low resolution spectra, see fig. 4.57 b. High resolution spectrometer showed evidence of N_2^+ lines at 391.4 and 423.6 nm, and also the atomic oxygen triplet at 777 nm. From N_2 spectra the rotational and the vibrational temperatures have been calculated according to [Herzberg_1950]. The results of the pressure and power scans

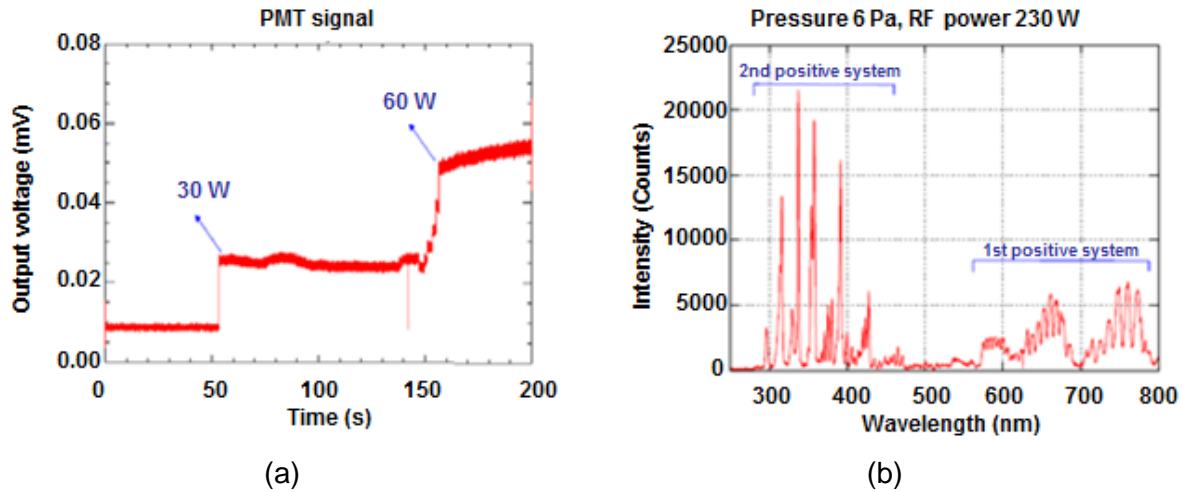


Fig. 4.57: (a) PMT signal for the first NIO1 run on July 2014. To be noted not only the rise in plasma emission intensity during the RF power variations, but also the continuous functioning of the source. (b) Source spectrum recorded by the low resolution spectrometer showing the intense roto-vibrational bands of molecular nitrogen.

are reported in the following. Fig. 4.58 reports the PMT signals recorded during the pressure and the power scans. The data clearly show saturation at high pressure values, and the transition from an exponential growth to a linear growth in the PMT signal, while increasing the power, with a threshold at about 100 W.

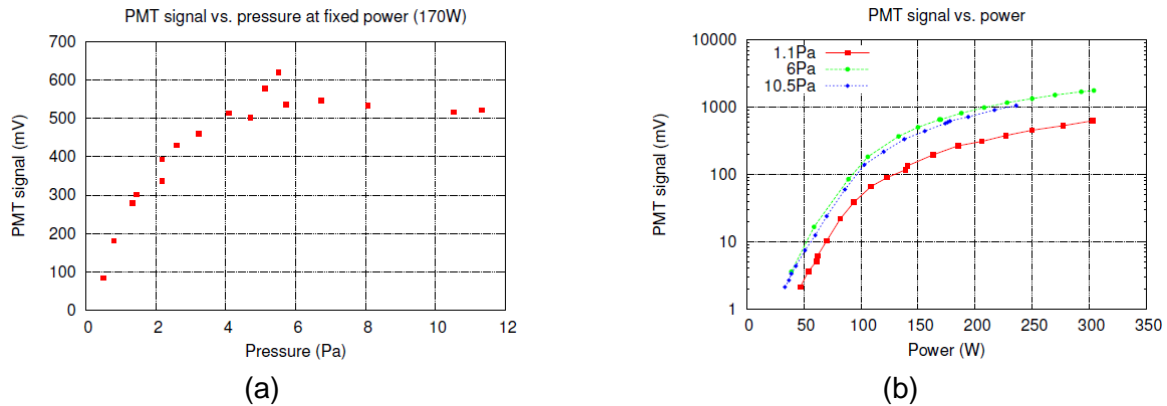


Fig. 4.58: PMT pressure (a) and power (b) scans.

The vibrational temperatures derived from the Boltzman plot of the 2nd positive system $\Delta u=2$ transition intensities of N₂, are reported in fig. 4.59. The temperature increases at first both raising the pressure and the power, but in the first case it soon starts to decrease down to the initial values, while in the second case it saturates at higher power, above 200 W.

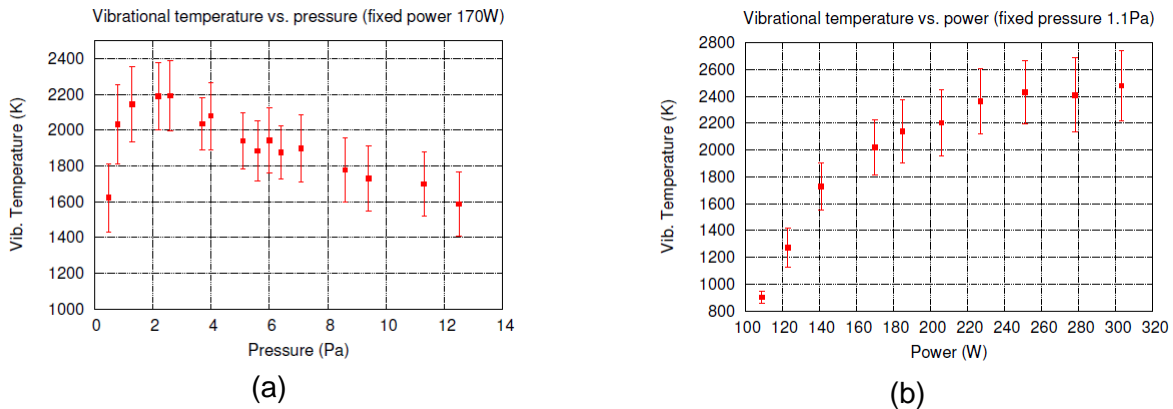
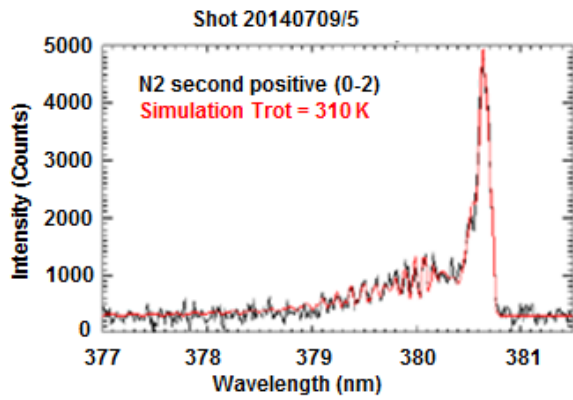


Fig. 4.59: N₂ vibrational temperature measured during a pressure (a) and a power (b) scans.

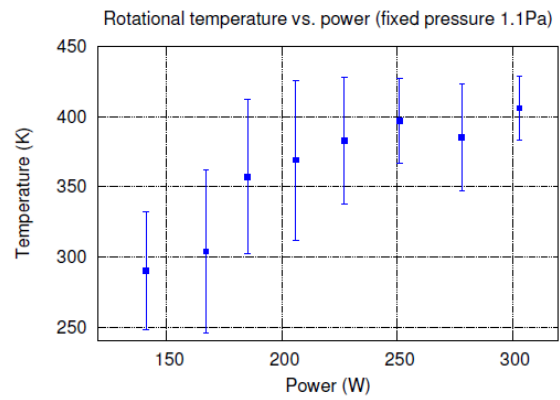
N₂ rotational temperature has been derived from the simulation of the rotational bands. The simulated spectra at different rotational temperatures were superimposed to the experimental data in order to find the best match, see fig. 4.60a. The selected band corresponds to the (0-2) transitions of the 2nd positive system, but similar temperatures have been found using other bands. The results of the power scan are reported in fig. 4.60b. As for the vibrational temperature, the rotational temperature increases with the power until it saturates at power values similar for the two temperatures.

These measurements have provided the first preliminary characterization of NIO1. They will be further optimized while other system now under development will be completed and installed before the next experimental campaign in 2015.

In 2014 concept study and experimental optimisation of a fixing system for thermocouples to be used for water calorimetry were performed. Moreover, after tests in various beam sources to optimise the rejection of electromagnetic noise, the latest version of the conditioning circuitry for source thermocouples was realised (Fig. 4.61) and will be installed in the high voltage deck at the beginning of 2015 together with the thermocouples themselves.



(a)



(b)

Fig. 4.60: (a) Example of a good match between data and simulation of a N_2 rotational band. (b) N_2 rotational temperature power scan.

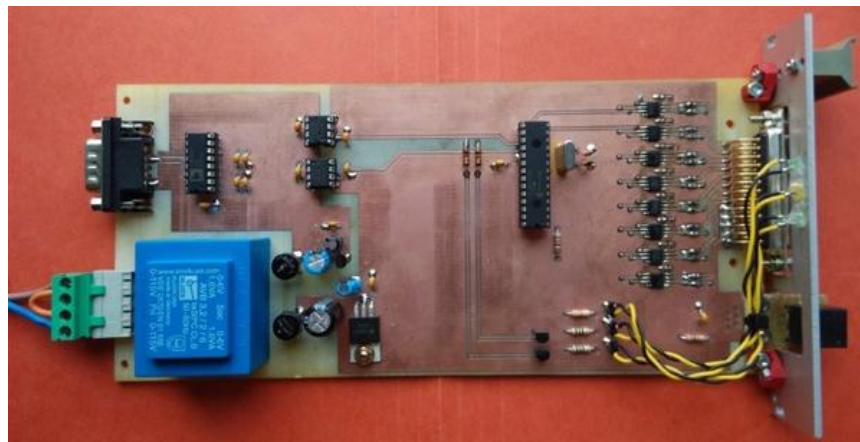


Fig. 4.61: conditioning circuit for thermocouple signals

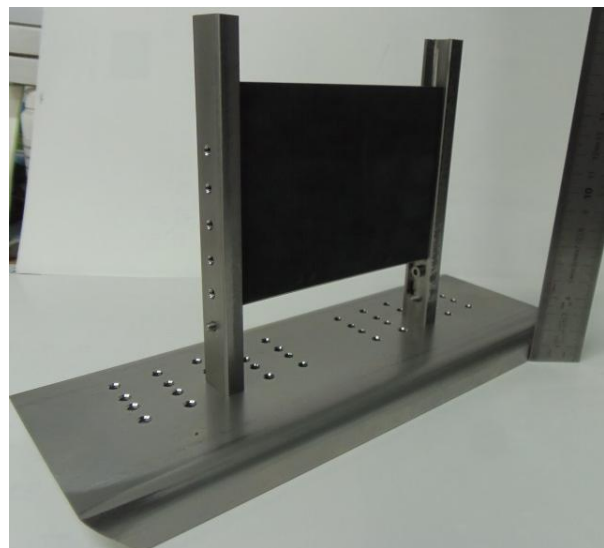
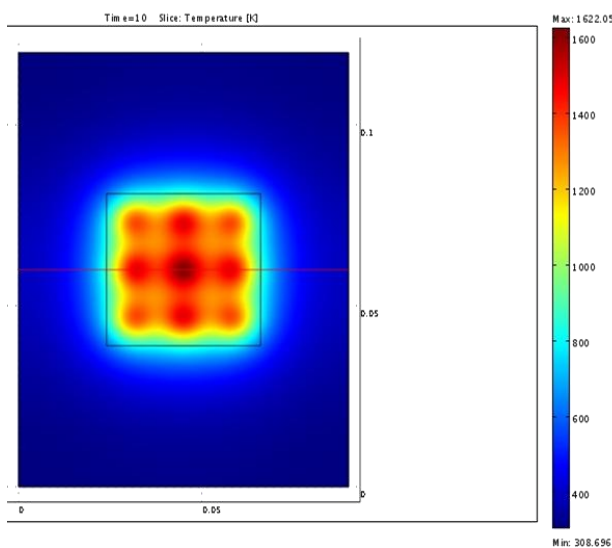


Fig. 4.62: left: simulation of the temperature pattern expected on the rear side of a CFC tile exposed to the NIO1 beam; right: CFC tile and its supporting structure.

In view of the extraction and acceleration of a beam, a diagnostic calorimeter, mini-STRIKE, was designed and built (Fig. 4.62); it will be installed in January 2015.

In order to interpret the experimental results and to guide the future experimentation, a strong numerical effort was dedicated to modelling the behaviour of the source, the expected beam and the background gas density.

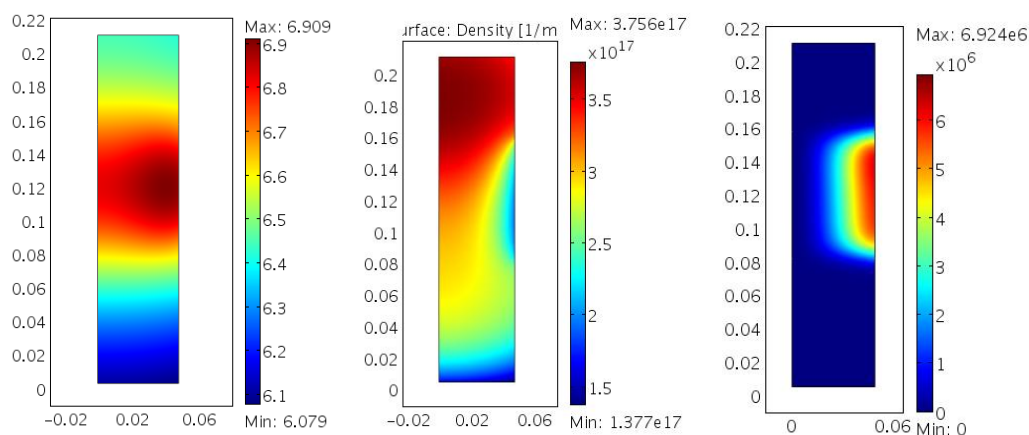


Fig. 4.63: simulation of the expected profiles of electron temperature (left), electron density (centre) and deposited power density (right) in NIO1 source.

An analytic model for the RF coupling was realised, which gives an estimate of the power coupling efficiency as a function of the plasma temperature and density and allows dimensioning the matching circuit used to couple the RF power supply to the plasma. Plasma heating is due to local and non-local effects, which were introduced in the model by the use of an effective collision frequency, defined as the sum of the electron collision frequencies with ions and neutrals and a stochastic collision frequency. A model for the profile of plasma parameters (Fig. 4.63), which considers the electron diffusion and energy equation and a multipole magnetic confinement, was implemented numerically for hydrogen, nitrogen and oxygen gases: the results well agree with other numerical simulations and experimental measurements. By adopting a Monte Carlo approach, a sample of Maxwellian electrons was then evolved through the magnetic filter field in NIO1 in order to calculate the electron temperature and density as a function of the distance from the plasma grid: the simulation confirms that there is an effective electron cooling, which could be further improved by increasing the magnetic field strength. As a last step in the experiment modelisation, a hydrogen and an oxygen (Fig. 4.64) beam have been simulated in the case of a low current density, typical of the first operations of NIO1 without caesium. The optimal electrode potentials have been studied and the results show the necessity of an appropriate scaling in the strength of the permanent magnets when operating in hydrogen. A multi-beamlet simulation of

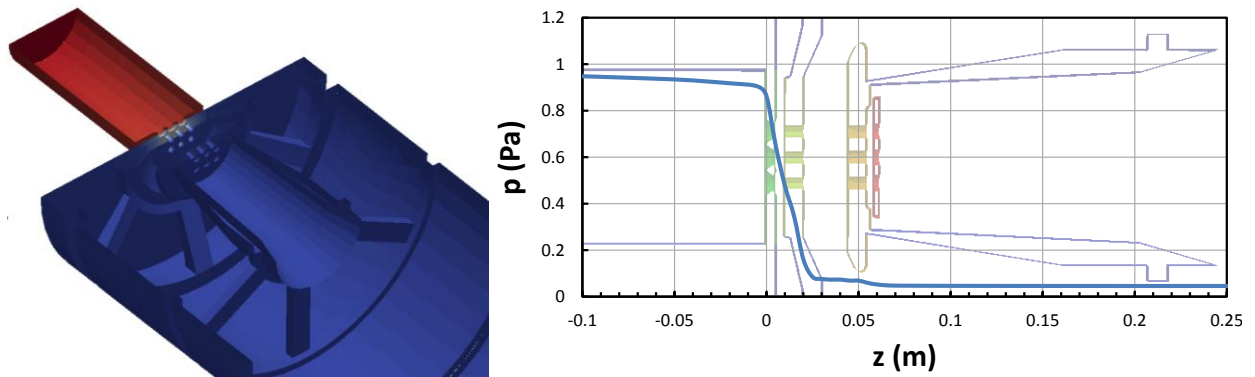


Fig. 4.65: left: mesh and pressure distribution over the NIO1 surfaces; right: profile of the background gas density

NIO1 beam acceleration has also been performed to optimise the shape of the extraction grid including the most recent features of MITICA accelerator [Veltri_2014].

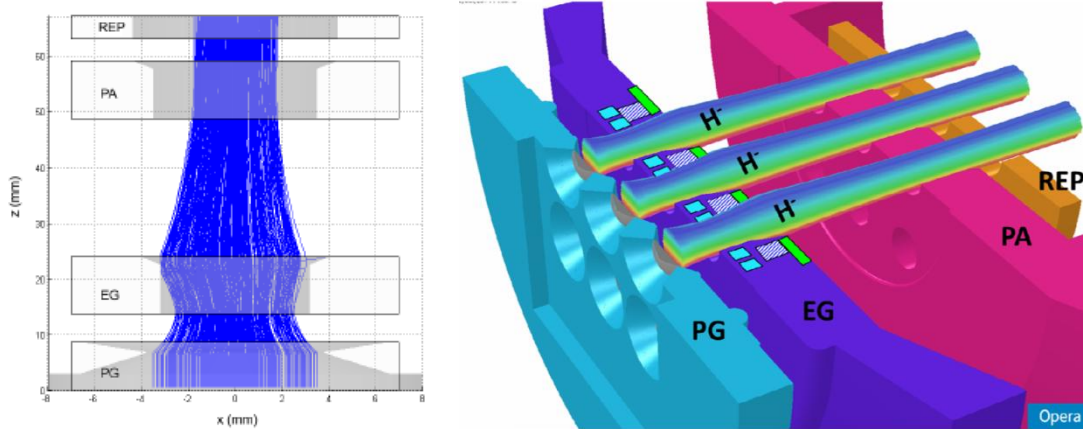


Fig. 4.64: left: simulation of the expected propagation of an oxygen beam inside NIO1 accelerator; right: multi-beamlet simulation of NIO1 beam acceleration to optimise the extraction grid shape

Motivated by the experimental linearity of source and vessel pressure in the relevant pressure regimes (

Fig. 4.56), the free molecular flow code Avocado has been used to simulate the gas flow and calculate the pressure profile through the electrodes of NIO1. To this purpose a model of the complete vacuum vessel, pumping system and pressure measurement was realised, together with the detailed geometry of the grids and their supports, and the resulting pressure three-dimensional pressure profile was obtained (Fig. 4.56). The relationship between source and vessel pressures reproduces the measured value.

4.2.4 Modelling

4.2.4.1 EAMCC numerical simulations

In the MITICA accelerator now under design finalization (MITICA is the full size prototype of the ITER neutral beam injector under construction at RFX), a significant amount of electrons is extracted together with the negative ions, while other electrons are generated inside the accelerator by means of stripping reactions, because the negative ions are very likely to lose their extra electron when they collide with the background gas. These electrons impinge on the grids, where they can give high heat loads, or are transmitted out of the accelerator together with the negative ion beam. The amount of transmitted electrons must be as small as possible because it gives problems to the beam line components located downstream of the accelerator, like the neutralizer and the cryopumps.

The thermo-mechanical analysis and the mechanical design of the accelerator of MITICA are based on the calculation of the power deposition induced by particle impacts. This calculation is performed by EAMCC, a relativistic particle tracking code based on the Monte-Carlo method for describing collisions inside the accelerator, under prescribed electric and magnetic fields. The magnetic field maps are produced by 3D codes [Chitarin_2014], while the electric field maps come from the 2D axi-symmetric code SLACCAD (bi-dimensional version of the EAMCC code) or from the fully 3D code Cobham OPERA (three-dimensional version of the EAMCC code) [OPERA]. The main activities have been carried out in 2014 regarding the EAMCC code were the following:

1. The bi-dimensional version of the code has been extensively used to calculate the heat loads deposited on the MITICA accelerator grids, and the particles transmitted at the accelerator exit. The output of these analyses has been used for the thermo-mechanical simulations of the accelerator. These results are reported in several technical notes delivered to Fusion for Energy and in a paper on the MITICA accelerator that will be published in 2015.
2. The three-dimensional version of the code have been applied to the MITICA accelerator in order to evaluate the effect of the interactions among beamlets regarding the heat loads and the trajectories of the particles inside the accelerator. This work has been described in the paper "A Multi-beamlet Analysis of the MITICA Accelerator" presented at the 4th International Symposium on Negative Ions, Beams and Sources (NIBS 2014) held in Garching bei Muenchen (Germany).

Regarding the first point (bi-dimensional version of EAMCC), the simulation of the heat loads on the MITICA accelerator was carried out upon considering three contributions: the beam core, the beam halo and the co-extracted electrons. For the beam core simulation (see for example Fig.

4.66a), an D⁻ extracted current density of 286 A m⁻² was considered, able to give 40 A of negative ion beam at the accelerator exit with the considered density profile.

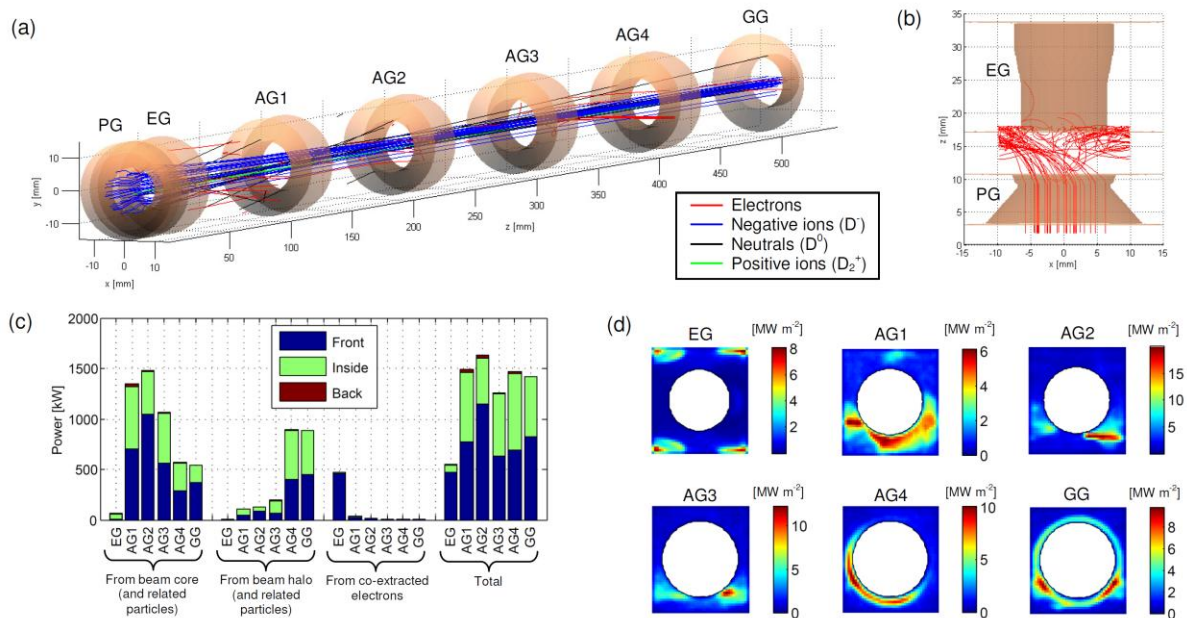


Fig. 4.66: Estimation of the transmitted and dumped heat loads with EAMCC: (a) simulation of the negative ion beam and related particles generated by stripping; (b) simulation of the co-extracted electrons; (c) heat loads on the grids; (d) power densities in MW m⁻² on the aperture area.

The beam halo, that in EAMCC is considered to be generated by ions starting from the downstream surface of the PG, is assumed to carry a current equal to 8% of the core current. This assumption is suggested by some experimental evidence. For the simulation of the co-extracted electrons (see for example Fig. 4.66b), the extracted current density is assumed to be the same of the negative ions one, as typically measured in the IPP ion source.

The global heat loads impinging on each grid are summarized in Fig. 4.66c, where also the source of the heat load (beam core, beam halo or co-extracted electrons) and the zone of deposition (front of the grid, internal part of the aperture or back) are indicated. It can be observed that the heat loads on the AGs and GG are significantly high, above 1.2 MW per grid. In order to reduce them (which leads to a higher efficiency of the accelerator and influences the design of the cooling system of the grids) and to make them similar among the five acceleration grids (which makes it easier the alignment among the grids) several approaches have been tried. Among them, the most effective ones were:

- to adopt a diagonal deflection of the stripped electrons;
- to adopt a 14 mm diameter for the first two acceleration grids (AG1 and AG2), and a 16 mm diameter for the last three (AG3, AG4 and GG). This permits to limit the heat load from halo on

the last grids, by dumping a good percentage of it in the first two acceleration grids (AG1 and AG2).

The final results of this optimization process were to obtain, with the nominal operating conditions (40 A of D- at the accelerator exit), a total heat load on each grid lower than 1.6 MW, and fairly shared loads among the five acceleration grids, ranging between 1.2 and 1.6 MW. The peak power densities are in any case quite high, with a maximum of about 20 MW m⁻² reached in the AG2. From the power density plots (see Fig. 4.66d) it can be observed that the most heated areas on the first acceleration grids (AG1, AG2 and AG3) are located below the apertures, because they are mostly given by the stripped electrons deflected by magnetic fields (the long range field deflects them downwards along the -y direction and the short range field laterally along the x direction). On the other hand the heat loads on the last acceleration grids (AG4 and GG) are located on the aperture border, because they are mostly due to the halo particles (D- and D0). This is confirmed by the fact that a large fraction of the heat load on these grids comes from the halo simulation, as shown in Fig. 4.66c.

Regarding the second point, a modified version of EAMCC, fully 3D, capable of modifying the mesh of the 3D maps and of dealing with uneven meshes has been developed and used for the MITICA accelerator, in order to confirm the results obtained with the bi-dimensional version of the code [Fonnesu2_2014]. An example of the fully 3D version of EAMCC is reported in Fig. 4.67. A finer mesh was used just in the regions where a more detailed description of the fields is required, for a more realistic simulation. A comparison between the original code and the modified version was made at first, as a validation of the modifications introduced in the latter. Subsequently, the main results of a single-beamlet analysis was performed with the two versions of the code are shown and the differences between the 2D and the 3D simulations analysed.

4.2.5.2 OPERA numerical simulations

During the present year, several modeling activities related with NBI physics were carried out at RFX. These involve both the use of commercial codes, the refinement of the numerical tools developed in the past years, and the development of new codes.

The OPERA code [OPERA] was extensively used to finalize the design of the MITICA accelerator. The large amount of data to be compared and analyzed, required the development of a series of tools (in MATLAB) capable of interpret OPERA data, interpolate the results in the most delicate points, evaluate the relevant quantity and record them in a convenient way, to form a kind of

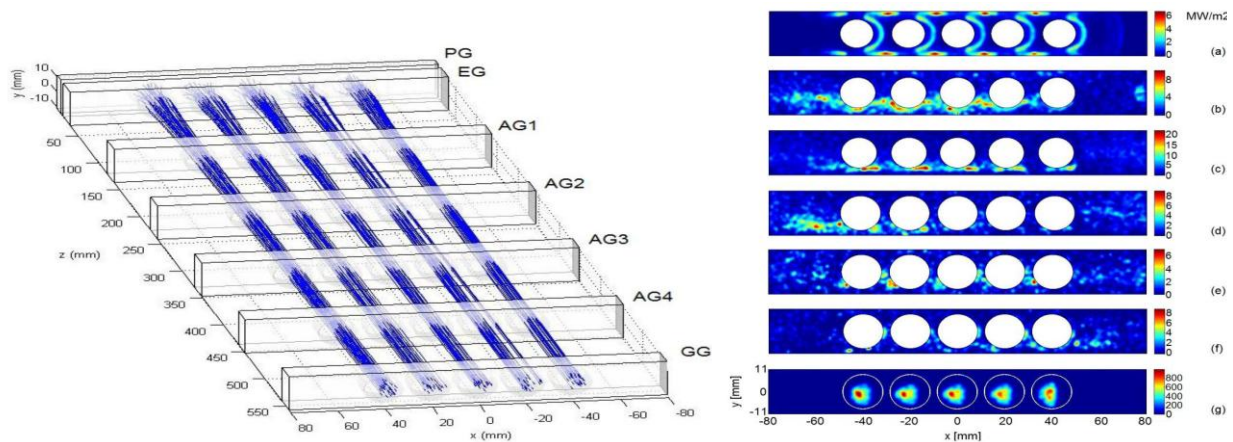


Fig. 4.67: (left) trajectories of 1000 D- macro-particles in a 5-beam simulation. (right) power densities evaluated considering a beam of D- and co-extracted e- on the upstream surface of the EG (a), AG1 (b), AG2 (c), AG3 (d), AG4 (e), GG (f) and transmitted beam at the exit of the GG (g) resulting from the 5 beamlet simulation.

simulation database useful for future investigations. A partial list of the topic addressed by means of the code during 2014 includes:

- Study the effects of the beam deflection induced by the magnets embedded in the EG, to decide the optimal size of the magnets, in terms of electron filtering and cancellation of the residual ion deflection
- Comparison of the strategies of beam aiming to select the more suitable method (use of steering plates, usually named kerbs, at the edges of each accelerator grid) and to define kerb size and positioning
- Optimization of beamlet clearance, by a careful positioning of the apertures on each grid (centering)
- Effects of non-perfect grid positioning or aperture concentricity on beamlet deflection
- Designs of the new extractor for the NIO1 experiment
- Modeling of the experimental test bed for negative ions at NIFS (national Institute for Fusion Science, Japan), for benchmark purposes

The OPERA calculations were also supported by several analyses in COMSOL environment, useful to have fast estimation of specific phenomena, whose modeling in OPERA would require extremely long and time consuming runs. Among them: the effect of 3D supporting structures on beamlet optics and the steering constant of kerbs.

Other codes, internally developed at RFX, underwent major upgrades during 2014; this is the case of the ACCPIC code, a 2D axial-symmetric particle in cell code, devoted to study the beamlet optics, that is now capable of taking into account the ionic temperature of the beam, and to

simulate parametric geometries with a large degree of flexibility. This tool was particularly helpful in optimizing the extraction system of the NIO1 accelerator and to finalize the design of a new grid [Veltri2014].

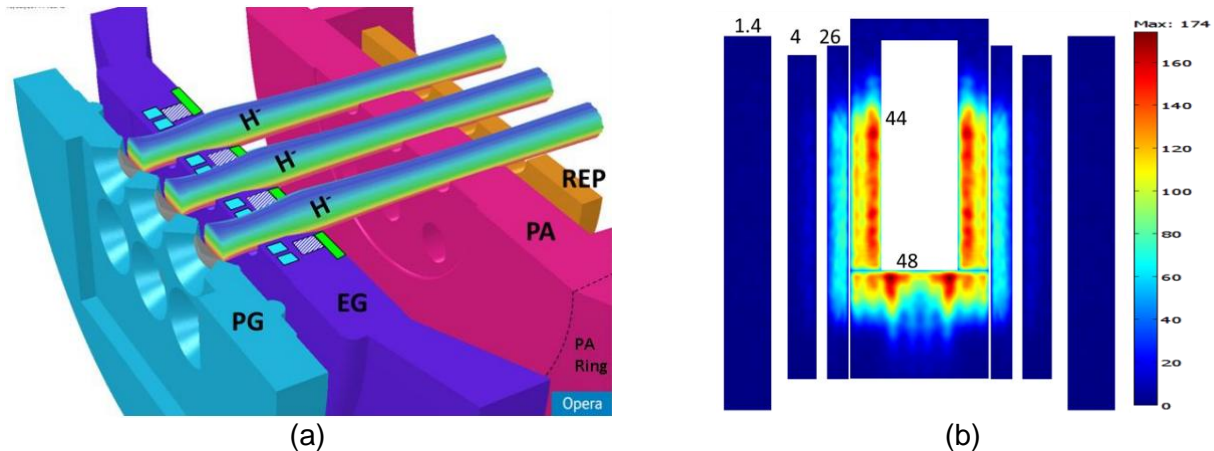


Fig. 4.68: (a) Self-consistent particles trajectories calculated with OPERA for the beamlet of NIO1 accelerator. Only 3 beamlets are shown for image readability. (b) the power load deposition on the electron dump panels and on the cryopumps front panel, calculated with BACKSCAT. Labels refers to the total load on each component, in kW.

The BACKSCAT code [Veltri2_2014], developed to evaluate the power load due to transmitted electrons along the beam line was modified to take into account an arbitrary large number of magnetic fields profiles, taking into account the relativistic equation of motion. This supported the design of the electron dump at the neutralizer entrance, to protect the cryopumps [DallilaPalma5].

The SAMANTHA code[Sartori5], written during 2013 to simulate the beam transport, the production of secondary particles and the power loads on beam-line components was optimized during this year and it is now able to efficiently simulate larger number of particles ($>10^6$) to correctly sample the 1280 beamlet of the MITICA/HNB. The code was also successfully compared [Sartori6] with the BTR code [BTR], the standard code used for this kind of simulation in the past decades. The new features of Samantha with respect to BTR allow to identify new possible sources of power load on the cryopumps.

A set of numerical tool in Comsol environment was also developed [Cazzador_2014], in the framework of a bachelor thesis [Cazzador2_2014], to simulate the behavior of the plasma in radiofrequency (RF) plasma sources. It consist of a simplified model for a 2 species plasma, able to predict the coupling with the RF power and the plasma evolution of plasma properties across magnetic fields used to filter hot electrons in negative ions sources. The model was applied to NIO1 geometry giving satisfactory results.

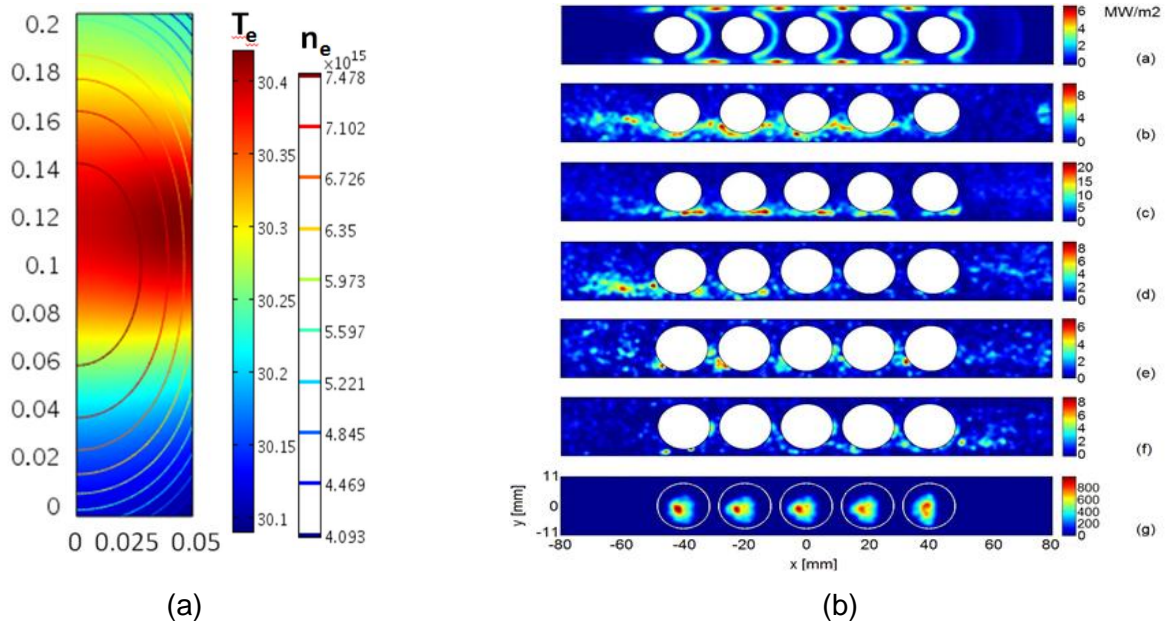


Fig. 4.69: (a) Results of the Model implemented in comsol for RF coupling with plasma in negative ions sources. Here the electron density and temperature of an H₂ plasma, for $P_{RF} = 2\text{kW}$ and pressure of 0.3 Pa for the case of NIO1 is reported. (b) the Power loads on the EG and AGs of MITICA, evaluated with the new 3D multi-beamlet versione of EAMCC.

Finally, a completely new version of the EAMCC code was issued [Fonnesu2_2014], able to account for completely 3D electric fields and to simulate multiple beamlets (the standard version simulates 1 beamlet in an axial-symmetric environment). This version of the code is now able to completely model small scale accelerator (as NIO1) or larger portion of MITICA/HNB accelerator: the limit is now given by the OPERA domain.

4.2.5 Participation to operation of Ion sources and Neutral beam injectors at other facilities

In 2014, in collaboration with IPP, it was possible to start the training of researchers in view of the operation of SPIDER and MITICA. A group of 14 people from Consorzio RFX spent a total of 23 weeks at IPP for the training on ELISE, which involved: information about plants (pumping, gas injection, safety, cooling, cryopumps, caesium ovens, etc.); description of the diagnostics systems (optical emission spectroscopy, beam emission spectroscopy, tungsten wire and copper calorimeters, thermography, calorimetry, etc.); instruction on the management of source and beam pulses (breakdowns, interlocks, acquisition, timing, control, etc.), joint experimental campaigns at low power in hydrogen (Fig. 4.70).

Some prototype tiles for the diagnostic calorimeter for SPIDER were employed in 2014 as a small-scale version (mini-STRIKE) of the entire system to investigate the features of the beam of the

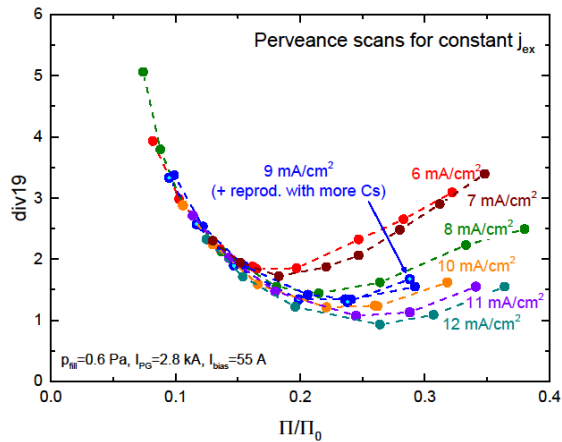


Fig. 4.70: multiple scan of divergence versus normalised perveance;

measurement system has been realized for the thermocouple signals and employed in BATMAN in view of its use in SPIDER. A new series of measurements has been carried out to characterise the BATMAN beam in different experimental conditions, obtaining an approximation to the 2D profile of the beam power density (Fig. 4.71) [Cristofaro_2014].

The mini-STRIKE was also used to characterise the beam of the test stand of LHD negative ion beam injectors [Antoni_2014]. The extraction system of the NIFS test stand source was modified and only a subset of the beamlets was isolated, arranged in two 3x5 matrices, resembling the beamlet groups of the ITER beam sources. The beamlet monitor was successfully used for a full experimental campaign, during which the main parameters of the source, mainly the arc power and the grid voltages, were varied. Correspondingly the beam pattern was modified as shown in fig.4.72.

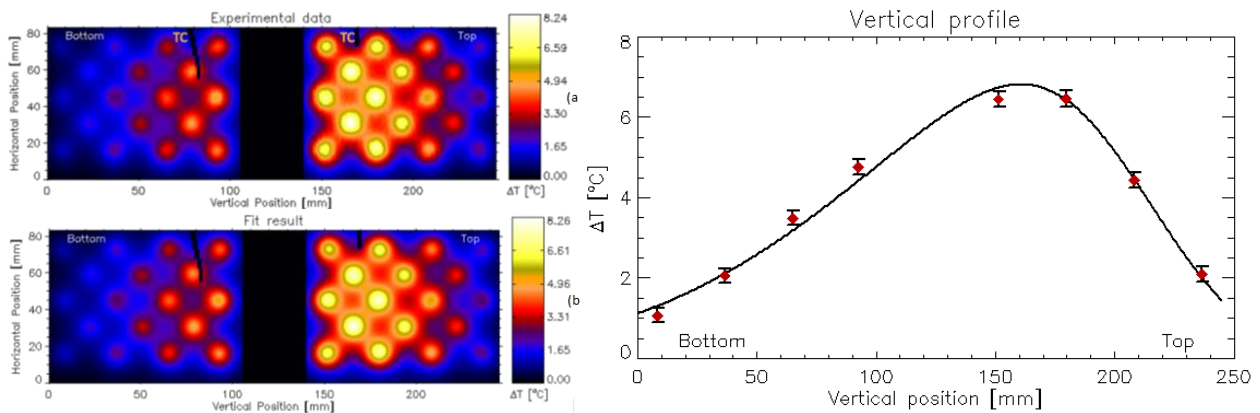


Fig. 4.71: left: data and corresponding fitting of 2D thermal pattern on the rear side of the CFC tiles used in BATMAN; right: peaks as obtained from the 2D fit and corresponding best fitting function

device BATMAN at IPP-Garching [Serianni2_2014]. As the BATMAN beamlets are superposed at the measurement position, about 1m from the grounded grid, an actively cooled copper mask is located in front of the tiles; holes in the mask create an artificial beamlet structure. Recently the mini-STRIKE was updated, taking into account the results obtained in the first campaign [De Muri_2014]. In particular the spatial resolution of the system was improved by increasing the number of the copper mask holes. Moreover a custom

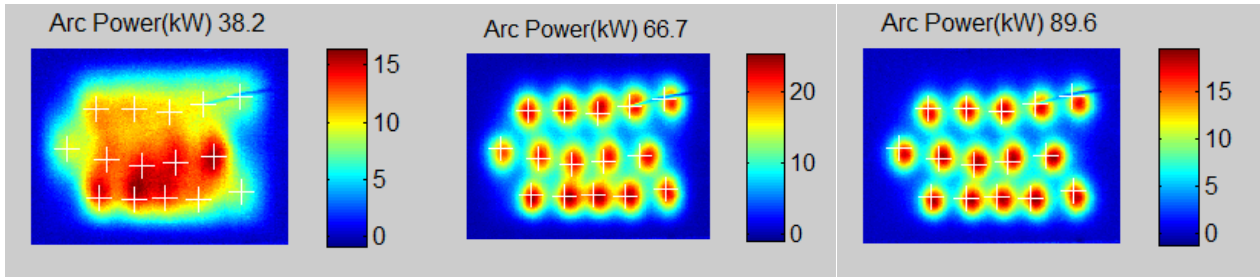


Fig. 4.72: thermal pattern on the rear side of the CFC tiles used at NIFS as the arc power varies

4.2.6 Photoneutralization

One of the most important issues for DEMO will be to improve the neutralization efficiency of the neutral beam injectors. As an alternative to the standard gas neutralizer, with about 60% efficiency, laser photoneutralization is being considered, with potentially 100% efficiency. It would use electron photodetachment, which has a low cross section and then requires very high power laser beams, in the multi MW range.

RFX just entered into this field where other EU laboratories are active in the EUROFUSION framework. RFX focused on reviewing the approaches proposed so far, especially of the cavity coupling the laser to the particle beam, balancing advantages and drawbacks. While Fabry-Perot cavities are extensively studied by CEA, an alternative multi-mirrors open cavity has been studied using a custom developed simple model, with lower performances but compensated by greater resilience to harsh environment, lower optical load on mirrors, easier alignment and control: results indicate that 60-70 % efficiency could be achieved with 100 kW laser input. Also an

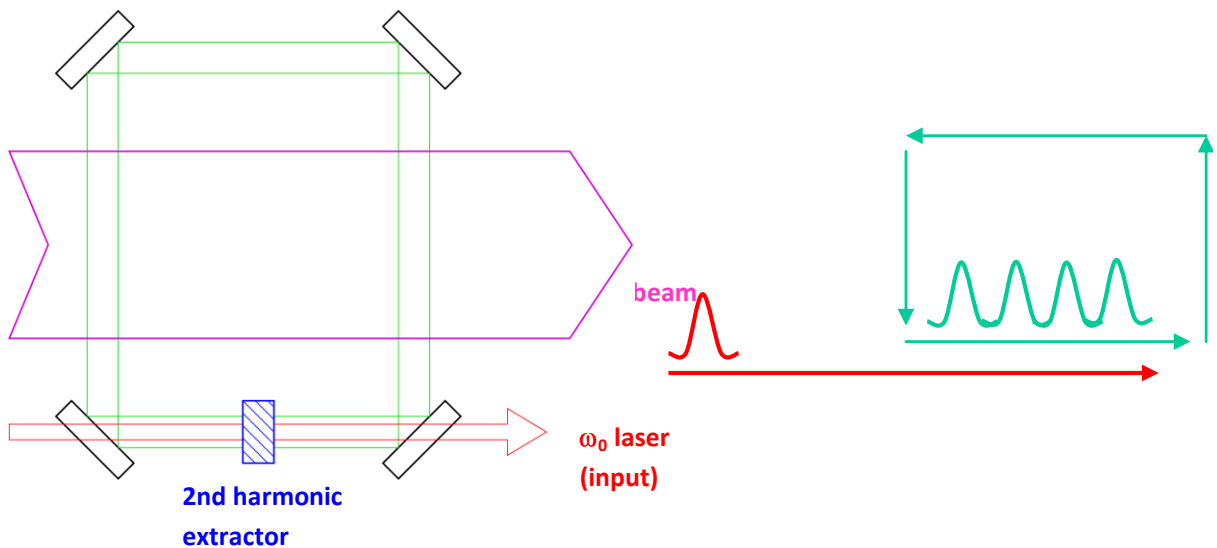


Fig 4.73: annular storage cavity concept and, on the right, proposed pulse accumulation

annular storage cavity has been explored as a possible alternative and a preliminary analysis was conducted of the improvements to the present schemes required to make it suitable for this application (fig. 4.73).

The study included also investigation of lasers other than YAG, with potential advantages in terms of scalability, efficiency, reliability: FEL, metal vapor alkali lasers and chemical lasers have interesting features that are worth considering.

4.3 ITER MODELLING: Disruptions

As a follow up of the ITER contract signed in November 2013 with 16 month duration (extensible to 24 month), in 2014 the activity was mainly oriented to fulfil the contract deliverables. In particular the problem of the mode and halo current rotations that can arise in the final stage of a disruption, i.e. during the current quench, has been addressed. Low frequency 10-100 Hz halo rotations could be risky in ITER because of the resonant response of the mechanical structure. On the other hand halo rotations have been experimentally observed in JET, DIII-D and NSTX during disruptions.

The activity has been divided in several subtasks. One task was to continue the 3D MHD nonlinear simulations employing the M3D code. In doing that we discover a new mechanism, due to non axis-symmetry, that can provide plasma acceleration and mode rotation. In particular it has been shown [Strauss 2014] that the plasma can be accelerated by the vertical movement linked to the Vertical Displacement Event (VDE), and that the non axis-symmetric forces generated by perturbed halo currents can also rotate as a consequence. Although this work has clearly shown that mode rotation is possible during disruptions, several points remain to be clarified, as the detailed mechanism of plasma acceleration, the coupling between the plasma velocity and the mode angular frequency, the scaling to ITER etc.

To address these issues and to clarify some of the basic physics questions, another activity began in 2014, regarding the application of the RFXlocking code to the study of mode-plasma-wall interactions. We consider parameters relevant for ITER in an equivalent cylindrical geometry. Preliminary results, presented at the ITPA meeting held in Padua in October, has shown the importance of the poloidal flow velocity in determining the mode locking dynamics. This activity has suggested therefore the necessity to understand the problem of poloidal flow generation and damping in toroidal plasmas. Some work aimed at clarifying this problem by considering the effect of the so called Neoclassical Toroidal Viscosity (NTV) has already started.

Finally, a further activity carried on in 2014 was the assessment of the importance of the so called surface-currents that can originate during fast plasma instabilities. This effect, which is not directly included in the present M3D code halo modelling, could be in principle important in determining the disruption dynamics . Some semi-analytical models have shown however that surface currents seem to play a role only in very specific conditions, i.e. for flat current profiles with an exactly resonant q through the plasma minor radius. These conditions seem not realized in experiments.

4.4 ITER magnetic diagnostics

During 2014 the activities related to the design of electro-magnetic sensors for ITER have been progressing in the framework of a Grant supported by Fusion for Energy started in 2011 with the involvement of Consorzio RFX as “single beneficiary” (F4E-2010-GRT-155).

The activities have been focused on the preliminary design of the two main components of the “in-vessel magnetic diagnostic system”:

- the “In-Vessel Discrete Inductive Sensors” (transducers designed for local magnetic field measurements at low-frequency, for plasma equilibrium control) [Peruzzo];
- the “In-Vessel Magnetic platform” (the assembly of parts which guarantee the support of the actual magnetic sensors within the Vacuum Vessel and the electrical connection to the in-vessel wiring, for the transmission of the measurement signal) [Peruzzo2].

Concerning the development of the transducers, a batch of 40 sensor prototypes based on LTCC technology (Low Temperature Co-fired Ceramic) has been procured in the framework of a F4E manufacturing contract (F4E-OPE-449) and tested with RFX facilities to characterise the electro-magnetic and thermo-electrical behaviour. The results of the tests performed so far are partially satisfactory, since some issues still remain open regarding the thermo-electrical reliability of the sensors under irradiation; the assessment of radiation induced effects are expected to be completed by the next year with a specific irradiation test program managed by F4E.

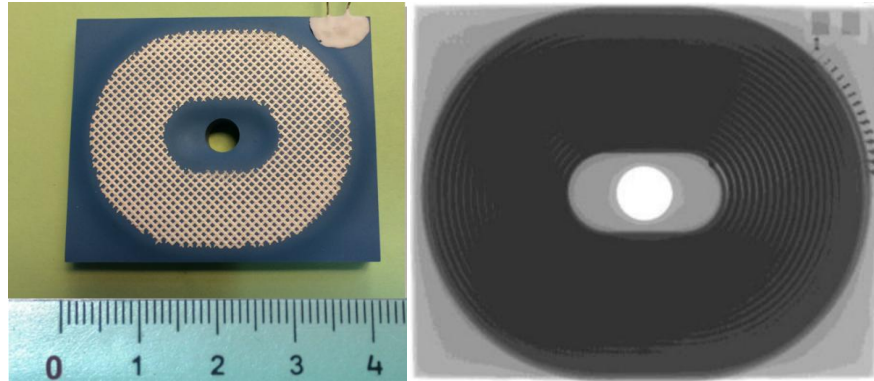


Fig. 4.74: LTCC sensors photo (left) & X-ray (right)

The development of an alternative concept of magnetic sensors, based on Mineral Insulated Cables (MIC) winding, has been carried on for a specific sensor type (Diamagnetic compensation coils) which requires a considerable magnetic effective area with respect to the previous (2 m^2 instead of 0.25 m^2). The main issue related to this sensor type is the capability to transmit the nuclear heat to the VV to limit the temperature induced emf within the MIC. To this purpose, technical specifications for the manufacture and test of MIC winding (0.5 mm outer diameter) brazed onto metallic supports have been prepared and discussed with potential suppliers. The results of these manufacturing contracts and relative tests (under the responsibility of IO) are expected in the first quarter of 2015.

As far as the magnetic platform is concerned, the design has been advanced in order to comply with several functional requirements: mechanical attachment to vacuum vessel; electrical connection to in-vessel wiring; heat

transfer to vacuum vessel; installation and replacement by means of Remote Handling (RH) system; housing of metrology features for post-installation control; shielding from ECH interference. Significant effort has been dedicated to the development of the proper CAD modeling, integrated within the ITER In-Vessel Configuration Model, to demonstrate in particular the geometrical compliance with the Blanket modules (modified in order to accommodate the magnetic sensors in suitable grooves) and the RH compatibility. Thorough thermo-mechanical and electro-magnetic

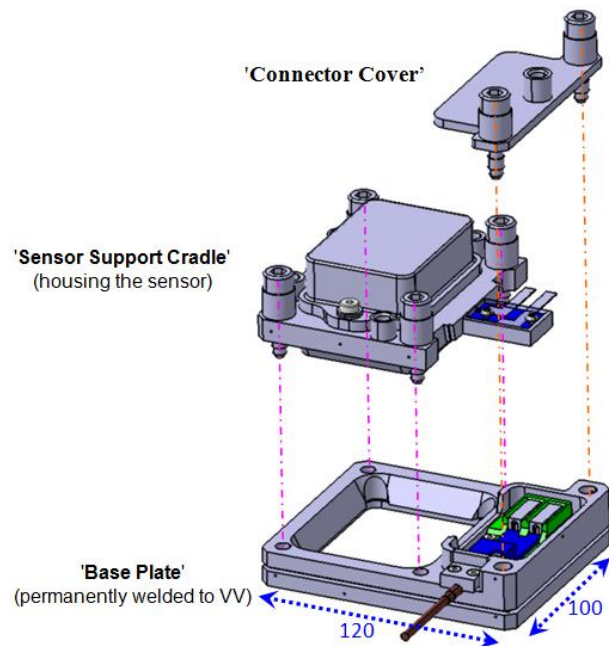


Fig. 4.75: Exploded view of the 'magnetic platform' and relative main sub-assemblies

fem analyses have been performed to demonstrate the reliability of the system in standard and off-normal operating conditions.

The above mentioned design activities have been presented at two Preliminary Design Reviews held at ITER in May and December 2014 for the magnetic platform and the magnetic sensors respectively.

4.5 ITER CORE THOMSON SCATTERING

RFX is a member of the ITER Thomson scattering (TS) Consortium, a collaboration between several EU fusion laboratories involved in the design and the development of this important ITER diagnostic. In 2014, following the negative outcome of the Call for Proposals F4E-FPA-409 (DG) issued in the previous year and the disappointing results of the subsequent market survey aimed to verify which other parties in Europe were interested in contributing to this diagnostic, F4E delayed the issue of a new Call, originally expected by the end of the year. In the meantime, due to technological problems of the LIDAR approach, IO started an internal activity aimed to advance the design of a core TS system based on a conventional (i.e. non LIDAR) approach. RFX contributed to this activity participating to a set of experimental tests, carried out at CCFE, for the preliminary evaluation of new commercial Si APD detectors. RFX also contributed marginally to the performance simulation of the ITER divertor TS scattering system in a collaboration with the TS team of the Joffe Institute in St. Petersburg [Mukhin 2014]. In addition in 2014 two important studies related to TS were carried out: the first was the analysis of a self-calibrating, dual-laser TS technique for ITER [Giudicotti 2014], including also an experimental test of dual-angle TS measurements in RFX-mod, a variant of the method, [Giudicotti_2 2014], the second was a theoretical study on the polarization of Raman scattering radiation, useful for calibration purposes [Giudicotti 2015]. Following recent advances in ultra-fast X-ray detectors for high energy physics experiments, appeared in the literature, the study of a new NIR detector based on a multipixel APD array, fast enough for the LIDAR approach, was also started. Finally a research project on "Advanced Thomson scattering diagnostics for burning plasmas" was prepared and submitted for the Enabling Research work package of the 2015 Eurofusion Work Plan. The project was a collaboration between RFX and CCFE/JET aimed to carry out an experimental test in JET of two advanced Thomson scattering techniques of interest to ITER. The project however was not funded. In the last part of the year F4E made the members of the ITER TS Consortium aware of a change of strategy about the development of the core TS Diagnostics, which was moving to a new scheme in which the design and construction work would be carried out via a 100% contract with

an industrial organization. This started a discussion among the members about the opportunity to continue or terminate the Consortium itself. At the end of the year the discussion is still going on.

REFERENCES

[Toigo2014] V. Toigo, D. Boilson, T. Bonicelli, M. Hanada, A. Chakraborty and NBTf Team, "Progress in the Realization of the PRIMA Neutral Beam Test Facility", 25th Fusion Energy Conference (FEC2014), 13-18 October, 2014 Saint Petersburg, Russia, Proceeding under publication

[Masiello2014] A. Masiello et al., "Progress Status of the Activities in EU for the Development of the ITER Neutral Beam Injector and Test Facility", 25th Fusion Energy Conference (FEC2014), 13-18 October, 2014 Saint Petersburg, Russia, Proceeding under publication

[Fellin1_2014] F. Fellin et al., "Plant integration of MITICA and SPIDER experiments with auxiliary plants and buildings on PRIMA site", 28th Symposium on Fusion Technology, San Sebastian, Spain, Sept 29th – Oct 3rd, submitted to Fusion Engineering and Design

[Pomaro2014] N. Pomaro et al., "The Earthing System of the PRIMA Neutral Beam Test Facility based on the Mesh Common Bonding Network Topology", 28th Symposium on Fusion Technology, San Sebastian, Spain, Sept 29th – Oct 3rd, submitted to Fusion Engineering and Design

[Fellin2_2014] F. Fellin et al., "The SPIDER Cooling Plant from design to realization", 28th Symposium on Fusion Technology, San Sebastian, Spain, Sept 29th – Oct 3rd, submitted to Fusion Engineering and Design

[Fellin3_2014] F. Fellin et al., "Design and radiation protection aspects for the PRIMA Cooling Plant", 28th Symposium on Fusion Technology, San Sebastian, Spain, Sept 29th – Oct 3rd, submitted to Fusion Engineering and Design

[Zaccaria2014] P. Zaccaria et al., "Manufacturing, assembly and tests of SPIDER Vacuum Vessel to develop and test a prototype of ITER Neutral Beam Ion Source", 28th Symposium on Fusion Technology, San Sebastian, Spain, Sept 29th – Oct 3rd, submitted to Fusion Engineering and Design

[Pavei2014] M. Pavei et al., "Manufacturing of the full size prototype of the ion source for the ITER Neutral Beam Injector – the SPIDER Beam Source", 28th Symposium on Fusion Technology, San Sebastian, Spain, Sept 29th – Oct 3rd, submitted to Fusion Engineering and Design

[Sartori2014] E. Sartori et al., "Non-ideal operating conditions of the ion source prototype for the ITER neutral beam injector due to thermal deformation of the support structure", REV SCI INSTRUM, 85 Issue: 2 (2014) 02B313

[Bigi2014] M. Bigi et al., "Design, manufacture and factory testing of the Ion Source and Extraction Power Supplies for the SPIDER experiment", 28th Symposium on Fusion Technology, San Sebastian, Spain, Sept 29th – Oct 3rd, submitted to Fusion Engineering and Design

[Boldrin2014] M. Boldrin et al., “The 100kV Faraday cage (High Voltage Deck) for the SPIDER experiment”, 28th Symposium on Fusion Technology, San Sebastian, Spain, Sept 29th – Oct 3rd, submitted to Fusion Engineering and Design

[Brombin2014] M. Brombin et al., “Langmuir probes for SPIDER (source for the production of ions of deuterium extracted from radio frequency plasma) experiment: Tests in BATMAN (Bavarian test machine for negative ions)” Rev. Sci. Instrum. 85, 11D832 (2014)

[Delogu2014] Delogu et al., “Optical Layout and Alignment Methods for Visible Tomography and Emission Spectroscopy Diagnostics in SPIDER”, IEEE T PLASMA SCI, 42 Issue: 6 (2014) 1802-1806 Part: 2

[Fonnesu2014] N. Fonnesu et al., “An image filtering technique for SPIDER visible tomography”, Rev. Sci. Instrum., 85 Issue: 2 (2014) 02A730

[Serianni2014] G. Serianni et al., “First negative ion beam measurement by the Short-Time Retractable Instrumented Kalorimeter Experiment (STRIKE)”, Rev. Sci. Instrum., 85 Issue: 2 (2014) 02A736

[DeMuri2014] M. De Muri et al., “High energy flux thermo-mechanical test of 1D-carbon-carbon fibre composite prototypes for the SPIDER diagnostic calorimeter”, Rev. Sci. Instrum., 85 Issue: 2 (2014) 02A718

[Pasqualotto2014] R. Pasqualotto et al., “A Wire Calorimeter for the SPIDER Beam: Experimental Tests and Feasibility Study”, accepted for publication on AIP Conference Proceedings, Proceedings of the 4th International Symposium on Negative Ions, Beams and Sources, 6-10 October 2014, Garching, Germany

[Muraro2014] A. Muraro et al., “Status of the CNESM diagnostic for SPIDER”, submitted to Fusion Engineering and Design

[Barbisan2014] M. Barbisan et al., “Modeling and simulation of a beam emission spectroscopy diagnostic for the ITER prototype neutral beam injector”, Rev. Sci. Instrum. 85, 11E430 (2014)

[Nocentini2014] R. Nocentini et al., “Advanced ion beam calorimetry for the test facility ELISE”, accepted for publication on AIP Conference Proceedings, Proceedings of the 4th International Symposium on Negative Ions, Beams and Sources, 6-10 October 2014, Garching, Germany

[Brombin2_2014] M. Brombin et al. “Electrostatic sensors for SPIDER experiment: Design, manufacture of prototypes, and first tests”, Rev. Sci. Instrum, 85 Issue: 2 (2014) 02A715

[Luchetta2014] A. Luchetta et al., “Control and Data Acquisition of the ITER Full-scale Ion Source for the Neutral Beam Test Facility”, 28th Symposium on Fusion Technology, San Sebastian, Spain, Sept 29th – Oct 3rd, submitted to Fusion Engineering and Design

[Barbato2014] P. Barbato, RFX-SPIDER-TN-268_r2 SPIDER Central CODAS Hardware Design – Networks, 28-7-2014, RFX Internal report

[Luchetta2014] A. Luchetta et al., "Fast control and data acquisition in the neutral beam test facility", Fusion Engineering and Design, 89, Issue 5, May 2014, Pages 663-668

[Pomaro2_2014] N. Pomaro et al., RFX_SPIDER_TN_22 Technical Specifications for the SPIDER Central Interlock System, 19-12-2014, RFX Internal report

[Luchetta2014] A. Luchetta, T4.19/P1.2 - Report on MITICA CODAS Conceptual Design, RFX-MITICA-TN-276, RFX Internal report

[Pomaro3_2014] N. Pomaro, T4.20/P1.2 - Report on MITICA Interlock Conceptual Design, RFX-MITICA-TN-277, RFX Internal report

[DallaPalma2_2014] M. Dalla Palma et al., "Design and R&D of Thermal Sensors for ITER Neutral Beam Injectors", IEEE T PLASMA SCI, **42** Issue: 3 Special Issue: SI (2014) 610-615 Part:1

[DallaPalma2_2014] M. Dalla Palma et al., "Design and Test of a Thermal Measurement System Prototype for SPIDER Experiment", IEEE T PLASMA SCI, **42** Issue: 7 (2014) 1971-197

[Agostinetti2014] P. Agostinetti et al., "Manufacturing and Testing of Grid Prototypes for the ITER Neutral Beam Injectors", IEEE T PLASMA SCI, **42** Issue: 3 Special Issue: SI (2014) 628-632 Part:1

[Agostinetti2_2014] P. Agostinetti et al., "Vacuum Tight Threaded Junctions (VTTJ): a new solution for reliable heterogeneous junctions in ITER", 28th Symposium on Fusion Technology, San Sebastian, Spain, Sept 29th – Oct 3rd, submitted to Fusion Engineering and Design

[Pilan2014] N. Pilan et al., "Electrical and structural R&D activities on high voltage DC solid insulators in vacuum", 28th Symposium on Fusion Technology, San Sebastian, Spain, Sept 29th – Oct 3rd, submitted to Fusion Engineering and Design

[DallaPalma3_2014] M. Dalla Palma et al., "First boundary electrical feedthroughs for the Heating Neutral Beams injectors of ITER", 28th Symposium on Fusion Technology, San Sebastian, Spain, Sept 29th – Oct 3rd, submitted to Fusion Engineering and Design

[Pilan2_2014] N. Pilan et al., "Magnetic Field Effect on Voltage Holding in the MITICA Electrostatic Accelerator", IEEE T PLASMA SCI, **42** Issue: 4 (2014) 1012-1020

[Sartori2_2014] E. Sartori et al., "Comparative study of beam losses and heat loads reduction methods in MITICA beam source", REV SCI INSTRUM, 85 Issue: 2 (2014) 02B308

[Sartori3_2014] E. Sartori et al., "Experimental Validation of the 3-D Molecular Flow Code AVOCADO", IEEE T PLASMA SCI Volume: 42 Issue: 9 Pages: 2291-2297

[Sartori4_2014] E. Sartori et al., "Multi-scale simulation of gas density distribution in a fusion-relevant particle accelerator", 13th European Vacuum Conference, 8-12 September, 2014 Aveiro, Portugal, To be published after peer review in Vacuum journal

[Marconato2014] N. Marconato et al., "Magnetic and thermo-structural design optimization of the Plasma Grid for the MITICA Neutral Beam Injector", 28th Symposium on Fusion Technology, San Sebastian, Spain, Sept 29th – Oct 3rd, submitted to Fusion Engineering and Design

[DallaPalma4_2014] M. Dalla Palma et al., "Design and R&D for manufacturing the Beamline Components of MITICA and ITER HNB", 28th Symposium on Fusion Technology, San Sebastian, Spain, Sept 29th – Oct 3rd, submitted to Fusion Engineering and Design

[Zanotto2014] L. Zanotto et al., "Control, Protection and Breakdown Management in the Acceleration Grid Power Supply of the ITER Heating Neutral Beam Injector", 28th Symposium on Fusion Technology, San Sebastian, Spain, Sept 29th – Oct 3rd, submitted to Fusion Engineering and Design

[Chitarin_2014] G. Chitarin et al., submitted to AIP Conference Proceedings of IV Symposium on negative ions, beams and sources (2014)

[OPERA] OPERA-3D software, Cobham plc Brook Road, Wimborne, Dorset, BH21 2BJ, UK.
<http://www.cobham.com>

[Zaniol_2014] B. Zaniol et al., submitted to AIP Conference Proceedings of IV Symposium on negative ions, beams and sources (2014)

[Herzberg_1950] Herzberg, "Molecular Spectra and Molecular Structure I: Spectra of Diatomic Molecules", New York: Van Nostrand, 1950

[Veltri_2014] P. Veltri, M. Cavenago and C. Baltador, submitted to AIP Conference Proceedings of IV Symposium on negative ions, beams and sources (2014)

[Veltri2_2014] P. Veltri, P. Agostinetti, M. Dalla Palma, E. Sartori and G. Serianni, Fusion engineering and design 88 (6-8) (2013)

[DallaPalma5_2014] M. Dalla Palma et al, submitted to Fusion engineering and design (2014)

[Sartori5_2014] E. Sartori, P. Veltri, G. Serianni, M. Dalla Palma, G. Chitarin and P. Sonato, IEEE Transaction on Plasma Science, Vol 42 n. 3 (2014)

[BTR] <http://www.btr.org.ru/>

[Sartori6_2014] E. Sartori, P. Veltri, E. Dlougach, R. Hemsworth, G. Serianni and M. Singh, Submitted to Aip Conference Proceedings of IV Symposium on negative ion beams and sources (2014)

[Cavenago_2014] M. Cavenago et al., submitted to AIP Conference Proceedings of IV Symposium on negative ions, beams and sources (2014)

[Cazzador2014] M Cazzador, M Cavenago, G. Serianni and P. Veltri, Submitted to Aip Conference Proceedings of IV Symposium on negative ion beams and sources (2014)

[Cazzador2_2014] M. Cazzador, Bachelor Thesis, University of Padova, 2014.

[Fonnesu2_2014] N. Fonnesu et al., Submitted to AIP Conference Proceedings of IV Symposium on negative ion beams and sources (2014)

[De Muri2_2014] M. De Muri et al., 28th Symposium On Fusion Technology, 29 September – 3 October 2014, San Sebastian, Spain; under revision for publication in Fusion Eng. Des.

[Serianni2_2014] M. Cavenago et al., submitted to AIP Conference Proceedings of IV Symposium on negative ions, beams and sources (2014)

[Cristofaro_2014] S. Cristofaro, Bachelor Thesis, University of Padova, 2014.

[Antoni_2014] M. Cavenago et al., submitted to AIP Conference Proceedings of IV Symposium on negative ions, beams and sources (2014)

[Strauss 2014] H. Strauss, L. Sugiyama, R. Paccagnella, J. Breslau and S. Jardin., "Tokamak toroidal rotation caused by AVDEs and ELMs" Nuclear Fusion **54** (2014) 043017

[Peruzzo2014] "Design Description of the Generic In-vessel Magnetic Platform" (RFX-IP-TN-180, 23 May 2014), (ITER_D_PA23N9)

[Peruzzo2] "System Design Description (DDD) 55.AA,AB,AC,AG discrete inductive sensors", (RFX_IP_TN_190, 15 Dec 2014), (ITER_D_4GWCLQ)

[Mukhin2014] E.E. Mukhin, R.A. Pitts, P. Andrew, I.M. Bukreev, P.V. Chernakov, L. Giudicotti, G. Huijsmans, M.M. Kochergin, A.N. Koval, A.S. Kukushkin, G.S. Kurskiev, A.E. Litvinov, S.V. Masyukevich, R. Pasqualotto, A.G. Razdobarin, V.V. Semenov, S.Yu. Tolstyakov and M.J. Walsh, "Physical aspects of divertor Thomson scattering implementation on ITER", Nucl. Fusion 54, 043007, (2014) doi:10.1088/0029-5515/54/4/043007

[Giudicotti 2014] L. Giudicotti and R. Pasqualotto, "Dual-laser calibration of Thomson scattering systems in ITER and RFX-mod", Nucl. Fusion 54, 043005 (2014) doi:10.1088/0029-5515/54/4/043005

[Giudicotti_2 2014]: L. Giudicotti, R. Pasqualotto and A. Fassina, "Dual-angle, self-calibrating, Thomson scattering measurements in RFX-MOD", Rev. of Sci. Instrum. 85, 11D823 (2014) doi: 10.1063/1.4890409

[Giudicotti 2015]: L. Giudicotti and R. Pasqualotto, "Rotational Raman scattering as a source of polarized radiation for the calibration of polarization-based Thomson scattering", accepted for publication in Plasma Physics and Controlled Fusion, 2015.

5. PPPT: POWER PLANT PHYSICS & TECHNOLOGY PROJECTS

The H2020 roadmap foresees to develop key technologies in view of DEMO design to be completed by 2030.

Relevant outcomes are expected from the construction of ITER, but in many areas R&D activities are required in particular in the breeding blanket concept and technologies and in the area of the materials that have to withstand to a significant amount of radiation.

In 2014 the activities of all the WPs started with the development of the PMP (Project Management Plan) for the activities to be developed from 2014 to 2018 and have been dedicated to organize the work in cooperation with all the other RUs (Research Units) contributing to each WP.

In the other technology areas the main scope defined in the Roadmap is focused in limited R&D, in exploration of defined alternatives concepts and in the development of the conceptual design.

The overall involvement of Consorzio RFX in the different WPs for 2014 is described in the following table.

H2020-PPPT 2014	ppy	Hardware
WPHCD: Heating and Current Drive Systems	1,5	120
WPTFV: Tritium, Fuelling and Vacuum Pumping Systems	0,2	0
WPMAG: Magnet system	0,1	0
WPPMI: Plant Level System Engineering, Design Integration & Physics Integration	0,75	0
OVERALL TOTAL	2,55	120

There is also an additional WP in which Consorzio RFX is involved the *WPSES-Work Package on Socio-Economic Studies* in which there is a significant contribution that is described in section 5.5

5.1 WPHCD: Heating and Current Drive Systems

Consorzio RFX is involved in the R&D and conceptual design development of the Neutral Beam system for DEMO.

In the R&D activities Consorzio RFX is working in all the main three areas of development:

1. Development of optimized negative ion sources. In this topic Consorzio RFX is contributing through the operation of NIO1. Most of the HW contribution from EUROfusion is supporting the operation of this facility. For the detail of the operation of NIO1 a dedicated session is included in this document. The main objectives of negative ion sources development are:

-
- Caesium physical vapour deposition free sources
 - Maximization of volume negative ion production
 - Alternative and optimized RF sources
 - Maximization of negative ion production with the lowest neutral density
2. Development of alternative neutralisation systems to maximize the neutralisation efficiency actually limited to less than 60% for the gas neutralisation concept adopted in ITER. One of the most promising set of alternative concepts is the photoneutralisation. Consorzio RFX in 2014 has studied and compared different options of neutralisation systems as discussed in section 4.2.6.
 3. Development of an Energy Recovery System from the power adsorbed by the Residual Ion Dump or any other component collecting energetic particles. Consorzio RFX has analysed the electric circuit and has designed a possible test to be installed in NIO1. The purchase of the first components has started and will continue. In the figures here below the electric circuit for the Energy Recovery System for NIO1 is shown.

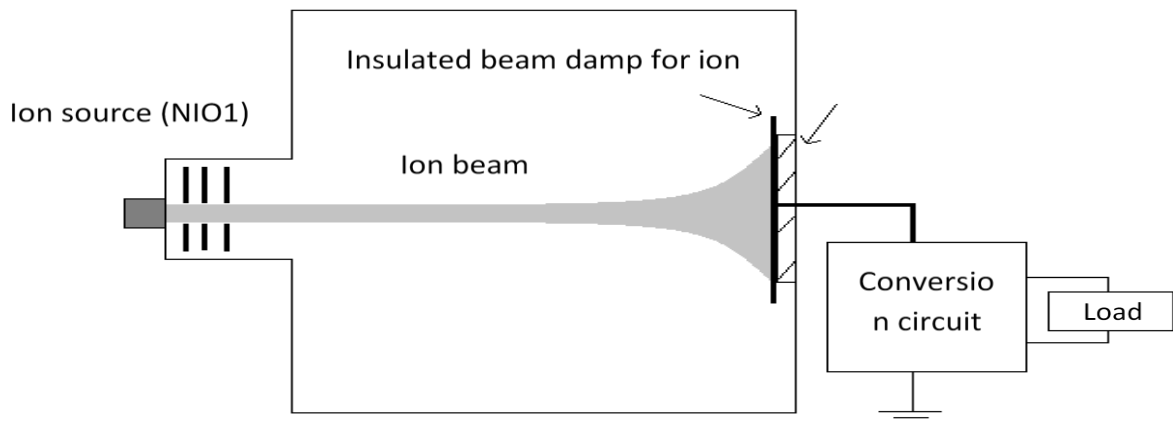


Fig. 5.1.1: conceptual layout of the Energy recovery system applied to NIO1 beam source

With regards to the development of the conceptual design the first concept of injector has been developed in a CAD model integrating the photoneutralisation concept.

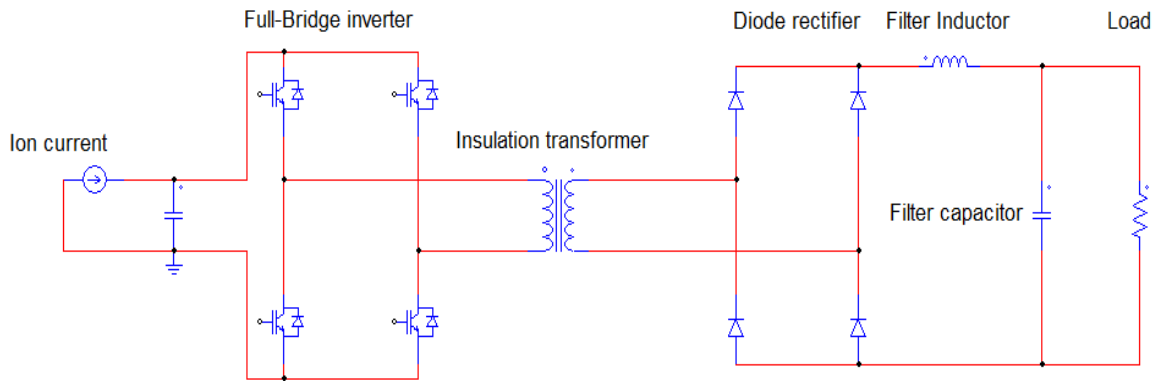


Fig. 5.1.2: electric circuit of the energy recovery system for NIO1

In the next figures the overall view of the injector integrated in the DEMO1 CAD is shown as well as a horizontal cut of the injector showing the internal components where it is visible the source and the duct components connecting the injector to the Tokamak. In fig. 5.1.5 the exploded view of

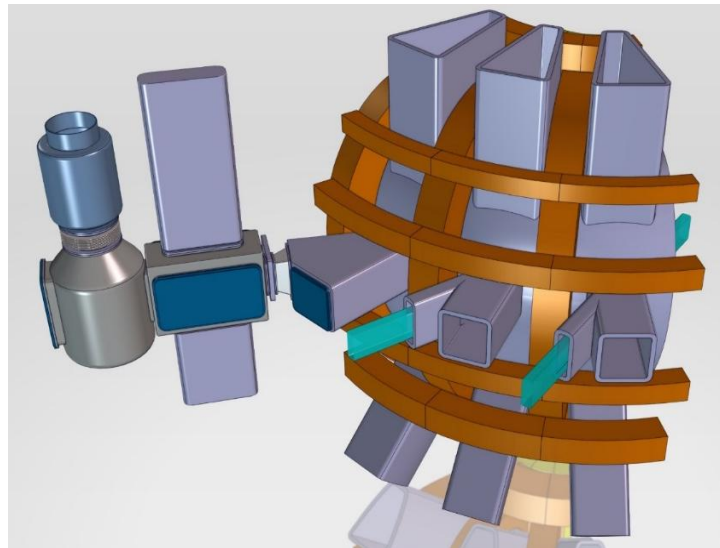


Fig. 5.1.3: conceptual design of DEMO1 NBI with photoneutraliser

the injector components is shown for the option with gas neutraliser.

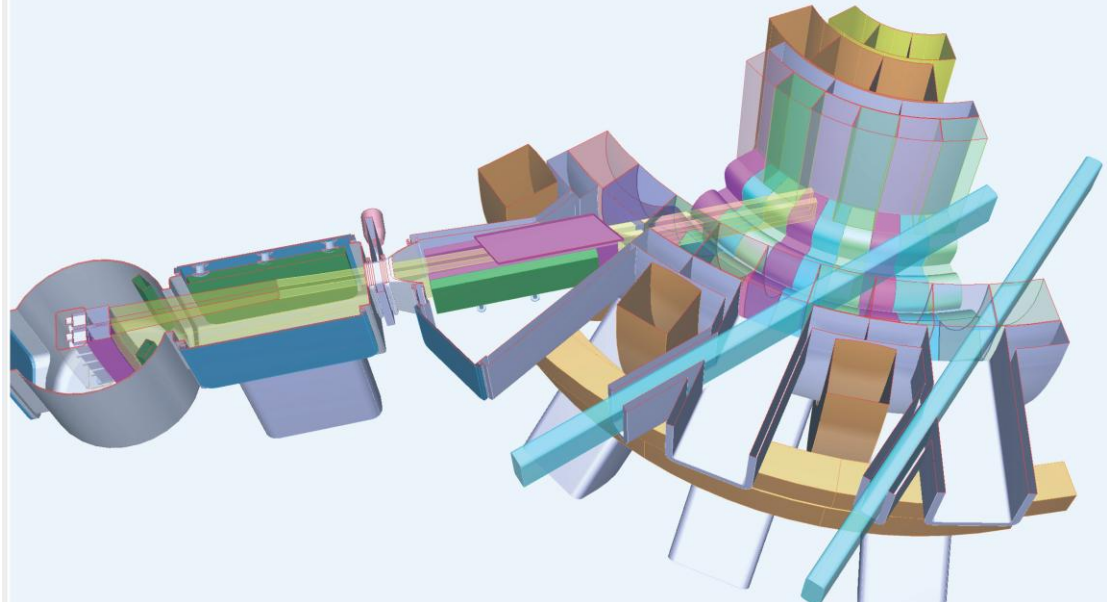


Fig. 5.1.4: cut view of the NBI for DEMO1 where the beam source and the components connecting the injector to the Tokamak are shown

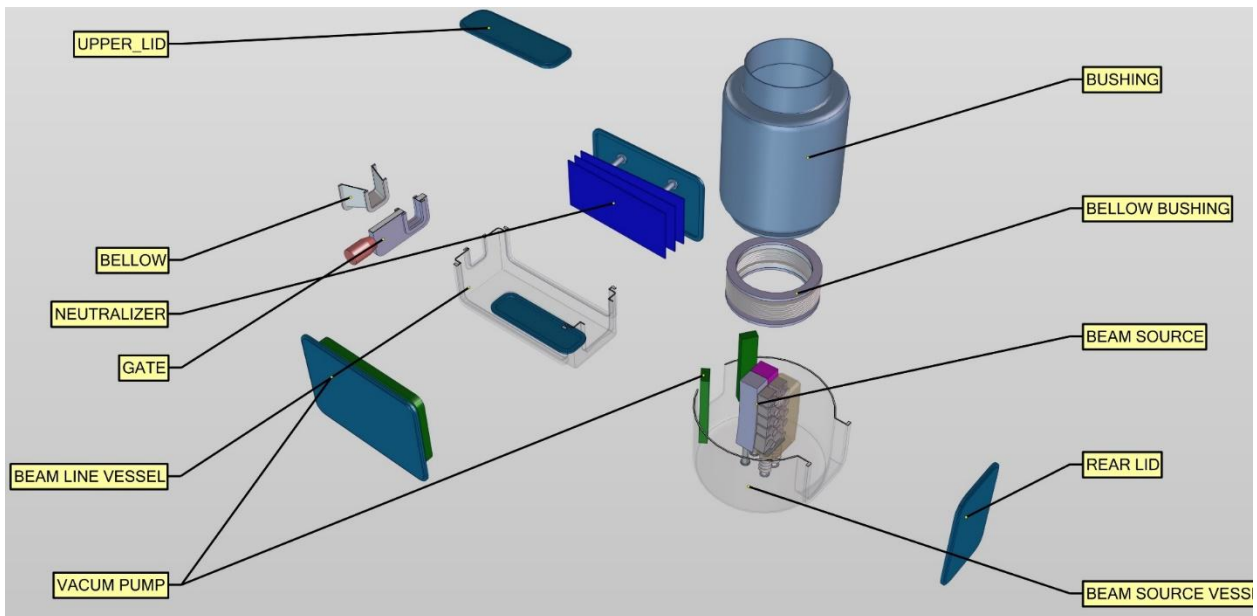


Fig. 5.1.5: exploded view of the compoents in the NBI fro DEMO1 in the option with gas neutraliser

One of the most important part of the work has been dedicated to the development of the requirements for the injector. This work has been also developed in conjunction with the activities to define the operational scenarios of the DEMO plasma (see section 5.4).

5.2 WPTFV: Tritium, Fuelling and Vacuum Pumping Systems

Since the concept of vacuum systems actually applied in the fusion experiments are not suitable for their application in a fusion reactor most of the development work under this work package is dedicated to develop viable alternative concepts. In collaboration with a company leader in vacuum systems it has been proposed to develop an innovative concept that is significantly less expensive both on investment and running costs and guarantees an intrinsically safe operation, high reliability and high availability with respect to the commonly used cryogenic system.

In 2014 the cooperation with an Italian company leader in the development of NEG (Non Evaporable Getters) materials and pumps started to develop a pump for the Neutral Beam System for DEMO. The development is also done with the scope to compare the performances with the actual cryogenic systems in a dedicated testbed available at KIT. In the following figures the honeycomb concept of the NEG pump is presented.

5.3 WPMAG: Magnet System

Consorzio RFX is a leading group in the development of PS systems and of active protection

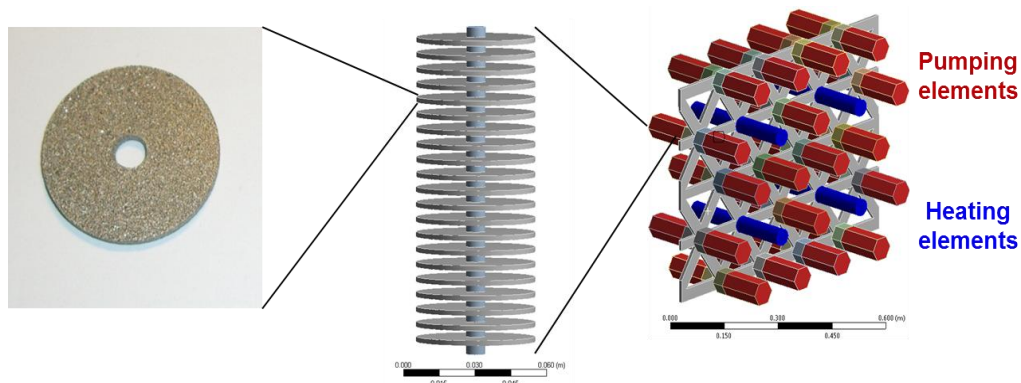


Fig. 5.2.1: single disk, stack and honeycomb concept of the NEG pump mock up for the DEMO NBI

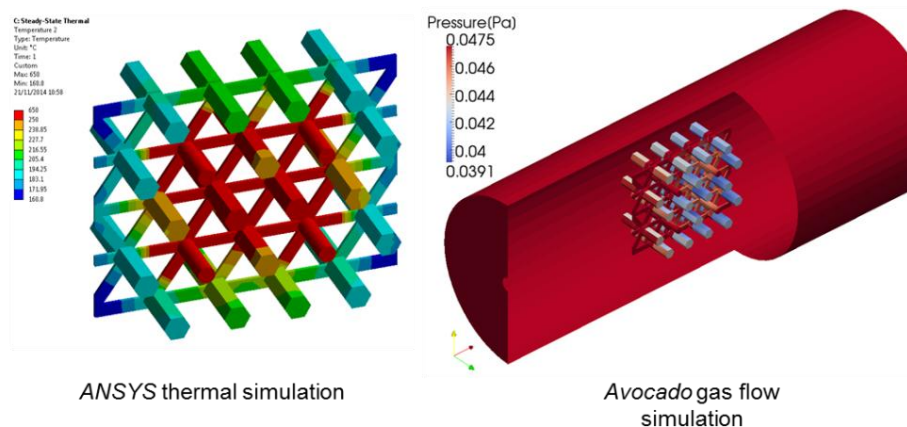


Fig. 5.2.2: thermal analysis and vacuum gas flow analysis in the TIMO facility at KIT

systems for fusion relevant magnet systems.

Despite the scarce relevance dedicated to this essential aspect of a Magnet System for a fusion reactor in the EUROfusion Work Programme it has been proposed to contribute and to guarantee the competence for the development of these systems to be developed for DEMO.

In particular in 2014 the work has been dedicated to collect the information and the requirements for the development of the Quench Protection System (QPS) and, based on the experience gained in the past by Consorzio RFX, the review of the key aspects for the design of the QPS for DEMO is started.

5.4 WPPMI: Plant Level System Engineering, Design Integration and Physics Integration

This is a Work Package in which it is required to define the plant system requirements and develop conceptual solution for almost all subsystems of a fusion reactor from diagnostic dedicated to the control up to the actuators and control systems and from the assessment of physics scenarios up to the analysis of requirements for auxiliary plant systems and finally up to the engineering integration of a fusion power plant.

Consorzio RFX has worked in two areas:

1. Design of the Plant Electrical System. In 2014 the work started in the following areas:
 - Collection of input data for the design of the Plant Electrical System from all the subsystems of DEMO including not only the available data , but also highlighting the missing parameters necessary for the development of the design.
 - First development of conceptual design of various Electrical Plant subsystems
 - Preliminary technological survey and first identification of issues, limits and analyses useful for the design development of the Plant Electrical System.
2. Plasma scenario development. A substantial work has been developed to explore different

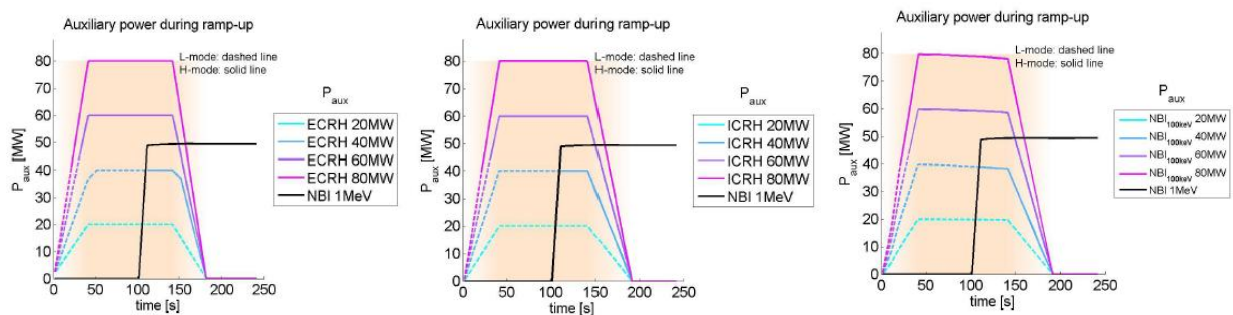


Fig. 5.4.1: three different heating scenario developed under WPPMI to study the ramp-up phase of the plasma current to assist the L-H transition

plasma scenario including a parametric scan on the aspect ratio. The in 2014 has been mainly dedicated to the parametric scan with the code METIS and with JINTRAC of different scenario for the Ramp Up and Ramp Down of the current with different heating systems and parameters. Examples of different ramp up scenario with different choices of additional heating system explored in this year are given in the following figures. It has to be noted that a closer interaction between different WPs are necessary to better define the requirements and the operation of the auxiliary heating systems to be considered for the plasma scenario development.

5.5 Energy Strategies

Fusion Energy as base-load electricity source.

A further development of the FRESCO (Fusion REactor Simplified COsts) code was carried out so as stochastic computation of the Fusion Levelised Cost of Electricity (LCE) was performed. This allowed a more reliable assessment (in terms of probability distribution) of the impact on the cost of electricity of both the reactor architecture and the long-term assumptions on key parameters, e.g. divertor and blanket lifetime and replacement time, financial parameters, cost of materials. The analyses carried out allowed finding the technical and economical parameters with the highest impact on the LCE of a Demo-like fusion power plant.

Preliminary assessments for the evaluation of the impact of the level of the safety of a Fusion Power Plant on the investment cost and generation cost of the electricity.

Long term scenarios for power generation and the role of Fusion.

Preliminary analyses were carried out he COMESE (*COsto MEdio del Sistema Elettrico*) code, set up in the past years, able to compute the average cost of electricity for different mix of technologies and energy sources, including energy storage; Fusion power plants for base load generation will be includes, in a post 2070 scenario, in order to evaluate under which conditions Fusion might have a key role.

6. APPLICATIONS

6.1 Plasma applications in medicine

The activity on plasma applications in medicine has been continued in the course of 2014. First of all, Consorzio RFX has actively participated to the development of the prototype of the plasma source for the treatment of corneal infections. This activity has been carried out in close contact with the company which acquired the license for the patent jointly filed by Consorzio RFX and University of Padova. The plasma source has been integrated in a piece of equipment already produced by the company. The mechanical part of the prototype is now ready, and the power supply is at an advanced stage of development. Thus, it is foreseen that electromagnetic compatibility certification will be achieved in the first months of 2015, and after that clinical trials will start. Meanwhile, research activity concerning in-vitro effects of the plasma on cells and has been continued, in collaboration with the Department of Molecular Medicine of the University of Padova. In particular, the role of the low-power atmospheric pressure plasma in the tissue repairing process was investigated in cultured human fibroblast-like primary cells. It was found that five minutes after treatment, plasma induced formation of reactive oxygen species (ROS) in cultured cells, as already previously found. Moreover, the ROS generated by the plasma treatment increased the expression of peroxisome proliferator activated receptor (PPAR)- γ , a nuclear

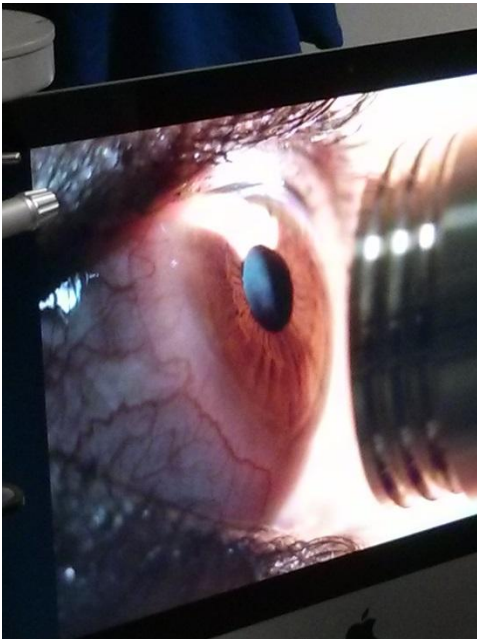


Fig. 6.1: Testing of the usability of the plasma source prototype performed by medical personnel (left) and close-up of the prototype positioned in proximity of the eye to be treated (right).

receptor that modulates the inflammatory responses. Plasma exposure promoted wound healing in an in-vitro model and induced fibroblast migration and proliferation. Since plasma-evoked ROS are time-restricted and elicit the PPAR- γ anti-inflammatory molecular pathway, this strategy ensures precise regulation of human fibroblast activation and could yield a valid therapeutic approach for liver and gut lesions [Brun 2014].

6.2 Vacuum Tight Threaded Junction

A new technique, called Vacuum Tight Threaded Junction (VTTJ), has been developed and patented by Consorzio RFX, permitting to obtain low-cost and reliable non welded junctions, able to maintain vacuum tightness also in heavy loading conditions (high temperature and high mechanical loads). The technique can be applied also if the materials to be joint are not weldable

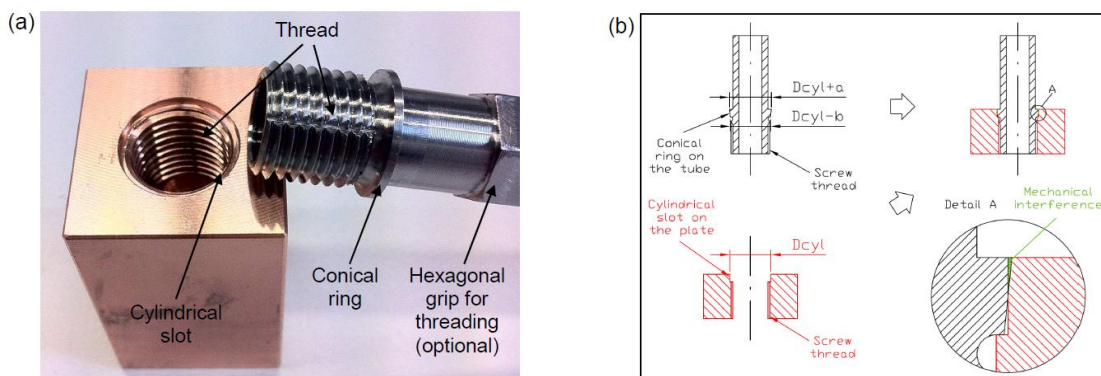


Fig. 6.2: The VTTJ concept: (a) VTTJ sample; (b) Section drawing.

and for heterogeneous junctions (for example, between steel and copper) and has been tested up to 500 bar internal pressure and up to 700 °C, showing excellent leak tightness in vacuum conditions and high mechanical resistance. The main advantages with respect to existing technologies (for example, friction welding and electron beam welding) are an easy construction, a low cost, a precise positioning of the junction and a high repeatability of the process. Due to these advantages, the new technique has been adopted for several components of the SPIDER experiment and it is proposed for ITER, in particular for the ITER Heat and Current Drive Neutral Beam Injector and for its prototype, the MITICA experiment, to be tested at Consorzio RFX.

The working principle of VTTJ is extremely simple. Two parts (at least one with tube shape) are screwed one into the other with a mechanical interference that creates a metallic seal. As an example, the sample of Fig. 6.2a represents a junction between a stainless steel tube and a copper block. A section drawing of the sample is given in Fig. 6.2b. The block presents a

cylindrical slot with a certain diameter D_{cyl} . On the other hand, the tube presents a conical ring, whose diameter on the external part is slightly larger than the one of the slot $D_{cyl}+a$, while on the internal part (toward the thread) it is slightly smaller $D_{cyl}-b$. For a junction between steel and copper, the a and b dimensions are of about a tenth of a millimeter. In this way, when the tube is screwed into the block, a plastic deformation of the cylindrical slot occurs in the mechanical interference region (highlighted in green in Fig. 6.2b). It has to be noted that this interference region is located on the surface of the sample; this fact is important because it represents an optimal starting point for the subsequent finishing operations. As a consequence of the plastic deformation of the softer material (in this case, copper) there is a certain increase on the screwing torque. The plastic deformation of copper generates an absolutely hermetic seal, as demonstrated by several tests carried out on various geometries of the junction.

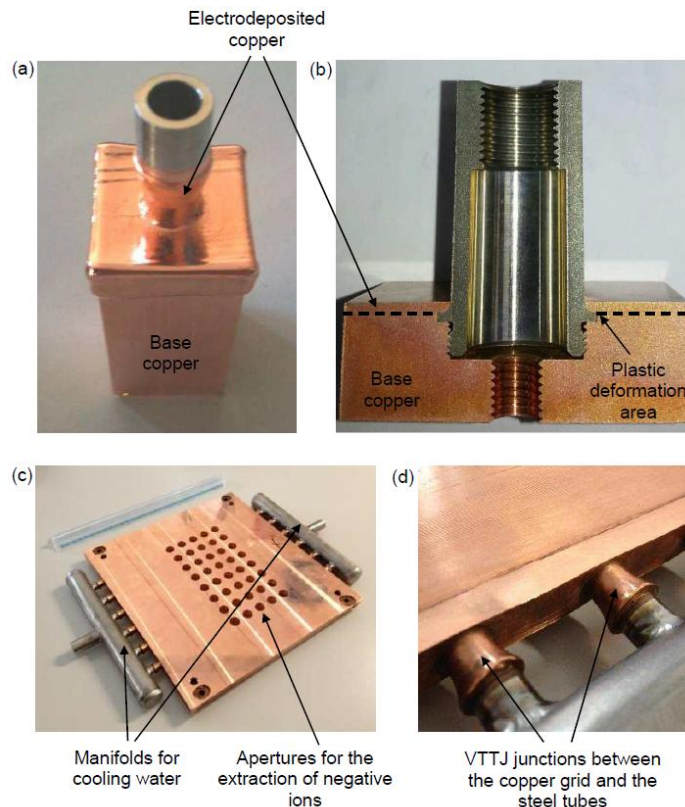


Fig. 6.3: Finishing with copper electrodepositions: (a) sample for the application on the SPIDER extraction grid; (b) section of the sample for the application on the SPIDER grounded grid; (c) prototype of an extraction grid for the SPIDER experiment; (d) detail view of the VTTJ junctions.

To avoid the unscrewing of the two components, and to make the junction compatible also with high thermal and/or structural loads, one can proceed with a finishing phase using galvanic electrodeposition of copper. Practically, the junction region is covered with a layer of about one

millimeter of copper. To have a good adhesion between the base materials and the electrodeposited copper, the base materials are subjected to a suitable surface cleaning and activation process. This can be made for example by treating the surfaces to be electrodeposited with a solution of water and hydrochloric acid. After the electrodeposition, the junction appears like in Fig. 6.3. In particular, the electrodeposited surface can be left as it is like in Fig. 6.3a, or flattened by milling like in Fig. 6.3b. The former sample was made for the SPIDER extraction grid, while the latter one for the SPIDER grounded grid. The pressure tests and leak tests were successful for both the samples.

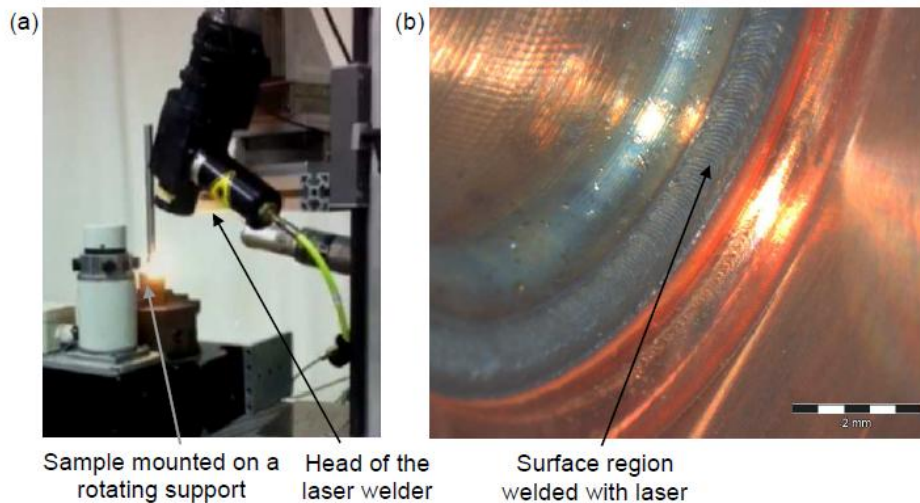


Fig. 6.4: Finishing with laser welding: (a) equipment set-up; (b) sample after finishing, where the optimal quality of the welding is visible.

As an alternative to the copper electrodeposition, some tests have been carried out also with a second finishing option, that foresees a surface laser welding. In this case, after screwing the tube, the surface of the junction circular border is heated with laser, so that a small quantity of material melts in the region that has been previously subjected to plastic deformation. The perfect contact between the two materials in that area, guaranteed by the previous plastic deformation, permits to obtain with a certain reliability an good quality of the laser welding, once suitable process parameters have been set up.

Summarizing, the new VTTJ technique permits to manufacture junctions between copper and steel having a perfect seal (compatible with the requirements of high vacuum environments) that is reliable in time also in presence of high temperatures and high structural loads. In the version with electrodeposited copper finishing, the process is carried out completely in room temperature conditions, hence in any phase the materials are prevented from possible damages due to overheating. On the other hand, using any other existing technique able to give a vacuum

compatible seal (like friction welding, electron beam welding, brazing etc.) there is always a certain overheating in the junction area, with possible cracks or other types of degradation of the materials (annealing, recrystallization, inclusions etc.). Following the second option, that entails a laser welding finishing, although the process is not completely cold, the heat affected zone has in any case a very limited volume, because the penetration depth of the laser welding is of the order of some tenth of millimeter.

The principle of VTTJ junction is also applicable if other materials are used (like aluminum, magnesium, nickel, chromium, bronze, zirconium etc.) or other geometries (for example, tube-tube junctions instead of tube-plate ones).

The VTTJ junction has been used so far in the all grids of the SPIDER extractor/acceleration system. In this regard, Fig. 6.3c and Fig. 6.3d show the applications on the Multi Channel Prototype of the SPIDER extraction grid. This is a prototype featuring all the possible manufacturing issues of the SPIDER and MITICA grids. A comprehensive testing campaign has been carried out on this prototype, with all the tests successfully passed. Moreover, VTTJ is presently one of the design options for the junctions of the MITICA accelerator grids. In principle, it could be used in other components of the ITER experiment, that are required to operate in vacuum conditions and under high heat loads. Among these, we can cite the Beam Line Components of the Neutral Beam Injectors, the blanket and the divertor.

Although developed for nuclear fusion applications, the new junction technique is applicable also to large scale production, in particular in the fields of heat engineering, thermotechnics, chemistry, cryogenics, nuclear, vacuum equipment, food and pharmaceutical industry.

The VTTJ has been patented by Consorzio RFX. In particular, the following patents of the VTTJ technique have been deposited:

- Italian patent, deposited on June 7th 2012
- International patent according to PCT, deposited on December 12th 2013 and visible at the following websites:
<http://patentscope.wipo.int/search/en/WO2013182962>
<http://worldwide.espacenet.com/publicationDetails/biblio?CC=WO&NR=2013182962A1&KC=A1&FT=D>
- Indian patent, deposited on November 19th 2014
- Japanese patent, deposited on November 20th 2014
- South-corean patent, deposited on November 26th 2014

-
- Chinese patent, deposited on November 26th 2014
 - USA patent, deposited on December 2nd 2014
 - European patent, to be deposited within December 31st 2014

6.3 Investigation on Voltage Holding properties of Siemens Vacuum Interrupters

In the last six years, the Padova Research Group gained significant expertise in the field of High Voltage Holding in Vacuum, as a consequence of the R&D activities related to the design and construction of the accelerator of the 1 MeV Neutral Beam Injector prototype of the Neutral beam Test Facility.

Both experimental and modeling skill have been thus developed. In particular, a High Voltage Test Facility (HVPTF) [De Lorenzi 2014] has been realized, designed to perform experiments up to 800 kV in bipolar configuration (+400 kV; -400 kV). On the modeling side, it has been developed an innovative design tool to predict, for any multi-voltage and multi-electrode configuration the breakdown probability for a given voltage distribution (Voltage Holding Predictive Model VHPM [Pilan 2014]).



High-voltage VI
145kV / 40kA

On the basis of this recent expertise, supported by the very fruitful, long time collaboration in the development of special Vacuum Interrupters for DC current used in the RFX Ohmic Heating Circuit and then in ITER Fast Discharge Units, the Siemens Departments CT RTC PET REG-DE – Erlangen and AG, IC LMV MS R&D OC 3 - Berlin in charge for the development of a new generation of Vacuum Interrupters, asked the Consorzio RFX to implement an Agreement for the characterization of the Voltage Holding properties of Vacuum Interrupter for medium Voltage applications, using the VHPM tool developed by RFX.

An example of a Vacuum Tube
(Courtesy of IC LMV MS –Berlin)

The technical content of the Agreement is summarized below:

- Statistical Analysis of the pulse voltage conditioning processes,
- Application of the Voltage Holding Predictive Model (VHPM) originally developed for DC application.

-
- Application of VHPM to the test cases (Vacuum Tubes from standard production)
 - Assessment of the predictive capability of VHPM in non DC conditions.
 - Further usage of the VHPM for the development of the geometry of an alternative /optimized tube design.

The Agreement has been signed by the Director of the Centro Ricerche Fusione, the Representative of the Padova University in the Consorzio RFX and by the Heads of the two Siemens Units in Erlangen (CT-RTC-PET) and Munich (CT-TIM-EC-UR) and entered into force the 2 December 2014.

Immediately after the signature of the Agreement; the Erlangen Unit sent to RFX the first data set to start the first activity block planned in the workplan, namely the electrostatic analyses of a specific VCB in 2D and 3D geometry, as a first benchmarking of the analyses carried out by the Siemens R&D Department. The work at RFX has officially on 15 December 2014.

REFERENCES

[Brun 2014] P. Brun, S. Pathak, I. Castagliuolo, G. Palù, P. Brun, M. Zuin, R. Cavazzana, E. Martines, *Helium Generated Cold Plasma Finely Regulates Activation of Human Fibroblast-Like Primary Cells*, PLoS One **9**, e104397 (2014).

[De Lorenzi 2014] A. De Lorenzi, N. Pilan L. Lotto, M. Fincato, G. Pesavento, R. Gobbo *HVPTF—The high voltage laboratory for the ITER Neutral Beam test facility* Fusion Engineering and Design Volume 86, Issues 6–8, October 2011, Pages 742–745

[Pilan 2014] Pilan, N.; Veltri, P.; De Lorenzi, A., *Voltage holding prediction in multi electrode-multi voltage systems insulated in vacuum* IEEE Transactions on Dielectrics and Electrical Insulation, Volume: 18 , Issue: 2 DOI 10.1109/TDEI.2011.5739461

7. EDUCATION, TRAINING AND INFORMATION TO THE PUBLIC

7.1 International Doctorate in Fusion Science and Engineering

In 2014, the activity of both the “Joint Research Doctorate in Fusion Science and Engineering” (by Padua and Lisbon universities), and the “European Interuniversity Doctoral Network in Fusion Science and Engineering”, among the same two universities and the Ludwig Maximilian University of Munich, continued under the responsibility of Padua University and of Consorzio RFX. Moreover, also the participation to the Erasmus Mundus International Doctoral College in Fusion Science and Engineering (Fusion DC), led by Ghent University, continued very fruitfully

In particular, 6 new PhD students entered RFX in 2014: 4 from our International Doctorate and 2 from Fusion DC, bringing to 19 the number of PhD students working at Consorzio RFX over a total of 28 students participating to the three year of the doctorate on the three Universities of the Network.

Furthermore, at beginning of 2014, 4 students completed the Doctorate, passing the doctoral final examination and obtaining the Joint International Doctoral Diploma.

As usual, for the students of the Doctorate, during 2014, 4 courses were organized, 2 at RFX, one at IST (Lisbon) and one at IPP (Garching).

The 2 courses at RFX were: a Basic course, organized for the students starting the first year of the doctorate, divided into a Basic Physics and a Basic Engineering, and an Engineering Advanced Course, for the students at the second year.

Topics and teachers of these Courses were:

1. Basic Course

a). Basic Physics (36 hrs)

- Introduction to plasma physics (G. Serianni, RFX)
- Collision and MHD plasma description (T. Bolzonella, RFX)
- Magnetic Configurations (E. Martines, RFX)
- Equilibrium, stability and shaping of toroidal plasmas (F. Gesotto, RFX and UniPD)
- Transport and turbulence (N. Vianello, RFX)
- Introduction to plasma diagnostics (L. Giudicotti, RFX and UniPD).

b) Basic Engineering (36 hrs)

- Fusion power plants (M. Dalla Palma, RFX)
- First wall, divertor, vacuum vessel (P. Zaccaria, RFX)
- Magnets (G. Chitarin, RFX and UniPD)

-
- Power systems for fusion experiments (E. Gaio, RFX)
 - Feedback control theory with application to Tokamak control (G. Manduchi, RFX)
 - Basic data acquisition (G. Manduchi, RFX).

2. **Engineering Advanced Course** (50hrs)

- *Introduction*

Introduction to the Course (P. Bettini, RFX and UniPD)

Energy scenarios for the next century and the role of fusion (G. Zollino, RFX and UniPD),

The fusion reactor (G. Zollino, RFX and UniPD)

- *Materials for fusion reactors:*

The role of materials in fusion devices and structural materials (S. Dudarev, CCFE Culham),

Superconducting magnets for fusion applications (P. Bruzzone, CRPP Lausanne), Liquid

metal for first wall (G. Mazzitelli, ENEA Frascati), Plasma Facing components in ITER (M.

Merola, ITER Cadarache),

- *Heating and current drive systems:*

Introduction: heating and current drive in fusion devices (A. Cardinali, ENEA Frascati),

Plasma heating and current drive by NBI (C. Hopf, IPP Garching), ITER NBI (P. Sonato,

RFX and UniPD), ECRH in fusion devices (G. Granucci, CNR Milano), ICRH and LHCD:

electromagnetic issues and system integration (F. Mirizzi, ENEA Frascati), Antenna design

for RF fusion systems (D. Milanese, Politecnico Torino).

- *Fusion plant studies, management, modeling:*

Managing the design of the tokamak (JT60 SA) (G. Giruzzi, CEA Cadarache),

Electromagnetic modeling of fusion machines (R. Albanese, UniNA), ITER vacuum vessel

manufacturing preparation (P. Bonifazi, Walter Tosto SpA Chieti), Power Plant studies and

DEMO (D. MAisonnier, European Commission Bruxelles)

In addition in 2014, since the Italian doctoral calendar was changed, by anticipating the start of the doctorates from January 1st to November 1st, the first part of the Basic Course dedicated to Physics was repeated at the end of November for the new entering students.

Teachers from RFX contributed also to the courses held in Garching and Lisbon.

7.2 Other education and training activities

The other educational and training activities of Consorzio RFX continued also in 2014 with a significant effort.

In particular, the tutorial activity for development of bachelor and master thesis continued as in the past.

Also the organization of short (1-2 months) summer stages at Consorzio RFX of secondary school students continued as in the previous years.

In conclusion, RFX professionals were in charge of 19 PhD students, preparing their PhD thesis, of about 15 students, preparing their graduation thesis, and of a few secondary school students in summer stage.

In addition in 2014, the educational actions dedicated to the RFX staff have been intensified with goal oriented courses in specialized topics. In particular the following 4 courses were organized :

- *Distribuzione ed utilizzo di gas criogenici*
- *Compatibilità EMI e EMC e sorgenti di radiazione(2 times)*
- *CATIA*

Moreover 7 regular courses of Padua University, on fusion related disciplines, were given by teachers from Consorzio RFX.

In particular:

- 4 at Engineering Department: "Fission and Fusion Nuclear Plants", "Thermonuclear Fusion", "Industrial Applications of Plasmas" and "Energy Technology and Economics";
- 3 at Physics Department: "Introduction to Plasma Physics", "Fluid and Plasmas Physics" and "Physics of Nuclear Fusion and Applications of Plasmas".

In addition at Physics Department, for the 14° Master course in Comunicazione delle Scienze "Comunicazione negli enti di ricerca".

7.3 Information to the public

In 2014, the activity developed along the following main lines:

- Outreach and education

The effort devoted to the public understanding of fusion topics continued in 2014, in particular, with public talks and lectures and with overviews on fusion given to secondary students on the occasion of visits to the plant.

In September, Consorzio RFX participated to the European Night of Research in collaboration with the University of Padova; among the initiatives organized for the event, the participation to the scientific caffè held in downtown was particularly successful. Information material (brochures, posters and images) was updated and elaborated for an effective dissemination of the information.

Contacts with CNR communication office in Rome were started to evaluate further initiatives to be organized on local public transportation.

The website was updated as for the development of the Prima Project is concerned.

- Public information

Press notes were elaborated on the occasion for the best thesis in Fusion Science and Engineering Award 2014. Public speaking were given by researchers from Consorzio RFX and relations with stakeholders were reinforced to share points of view prior to programmatic decisions.

- EUROfusion activity

In the frame of the outreach and communication activity foreseen in the Road Map in support of fusion energy research, Consorzio RFX participated in 2014 Social Economic and outreach Studies (SES).

8. PUBLICATION LIST

SUMMARY

International and national journals

Conference proceedings

Communications to National and International Workshops and Conferences

International and national journals

1. Tomography feasibility study on the optical emission spectroscopy diagnostic for the negative ion source of the ELISE test facility
Bonomo, F.; Agostini, M.; Brombin, M.; U. Fantz, P. Franzen, R. Pasqualotto, U. Fantz, P. Franzen, D W"underlich and the NNBI Team
PLASMA PHYS CONTR F, **56** Issue: 1, (2014) 015006 (14 pp)
2. Characterization of temperature profiles in the outer region of RFX-mod
Scaggion, A.; Agostini, M.; Fassina, A., P. Franz
PLASMA PHYS CONTR F, **56** Issue: 1 (2014) 015008 (13 pp)
3. First scenario development with the JET new ITER-like wall
E. Joffrin, M. Baruzzo, M. Beurskens, C. Bourdelle, S. Brezinsek, J. Bucalossi, P. Buratti, G. Calabro, C.D. Challis, M. Clever, J. Coenen, E. Delabie, R. Dux, P. Lomas, E. de la Luna, P. de Vries, J. Flanagan, L. Frassinetti, D. Frigione, C. Giroud, M. Groth, N. Hawkes, J. Hobirk, M. Lehnen, G. Maddison³, J. Mailloux, C.F. Maggi, G. Matthews, M. Mayoral, A. Meigs, R. Neu, I. Nunes, T. Puetterich, F. Rimini, M. Sertoli, B. Sieglin, A.C.C. Sips, G. van Rooij, I. Voitsekhoovitch and JET-EFDA Contributors
NUCL FUSION, **54** Issue: 1 (2014) 013011 (12 pp)
4. Calculation of 3-D Magnetic Fields Produced by MHD Active Control Systems in Fusion Devices
Bettini, Paolo; Marrelli, Lionello; Specogna, Ruben
IEEE T MAGN, **50** Issue: 2 (2014) 7000904 (4 pp)
5. A Novel Tool for Breakdown Probability Predictions on Multi-Electrode Multi-Voltage Systems
Bettini, Paolo; Pilan, Nicola; Specogna, Ruben
IEEE T MAGN, **50** Issue: 2 (2014) 7002104 (4 pp)
6. Lazy Cohomology Generators Enable the Use of Complementarity for Computing Halo Current Resistive Distribution in Fusion Reactors
Bettini, Paolo; Specogna, Ruben
IEEE T MAGN, **50** Issue: 2 (2014) 7012004 (4 pp)
7. A 2D Particle in Cell model for ion extraction and focusing in electrostatic accelerators
Veltri, P; Cavenago, M; Serianni, G
REV SCI INSTRUM, **85** Issue: 2 (2014) 02A711
8. Ferromagnetic effects in the theory of slow and fast resistive wall modes in tokamaks
Pustovitov, V. D.; Yanovskiy, V. V.
PHYS PLASMAS, **21** Issue: 2 (2014) 022516

-
9. Modeling and design of a beam emission spectroscopy diagnostic for the negative ion source NIO1
Barbisan, M.; Zaniol, B.; Cavenago, M.; R. Pasqualotto
REV SCI INSTRUM, **85** Issue: 2 (2014) 02A708
 10. Electrostatic sensors for SPIDER experiment: Design, manufacture of prototypes, and first tests
M. Brombin, M. Spolaore, G. Serianni, A. Barzon, L. Franchin, R. Pasqualotto, N. Pomaro, L. Schiesko, C. Taliercio, and L. Trevisan
REV SCI INSTRUM, **85** Issue: 2 (2014) 02A715
 11. Installation of a versatile multiaperture negative ion source
M. Cavenago, G. Serianni, V. Antoni, M. Barbisan, M. Bigi, M. De Muri, E. Fagotti, F. Fellin, T. Kulevoy, A. Minarello, R. Pasqualotto, S. Petrenko, M. Poggi, M. Recchia, F. Rossetto, M. Sattin, M. Valente, and P. Veltri
REV SCI INSTRUM, **85** Issue: 2 (2014) 02A704
 12. High energy flux thermo-mechanical test of 1D-carbon-carbon fibre composite prototypes for the SPIDER diagnostic calorimeter
M. De Muri, T. Cavallin, R. Pasqualotto, M. Dalla Palma, V. Cervaro, D. Fasolo, L. Franchin, M. Tollin, H. Greuner, B. Böswirth, and G. Serianni
REV SCI INSTRUM, **85** Issue: 2 (2014) 02A718
 13. An image filtering technique for SPIDER visible tomography
N. Fonnesu, M. Agostini, M. Brombin, R. Pasqualotto, and G. Serianni
REV SCI INSTRUM, **85** Issue: 2 (2014) 02A730
 14. First negative ion beam measurement by the Short-Time Retractable Instrumented Calorimeter Experiment (STRIKE)
G. Serianni, M. De Muri, A. Muraro, P. Veltri, F. Bonomo, G. Chitarin, R. Pasqualotto, M. Pavei, A. Rizzolo, M. Valente, P. Franzen, B. Ruf, and L. Schiesko
REV SCI INSTRUM, **85** Issue: 2 (2014) 02A736
 15. A 2D Particle in Cell model for ion extraction and focusing in electrostatic accelerators
Veltri, P.; Cavenago, M.; Serianni, G.
REV SCI INSTRUM, **85** Issue: 2 (2014) 02A711
 16. Physics design of the injector source for ITER neutral beam injector (invited)
V. Antoni, P. Agostinetti, D. Aprile, M. Cavenago, G. Chitarin, N. Fonnesu, N. Marconato, N. Pilan, E. Sartori, G. Serianni, and P. Veltri
REV SCI INSTRUM, **85** Issue: 2 (2014) 02B128
 17. Cancellation of the ion deflection due to electron-suppression magnetic field in a negative-ion accelerator
Chitarin, G.; Agostinetti, P.; Aprile, D.; N. Marconato, P. Veltri
REV SCI INSTRUM, **85** Issue: 2 (2014) 02B317
 18. Non-ideal operating conditions of the ion source prototype for the ITER neutral beam injector due to thermal deformation of the support structure
E. Sartori, M. Pavei, D. Marcuzzi, and P. Zaccaria

REV SCI INSTRUM, **85** Issue: 2 (2014) 02B313

19. Comparative study of beam losses and heat loads reduction methods in MITICA beam source
E. Sartori, P. Agostinetti, S. Dal Bello, D. Marcuzzi, G. Serianni, P. Sonato, and P. Veltri
REV SCI INSTRUM, **85** Issue: 2 (2014) 02B308
20. Resistive wall stabilization of rotating edge modes in tokamaks
Pustovitov, V. D.; Yanovski, V. V.
PLASMA PHYS CONTR F, **56** Issue: 3 (2014) 035003
21. Design and R&D of Thermal Sensors for ITER Neutral Beam Injectors
Mauro Dalla Palma, Nicola Pomaro, Moreno Maniero, Roberto Pasqualotto, Lauro Trevisan,
and Piergiorgio Sonato
IEEE T PLASMA SCI, **42** Issue: 3 Special Issue: SI (2014) 610-615 Part:1
22. Manufacturing and Testing of Grid Prototypes for the ITER Neutral Beam Injectors
Piero Agostinetti, Giuseppe Chitarin, Nicolò Marconato, Diego Marcuzzi, and Andrea Rizzolo
IEEE T PLASMA SCI, **42** Issue: 3 Special Issue: SI (2014) 628-632 Part:1
23. Modeling of Beam Transport, Secondary Emission and Interactions With Beam-Line
Components in the ITER Neutral Beam Injector
Emanuele Sartori, Pierluigi Veltri, Gianluigi Serianni, Mauro Dalla Palma, Giuseppe Chitarin,
and Piergiorgio Sonato
IEEE T PLASMA SCI, **42** Issue: 3 Special Issue: SI (2014) 633-639 Part:1
24. Review of the RFX-Mod AC/DC Conversion System and Possible Improvements for New
Plasma Scenarios
Ferro, Alberto; Framarin, Junior Jader; Novello, Luca; A. Zamengo, L. Zanotto, E. Gaio
IEEE T PLASMA SCI, **42** Issue: 3 Special Issue: SI (2014) 645-650 Part:1
25. Chaoticity threshold in magnetized plasmas: Numerical results in the weak coupling regime
Carati, A.; Benfenati, F.; Maiocchi, A.; M. Zuin
CHAOS, **24** Issue: 1 (2014) 013118
26. Pressure-driven reconnection and quasi periodical oscillations in plasmas
Paccagnella, R.
PHYS PLASMAS, **21** Issue: 3 (2014) 032307
27. From distributed to multicore architecture in the RFX-mod real time control system
Manduchi, G.; Luchetta, A.; Soppelsa, A.; C. Taliercio
FUSION ENG DES, **89** Issue: 3 (2014) 224-232
Published: MAR 2014
28. Tearing modes transition from slow to fast rotation branch in the presence of magnetic
feedback
P. Innocente, P. Zanca, M. Zuin, T. Bolzonella and B. Zaniol
NUCL FUSION, **54** Issue: 12 (2014) 122001
29. Dual-laser calibration of Thomson scattering systems in ITER and RFX-mod
Giudicotti, L.; Pasqualotto, R.

NUCL FUSION, **54** Issue: 4 (2014) 043005

30. Trapped electron effects eta(i)-mode and trapped electron mode in RFP plasmas
Liu, S. F.; Guo, S. C.; W. Kong and J.Q. Dong
NUCL FUSION, **54** Issue: 4 (2014) 043006
31. Physical aspects of divertor Thomson scattering implementation on ITER
E.E. Mukhin, R.A. Pitts, P. Andrew, I.M. Bukreev, P.V. Chernakov, L. Giudicotti, G. Huijsmans, M.M. Kochergin, A.N. Koval, A.S. Kukushkin, G.S. Kurskiev, A.E. Litvinov, S.V. Masyukevich, R. Pasqualotto, A.G. Razdobarin, V.V. Semenov, S.Yu. Tolstyakov and M.J. Walsh
NUCL FUSION, **54** Issue: 4 (2014) 043007
32. Tokamak toroidal rotation caused by AVDEs and ELMs
Strauss, H.; Sugiyama, L.; Paccagnella, R.; J. Breslau
NUCL FUSION, **54** Issue: 4 (2014) 043017
33. Electric Probe Measurements of the Poloidal Velocity in the Scrape-Off Layer of ASDEX Upgrade
F. Mehlmann, S. Costea, R. Schrittwieser, V. Naulin, J. J. Rasmussen, H. W. Mueller, A.H. Nielsen, N. Vianello, D. Carralero, V. Rohde, C. Lux, C. Ionita, and ASDEX Upgrade Team
CONTRIB PLASM PHYS, **54** Issue: 3 Special Issue: SI (2014) 273-278
34. Magnetic Field Effect on Voltage Holding in the MITICA Electrostatic Accelerator
Pilan, Nicola; Chitarin, Giuseppe; De Lorenzi, Antonio, G. Serianni
IEEE T PLASMA SCI, **42** Issue: 4 (2014) 1012-1020
35. Prototype of a Diagnostic Calorimeter for BATMAN: Design and Preliminary Measurements
Michela De Muri, Mauro Pavei, Andrea Rizzolo, Federica Bonomo, Peter Franzen, Rudolf Riedl,
Benjamin Ruf, Loic Schiesko, Matteo Valente, Vannino Cervaro, Daniele Fasolo, Luca Franchin, Marco Tollin, Roberto Pasqualotto, and Gianluigi Serianni
IEEE T PLASMA SCI, **42** Issue: 4 (2014) 1032-1035
36. Compensation of Beamlet Deflections and Focusing Methods in the Electrostatic Accelerator of MITICA Neutral Beam Injector
P. Veltri, P. Agostinetti, M. Cavenago, G. Chitarin, N. Marconato, E. Sartori, and G. Serianni
IEEE T PLASMA SCI, **42** Issue: 4 (2014) 1047-1052
37. A New Generation of Real-Time Systems in the JET Tokamak
Diogo Alves, André C. Neto, Member, IEEE, Daniel F. Valcárcel, Robert Felton, JuanM.López, Antonio Barbalace, Luca Boncagni, Peter Card, Gianmaria De Tommasi, Senior Member, IEEE, Alex Goodyear, Stefan Jachmich, Peter J. Lomas, Francesco Maviglia, Paul McCullen, Andrea Murari, Mark Rainford, Cedric Reux, Fernanda Rimini, Filippo Sartori, Adam V. Stephen, Jesus Vega, Riccardo Vitelli, Luca Zabeo, and Klaus-Dieter Zastrow
IEEE T NUCL SCI, **61** Issue: 2 (2014) 711-719
38. Implementation of the Disruption Predictor APODIS in JET's Real-Time Network Using the MARTe Framework

-
- J. M. López, J. Vega, D. Alves, Member, IEEE, S. Dormido-Canto, A. Murari, J. M. Ramírez, R. Felton, M. Ruiz, and G. de Arcas
IEEE T NUCL SCI, **61** Issue: 2 (2014) 741-744
39. An Original Method for Spot Detection and Analysis for Large Surveys of Videos in JET
Teddy Craciunescu, Andrea Murari, Bernhard Sieglin, Guy Matthews, and JET EFDA Contributors
IEEE T PLASMA SCI, **42** Issue: 5 (2014) 1358-1366 Part:1
40. The influence of an ITER-like wall on disruptions at JET
P. C. de Vries, M. Baruzzo, G. M. D. Hogeweij, S. Jachmich, E. Joffrin, P. J. Lomas, G. F. Matthews, A. Murari, I. Nunes, T. Pütterich, C. Reux, J. Vega, and JET-EFDA Contributors
PHYS PLASMAS, **21** Issue: 5 (2014) 056101
41. Edge ambipolar potential in toroidal fusion plasmas
G. Spizzo, N. Vianello, R. B. White, S. S. Abdullaev, M. Agostini, R. Cavazzana, G. Ciaccio, M. E. Puiatti, P. Scarin, O. Schmitz, M. Spolaore, D. Terranova, and RFX and TEXTOR Teams
PHYS PLASMAS, **21** Issue: 5 (2014) 056102
42. Real-time change detection in data streams with FPGAs
J. Vega, S. Dormido-Canto, T. Cruz, M. Ruiz, E. Barrera, R. Castro, A. Murari, M. Ochando
FUSION ENG DES, **89** Issue: 5 (2014) 644-648
43. MDSplus automated build and distribution system
Fredian, T.; Stillerman, J.; Manduchi, G.
FUSION ENG DESV, **89** Issue: 5 (2014) 649-651
44. Fast control and data acquisition in the neutral beam test facility
Luchetta, A.; Manduchi, G.; Taliercio, C.
FUSION ENG DES, **89** Issue: 5 (2014) 663-668
45. Future directions of MDSplus
Manduchi, G.; Fredian, T.; Stillerman, J.
FUSION ENG DES, **89** Issue: 5 (2014) 775-779
46. Input/output plugin architecture for MDSplus
Stillerman, Joshua; Fredian, Thomas; Manduchi, Gabriele
FUSION ENG DES, **89** Issue: 5 (2014) 784-786
47. Self-organized 3D equilibrium formation and its feedback control in RFX-mod
P. Piovesan, D. Bonfiglio, L. Marrelli, A. Soppelsa, M. Spolaore, D. Terranova and the RFX-Mod Team
NUCL FUSION, **54** Issue: 6 (2014) 064006
48. Plasma edge transport with magnetic islands-a comparison between tokamak and reversed-field pinch
G. Ciaccio, O. Schmitz, S.S. Abdullaev, H. Frerichs, M. Agostini, P. Scarin, G. Spizzo, N. Vianello and R. B. White
NUCL FUSION, **54** Issue: 6 (2014) 064008

-
49. Ideal saturated MHD helical structures in axisymmetric hybrid plasmas
Brunetti, D.; Graves, J. P.; Cooper, W. A., D. Terranova
NUCL FUSION, **54** Issue: 6 (2014) 064017
 50. Real-Time Processing System for the JET Hard X-Ray and Gamma-Ray Profile Monitor Enhancement
Ana M. Fernandes, Rita C. Pereira, André Neto, Daniel F. Valcárcel, Diogo Alves, Jorge Sousa,
Bernardo B. Carvalho, Vasily Kiptily, Brian Syme, Patrick Blanchard, Andrea Murari, Carlos M.
B. A. Correia, Carlos A. F. Varandas, Bruno Gonçalves, and JET EFDA contributors
IEEE T NUCL SCI , **61** Issue: 3 (2014) 1209-1215 Part: 2
 51. The New Feedback Control System of RFX-mod Based on the MARTe Real-Time Framework
Manduchi, G.; Luchetta, A.; Soppelsa, A.
IEEE T NUCL SCI , **61** Issue: 3 (2014) 1216-1221 Part: 2
 52. Optical Layout and Alignment Methods for Visible Tomography and Emission Spectroscopy Diagnostics in SPIDER
Delogu, Rita Sabrina; Brombin, Matteo; Zaniol, Barbara, M. Agostini, M. Barbisan, N. Fonesu, M. Tollin, R. Pasqualotto
IEEE T PLASMA SCI, **42** Issue: 6 (2014) 1802-1806 Part: 2
 53. UMEL: A new regression tool to identify measurement peaks in LIDAR/DIAL systems for environmental physics applications
Gelfusa, M.; Gaudio, P.; Malizia, A, A. Murari, J. Vega, M. Richetta, S. Gonzales
REV SCI INSTRUM, **85** Issue: 6 (2014) 063112
 54. Impurity transport studies in the Madison Symmetric Torus reversed-field pinch during standard and pulsed poloidal current drive regimes
Barbui, T.; Carraro, L.; Den Hartog, D. J, S.T.A. Kumar, M. Nornberg
PLASMA PHYS CONTR F, **56** Issue: 7 (2014) 075012
 55. Simulation of feedback control on tearing modes using different sensors in a reversed field pinch and application to the Keda Torus eXperiment
Li, Chenguang; Zanca, Paolo; Liu, Wandong
PLASMA PHYS CONTR F, **56** Issue: 7 (2014) 075015
 56. Design and Test of a Thermal Measurement System Prototype for SPIDER Experiment
Dalla Palma, Mauro; Pomaro, Nicola; Taliercio, Cesare
IEEE T PLASMA SCI, **42** Issue: 7 (2014) 1971-1976
 57. Feedback-assisted extension of the tokamak operating space to low safety factor
J. M. Hanson, J. M. Bialek, M. Baruzzo, T. Bolzonella, A. W. Hyatt, G. L. Jackson, J. King, R. J. La Haye, M. J. Lanctot, L. Marrelli, P. Martin, G. A. Navratil, M. Okabayashi, K. E. J. Olofsson, C. Paz-Soldan, P. Piovesan, C. Piron, L. Piron, D. Shiraki, E. J. Strait, D. Terranova, F. Turco, A. D. Turnbull,³ and P. Zanca
PHYS PLASMAS, **21** 072107 (2014)
 58. Tokamak Operation with Safety Factor $q_{(95)} < 2$ via Control of MHD Stability.

-
- P. Piovesan, J.M. Hanson, P. Martin, G.A. Navratil, F. Turco, J. Bialek, N.M. Ferraro, R.J. La Haye, M.J. Lanctot, M. Okabayashi, C. Paz-Soldan, E.J. Strait, A.D. Turnbull, P. Zanca, M. Baruzzo, T. Bolzonella, A.W. Hyatt, G.L. Jackson, L. Marrelli, L. Piron, and D. Shiraki
PHYS REV LETT, **113** Issue: 4 (2014) 045003
59. Parallel and perpendicular structure of the edge turbulence in a three-dimensional magnetic field
M Agostini, P Scarin, G Spizzo, N Vianello and L Carraro
PLASMA PHYS CONTR F **56** (2014) 095016 (10pp)
60. Magnetohydrodynamic modes analysis and control of Fusion Advanced Studies Torus high-current scenarios
F. Villone, G. Calabrò, G. Marchiori, S. Mastrostefano, G. Vlad, T. Bolzonella, F. Crisanti, V. Fusco, Y. Q. Liu, P. Mantica, L. Marrelli, and P. Martin
PHYS PLASMAS, **21** 082514 (2014)
61. Tungsten transport in JET H-mode plasmas in hybrid scenario, experimental observations and modelling
C. Angioni, P. Mantica, T. Pütterich, M. Valisa, M. Baruzzo, E.A. Belli, P. Belo, F.J. Casson, C. Challis, P. Drewelow, C. Giroud, N. Hawkes, T.C. Hender, J. Hobirk, T. Koskela⁸, L. Lauro Taroni, C.F. Maggi, J. Mlynar, T. Odstrcil, M.L. Reinke, M. Romanelli and JET EFDA Contributors
NUCL FUSION, **54** Issue: 8 (2014) 083028
62. Supervised Image Processing Learning for Wall MARFE Detection Prior to Disruption in JET With a Carbon Wall
Craciunescu, Teddy; Murari, Andrea; Tiseanu, Ion and JET EFDA Contributors
IEEE T PLASMA SCI, **42** Issue: 8 (2014) 2065-2072
- 1.
63. Helium Generated Cold Plasma Finely Regulates Activation of Human Fibroblast-Like Primary Cells
Surajit Pathak, Ignazio Castagliuolo, Giorgio Palù, Paola Brun, Matteo Zuin, Roberto Cavazzana, Emilio Martines
PLOS ONE, **9** Issue: 8 (2014) e104397
64. Computation of stationary 3D halo currents in fusion devices with accuracy control
Bettini, Paolo; Specogna, Ruben
J COMPUT PHYS, **273** (2014) 100-117
65. Joint 19th ISHW and 16th RFP workshop- Preface
David Terranova, Maria Ester Puiatti and Boyd Blackwell
PLASMA PHYS CONTR F, **56** (2014) 090301 (3pp)
66. Experimental Validation of the 3-D Molecular Flow Code AVOCADO
Emanuele Sartori, Samuele Dal Bello, Michele Fincato, Winder Gonzalez, Gianluigi Serianni, and Piergiorgio Sonato
IEEE T PLASMA SCI Volume: 42 Issue: 9 Pages: 2291-2297
67. Spatiotemporal synchronization of drift waves in a magnetron sputtering plasma

-
- E. Martines, M. Zuin, R. Cavazzana, J. Adánek, V. Antoni, G. Serianni, M. Spolaore, and N. Vianello
PHYS. PLASMAS, **21**, vol 2 issue 10 (2014) 102309
68. Difficulties and solutions for estimating transport by perturbative experiments
F Sattin, D F Escande, F Auriemma, G Urso and D Terranova
PLASMA PHYS CONTR F, **56** (2014) 114008 (14pp)
69. Physics-based optimization of plasma diagnostic information
A Murari and J Vega
PLASMA PHYS CONTR F, **56** (2014) 110301
70. An alternative approach to the determination of scaling law expressions for the L–H transition in Tokamaks utilizing classification tools instead of regression
P Gaudio, A Murari, M Gelfusa, I Lupelli and J Vega
PLASMA PHYS CONTR F, **56** (2014) 114002 (12pp)
71. A statistical method for model extraction and model selection applied to the temperature scaling of the L H transition
E Peluso, A Murari, M Gelfusa and P Gaudio
PLASMA PHYS CONTR F, **56** (2014) 114001 (10pp)
72. Robustness and increased time resolution of JET Advanced Predictor of Disruptions
R Moreno, J Vega, A Murari, S Dormido-Canto, J M Lopez, J M Ramirez and JET EFDA Contributors
PLASMA PHYS CONTR F, **56** (2014) 114003 (8pp)
73. Simulation and real-time replacement of missing plasma signals for disruption prediction: an implementation with APODIS
G A Rattà, J Vega¹, A Murari² and JET EFDA Contributors³
PLASMA PHYS CONTR F, **56** (2014) 114004 (11pp)
74. Overview of manifold learning techniques for the investigation of disruptions on JET
B Cannas, A Fanni, A Murari, A Pau, G Sias and JET EFDA Contributors
PLASMA PHYS CONTR F, **56** (2014) 114005 (14pp)
75. Overview of image processing tools to extract physical information from JET videos
T Craciunescu, A Murari, M Gelfusa, I Tiseanu¹, V Zoita and JET EFDA Contributors
PLASMA PHYS CONTR F, **56** (2014) 114006 (13pp)
76. Extensive statistical analysis of ELMs on JET with a carbon wall
A Murar, F Pisano, J Vega, B Cannas, A Fanni, S Gonzalez, M Gelfusa, M Grosso and JET EFDA Contributors
PLASMA PHYS CONTR F, **56** (2014) 114007 (26pp)
77. Continuous model in dq frame of Thyristor Controlled Reactors for stability analysis of high power electrical systems
Finotti, Claudio; Gaio, Elena
INT J ELEC POWER, **63** (2014) 836-845

-
78. An integrated data analysis tool for improving measurements on the MST RFP
L. M. Reusch, M. E. Galante, P. Franz, J. R. Johnson, M. B. McGarry, H. D. Stephens and D. J. Den Hartog
Rev. Sci. Instrum. **85** , 11D844 (2014).
 79. Note: Effect of photodiode aluminum cathode frame on spectral sensitivity in the soft x-ray energy band
M. B. McGarry, P. Franz, D. J. Den Hartog, J. A. Goetz and J. Johnson
REV. SCI. INSTRUM. **85** , 096105 (2014).
 80. Experimental Qualification of the Hybrid Circuit Breaker Developed for JT-60SA Quench Protection Circuit
Alberto Maistrello, Elena Gaio, Alberto Ferro, Mauro Perna, Carlo Panizza, Francesco Soso, Luca Novello, Makoto Matsukawa, and Kunihiro Yamauchi
IEEE T APPL SUPERCON **24**, NO. 3 (2014)
 81. Dual-angle, self-calibrating Thomson scattering measurements in RFX-MOD
L. Giudicotti, RT. Pasqualotto, A. Fassina
REV. SCI. INSTRUM. **85** , 11d823 (2014).
 82. Theoretical description of heavy impurity transport and its application to the modelling of tungsten in JET and ASDEX upgrade
F J Casson, C Angioni, E A Belli, R Bilato, P Mantica, T Odstrcil, T Pütterich, M Valisa, L Garzotti¹, C Giroud, J Hobirk, C F Maggi, J Mlynar and M L Reinke
PLASMA PHYS CONTR F, **57** N. 1 (2014) 014031
 83. Development of a new virtual diagnostic for V3FIT
G. L. Trevisan, M. R. Cianciosa, D. Terranova, and J. D. Hanson
PHYS. PLASMAS, **21**, vol 2 issue 12 122504 (2014)

Conference proceedings

International Conference on Fusion Reactor Diagnostics 2013

1. Gonzalez W., Rizzolo A., Peruzzo S., Arshad S., Portales M., Vayakis G.
Thermo-mechanical analyses of ITER in-vessel magnetic sensor assembly
AIP Conf. Proc. (), 1612 (2014) 179-183
2. CEFC 2014 – The 16th Biennial IEEE Conference on Electromagnetic Field Computation
May 25-28, 2014 Annecy, France
To be published on a special issue of IEEE Transactions on Magnetics
3. N. Marconato, D. Aprile, G. Chitarin
An efficient method for magnetic field and force calculation in complex permanent magnet and current
4. P. Bettini, Tommaso Bolzonella, Alberto Ferro, Murizio Furno Palumbo, Stefano Mastrostefano, Go Matsunaga, Ruben Specogna, Manabu Takechi, Fabio Villone

Advanced computational tools for the characterization of the dynamic response of MHD control systems

5. 21th International Conference on Plasma Surface Interactions 2014 (PSI)
May 26-30, 2014 Ongaku-do, Kanazawa Ishikawa, Japan
To be published in Journal of Nuclear Materials
6. P. Scarin, M. Agostini, L. Carraro, G. Ciaccio, G. De Masi, G. Spizzo, M. Spolaore, N. Vianello
Edge plasma physics modifications due to magnetic ripple in RFX-mod
P2-042
7. P. Innocente, M. Agostini, S. Barison, A. Canton, L. Carraro, R. Cavazzana, G. De Masi, A. Fassina, S. Fiameni, D.K. Mansfield, B. Rais, A.L. Roquemore, P. Scarin
Lithium wall conditioning by high frequency pellet injection in RFX-mod
P2-055
8. F. Ghezzi, R. Caniello, A. Cantona, P. Innocentea, L. Laguardia, B. Rais
Deuterium and oxygen bounding mechanism in boron coating film for graphite wall conditioning in RFX-mod
P2-112
9. 20th Topical Conference on High-Temperature Plasma Diagnostics (HTPD 2014)
June 1-5, 2014 Atlanta, USA
To be published in Review of Scientific Instruments
10. M. Brombin, M. Spolaore, G. Serianni, N. Pomaro, C. Taliercio, M. Dalla Palma, R. Pasqualotto, and L. Schiesko
Langmuir probes for SPIDER experiment: tests in BATMAN
11. L. Giudicotti, R. Pasqualotto, and A. Fassina
Dual-angle, self-calibrating Thomson scattering measurements in RFX-MOD
12. M. Barbisan, B.Zaniol, and R. Pasqualotto
Modeling and simulation of a beam emission spectroscopy diagnostic for the ITER prototype neutral beam injector
13. 41st EPS conference
June 23-27, 2014 Berlin, Germany
Europhysics Conference Abstracts Vol. 38F (2014)
14. T. Bolzonella, M. Baruzzo, P. Bettini, Y.Q. Liu, G. Marchiori, G. Matsunaga, L. Pigatto, M. Takechi, F. Villone
Physics and control of multiple external kink instabilities with realistic 3D boundaries: recent understandings from experiment and modelling
Europhysics Conference Abstracts Vol. 38F (2014) O4.132
15. L. Pigatto, P. Bettini, T. Bolzonella, G. Marchiori, F. Villone
MHD control system optimization to RFX-mod real passive boundary
Europhysics Conference Abstracts Vol. 38F (2014) P5.080

-
16. S. Spagnolo, M. Zuin, F. Auriemma, T. Barbui, R. Cavazzana, G. De Masi, P. Innocente, E. Martines, B. Momo, C. Rea, M. Spolaore, D. Spong, N. Vianello
Characterization of Alfvén Eigenmodes in RFX-mod plasmas
Europhysics Conference Abstracts Vol. 38F (2014) P5.085
 17. G. Marchiori, C. Finotti, R. Cavazzana, O. Kudlacek, G. Manduchi, L. Marrelli, F. Villone, P. Zanca, L. Zanotto, A. Cenedese, P. Merlo
Model based feedback control system of plasma shape in RFX-mod Tokamak discharges
Europhysics Conference Abstracts Vol. 38F (2014) P5.040
 - a. Kudláček, R. Cavazzana, C. Finotti, G. Marchiori, P. Zanca
Real time plasma boundary reconstruction in RFX-mod tokamak discharges
Europhysics Conference Abstracts Vol. 38F (2014) P5.062
 18. D. Terranova, R. Cavazzana, C. Finotti, O. Kudláček, G. Marchiori, L. Marrelli
Equilibrium reconstruction for shaped tokamak discharges in RFX-mod
Europhysics Conference Abstracts Vol. 38F (2014) P5.039
 19. L.Carraro, F.Auriemma, T.Barbui, A.Fassina, P.Franz, P.Innocente, I.Predebon, P.Scarin, G.Spizzo, M.Spolaore, B.Zaniol
Impurity screening in RFX-mod RFP plasmas
Europhysics Conference Abstracts Vol. 38F (2014) P5.078
 20. M. Spolaore, R. Cavazzana, G. De Masi, C. Finotti, O. Kudlacek, G. Marchiori, E. Martines, B. Momo, C. Rea, S. Spagnolo, N. Vianello, M. Zuin
Edge effects of dynamically shaped tokamak configuration in RFX-mod experiment
Europhysics Conference Abstracts Vol. 38F (2014) P5.073
 21. F. Auriemma, R. Lorenzini, M. Agostini, A. Fassina, M. Gobbin, P. Innocente, P. Scarin
Spontaneous mitigation of anomalous transport in RFX-mod helical regimes
Europhysics Conference Abstracts Vol. 38F (2014) P5.079
 22. B. Rais, S. Barison, A. Canton, S. Dal Bello, J. Fu, L. Grando, S. Fiameni, B. Koel, P. Innocente, C.H. Skinner, F. Degli Agostini, F. Rossetto
Study of the effect of the glow power on the growth of the boron coating obtained with boronizations in RFX-mod
Europhysics Conference Abstracts Vol. 38F (2014) P5.076
 23. M. Veranda, D. Bonfiglio, S. Cappello, L. Chacòn, D.F. Escande
Helical RFP states in 3D nonlinear MHD: intermittency and magnetic topology
Europhysics Conference Abstracts Vol. 38F (2014) P5.082
 24. M.Gobbin, F.Auriemma, A.Fassina, P.Franz, R.Lorenzini, L.Marrelli
Characterization of eITBs in high current deuterium and hydrogen helical shaped plasmas
Europhysics Conference Abstracts Vol. 38F (2014) P5.074
 25. P.Franz, M.B.McGarry, D.J.Den Hartog, J.A.Goetz, J.Johnson
Improvements in SXR and Te measurements in the Madison Symmetric Torus

-
- Europhysics Conference Abstracts Vol. 38F (2014) P5.081
26. C. Rea, N. Vianello, M. Agostini, R. Cavazzana, G. De Masi, E. Martines, B. Momo, P. Scarin, S. Spagnolo, G. Spizzo, M. Spolaore, M. Zuin
Investigation of edge transport properties in helically shaped RFP discharges
Europhysics Conference Abstracts Vol. 38F (2014) P5.077
 27. S. Munaretto, F. Auriemma, D. Brower, M. Cianciosa, B.E. Chapman, D.J. Den Hartog, W.X. Ding, J. Duff, P. Franz, J.A. Goetz, J.D. Hanson, D. Holly, P. Innocente, J.J. Koliner, L. Lin, M. McGarry, L. Morton, M.D. Nornberg, E. Parke, J.S. Sarff, D. Terranova, P.W. Terry, G.G. Whelan
Dynamics of helical states in MST
Europhysics Conference Abstracts Vol. 38F (2014) P5.075
 28. M. Komm, M. Kořcan, D. Carralero, H.W. Müller, J. Stöckel, C. Rea, COMPASS team and the ASDEX Upgrade Team
Fast measurements of ion temperature fluctuations in COMPASS and Asdex Upgrade scrape-off layer
Europhysics Conference Abstracts Vol. 38F (2014) P5.026
 29. F. Felici, P. Geelen, L. Giannone, D. Kim, E. Maljaars, P. Piovesan, C. Piron, C. J. Rapson, O. Sauter, A. Teplukhina, W. Treutterer, L. Barrera, E. Fable, M. Reich, G. Tardini and the ASDEX-Upgrade team
First results of real-time plasma state reconstruction using a model-based dynamic observer on ASDEX-Upgrade
Europhysics Conference Abstracts Vol. 38F (2014) P2.002
 30. M.Goniche, E.Lerche, P.Jacquet, D.Van Eester, V.Bobkov, S.Brezinsek, L.Colas, A.Czarnecka, P.Drewelow, R.Dumont1, N.Fedorczak, C.Giroud, M.Graham, J.P.Graves, I.Monakhov, P.Monier-Garbet, C.Noble, T.Pütterich, F.Rimini, M.Valisa and JET-EFDA Contributors
Optimization of ICRH for tungsten control in JET H-mode plasmas
Europhysics Conference Abstracts Vol. 38F (2014) O4.129
 31. P.Mantica, C.Angioni, F.J.Casson, T.Pütterich, M.Valisa, M.Baruzzo, P.C.da Silva Aresta Belo, I. Coffey, P. Drewelow, C.Giroud, N.C.Hawkes, T.C.Hender, T.Koskela, L. Lauro Taroni, E. Lerche, C.F. Maggi, J.Mlynar, M.O'Mullane, M.E.Puiatti, M.L.Reinke, M.Romanelli and JET EFDA contributors
Understanding and Controlling Tungsten Accumulation in JET Plasmas with the ITER-like Wall
Europhysics Conference Abstracts Vol. 38F (2014) P1.017
 32. C Perez von Thun, V G Kiptily, S Popovichev, V Yavorskij , V Goloborod'ko, P Buratti, M Baruzzo, G Pucella, and JET EFDA Contributors
Fast ion losses in JET hybrid scenarios - MHD sources overview
Europhysics Conference Abstracts Vol. 38F (2014) P1.007
 33. J. Vega, A. Murari, S. Dormido-Canto, D. Alves, G. Farias, J. M. López, R. Moreno, A. Pereira, J. M. Ramírez, G. A. Rattá and JET-EFDA Contributors
Overview of real-time disruption prediction in JET: applicability to ITER

-
- Europhysics Conference Abstracts Vol. 38F (2014) P1.024
34. UV.D. Pustovitov¹ U and V.V. Yanovskiy
Ferromagnetic destabilization of resistive wall modes in tokamaks
Europhysics Conference Abstracts Vol. 38F (2014) P4.008
 35. S. Costea, A.H. Nielsen, V. Naulin, J.J. Rasmussen, H.W. Müller, G.D. Conway, N. Vianello, D. Carralero, R. Schrittwieser, F. Mehlmann, C. Lux, C. Ionita, ASDEX Upgrade Team
Investigations of poloidal velocity and shear in the SOL of ASDEX Upgrade
Europhysics Conference Abstracts Vol. 38F (2014) P2.001
 36. J. Mailloux , M. Beurskens, I. Chapman, I. Nunes, B. Alper, M. Baruzzo, P. S. A. Belo, E. Belonohy, J. Bernardo, P. Buratti, C. D. Challis, E. de la Luna, L. Frassinetti, J. Garcia, C. Giroud, N. Hawkes, J. Hobirk , E. Joffrin, D. Keeling, M. Lennholm, P. J. Lomas, T. Luce, P. Mantica, C. Marchetto, M. Maslov, G. Pucella, S. Saarelma, S. Sharapov, E. R. Solano, C. Sozzi, G. Szepesi, M. Tsalas and JET EFDA contributors
Effect of 'baseline' and 'hybrid' operational parameters on plasma confinement and stability in JET with a Be/W ITER-Like Wall
Europhysics Conference Abstracts Vol. 38F (2014) P4.127
 37. E. Peluso, A. Murari, I. Lupelli, M. Gelfusa and P. Gaudio
Symbolic Regression via Genetic Programming to derive Empirical Models and Scaling Laws as Monomial or Polynomial Expansions.
Europhysics Conference Abstracts Vol. 38F (2014) P2.029
 38. K. Kovařík , M. Spolaore, I. Ďuran, J. Stöcke, J. Adámek, N. Vianello
First measurements of SOL plasma filament properties with U-probe on the COMPASS tokamak
Europhysics Conference Abstracts Vol. 38F (2014) P5.025
 39. L. Giudicotti
Gain saturation in microchannel plate detectors
To be published in a special issue of Nuclear Instruments and Methods in Physics Research Section A: Accelerators, Spectrometers, Detectors and Associated Equipment^{7th}
International Conference on New Developments In Photodetection
30 June- 4 July 2014, Tours, France
 40. E. Sartori, G. Serianni, S. Dal Bello
Multi-scale simulation of gas density distribution in a fusion-relevant particle accelerator
To be published after peer review in Vacuum journal
13th European Vacuum Conference
September, 2014 Aveiro, Portugal
 41. Piero Agostinetti Mauro Dalla Palma Fabio Degli Agostini Diego Marcuzzi Federico Rossetto Piergiorgio Sonato Pierluigi Zaccaria
Vacuum Tight Threaded Junctions (VTTJ): a new solution for reliable heterogeneous junctions in ITER
O5B.4
28th SOFT Symposium on Fusion Technology

29 September – 3 October, 2014 San Sebastian, Spain

To be published in a special edition of the International Journal “Fusion Engineering and Design”

42. Mauro Pavei, Deirdre Boilson, Tullio Bonicelli, Marco Bigi, Jacques Boury, Michael Bush, Andrea Ceracchi, Diego Faso, Joseph Graceffa, Bernd Heinemann, Ronald Hemsworth, Cristophe Lievin, Diego Marcuzzi, Antonio Masiello, Roberto Pasqualotto, Nicola Pomaro, Andrea Rizzolo, Bernd Sczepaniak, Mahendrajit Singh, Pierluigi Zaccaria
Manufacturing of the full size prototype of the ion source for the ITER neutral beam injector. The spider beam source
P2.005
43. Paolo Bettini, Tommaso Bolzonella, Maurizio Furno Palumbo, Stefano Mastrostefano, Go Matsunaga, M. Takechi, Fabio Villone
Three-dimensional electromagnetic analysis of JT-60SA conducting structures in view of RWM control
P2.035
44. Ruben Specogna, Paolo Bettini
A novel approach for solving three dimensional eddy current problems in fusion devices
P4.042
45. Paolo Bettini , Ruben Specogna
A boundary integral method for eddy-current problems in fusion devices
P1.041
46. Nicola Pomaro, Marco Boldrin, Gabriele Lazzaro
The Earthing System of the PRIMA Neutral Beam Test Facility based on the Mesh Common Bonding Network Topology
P2.002
47. Michela De Muri , Marco Cavenago, Gianluigi Serianni, Pierluigi Veltri, Marco Bigi, Roberto Pasqualotto, Marco Barbisan, Mauro Recchia, Barbara Zaniol, Timour KulevoySergey Petrenko, Lucio Baseggio, Vannino Cervaro, Fabio Degli Agostini, Luca Franchin, Bruno Laterza, Alessandro Minarello, Federico Rossetto, Manuele Sattin, Simone Zucchetti
Installation and Commissioning of the Negative Ion Optimization Experiment
P3.003
48. Nicolò Marconato, Piero Agostinetti, Giuseppe Chitarin
Magnetic and thermo-structural design optimization of the Plasma Grid for the MITICA Neutral Beam Injector
P2.019
49. Mauro Recchia, Alberto Ferro, Fabio Baldo, Gabriele Manduchi, Cesare Taliercio, Elena Gaio,
Improvements of the RFX-mod power supply system for MHD mode control
P2.071
50. Giuseppe Marchiori, Paolo Bettini, Luca Grandò

-
- Feasibility study of a local active correction system of magnetic field errors in RFX-mod
P1.042
51. Mauro Dalla Palma, Emanuele Sartori, Peter W Blatchford, Benjamin Chuilon, Joseph Graceffa, Stefan Hanke, Christopher Hardie, Antonio Masiello, Andrea Muraro, Santiago Ludgardo Ochoa Guaman, Darshan Shah, Pierluigi Veltri, Pierluigi Zaccaria, Matteo Zaupa
Design and R&D for manufacturing the Beamline Components for MITICA and ITER HNB
P2.024
52. Chiara Bustreo, Tommaso Bolzonella , Giuseppe Zollino
The Monte Carlo approach to the economics of a DEMO-like power plant.
P2.189
53. Gabriele Manduchi , Adriano Luchetta, Cesare Taliercio
Integration of Simulink, MARTe and MDSplus for rapid development of real-time applications
P1.040
54. Leonardo Pigatto, Paolo Bettini, Tommaso Bolzonella, Giuseppe Marchiori, Fabio Villone,
P1.043
Strategies for real-time actuator decoupling in closed-loop MHD control operations
55. Francesco Fellin, Pierluigi Zaccaria, Manuela Battistella, Samuele Dal Bello, Marco D'Arienzo, Sandro Sandri, Angela Coniglio, Gilbert Agarici, Giovanni Dell'Orco, Roberto Bozzi, Gabriele Cenedella
Design and radiation protection aspects for the PRIMA Cooling Plant
P2.004
56. Francesco Fellin, Pierluigi Zaccaria, Marco Bigi, Adriano Luchetta, Nicola Pomaro, Matteo Zaupa, Mauro Breda, Gabriele Lazzaro, Moreno Maniero, Gilbert Agarici, Vincent Pilard, Daniel Gutierrez, Lennart Svensson, Carmelenzo Labate, Marco Simonetti, Roberto Bozzi, Gabriele Cenedella
The SPIDER Cooling Plant from design to realization
P2.003
57. Francesco Fellin, Marco Boldrin, Pierluigi Zaccaria, Piero Agostinetti, Manuela Battistella, Marco Bigi, Mauro Dalla Palma, Samuele Dal Bello, Aldo Fiorentin, Adriano Luchetta, Alberto Maistrello, Diego Marcuzzi, Edoardo Ocello, Roberto Pasqualotto, Mauro Pavei, Andrea Rizzolo, Vanni Toigo, Matteo Valente, Loris Zanotto, Luca Calore, Federico Caon, Massimo Caon, Michele Fincato, Gabriele Lazzaro, Michele Visentin, Enrico Zampiva, Simone Zucchetti
Plant integration of MITICA and SPIDER experiments with auxiliary plants and buildings on PRIMA site
P2.006
58. Alberto Ferro, Elena Gaio, Luca Novello, Makoto Matsukawa, Katsuhiko Shimada, Yoichi Kawamata, Manabu Takechi
Reference design of the Power Supply system for the Resistive-Wall-Mode control in JT-60SA
P2.069

-
59. Alberto Maistrello, Elena Gaio, Luca Novello, Makoto Matsukawa, Kunihito Yamauchi
Analyses of the impact of connections layout on the coil transient voltage at the Quench Protection Circuit intervention in JT-60SA
P2.072
 60. Loris Zanotto, Marco Bigi, Alberto Ferro, Elena Gaio, Nicola Pomaro, Andrea Zamengo, Vanni Toigo, Mieko Kashiwagi, Haruiko Yamanaka, Tetsuya Maejima, Yasuo Yamashita, Kazuhiro Watanabe, Masaya Hanada, Hans Decamps, Daniel Gutierrez
Control, Protection and Breakdown Management in the Acceleration Grid Power Supply of the ITER Heating Neutral Beam Injector
P2.022
 61. Paolo Innocente, Jonathan Farthing, Gerardo Giruzzi, Shunsuke Ide, Emmanuel Joffrin, Yutaka Kamada, Georg Kühner, Osamu Naito, Hajime Urano, Maiko Yoshida
Requirements for tokamak remote operation: application to JT-60SA
P1.063
 62. Claudio Finotti, Elena Gaio, Inho Song, Jun Tao, Ivone Benfatto
Improvement of the dynamic response of the ITER Reactive Power Compensation system
P2.070
 63. Marco Boldrin, Luca Grando, Mauro Recchia, Alberto Pesce, Vanni Toigo, Daniel Gutierrez, Muriel Simon, Giovanni Faoro, Edoardo Maggiora, Anita Roman, Hans Decamps
The 100kV Faraday cage (High Voltage Deck) for the SPIDER experiment
P2.021
 64. Nicola Pilan, Diego Marcuzzi, Andrea Rizzolo, Luca Grando, Stefania Dalla Rosa, Volker Kraemer, Thomas Quirnbach, Giuseppe Chitarin, Renato Gobbo, Giancarlo Pesavento, Antonio De Lorenzi, Luca Lotto, Roberto Rizzieri, Michele Fincato, Livio Romanato, Lauro Trevisan, Vannino Cervaro, Luca Franchin
Electrical and structural R&D activities on high voltage DC solid insulators in vacuum
P2.020
 65. Pierluigi Zaccaria, Matteo Valente, Wladi Rigato, Diego Marcuzzi, Samuele Dal Bello, Marco Tollin, Giorgio Corniani, Matteo Badalocchi, Riccardo Bettero, Massimo Sacchiero, Antonio Masiello, Federico Rossetto, Fabio Degli Agostini
Manufacturing, assembly and tests of SPIDER Vacuum Vessel to develop and test a prototype of ITER Neutral Beam Ion Source
P2.001
 66. Adriano Luchetta, Gabriele Maduchi, Cesare Taliercio, Francesco Paolucci, Filippo Sartori, Lennart Svensson, Carmelo Vincenzo Labate, Mauro Breda, Roberto Capobianco, Federico Molon, Modesto Moressa, Paola Simionato, Enrico Zampiva, Paolo Barbato, Sandro Polato
Control and Data Acquisition of the ITER Full-scale Ion Source for the Neutral Beam Test Facility
P2.026

-
67. Marco Bigi, Luigi Rinaldi, Muriel Simon, Luca Sita, Giuseppe Taddia, Saverino Carrozza, Hans Decamps, Adriano Luchetta, Abdelraouf Meddour, Modesto Moressa, Cristiano Morri, Antonio Musile Tanzi, Mauro Recchia, Uwe Wagner, Andrea Zamengo, Vanni Toigo
Design, manufacture and factory testing of the Ion Source and Extraction Power Supplies for the SPIDER experiment
P2.023
 68. Gianmaria De Tommasi, Gabriele Manduchi, David G. Muir, Shunsuke Ide, Osamu Naito, Hajime Urano, Susana Clement-Lorenzo, Noriyoshi Nakajima, Takahisa Ozeki, Filippo Sartori
Current status of EU activities for the Remote Data Access System of the ITER Remote Experimentation Centre
P4.060
 69. Etienne Delmas, Deirdre Boilson, Chang-Hwan Choi, Mauro Dalla Palma, Miguel Dapena-Febrer, Joseph Graceffa, Marcus Iseli, Antonio Masiello, Gonzalo Micó-Montava, Kevin Roux, Darshan Shah, Lennart Svensson, Matteo Valente
First boundary electrical feedthroughs for the Heating Neutral Beams injectors of ITER
P3.111
 70. Luca Novello, Olivier Baulaigue, Alberto Coletti, Nicolas Dumas, Alberto Ferro, Elena Gaio, Alessandro Lampasi, Alberto Maistrello, Makoto Matsukawa, Kunihito Yamauchi, Katsuhiko Shimada, Pietro Zito
Present status of the new Power Supply Systems of JT-60SA procured by EU
P3.069
 71. Alessandro Pau, Raffaele Aledda, Barbara Cannas, Alessandra Fanni, Andrea Murari, Giuliana Sias, JET EFDA Contributors
An adaptive disruption predictor based on FDI approach for next generation Tokamaks
P2.034
 72. Marco D'Arienzo, Angela Coniglio, Sandro Sandri, Manuela Battistella, Samuele Dal Bello, Luca Grando, Roberto Piovan, Maria Ester Puiatti
RFX radiological analysis and testing for improved tokamak and deuterium operation mode
P2.010
 73. Teddy Craciunescu, Andrea Murari, Michela Gelfusa, Ion Tiseanu, Vasile Zoita, Gilles Arnoux
Advanced Methods for Image Registration Applied to JET Videos
P1.068
 74. Philippe Moreau, Pascal Spuig, Alain Le-Luyer, Philippe Malard, Bruno Cantone, Patrick Pastor, François Saint-Laurent, George Vayakis, Dominique Delhom, Shakeib Arshad, Jonathan Lister, Matthieu Toussaint, Philippe Marmillod, Duccio Testa, Christian Schlatter, Simone Perruzo, Giuseppe Chitarin
Development of the ITER Continuous External Rogowski: from conceptual design to final design
P1.053

-
75. Philippe Moreau, Pascal Spuig, Alain Le-luyer, Philippe Malard, B. Cantone, Patrick Pastor, F. Saint-Laurent, George Vayakis, Dominique Delhom, Shakeib Arshad, Jonathan Lister, Matthieu Toussaint, Philippe Marmillod, Duccio Testa, Christian Schlatter, Simone Peruzzo
Development of the ITER Continuous External Rogowski: from conceptual design to final design

**4th International Symposium on Negative Ions, Beams and Sources (NIBS 2014)
6 - 10 October 2014, IPP Garching, Germany**

To be published by AIP, in their conference proceedings series

E. Sartori, P. Veltri, E. Dlugach, R. Hemsworth, G. Serianni, M. Singh

Benchmark of Numerical Tools Simulating Beam Propagation and Secondary Particles in ITER NBI

G. Serianni, R. Pasqualotto, I. Mario, M. Zanini

A Wire Calorimeter for the SPIDER Beam: Experimental Tests and Feasibility Study

V. Antoni, P. Agostinetti, M. Brombin, V. Cervaro, R. Delogu, M. De Muri, D. Fasolo, L. Franchin, R. Ghiraldelli, K. Ikeda, M. Kasaki, F. Molon, A. Muraro, H. Nakano, R. Pasqualotto, G. Serianni, Y. Takeiri, M. Tollin, K. Tsumori³ and P. Veltri

Design, Installation, Commissioning and Operation of a Beamlet Monitor in the negative ion beam test stand at NIFS

Oral

P. Veltri, M. Cazzador, M. Cavenago, G. Serianni

Semi-analytical Modeling of the NIO1 Source

B. Zaniol, M. Cavenago, G. Serianni, M. De Muri, M. Barbisan, A. Mimo, R. Pasqualotto

NIO1 Diagnostics

G. Serianni, F. Bonomo, M. Brombin, V. Cervaro, G. Chitarin, S. Cristofaro, R. Delogu, M. De Muri, D. Fasolo, N. Fonnesu, L. Franchin, P. Franzen, R. Ghiraldelli, F. Molon, A. Muraro, R. Pasqualotto, B. Ruf, L. Schiesko, P. Veltri

Negative Ion Beam Characterisation in BATMAN by mini-STRIKE: Improved Design and New Measurements

P. Veltri, M. Cavenago, G. Chitarin, D. Marcuzzi, E. Sartori, G. Serianni, P. Sonato

Electrostatic steering and beamlet aiming in large neutral beam injectors

P. Veltri, M. Cavenago, C. Baltador

Design of the new extraction grid for the NIO1 negative ion source

G. Chitarin, P. Agostinetti, D. Aprile, N. Marconato, P. Veltri

Integration of the Magnetic Field Design for SPIDER and MITICA Negative Ion Beam Sources

oral

N. Fomesu, P. Agostinetti, G. Serianni, M. Kasaki, P. Veltri
A multi-beamlet analysis of the MITICA accelerator

R. Nocentini, F. Bonomo, A. Pimazzoni, U. Fantz, P. Franzen, M. Frösche, B. Heinemann, R. Pasqualotto, R. Riedl, B. Ruf, D. Wunderlich

Advanced ion beam calorimetry for the test facility ELISE

F. Bonomo, B. Ruf, M. Barbisan, S. Cristofaro, L. Schiesko, U. Fantz, P. Franzen, R. Pasqualotto, R. Riedl, G. Serianni, D. Wunderlich and the NNBI-Team

BATMAN Beam Properties Characterization by the Beam Emission Spectroscopy Diagnostic

The development of the Neutral Beam Injector for DEMO within the EUROFUSION Activities

P. Sonato

Oral

25th Fusion Energy Conference (FEC2014)

13-18 October, 2014 Saint Petersburg, Russia

The papers will be published by the IAEA as unedited proceedings in electronic format on a CD-ROM and on the IAEA Physics Section website by march 2015

Possible submission to Nuclear Fusion

A. Masiello, V. Antoni, D. Marcuzzi, V. Toigo et al.

Progress Status of the Activities in EU for the Development of the ITER Neutral Beam Injector and Test Facility

FIP/2-4Ra

M. Nornberg, F. Aureimma, P. Innocente, D. Terranova, D. Brower, M. Cianciosa, B. Chapman

Predator-Prey Time Dynamics and Locking Control of Spontaneous Helical States in the RFP

EX/P3-50

B. Chapman, F. Auriemma, S. Cappello, E. Martines, B. Momo, P. Piovesan, M.E. Puiatti, M. Spolaore, D. Terranova, P. Zanca, P. Innocente, R. Lorenzini et al.

Overview of Results from the MST Reversed Field Pinch Experiment

OV/5-3

S.C. Guo, X.Y. Xu, Y.Q. Liu, M. Baruzzo, T. Bolzonella, R. Wang, S. Cappello, M. Veranda, D. Bonfiglio, D. Escande

Progress in Theoretical Studies of Resistive Wall Modes for RFP plasmas and Comparison with Tokamaks

TH/P5-10

P. Martin, M. Baruzzo, J. Bialek, T. Bolzonella, D. Bonfiglio, R. Cavazzana, M. Ferraro, M. Garofalo, J. Hanson, A.W. Hyatt, G.L. Jackson, J. King, R.J. La haye, M. Lanctot, L. Marrelli, G.A. Navratil, M. Okabayashi, E. Olofsson, R. Paccagnella, C. Paz-Soldan, P. Piovesan, C. Piron, L. Piron, D. Shiraki, E.J. Strait, D. Terranova, F. Turco, A. Turnbull, P. Zanca, B. Zaniol

Extreme Low-Edge Safety Factor Tokamak Scenarios via Active Control of Three-Dimensional Magnetic Field on RFX and DIII-D

EX/P2-41

S. Gerasimov, M. Baruzzo et al.
JET Asymmetrical Disruptions
EX/P5-33

M. Valisa, C. Angioni, P. Mantica, T. Puetterich, M. Baruzzo, P. Della Silva Aresta, E.A. Belli, F. Casson, I. Coffey, P. Drewelow, C. Giroud, N. Hawkes, T. Hender, T. Koskela, E. Lerche, L. Lauro Taroni, C. Maggi, J. Mlynar, M. O'mullane, M.E. Puiatti, M. Reinke, M. Romanelli
Heavy Impurity Transport in the Core of JET Plasmas
EX/6-1

G. Giruzzi, M. Baruzzo, T. Bolzonella, P. Vincenzi et al.
Modelling of Pulsed and Steady-State DEMO Scenarios
TH/P1-14

I.Nunez, M. Baruzzo et al
Compatibility of High Performance Operation with JET ILW
EX/9-2
E. Gaio, A. Maistrello, L. NOvello, M. Matsukawa, A. Ferro, K. Yanauchi, R. Piovan
Protection of Superconducting Magnets in Fusion Experiments: the New Technological Solution for JT-60SA
FIP/P8-22

R. Lorenzini
The Isotope Effect in the RFX-Mod Experiment
EX/P1-41

F. Imbeaux, G. Manduchi et al.
Design and First Applications of the ITER Integrated Modelling & Analysis Suite
TH/P3-41

L. Marrelli, P. Zanca, E.J. Strait, M. Garofalo, J. Hanson, Y. In, R. La Haye, P. Martin, P. Piovesan, C. Piron, L. Piron, D. Shiraki, F. Volpe
Avoidance of Tearing Mode Locking and Disruption with Electro-Magnetic Torque Introduced by Feedback-Based Mode Rotation Control in DIII-D and RFX-Mod
EX/P2-42

M. E. Puiatti, L. Marrelli, P. Martin
Overview of the RFX-Mod Contribution to the International Fusion Science Program
OV/5-2

H. R. Strauss, R. Paccagnella, L. Sugiyama, J. Breslau, S. Jardin
Toroidal Rotation Produced by Disruptions and ELMs
TH/P2-16

S. Masamune, R. Paccagnella et al.
Attainment of High Electron Poloidal Beta in Axisymmetric State and Two Routes to Self-Organized Helical State in Low-Aspect-Ratio RFP
EX/P3-52

R. Paccagnella, L. Sugiyama, J. Breslau, S. Jardin, H. R. Strauss
Progresses in 3D Nonlinear Numerical Simulation of Tokamak Disruptions
TH/P4-13

G. Spizzo, O. Tudisco, M. Zuin, G. Pucella
Density Limit Studies in the Tokamak and the Reversed-Field Pinch
EX/P1-42

M. Spolaore
Turbulent Electromagnetic Filaments in Toroidal Plasma Edge
EX/P1-40

V. Toigo, D. Boilson, T. Bonicelli, M. Hanada, A. Chakraborty, and NBTF Team
Progress in the Realization of the PRIMA Neutral Beam Test Facility
FIP/2-4Rc

E. Lerche, M. Valisa et al.
ICRH for Mitigation of Core Impurity Accumulation in JET-ILW
EX/P5-22

Communications to National and International Workshops and Conferences

5th International Conference on Plasma Medicine (ICPM5)
May 18-23, 2014 Nara, Japan
Book of abstracts

M. Zuin, P. Brun, E. Martines, S. Pathak, P. Brun, R. Cavazzana
Control of time-limited activation of human primary fibroblasts through ROS generation induced by cold atmospheric plasma treatment

Theory and Simulation of Disruptions Workshop
July 9-11, 2014, Princeton, New Jersey USA

R. Paccagnella, V. Yanovskiy, P. Zanca, R. Cavazzana, C. Finotti, G. Manduchi, L. Piron
Progresses in disruptions theory and some new experiments in disruption control

Theory of fusion plasmas, joint Varenna - Lausanne international workshop
September 1-5, 2014 Villa Monastero, Varenna, Italy

Xu Xinyang, S. C. Guo, Y. Q. Liu, Z. R. Wang
Trapped Energetic Particles Effect on Resistive Wall Mode and Excitation of Fishbone-Like Mode in RFP plasmas

M. Veranda, Bonfiglio Daniele, Cappello Susanna, Escande Dominique, Chacon Luis
Helical features in nonlinear 3D MHD simulations of reversed-field pinch

ICPP 2014 International Congress on Plasma Physics
15-19 September, 2014 Lisbona, Portugal

D. Bonfiglio, S. Cappello, M. Veranda, D. F. Escande and L. Chacón

Helical Self-Organization in 3D MHD Modeling of Fusion Plasmas

Book of abstracts MCF.I1

E. Martines, D. Bonfiglio, S. Cappello, P. Innocente, H. Isliker, R. Lorenzini, B. Momo, C. Rea, M. Veranda, L. Vlahos, P. Zanca, and M. Zuin

Magnetic Topology Change Induced By Discrete Relaxation Events In Reversed Field Pinch Plasmas

Book of abstracts MCF.P26

**Joint 24th MHD, Disruptions & Control and 13th Energetic Particle Physics Topical Groups of the International Tokamak Physics Activity (ITPA)
21-23 October, 2014 Padova, Italy**

P. Piovesan

Measurement and modelling of plasma response to 3D fields at high-beta in ASDEX Upgrade

T. Bolzonella

Systematic approach to 3D dynamic e.m. modeling of fusion devices and its validation

R. Paccagnella

Update on disruptions simulations

M. Gobbin/M. Valisa

Runaway electron dynamics in RFX-mod tokamak discharges

P. Zanca

An active feedback avoidance technique for disruption events induced by m=2 n=1 tearing modes in ohm ically heated tokamak

**56th Annual Meeting of the APS Division of Plasma Physics
October 27-31, 2014 • New Orleans, Louisiana**

Bulletin of the American Physical Society 56th Annual Meeting of the APS Division of Plasma Physics Volume 59, Number 15

Vadim Yanovskiy, Roberto Paccagnella

Plasma surface and wall eddy currents and their connection to Halo currents during disruptions in tokamaks

BP8.00015

I. Predebon, P. Xanthopoulos, D. Terranova

Gyrokinetic investigation of ITG turbulence in helical RFPs I.

JP8.00067

A.D. Turnbull, N.M. Ferraro, L.L. Lao, General Atomics, J.M. Hanson, F. Turco, P. Piovesan

External Kink Mode in Diverted Tokamaks

NP8.00021

Roberto Paccagnella, Paolo Zanca, Vadimyanovskiy, Claudio Finotti, Gabriele Manduchi, Chiara Piron Lorella Carraro, Paolo Franz

Disruption avoidance through active magnetic feedback in tokamak plasmas,
NP8.00044

P. Piovesan, , V. Igochine, Ipp, A. Kirk, M. Maraschek, Ipp, L. Marrelli, , W. Suttrop, D. Yadykin, M. Cavedon, I.G.J. Classen, Differ, B. Gude, M. Reich, E. Viezzer, E. Wolfrum, Asdex Upgrade Team
Measurement of plasma response to 3D fields at high- β in ASDEX Upgrade
PO3.00014

L.M. Reusch, M.E. Galante, D.J. Den Hartog, P. Franz, J.R. Johnson, M.B. MCGARRY, H.D. Stephens
Using IDA to Understand Electron Temperature Structures in High Temperature Discharges in the Madison Symmetric Torus
PP8.00012

Matthew Galante, Lisa Reusch, Daniel Den Hartog, Paolo Franz, Jay Johnson, Meghan MCGARRY
DETERMINATION OF ZEFF IN MST PLASMAS THROUGH INTEGRATED DATA ANALYSIS
PP8.00013

J.A. Goetz, M.B. MCGARRY, P. Franz, D.J. Den Hartog , J. Johnson
Improvements in SXR and Te Measurements on MST
PP8.00014

Stefano Munaretto, F. Auriemma, D. Brower, B.E. Chapman, D.J. Den Hartog, W.X. Ding, J. Duff, P. Franz, J.A. Goetz, D. Holly, L. Lin, K.J. Mccollam, M. MCGARRY, L. Morton, M.D. Nornberg, E. Parke, J.S. Sarff
Dynamics of helical states in MST
PP8.00022

3D MHD modeling of fusion plasmas with the PIXIE3D and SpeCyl codes
D. BONFIGLIO, S. CAPPELLO, M. VERANDA, L. CHACÓN, LANL, NM, D.F. ESCANDE
PP8.00037

Gianluca De Masi, Fulvio Auriemma, Roberto Cavazzana, Emilio Martines, Gianluca Spizzo
A new technique for effective core fueling and density control in RFX-mod
PP8.00038

Matteo Zuin, Luca Stevanato, Emilio Martines, Winder Gonzalez, Roberto Cavazzana, Davide Cester, G. Nebbia, Laszlo Sajo-Bohus, Giuseppe Viesti
Neutron and Gamma-ray Detection in Reversed-Field Pinch Deuterium Plasmas in the RFX-mod Device
PP8.00039

Barbara Momo, Emilio Martines, Paolo Innocente, Rita Lorenzini, Cristina Rea, Paolo Zanca, Matteo Zuin
Magnetic topology change induced by reconnection events in RFP plasmas
PP8.00040

Daniele Brunetti, Jonathan Graves, Wilfred Cooper, David Terranova, Christer Wahlberg

Fast growing instabilities and non-linear saturated states in hybrid tokamak and RFP plasmas

PP8.00041

Roberto Cavazzana, Matteo Agostini, Lorella Carraro, Paolo Innocente, Lionello Marrelli, Paolo Scarin, Gianluca Spizzo, Monica Spolaore, Nicola Vianello, Matteo Zuin

Direct Measurement of the First Wall Recycling Coefficient on RFX mod

TP8.00030

Matteo Agostini, Lorella Carraro, Giovanni Ciaccio, Gianluca De Masi, Cristina Rea, Paolo Scarin, Gianluca Spizzo, Monica Spolaore, Nicola Vianello

Turbulence and transport in a 3D magnetic boundary

TP8.00072

Vadim Yanovskiy, Paolo Zanca, Roberto Paccagnella

MHD modes rotation and locking threshold studies in ITER-like plasmas

YP8.00017

Vadim Yanovskiy, Vladimir Pustovitov

Ferromagnetic effect on the rotational stabilization of the resistive wall modes in tokamaks

YP8.00018

19th Workshop on MHD Stability Control - A US-Japan Workshop

Auburn University November 3-5, 2014

C. Piron: "Coupling of externally applied 3D fields with internal MHD, with focus on sawteeth and their control"